



HAL
open science

Two-dimensional complex modeling of bone and joint infections using agent-based simulation

Salma Alsassa

► **To cite this version:**

Salma Alsassa. Two-dimensional complex modeling of bone and joint infections using agent-based simulation. Imaging. Université de Bretagne occidentale - Brest, 2019. English. NNT : 2019BRES0022 . tel-02918081

HAL Id: tel-02918081

<https://theses.hal.science/tel-02918081>

Submitted on 20 Aug 2020

HAL is a multi-disciplinary open access archive for the deposit and dissemination of scientific research documents, whether they are published or not. The documents may come from teaching and research institutions in France or abroad, or from public or private research centers.

L'archive ouverte pluridisciplinaire **HAL**, est destinée au dépôt et à la diffusion de documents scientifiques de niveau recherche, publiés ou non, émanant des établissements d'enseignement et de recherche français ou étrangers, des laboratoires publics ou privés.

THESE DE DOCTORAT DE

L'UNIVERSITE
DE BRETAGNE OCCIDENTALE
COMUE UNIVERSITE BRETAGNE LOIRE

ECOLE DOCTORALE N° 605

Biologie Santé

Spécialité : Analyse et Traitement de l'Information et des Images Médicales

Par

Salma ALSASSA

Two-Dimensional Complex Modeling of Bone and Joint Infections Using Agent-Based Simulation

Thèse présentée et soutenue à « Brest », le « 25 Février 2019 »

Unité de recherche : UMR1101 Inserm, LaTIM

Rapporteurs avant soutenance :

Pr. Pierre-Yves BOËLLE PUPH, Institut Pierre Louis
d'Epidémiologie et de
Santé Publique

Pr. Tristan FERRY PUPH, Service Maladies
Infectieuses et tropicales ,
Hospices Civils de Lyon

Composition du Jury :

Pr. Pierre-Yves BOËLLE PUPH, Institut Pierre Louis
d'Epidémiologie et de Santé Publique

Pr. Tristan FERRY PUPH, Service Maladies Infectieuses et
tropicales, Hospices Civils de Lyon

Président du jury PU, Laboratoire des Sciences et
Techniques de l'Information, de la
Communication et de la
Connaissance (Lab-STICC)

Directeur de thèse
Pr. Séverine ANSART PUPH, Service Maladies Infectieuses
et Tropicales, CHRU Brest, LaTIM

Invité(s)
Pr. Eric STINDEL PUPH, UMR 1101 LaTIM, CHRU Brest

Dr. Thomas LEFEVRE MCU PH - AP-HP, Hôpital Jean Verdier,
Service de médecine légale et sociale,
IRIS - Institut de Recherche
Interdisciplinaire sur les enjeux Sociaux

M. Alcibiade LICHTEROWICZ Gérant de l'entreprise Tekliko

Acknowledgments

I shall start my acknowledgment and appreciation to Tekliko enterprise since this work was accomplished by the collaboration between industry and laboratory in the frame of contract CIFRE between Tekliko and LaTIM.

I would like to express my great gratitude to Prof. Eric Stindel for giving me the opportunity to do this Ph.D. and to join LaTIM laboratory during this work. I appreciate all the support, scientific guidance and valuable advice he has given me to accomplish this work. It has been a privilege of learning from and working with him.

I am proud to acknowledge the guidance of Prof. Séverine Ansart, my thesis director. She has given great support and academic knowledge that contributed to the completion of this thesis. I appreciate very much her expert advice and tireless patience that accompanied me, especially when writing this dissertation.

I am deeply grateful to my supervisor Dr. Thomas Lefèvre, for his insightful guidance and invaluable suggestions that contributed to realizing the work. I highly appreciate his scientific support, expert ideas, patience, and assistance to achieve the goal.

I am deeply grateful to Alcibiade Lichterowicz and Vincent Laugier, first for giving me the opportunity to do this work within Tekliko team, and then for the financial support, confidence, help, and enthusiasm for this project.

I would also like to express my gratitude to the reviewers, who examined my work of thesis and provided insightful suggestions. I would like as well to thank the jury members for their acceptance to be in the committee and examine the work.

This acknowledgment would be incomplete without expressing my gratitude to my family, especially my parents for all their moral support, advice, and encouragement. They have always raised me to love science, knowledge, and learning. My great thanks to my husband Mahmoud, who accompanied me with his unconditional support, confidence, patience, and sacrifices to complete this thesis that otherwise would not have been possible.

A great thanks go out to all my friends and labmates for their support. A special thanks to Dr. Bhushan Borotikar, Dr. Ammar Ghaibeh, and Prof. Pascal Ballet for their advices and valuable discussions during this thesis.

Abstract

Bone and joint infections are one of the most challenging bone pathologies that associated with irreversible bone loss and long costly treatment. Early diagnosis and management of bone and joint infections (BJI) is a difficult task. The high intra and inter patient's variability in terms of clinical presentation makes it impossible to rely on the systematic description or classical statistical analysis for its diagnosis or studying, particularly with regard to the number of cases. The development of BJI encompasses a complex interplay between the cellular and molecular mechanisms of the host bone tissue and the infecting bacteria. The objective of this thesis is to provide a novel computational modeling framework that simulates the behavior resulting from the interactions on the cellular and molecular levels to explore the BJI dynamics qualitatively and comprehensively, using an agent-based modeling approach. We relied on a meta-analysis-like method to extract the quantitative and qualitative data from the literature and used it for two aspects. First, elaborating the structure of the model by identifying the agents and the interactions, and second estimating quantitatively the different parameters of the model. The BJI system's response to different microbial inoculum sizes was simulated with respect to the variation of several critical parameters. The simulation output data was then analyzed using a data-driven methodology and system dynamics approach, through which we summarized the BJI complex system and identified plausible relationships between the agents using differential equations. The BJI model succeeded in imitating the dynamics of bacteria, the innate immune cells, and the bone cells during the first stage of BJI and for different inoculum size in a compatible way. The simulation displayed the damage in bone tissue as a result of the variation in bone remodeling process during BJI. These findings can be considered as a foundation for further analysis and for the proposition of different hypotheses and simulation scenarios that could be investigated through this BJI model as a virtual lab.

Table of Contents

Abstract.....	iv
Abbreviations List.....	viii
List of Figures.....	ix
List of Tables.....	xii
CHAPTER.....	1
1. Introduction.....	1
1.1. Bone and Joint Infections (BJI) : Introduction.....	1
1.2. Aims and Scope of This Thesis.....	5
2. Overview of the Bone and Joint Infections Biological System.....	9
2.1. Bone.....	10
2.1.1. Bone Tissue Structure and Function.....	10
2.1.2. Bone Cells.....	11
2.1.3. Bone Remodeling Process.....	17
2.2. Immune System.....	20
2.2.1. The Innate and Adaptive Immune Response.....	20
2.2.2. Innate Immune Cells.....	22
2.2.3. Cytokines and an Insight into TGF-beta.....	25
2.2.4. Different Stages of Innate Immune Response.....	25
2.3. Bacteria.....	26
2.3.1. Bacterial Growth Style and Characteristics.....	26
2.3.2. <i>Staphylococcus aureus</i> Resistance Mechanisms.....	28
3. Modeling Biological System Approaches.....	30
3.1. Traditional Modeling Approach (Animal Models).....	30
3.2. Characteristics of Complex Biological Systems.....	32
3.3. Computational Modeling of Complex Biological Systems.....	32
3.3.1. Strength of Computational Modeling Approach.....	32
3.3.2. Computational Modeling Approaches.....	34
3.4. Agent-Based Modeling (ABM) Approach.....	35
3.4.1. ABM in Modeling Biological System.....	35
3.4.2. Agent-Based Modeling Applications in Bone Biology and Infections.....	39
3.4.3. Limitations of ABM approach.....	40

4. Parameters Identification of BJI Model.....	43
4.1. Bibliography Search Method	44
4.2. Literature Review Results	48
5. Two-Dimensional Agent-Based Model of BJI.....	55
5.1. Model Development.....	56
5.1.1. The Model Platform.....	56
5.1.2. The Agents in the Model	58
5.1.3. BJI Logical Model	60
5.1.4. Model Implementation in NetLogo and Parameters Identification	74
5.1.5. Process Review and Event Series	81
5.2. Simulation Design.....	83
5.3. Results	84
5.3.1. The Developed Agent-Based Model of BJI	84
5.3.2. Simulation Result	85
5.4. Discussion	95
6. Analyzing BJI Model Simulation Output Data Using System Dynamics Approach.....	99
6.1. System Dynamics Approach	100
6.2. Methods.....	103
6.2.1. Software.....	103
6.2.2. Methods of analysis	104
6.3. Results	108
6.4. Analysis of Results: Optimal Selection of System Dynamics Model.....	120
6.5. Discussion	125
7. Conclusion.....	127
7.1. Brief Summary of the Study.....	127
7.2. Contribution	128
7.3. Limitation and Future Work.....	129
Publication and Communication.....	132
References.....	133
Appendix.....	159

Abbreviations List

BJI – Bone and Joint Infections

ABM – Agent-Based Model

ECM – Extra-Cellular Matrix

MCP-1 – Monocyte Chemo-Attractant Protein-1

MRI – Magnetic Resonance Imaging

OPG – Osteoprotegerin

RANK – Receptor Activator of Nuclear factor -B

RANK – Receptor Activator of Nuclear factor -B ligand

TGF- β – Transforming Growth Factor

TNF- α – Tumor Necrosis Factor Alpha

BMU – Basic Multicellular Unit

OB – Osteoblasts

OC – Osteoclasts

OS – Osteocytes

MA – Macrophages

PMN – Polymorphonuclear Neutrophil

MAM – Monocyte-Derived Macrophages

ODE – Ordinary Differential Equation

BDynSys – Bayesian Dynamical System

MLL – Maximum Log-Likelihood

Bf – Bayes factor

SD – Standard Deviation

List of Figures

Figure 1.1. Recurrence and prevalence of BJI in France, 2008.	3
Figure 2.1. A cross-section of a monkey jawbone showing the different parts of cortical bone.	11
Figure 2.2. Enlarged space of trabeculae bone shows its different cells.	12
Figure 2.3. The osteoblast cells activity in a remodeling cite.	13
Figure 2.4. Human cortical bone section of osteocytes located in their lacunae	14
Figure 2.5. A micrograph shows several human bone-lining cells	15
Figure 2.6. A microscopic photo shows tow active osteoclasts cells (OC) while resorbing the bone matrix	17
Figure 2.7. Steps of the bone remodeling process	18
Figure 2.8. Bacteria effects on bone remodeling	20
Figure 2.9. The dynamics of prenatal tissue-resident macrophage and monocyte-derived macrophage	23
Figure 2.10. Electron micrograph of a neutrophil during the process of phagocytosing a bacterium	24
Figure 2.11. Ideal growth curve of bacteria with time	27
Figure 3.1. An abstract map of computational modeling methods classified according to the most fitting biological spatial scale within discrete and continuous classes.	34
Figure 3.2. Mapping of the ABM approach to the research organization at each biological level of representation in multi-scale biological system structure	37
Figure 3.3. The cycle work of integrating the ABM model with experimental work .	39
Figure 4.1. Flowchart of the review method steps to identify the parameters of bone cells and signals.	50
Figure 4.2. Flowchart of the review method steps to identify the parameters of innate immune cells and signals.	51
Figure 4.3. Flowchart of the review method steps to identify the parameters of bacteria (<i>S. aureus</i>).	52
Figure 4.4. Flowchart of the review method steps to identify the interactions between agents.	53
Figure 5.1. Method flow of the model development.	55
Figure 5.2. Schematic of the agents in the BJI model.	60
Figure 5.3. Schematic diagram showing agents used in the model, interactions between them, and governing functions for each of them.	66
Figure 5.4. A flowchart of the main body of the ABM code	67
Figure 5.5. Logical flowcharts of the code run by the osteoclasts agents.	68
Figure 5.6. Logical flowcharts of the code run by the osteoblasts agents.	69
Figure 5.7. Logical flowcharts of the code run by the bacteria agents.	70
Figure 5.8. Logical flowcharts of the code run by the macrophage agents.	71
Figure 5.9. Logical flowcharts of the code run by the neutrophil agents.	72

Figure 5.10. Logical flowcharts of the code run by the monocyte agents.	73
Figure 5.11. Snapshot BJI model interface using NetLogo platform.	75
Figure 5.12. Snapshots of the ABM space at three different time steps	84
Figure 5.13. The mean and standard deviation (SD) for 100 iterations for bacterial populations over time.....	87
Figure 5.14. The mean and standard deviation (SD) for 100 iterations for neutrophil populations over time.....	88
Figure 5.15. The mean and standard deviation (SD) for 100 iterations for osteocyte populations over.....	89
Figure 5.16. Comparisons of system response for three inoculum infection state of bacteria	90
Figure 5.17. 3D surface graphs to analyze the relationship between the bacteria vs. neutrophils (PMN)	92
Figure 5.18. 3D surface graphs to analyze the relationship between the bacteria vs. osteocytes (OS)	93
Figure 5.19. 3D surface graphs to analyze the relationship between the neutrophils (PMN) vs. osteocytes (OS)	94
Figure 6.1. Comparison between the BJI model simulation outputs and the system dynamics model outputs of bacteria population over time	113
Figure 6.2. Comparison between BJI model simulation outputs and the system dynamics model outputs of the neutrophil (PMN) population over time	115
Figure 6.3. Comparison between BJI model simulation outputs and the system dynamics model outputs of the osteocyte population over time.....	119
Figure 6.4. Log Bf for the bacteria and neutrophils system dynamics models.....	121
Figure 6.5. Log Bf for bacteria and osteocytes system dynamics model	122
Figure B.1. Comparison between the BJI model simulation and the system dynamics model of bacteria population for inoculum size= 100 (CFU/mm ²)	172
Figure B.2. Comparison between the BJI model simulation outputs and the system dynamics model of bacteria population for inoculum size= 150 (CFU/mm ²).....	173
Figure B.3. Comparison between the BJI model simulation outputs and the system dynamics model of bacteria population for inoculum size= 250 (CFU/mm ²).....	174
Figure B.4. Comparison between the BJI model simulation outputs and the system dynamics model of neutrophil population for inoculum size= 100 (CFU/mm ²).....	175
Figure B.5. Comparison between the BJI model simulation outputs and the system dynamics model of neutrophil population for inoculum size= 150 (CFU/mm ²).....	176
Figure B.6. Comparison between the BJI model simulation outputs and the system dynamics model of neutrophil population inoculum size= 250 (CFU/mm ²).....	177
Figure B.7. Comparison between the BJI model simulation outputs and the system dynamics model of bacteria population for bacteria and osteocyte dynamic system for inoculum size= 100, 150 (CFU/mm ²).....	178
Figure B.8. Comparison between the BJI model simulation outputs and the system dynamics models of bacteria population for bacteria and osteocyte system for inoculum size= 250 (CFU/mm ²).....	179

Figure B.9. Comparison between the BJI model simulation outputs and the system dynamics models of osteocyte population for bacteria and osteocyte system for inoculum size= 100 (CFU/mm²)..... 180

Figure B.10. Comparison between the BJI model simulation outputs and the system dynamics models of osteocyte population for bacteria and osteocyte system for inoculum size= 150 (CFU/mm²)..... 181

Figure B.11. Comparison between the BJI model simulation outputs and the system dynamics models of osteocyte population over time for bacteria and osteocyte system for inoculum size= 250 (CFU/mm²) 182

List of Tables

Table 2.1. Vitale data of bone basic multicellular unit (BMU)	19
Table 4.1. Table of research equations used in the literature review with corresponding inclusion and the exclusion criteria.....	47
Table 4.2. Agent parameters and their values retrieved from the literature search.	48
Table 5.1. A comparison between ABM platforms according to general features.....	58
Table 5.2. List of the agents in the bone and joint infections agent-based model, their rules, and behaviors.	62
Table 5.3. List of mediators and their effects that are represented in BJI model.	65
Table 5.4. Table of agent's parameters, their range of applicable values	80
Table 5.5. List of the observed variables through the BJI model time courses	82
Table 6.1. The parameters' values at the initial state during 200 iterations of BJI model simulation for testing the system behavior coherence	105
Table 6.2. The initial conditions used to identify relationships between variables. ..	107
Table 6.3. The two terms DE systems that result from the Bayesian dynamical system modeling method with their R-squared values.	108
Table 6.4. The form, coefficient values and R-squared values for each variables' models that are represented in (Table 6.3).....	109
Table 6.5. The calculated three terms differential equations systems for bacteria (x) and neutrophils (y) dynamics.....	111
Table 6.6. The calculated three terms differential equations systems for bacteria population (x) and osteocyte population (y) dynamics.....	117
Table 6.7. System dynamics models of up to four terms with their maximum log-likelihood (MLL)	120
Table A.1. Table of the resulting articles of the literature review	159
Table B.1. The calculated three terms differential equations systems for the bacteria(x) and neutrophil (y) population for different initial conditions.....	165
Table B.2. The calculated three terms differential equations systems for the bacteria(x) and osteocyte (y) population for different initial conditions	168

1. Introduction

1.1. Bone and Joint Infections (BJI): Introduction

Bone and joint infections (BJI) are a group of clinical entities that all have in common the invasion and the progressive destruction of bone and cartilage tissue by microorganisms, most commonly bacteria. These infections constitute a very heterogeneous group of clinical cases, classified according to their anatomical location, their evolution time, the mechanism leading to infection, and the presence or not of orthopedic material (Mathews et al., 2010; Olson et al., 2013; Zimmerli et al., 2004). BJI can result from hematogenous spread of infection and develop within two weeks (acute hematogenous BJI) (Carek et al., 2001; Jorge et al., 2010). In adults, BJI develop more frequently from direct inoculation of bacteria secondary to trauma, internal fixation of a fracture, or prostheses placement and progress slowly within months (Birt et al., 2017; Smith et al., 2006). This class of BJI is representing the most prevalent type in the western countries and characterized as a long-lasting infection (Chronic BJI) (Lew et al., 2004). The incidence rate of post-operative/post-traumatic infections is showing an important annual increase due to the rising in arthroplasties procedures associated with mounting risk factors such as diabetes and peripheral vascular disease, in addition to the variation in the population's age structure (Walter et al., 2012).

In 2013, the BJI prevalence in France was 70 per 100,000 of the population, in comparison with 54/100,000 of the population in 2008 representing a high increase

within a short period (Grammatico-Guillon et al., 2012; Laurent et al., 2018) (Figure 1.1). In Olmsted County, USA, the BJI incidence has increased from 11.4/100,000 of the population per year in the period from 1969 to 1979 to 24.4/100,000 per year in the period from 2000 to 2009 (Kremers et al., 2015).

Surveys integrated inpatient database of several countries involving Western European countries along with the United States reported a considerable rise in total joint arthroplasties (TJA) in the last ten years (Kurtz et al., 2011; Niemeläinen et al., 2017; Patel et al., 2015). In 2008, the proceeded total hip (THA) and total knee (TKA) arthroplasties were 615,000 and 210,000 in the United States what represent an increase of 40% and 134%, respectively, compared to the year 1999 (Cram et al., 2011; Losina et al., 2012). In France, the number of performed TKA showed a compound annual growth of 5.3% between 2002 and 2007, and the demand continued rising to reach 33% higher in 2013 than 2008 (Colas et al., 2016; Kurtz et al., 2011). Projections expect that by 2030, the request for THA and TKA procedures will increase by 174%, and 673%, respectively (Kurtz et al., 2007a). For both THA and TKA, the demographics of recipients has become younger (< 65 years old), and it is projected that young patients will exceed 50% of the patient population by 2030 (Kurtz et al., 2009; Ravi et al., 2012).

The revisions of total hip and total knee are also estimated to increase by 173% and 601%, respectively, by 2030 in compare with 2005 (Kurtz et al., 2007a). It was reported that more than one-third of TKA revisions take place in the first two years, and the BJIs represent the second common failure cause (22.8%) of this group (Schroer et al., 2013). In France, a ten years' follow-up study shows that the failure rate of TKA patients operated during the year 2000 was 7.5%, and the infections represented the failure cause of 25% of this rate (Argenson et al., 2013; Colas et al., 2016). The infections have the prospect to become the most recurrent failure cause of TJA in the US in the following two decades. The revision procedures of THA and TKA were estimated to increase respectively from 8.4%, and 16.8% in 2005 to 47%, and 65.5% by 2030 (Kurtz et al., 2007b).

BJI incidents are associated with a high risk of therapeutic failure, a mortality rate of nearly 5%, and long-term consequences that impact the quality of life of 40% of patients, despite long and costly medical and surgical treatment (Cohen et al., 2004;

McHenry et al., 2002). For one prosthesis-related BJI case, the overall cost of the treatment was estimated to be between 45,000 and 80,000 euros (Parvizi et al., 2010). In France, the total cost of the healthcare of BJI is estimated to be more than 250 million euros per year, with an average hospital stay of 17.8 days per hospitalization (Grammatico-Guillon et al., 2012).

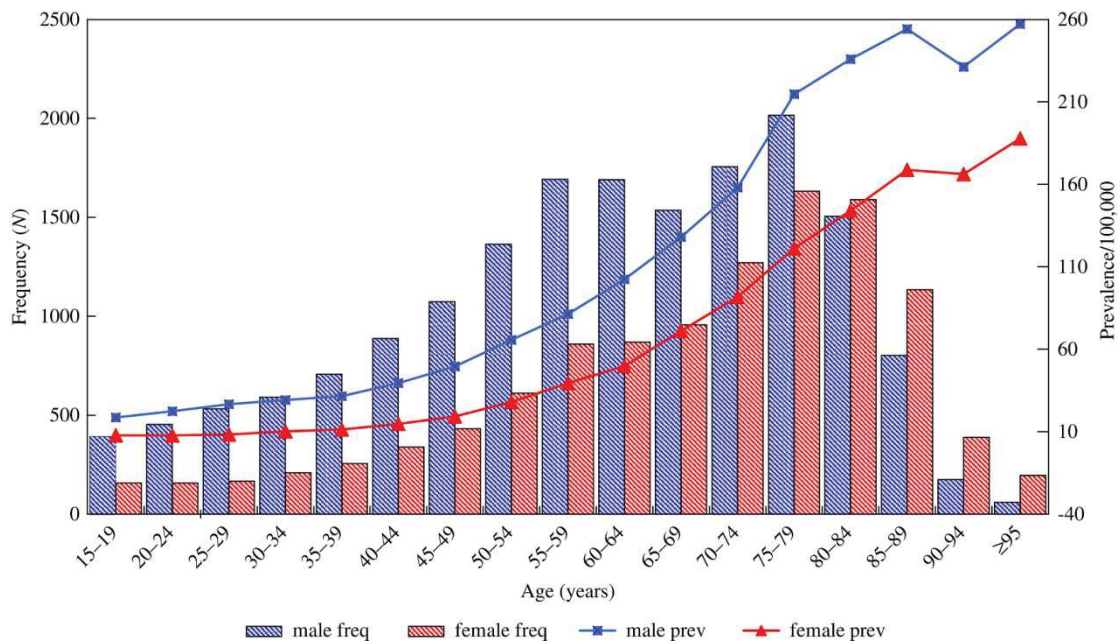


Figure 1.1. Recurrence and prevalence of BJI in France, 2008.
Source (Grammatico-Guillon et al., 2012)

The *Staphylococcus aureus* (*S. aureus*) is the predominant cause of BJI among the other types of causative micro-organisms (70% of cases) in both native and device-associated infections (Fritz et al., 2008; Grammatico-Guillon et al., 2012; Tande et al., 2014; Tong et al., 2015). Chronic BJI is still difficult to cure despite the prolonged treatment which usually combines various antimicrobial agents and surgical intervention (Bejon et al., 2017; Lew et al., 2004). This type is correlated with critical rates of relapse that could present after a long asymptomatic period (latent infection) (Osmon et al., 2013; Tande et al., 2014). This difficulty is due to bacterial avoidance of the host defense and the antibiotic treatment by forming biofilms or hiding intracellularly (Brady et al., 2008; Junka et al., 2017; Spellberg et al., 2012; Valour et al., 2013).

BJI pathogenesis is identified by different factors including the comorbidities and the patient's immune status, besides the vascularity, status, and location of the infected bone (Sia et al., 2006). BJI can affect the different structure of the bone tissue and even parts of the neighboring soft tissue (Pineda et al., 2006). It rapidly indicates acute bone loss and irregular bone signaling system.

The early diagnosis of BJI represents a challenge in its therapy due to the need of taking the best decision quickly and starting an aggressive treatment. BJI diagnosis relies on findings from different diagnostic methods include clinical examination, risk factors, laboratory results, diagnostic imaging (radiographs, computerized tomography, magnetic resonance imaging (MRI), scintigraphy, FDG-PET scans), and bone cultures (Forsberg et al., 2011). Despite the progress and accuracy of modern medical imaging techniques, it is still difficult to detect the BJI in its early hours or days. (Carek et al., 2001; Hatzenbuehler et al., 2011; Pineda et al., 2009). Also, it is difficult to rely on the systematic description or the statistical analysis tool to evaluate or predict the disease progress because of the great variety in disease presentations and pathophysiology intra and inter incident cases (Schmidt et al., 2011; Walter et al., 2012).

1.2. Aims and Scope of This Thesis

Improving the understanding and management of BJI development need to integrate a new tool that able to comprise different properties of the system and facilitate studying its dynamics. Due to the complex structure of BJI system and the impacts of various factors on BJI pathogenesis, significant progress in understanding the disease can be achieved from deep grasping of the behaviors that could result from the interactions between the system components.

A variety of experimental models range between simple in-vitro to complicated tissue or device-associated in-vivo models were proposed in the literature for imitating the behavior of microorganisms spreading during BJI or testing the effectiveness of a new treatment (Coenye et al., 2010). Nonetheless, these models increasingly improve our understanding of the BJI pathophysiology, as we yet away from an integral comprehension of the impact of various interactions that are managing and directing the dynamic of the system.

Computational modeling represents a unique way to construct a model of BJI systems that can simulate their complex and dynamic behavior, analyze their progression, and provide insights in selecting evidence-based treatment strategies.

Agent-based modeling (ABM) approach, even though is more consuming in terms of computational effort and time in comparison with the classical mathematical modeling approaches, provides a platform that has the capability to encompass various features of the biological system. The ABM approach can with its built-in structure involve the stochastic behaviors, the incremental changes, the multiple scales interactions, the heterogeneous components, and the multi-environment tissue characterizations. ABM is fitted to easily handle the cellular behaviors by embodying the information using the agent types, the local environment, rule-based behavior, and internal state.

The objective of this thesis is to introduce a novel computational modeling framework of BJI system that enables investigating and understanding the behaviors evolve from the spatiotemporal cellular and molecular (signals) mechanisms and interactions, using an agent-based modeling approach. The work of this thesis is set to achieve three tasks. The first task is to use the data from basic literature in a form that

allows quantitative and mechanistic description of cellular attitudes. To achieve this goal and extract the information from the different studies we will employ a systematic literature search and then identify the range of applicable values of the parameters.

The second task is to develop a two-dimensional agent-based model of BJI that introduces a plausible representation of the system and a simulated experimental environment to reproduce the infection and examine its dynamics as a result of cellular interactions. The BJI system will be modeled through the interaction between the components of three subsystems: the bacteria, the infected bone, and the immune response. The model simulation will be used to test several hypotheses that exist in the literature and to investigate the effect of different parameters changes on the cell dynamics, such as the initial concentration of bacteria and the quality of the immune system during the first stage of infection.

The third task is to analyze the different patterns of the system behavior that result from the BJI model simulation and to identify plausible relationships between its components using an effective data analysis technique. To achieve this goal, we will use the system dynamics approach that can summarize the BJI model outcomes using differential equations.

After a brief introduction of BJI, the motivation and objective of this work (**Chapter I**), the structure of this thesis is organized as follows:

Chapter II: introduces the biological background of BJI system at the level of its constituent cells beside the most important processes that are affected by the disease. The presentation of the biological system allows us to identify the points that we will focus on in our proposal for a BJI model.

Chapter III: is dedicated to presenting the state-of-the-art of the existing approaches to modeling the biological systems. Depending on several studies from the literature, we will compare in depth the two major approaches of modeling: the Top-down approach and the bottom-up approach. These details allow us to establish the following part of our thesis work, namely the proposal of a computational model of BJI.

Chapter IV: is devoted to explaining the method followed in this study for the literature review to describe and characterize the agent interactions and parameters, including the research questions, the inclusion and exclusion criteria, and the retrieved article that used to define the interactions between the components and the parameter ranges.

Chapter V: introduces the agent-based model that we propose to simulate the BJI system. It starts with presenting different elements of the model: the chosen ABM platform namely NetLogo, the model structure, the parameters' identifications, the agents' rules, and interactions, then the coupling between the conceptual model and the NetLogo platform. It followed by the simulation design and the investigation of system behavior that result from the interaction between each of the immune system, the bone tissue, and the bacteria.

Chapter VI: explains the Bayesian dynamic system modeling approach that we adopted to analyze the ABM outcomes under different hypotheses. This chapter includes the method followed in the analyses and the Bayesian selection method to identify the best dynamic models of the different variables of the system.

Chapter VII: concludes the work we have done and introduced in this dissertation in a summary followed by the limitations and the different perspectives of the work we plan to pursue.

2. Overview of the Bone and Joint Infections Biological System

BJI represents a complex biological system due to the nature of bone tissue, and to the overlapping elements and interactions on cellular and molecular levels. The infection and the manner of its development is a result of continued interaction between the bacteria and the host with its two parts: the infected bone and the immune defense system, on one side, and between the bacteria themselves on the other side (Lebeaux et al., 2013). These sub interacting systems consist of many components at the cellular and molecular level, which are the scales of interests of this thesis.

The pathogen invasion of the bone leads to a cascade of adverse changes in bone tissue components and severe activation of bone destruction (Claro et al., 2011; Josse et al., 2015). The balanced function between bone formation and bone resorption during bone remodeling process is regulated by RANK/RANKL/OPG signaling system (Boyce et al., 2008). This balance is altered by the presence of bacteria toward increasing osteoclasts activity and decreasing the osteoblasts related, what leads to bone loss (Eriksen, 2010).

At the same time, the presence of bacteria trigger the innate immune cells and signals to play their major role as the first line in defending the bacteria (Charles A Janeway et al., 2001; Dapunt et al., 2016). These cells, macrophages, neutrophils, and monocyte-derived macrophages, arrive consecutively to the site of infection under the stimulation by several signaling molecules and eradicate the bacteria by phagocytosis (Corrado et al., 2016; Shi et al., 2011). The infected bone cells also take place in

releasing cytokines, that may contribute either in directing immune cells reaction or in rising severe inflammatory damage (Bost et al., 1999; Marriott et al., 2005).

Building the simulation model of BJI goes hand in hand with the characteristics of the biological system, and it is necessary before starting any description of the modeling framework first to understand the structure of the biological system and the function of its components. This is important here since we are going to build a model for the cellular mechanisms and behavior of the real system. The different constituents of the BJI system have been studied in details in the literature in different contexts, including the macro and micro scale components and processes. In this chapter, we will introduce the biological system that we will study and model in the next chapters. We will start with a brief biological overview of the system structure, and the main cells and signals that constitute the system in the early stage of the infection.

2.1. Bone

2.1.1. Bone Tissue Structure and Function

Bone is a multifunction and multi-environment organ. It is a complex functional style of connected tissue that composite of cells surrounded by an extracellular matrix (Rodan, 1992). It is dynamic, renewable, and adaptable to always provide an architectural framework to support the soft tissue and protect the body organs (Steele et al., 1988). Bones are the site of blood cell production (in red marrow), and fat storage (in yellow marrow). Also, bones are the source of mineral homeostasis and have important roles in regulating various endocrine functions (Bilezikian et al., 2002).

In consequence of this variety of functions, bones have two principal osseous tissues. First, cortical (compact) bone, which represents the outer hard layer and composites of a dense matrix with osteon units (Figure 2.1). These units have the central Haversian canals through which the blood vessels and nerves pass. Second, cancellous (spongy) bone, which represents the non-organized porous network that hosts the marrow and takes on its mineral maintenance function (Parfitt, 1994; Sarko,

2005). Both of these tissues are characterized as an ever-change quality since they undergo a life-long regenerating process that called the bone remodeling process. When an area of bone is exposed to pathogen or strain, the quality of bone structure along with the harmony of the remodeling process are affected (Buckwalter et al., 1995).

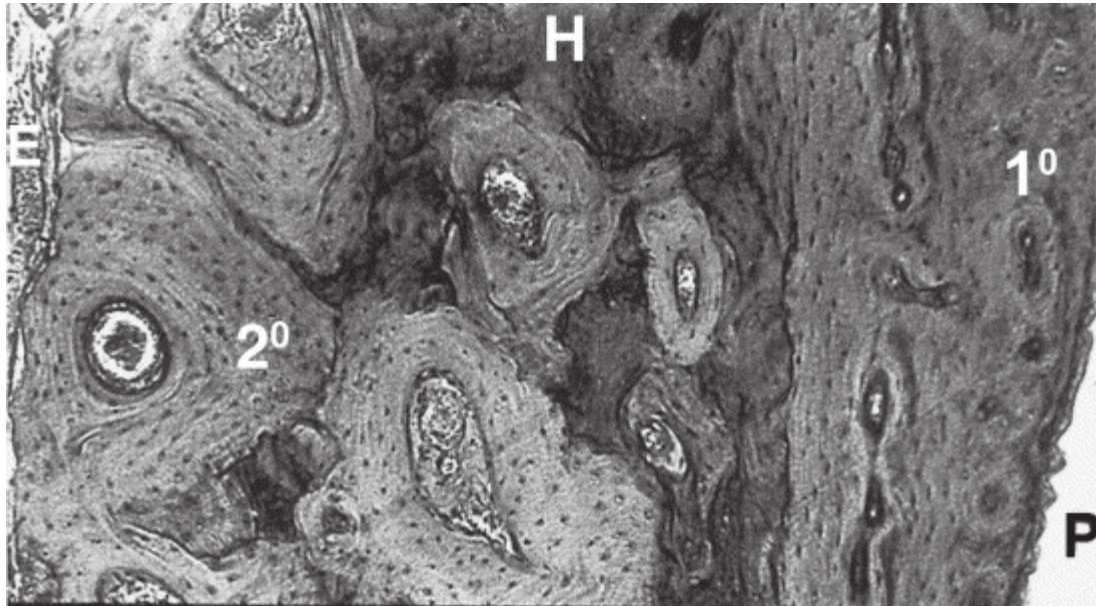


Figure 2.1. A cross-section of a monkey jawbone showing the different parts of cortical bone. The inner and outer surfaces, endosteum (E), periosteum (P), and between them, the Haversian bone (H), with its two types: the immature primary osteons (1°) and the mature bulls-eye shaped osteons (2°). Source (Roberts et al., 2006).

2.1.2. Bone Cells

There are four types of mature and specialized bone cells: osteoclasts, osteoblasts, lining bone cells, which all are found on the external and internal bone surfaces, periosteum and endosteum, and osteocytes which are trapped inside the bone matrix (Figure 2.2) (Rodan, 1992). Each of osteoblasts, osteocytes, and lining cells are arisen from osteoprogenitors cells, while on other hand osteoclasts are originated from the hematopoietic progenitors. These latter are also the origin of monocytes and macrophages blood cells (Bilezikian et al., 2002).

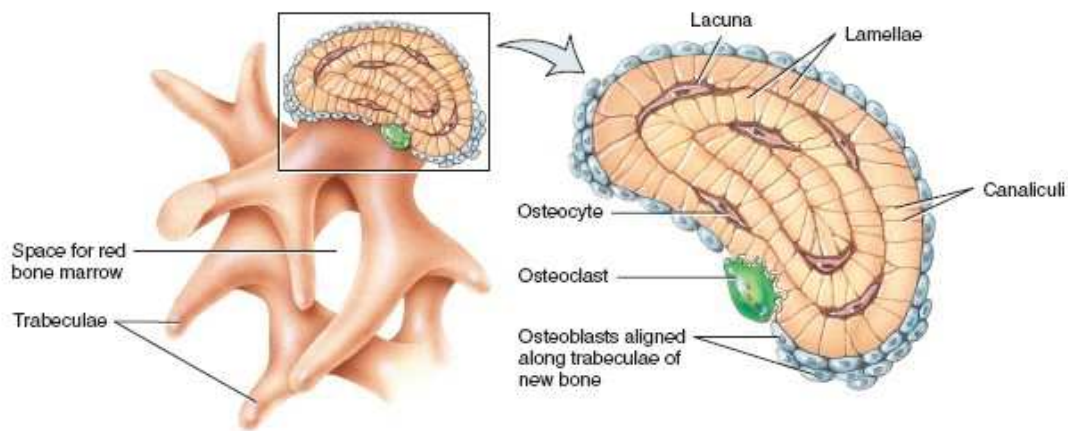


Figure 2.2. Enlarged space of trabeculae bone shows its different cells.

Source (<http://highereduc.wiley.com>).

Osteoblasts

They are the bone builder cells since they are responsible for forming new bone matrix either for replacing old bone by the life continuously bone remodeling process or for healing a damaged area (Figure 2.3) (Shapiro, 2008). They also have roles in activating osteoclasts and regulating bone matrix mineralization (Mackie, 2003; Yamashita et al., 2012). When they are activated, they secrete products such as collagen and other proteins in order to form the osteoid, and the non-mineralized bone matrix. Afterward, this osteoid is calcified to become a hard matrix where some osteoblasts are trapped inside and differentiate to osteocytes (Franz-Odenaal et al., 2006). This differentiation process from osteoblast to osteocyte generally takes three days (Knothe Tate et al., 2004). Osteoblasts might also flatten on the bone surface to form the lining cells while most of them, 50–70%, die in programmed cell death with an average lifespan of 3 months (Jilka et al., 1998; Parfitt, 1994). Considering their interaction with other systems, osteoblasts have impacts on the regulation and maintenance of the hematopoietic stem cells, which are produced in the bone marrow (Lorenzo et al., 2008; Takayanagi, 2007).

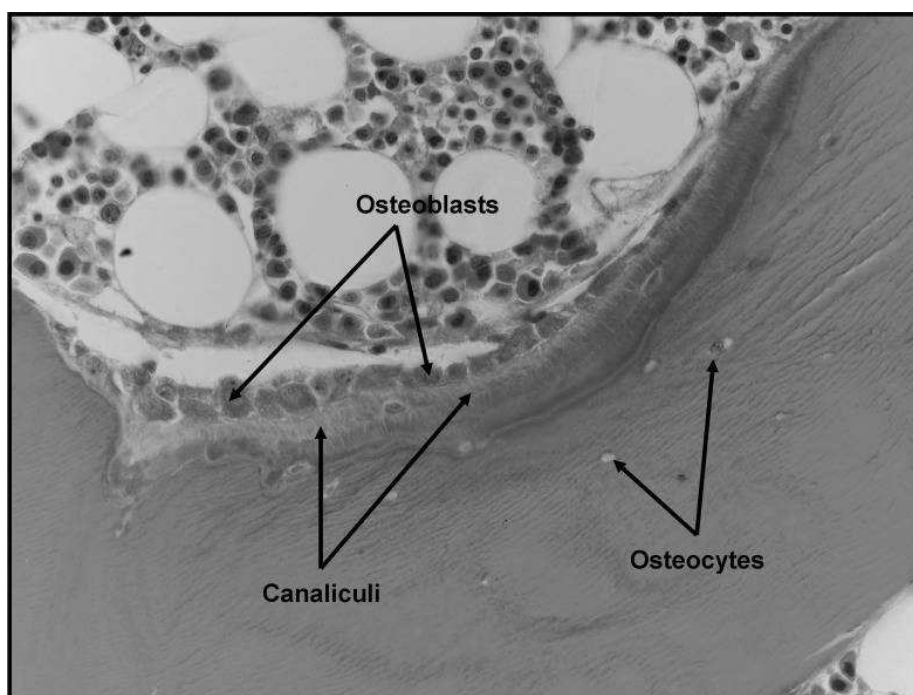


Figure 2.3. The osteoblast cells activity in a remodeling cite.

The image shows osteoblasts activity through the formation of the excavation area by synthesizing collagen to form new osteoids. These osteoids will be mineralized later to form the bone matrix.

Source (Clarke, 2008)

Osteocytes

They are the most common cells in bone tissue, 90-95% of all bone cells, and they have a long lifespan of 25 years (Franz-Ondendaal et al., 2006). Each osteocyte is located in space called lacunae within the mineralized bone matrix and communicates with other osteocytes and surfaces cells through gap junctions using their processes (Figure 2.4) (Schneider et al., 2010).

Osteocytes are recognized to be the main sensors that translate the mechanical tension to biochemical signals through which they could stimulate the remodeling process to respond to this load (Bonewald et al., 2008). They amazingly could adjust to several situations or to adapt the reaction under different conditions such as growth and strain (Bonewald, 2002). In addition, their location within the mineralized matrix

facilitates their responsibility for regulating the minerals level in the matrix and their transformation (Dallas et al., 2013). Moreover, they are in charge of the quality and status of the bone tissue. They manage the response if a part needs repair, nutrition, renewal or even if it counters damage. In other words, they stimulate, in an uncertain way, the osteoblasts formation function and the osteoclasts resorption function (Bonewald, 2011; Prideaux et al., 2016; Schaffler et al., 2012, 2014). The osteocyte death happens according to the apoptosis, bone destruction or resorption (Knothe Tate et al., 2004).

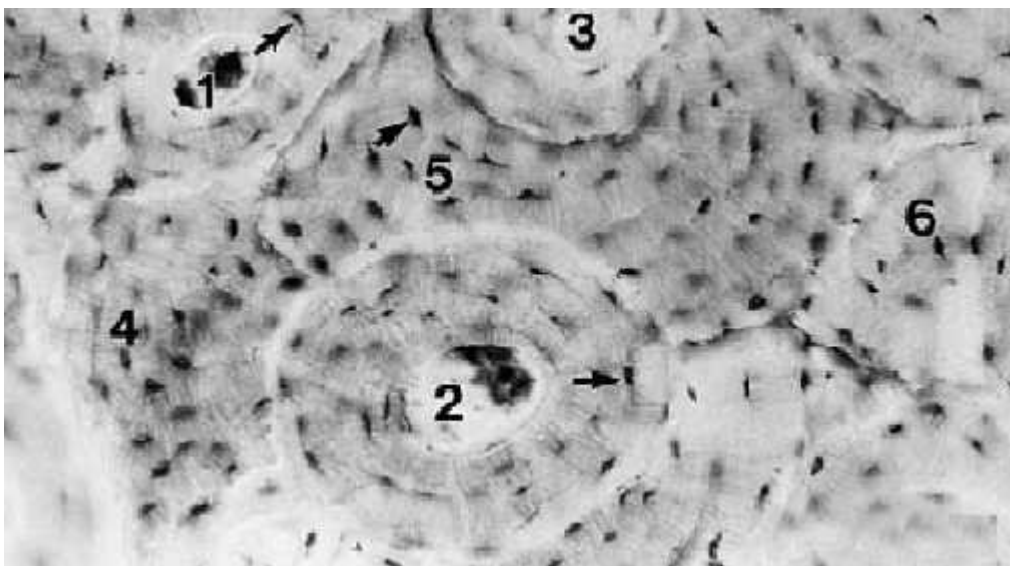


Figure 2.4. Human cortical bone section of osteocytes located in their lacunae (arrows). It shows the extended cell processes that are used to communicate with each other and with other cells. The osteocytes represent a network of cells that layout in Haversian system, (1, 2 and 3) are active Haversian, while (4, 5 and 6) are old Haversian where parts of them undergo the remodeling process. Source (Bilezikian et al., 2002)

Lining-bone cells

They derived from osteoblasts after they finish their role. They flatten on both inner and outer bone surfaces (Figure 2.5) (Florencio-Silva et al., 2015). They communicate with osteocytes through gap junctions and participate in regulating the mineral balance (Mullender et al., 1997). In addition, they take part in stimulating the osteoclasts and launching the remodeling process (Miller et al., 1987). They participate in initiating the bone formation by osteoblast through digesting the debris of the resorption phase (Everts et al., 2002). Due to their location, they inhibit the direct contact between osteoclasts and bone matrix in none remodeling site (Florencio-Silva et al., 2015).

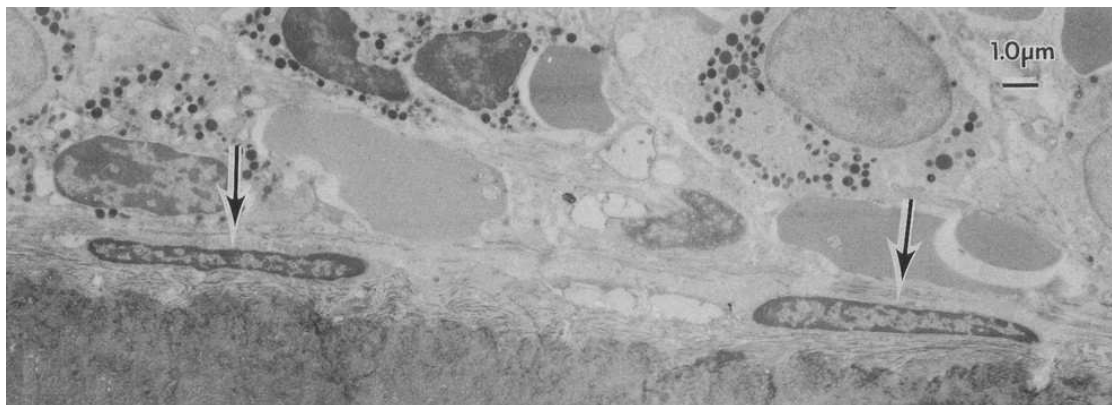


Figure 2.5. A micrograph shows several human bone-lining cells (arrows) alongside the endosteal bone surface.

Source (Miller et al., 1987)

Osteoclasts

They are phagocytic multinucleated huge cells that are derived from the hematopoietic precursor cells under the impact of various agents (Bar-Shavit, 2007). The hematopoietic precursor cells are also the source of originating monocytes and macrophages cells. The osteoclasts are known for their function as the bone eater cells, and they are found in the remodeling sites. Their lifespan is two weeks in general (Parfitt, 1994).

Their main function of bone resorption is to eliminate the old, dead, or damaged bone so the new bone formation could take place (Figure 2.6). The osteoclasts have a very important role in maintaining the mineral homeostasis hence they free minerals while degrading the bone matrix (Suda et al., 1997).

However, osteoclasts differentiation and activation are influenced by several mediators secreted by immune cells or another bone cells such as M-CSF, RANKL, IL-1, IL-7, TGF-beta, and TNF-alpha (Mori et al., 2013). Clues indicate that osteoclasts in return have roles in stimulating osteoblasts action (Sims et al., 2015), and activating immune cells such as T-cells through secreting special cytokines (Boyce, 2013; Boyce et al., 2009, 2012; Charles et al., 2014; Teti, 2013). It should be noted that not every deficiency of bone mass is a consequence of the extravagant activity of the osteoclasts, but it could result from the lack of harmony between osteoclasts and osteoblasts activities.

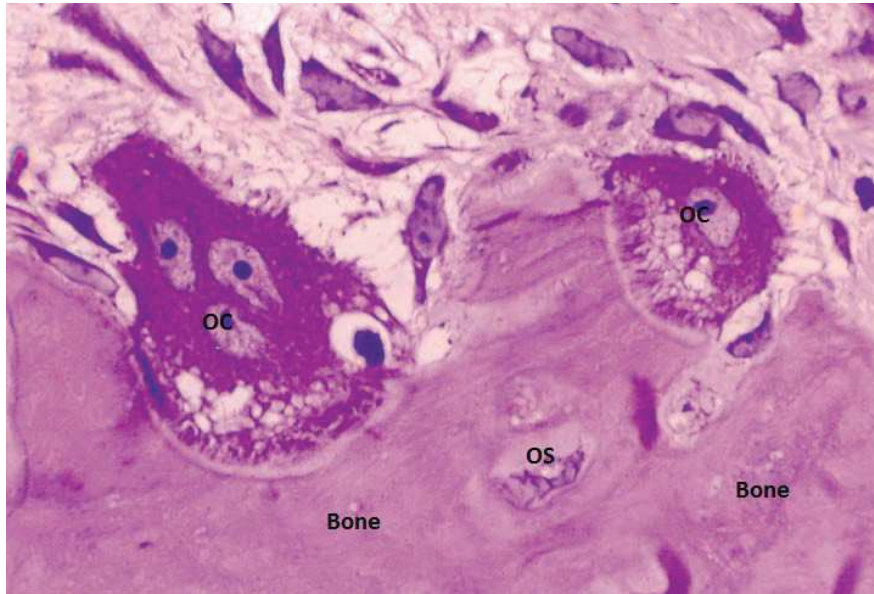


Figure 2.6. A microscopic photo shows two active osteoclasts cells (OC) while resorbing the bone matrix. An osteocyte (OS) with its lacunae is also distinguished. Source (Mescher 2013)

2.1.3. Bone Remodeling Process

Even after its growth, the skeleton undergoes a permanent regeneration process called bone remodeling process, whereby the bones replace the old tissue with new ones (Hadjidakis et al., 2006). This process is also essential to maintain the balance of minerals in the blood and bone matrix and to respond to external stress. In addition, it is the basis for bone repair after injury (Rucci, 2008).

This process is performed by the specialized bone cells, osteoclasts and osteoblasts, which work side by side harmoniously within groups called basic multicellular unit (BMU) (Zhou et al., 2010). When a site needs to go through remodeling, these units start their mission and move forward their aim destination. These units have a longer lifespan than their component cells; thus a continuous supply of new cells is needed to terminate the site remodeling (Table 2.1) (Manolagas, 2000). Accordingly, the number of cells in BMU and their lifespan are essential keys to evaluate the unit progress. The spatial and temporal correlation between osteoclasts and osteoblasts are well organized (Teti, 2013). The remodeling process starts by osteoclasts clinging to the tissue and secreting enzymes to acidify the

attached site of the matrix and result in decalcifying it, and consequently remove it (Figure 2.7). After that, the osteoclasts leave the corroded area and replaced by the osteoblasts, which start the phase of formation by restoring the site through emitting osteoid. This osteoid, at last, is mineralized to form the new bone (Raggatt et al., 2010).

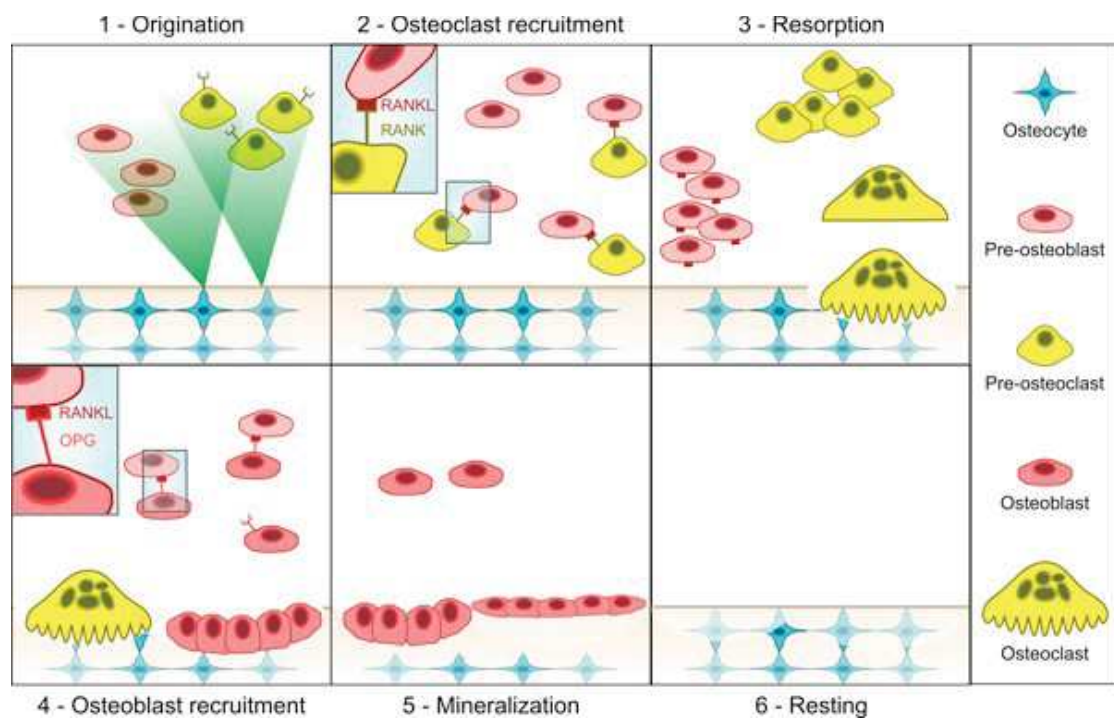


Figure 2.7. Steps of the bone remodeling process: 1) under the influence of stimulating signals from osteocytes, the pre-osteoclasts and pre-osteoblasts are activated. 2) Pre-osteoclasts extend RANK receptors that bind to pre-osteoblasts RANKL signals. 3) RANK/RANKL coupling persuade pre-osteoclasts proliferation and merging to found active mature osteoclasts that start degrading the site. 4) Mature osteoblasts express OPG receptor through which they bind to RANKL and start bone formation. 5) The newly formed osteoid is mineralized. 6) Finally, the primary state is rehabilitated. Source (Liò et al., 2012)

Table 2.1. Vitale data of bone basic multicellular unit (BMU). From (Parfitt, 1994)

- The lifespan of BMU ~6–9 months

- The speed ~25 $\mu\text{m}/\text{day}$

- The bone volume replaced by a single BMU ~0.025 mm^3

- The lifespan of osteoclasts ~2 weeks

- The lifespan of osteoblasts (active) ~3 months

- The interval between successive remodeling events at the same location ~2–5 years.

- The rate of turnover of the whole skeleton ~10% per year

The bone-remodeling process is controlled by the very important RANK/RANKL/OPG signaling system (Boyce et al., 2008). When a site of bone has to go through remodeling, the osteocytes send signals to bone lining cells, which in their turn pull away from the surface of the site. In the same time, they stimulate pre-osteoblasts to express RANKL signal that binds to RANK receptors on pre-osteoblasts (Jilka, 2003). This coupling between RANK/RANKL prompt the pre-osteoclasts to proliferate, combine, and generate active osteoclasts that in turn will start their resorption role (Eriksen, 2010). After the termination of the resorption phase, other cells will remove the debris, and the formation phase will begin by the maturity of pre-osteoblasts to osteoblasts which the latter express osteoprotegerin (OPG) receptors on their surfaces and form the osteoid layer (Sims et al., 2015). OPG is in competition with RANK to bind to RANKL in order to inhibit osteoclasts activation and imbalanced bone resorption (Sims et al., 2008, 2014). In healthy state, the BMU number in addition to the rate of resorption phase and formation phase are constant, while during bone infections, the bacteria affect the balance in this process and their signals by increasing RANKL/OPG ratio and inhibiting osteoblasts functions (Figure 2.8) (Cassat et al., 2013; Josse et al., 2015; Raisz, 1999).

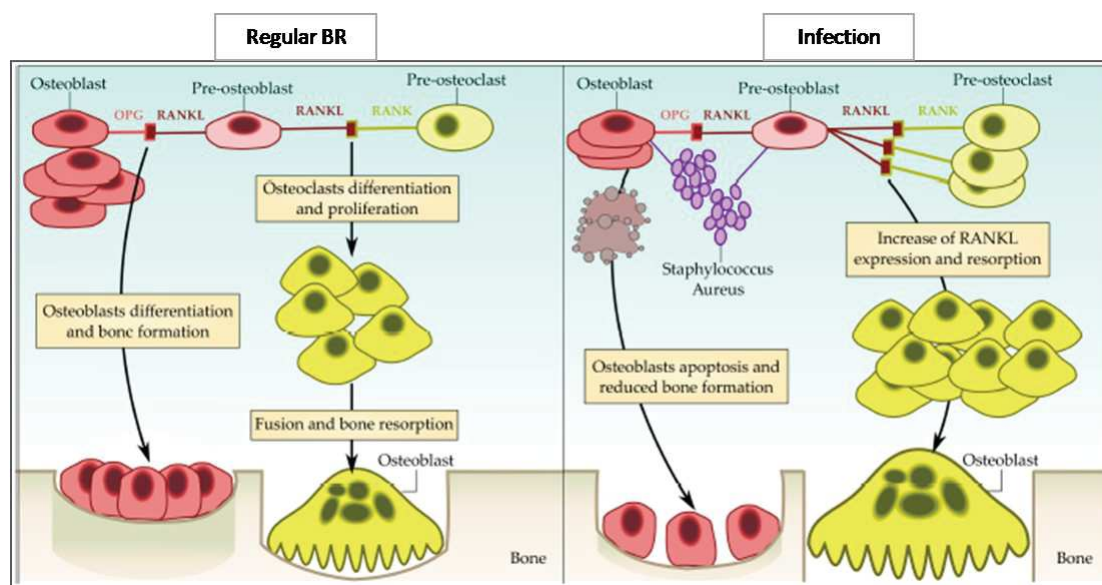


Figure 2.8. Bacteria effects on bone remodeling. During infections, the presence of bacteria stimulates osteoclasts proliferation and activity and increases osteoblasts apoptosis.

Source (Merelli, 2013)

2.2. Immune System

2.2.1. The Innate and Adaptive Immune Response

The immune system is a complex system that has a dynamic interactions network of cells. These cells communicate with each other through signals and receptors to apply a variety of mechanisms to encounter the infections. The immune system is classified into two subsystems: the innate immune system and the adaptive immune system. The innate immunity shoulder the first response against the invaders through their specialized phagocytes cells which have pre-existed defense mechanisms without the need for prior exposure to the pathogens (Alberts et al., 2002). The innate immune cells are capable to 1) detect and distinguish instantly the determinants of microorganisms from the self-ones, 2) hold effective humoral and cellular techniques which will exterminate these microorganisms, and 3) activate and regulate the adaptive immune response to attack the survival pathogens (Charles A Janeway et al., 2001). This class of immune response has the same degree of expansion for responding to infection regardless of the type of infection or how many

times it faces that infection (Beutler, 2004). In contrast, the acquired immunity is improved with the repeated encounter of the pathogen and its cells have a memory that provides them with effective destruction mechanisms in the next exposure (Delves et al., 2000).

The crucial role of the innate immune response is evident during the early hours of facing the pathogen, especially in the absence of the adaptive immunity. This latter can take several days and up to one week to initiate and become developed especially in the case of first exposure. In contrast, it takes only 10 generations for a bacterium to grow into a colony of 1024 cells, that means a lot of bacteria in less than 12 hours for *S.aureus* which divide very quickly (about every 40 minutes) in optimal laboratory conditions (Alberts et al., 2002; Pray, 2008). Thus, the body relies on its non-specific defense in the first hours of exposure to pathogenic bacteria to combat infection.

When recognizing the bacteria, the innate immune components immediately start the inflammatory response through macrophages, monocytes, neutrophils, and endothelial cells that are triggered by microbial products through receptors on their surfaces (Fearon et al., 1996). In turn, these cells take their action by releasing stimulating pro-inflammatory cytokines, such as interleukin-1 (IL-1), IL-6, IL-12 and tumor necrosis factor (TNF- α), to induce the intense stage response, promote the antibacterial function of macrophages and other innate immune cells, and boost the evolution of T cells (Vasselon et al., 2002).

The adaptive immune cells namely: the antigen-specific T and B cells, have receptors too and are activated when these receptors attach to antigen (Medzhitov et al., 1997). The structure of receptors and the type of signals or antigen, or in other words the way of pathogen recognition, in both of innate and adaptive immune cells represent an essential difference between those two classes of immunity (Delves et al., 2000). It is worth mentioning that the innate and adaptive immune system work side by side, and despite the effectiveness and vital role of the adaptive immune system, it cannot do so without the innate immune cells which present the antigens and release the cytokines (Beutler, 2004; Fearon, 1999).

2.2.2. Innate Immune Cells

There are a variety of specialized innate immune cells with different competencies, and which all derived from myeloid cells (Jr et al., 2001). They contain mononuclear phagocytes that include macrophages, derived monocytes, and dendritic cells, and polymorphonuclear phagocytes which contain neutrophils, basophils, and eosinophils. Macrophage, monocytes, and neutrophils are the main cells that responsible for engulfing the pathogen beside regulating the immune response (Savina et al., 2007). The other cells types are specialized in allergic and antigen presentation (Stone et al., 2010).

Macrophages

Recent evidence shows that tissue-resident macrophages are evolved and found prenatal, and they re-proliferate locally with little participation of monocytes (Figure 2.9) (Hashimoto et al., 2013; Mass et al., 2016; Patel et al., 2017; Yona et al., 2013a). Although they do not represent the most abundant phagocytes in the body, they are spread throughout the body tissue to be close and in a state of readiness to address any pathogen entering any site (Davies et al., 2013). The lifespan of macrophage is long that could range from days up to months (Parihar et al., 2010; Parwaresch et al., 1984).

Resident macrophages have several forms depending on the tissue (Kierdorf et al., 2015). Even though macrophages have a high ability to engulf and destroy the bacteria, their substantial function thought to be the regulation and management of following response steps (Gordon et al., 2017). They call up other phagocytes cells using their secreting signals, and they launch the adaptive immune response via presenting the pathogen antigen to T cells. Another function is subjected to macrophage which is cleaning the site by engulfing and digesting cells' debris in the inflammation site or cells go through apoptosis (Pinchuk, 2001). Macrophages keep controlling the site of inflammation for 1-2 days later. Macrophages have the ability to repopulate themselves locally (Ginhoux et al., 2014).

Monocytes

Monocytes are originated from bone marrow and then located in the bloodstream to begin performing their roles in tissue homeostasis and in regulating the initiation and recruitment of immune cells in a case of infection (Furth et al., 1968). Monocytes are responsible for refilling the tissue macrophage during infection since they migrate to the site of infection very quickly and differentiate to monocyte-derived-macrophage (Figure 2.9) (Ginhoux et al., 2014). Using in vivo deuterium labeling method, A. Patel et al. showed that classical monocytes have a lifespan of 24 hours in circulation in the steady state (Patel et al., 2017).

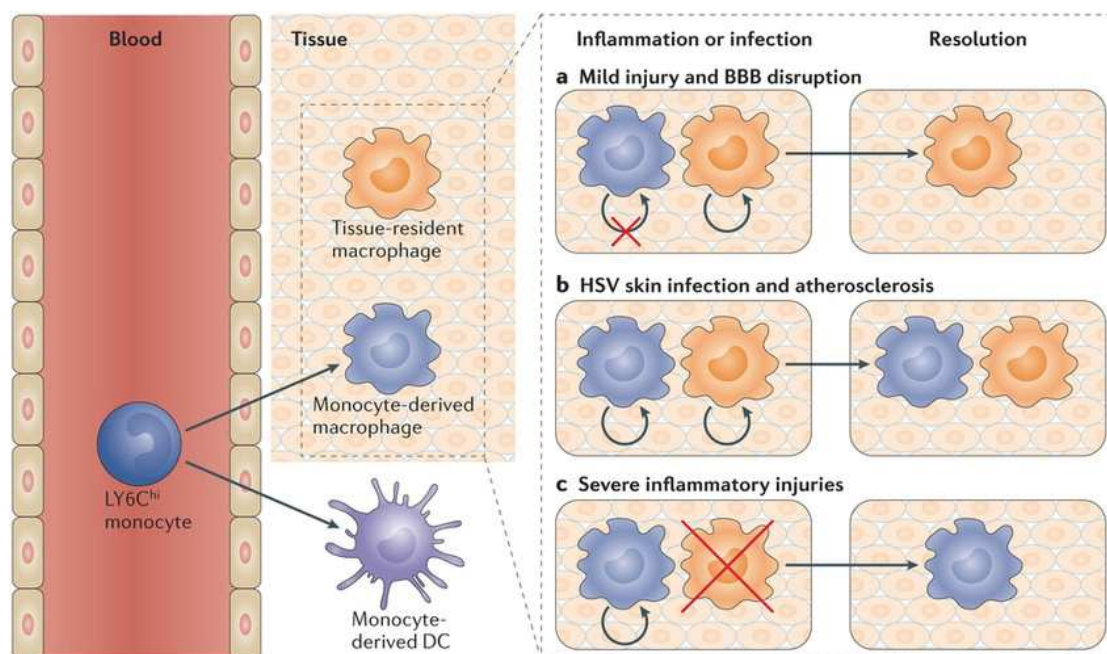


Figure 2.9. The dynamics of prenatal tissue-resident macrophage and monocyte-derived macrophage. In the infection, the monocyte migrates from blood circulation into the infected tissue to differentiate either to the monocyte-derived dendritic cell (DC) or to monocyte-derived macrophage (MDM) to increase their population. Even though the MDM will eventually boost tissue-resident macrophage population to getting rid of the infection, the nature and level of their contribution will be determined upon the type of infection and the volume of tissue-resident macrophage' damage. In the figure, several cases of infection are shown wherein (a) little MDM are needed, and the embryonic-derived macrophages are repopulating locally, in (b) both type are needed and proliferate, in (c) the tissue-resident macrophages are damaged what need to MDM to refill the macrophage population.

Source (Ginhoux et al., 2014)

Neutrophils

Neutrophils have a very important role in constraint the infection since they are highly efficient in eliminating the bacteria using different means (Figure 2.10) (Witko-Sarsat et al., 2000). They are regenerated in bone marrow under the stimulation of G-CSF cytokine with an average of 10^{11} cells/day what make them the most numerous leukocytes in blood, 5000 cells/mm^3 in normal case and it could increases 5-10 times in acute infection (Furze and Rankin, 2008; Summers et al., 2010). In spite of what is known of the short lifespan of the neutrophils (6-8 hours), recent studies show that they have a longer lifespan (5.4 days), what expand the insight of the function of neutrophils especially in mediating the activation of adaptive immune cells (Bekkering, 2013; Pillay et al., 2010; Rankin, 2010; Simon et al., 2010).



Figure 2.10. Electron micrograph of a neutrophil during the process of phagocytosing a bacterium, which is covered by antibodies and in the division phase.

Source (Williams et al., 1972)

2.2.3. Cytokines and an Insight into TGF-beta

Cytokines and their receptors represent the communication network between different cells, and not only immune cells (Van der Meide et al., 1996). One cytokine is secreted by more than several cells' type and has many activities which almost alike other cytokine functions (Cohen et al., 1996; Pinchuk, 2001). In addition, the cytokines have the ability to perform as a growth factor by inducing cells' reproduction and proliferation (Mousa et al., 2013; Renner et al., 2004). According to their functionality, the cytokines could be classified to three categories: mediators and stimulators for innate immune cells, for adaptive immune cells, or for blood stem cells (Turner et al., 2014).

Cytokines and their receptors occupy a big area of research to study the immune response during infection (Cobelli et al., 2011; Evans et al., 1998; Yoshii et al., 2002). One of the important cytokine in innate immune response is TGF- β that has an important function in modulating macrophages and monocytes recruitment (Bogdan et al., 1993; Kehrl, 1991). TGF- β is one of the important cytokines that released by activated macrophages and T helper cells in case of infection (Reed, 1999). It has shown that it has a double and contradictory effect on innate immunity (Lee et al., 2011). It stimulates the proliferation and recruitment of monocytes to the site of infection which in turn amplify and enhance the innate immune response (Ashcroft, 1999a). On the other side, it prohibits the macrophages activation which discouraged the innate response (Gong et al., 2012).

2.2.4. Different Stages of Innate Immune Response

When the bacteria success in breakthrough the host tissue, three types of innate immune cells reach the site of infection successively and engulf the pathogen: resident macrophages, monocyte-derived macrophages (MDMs), and neutrophils (Cheatle et al., 2013; Galli et al., 2011; Rochford et al., 2016; Silva, 2011). Resident Macrophages are the first line of cells defense that act against the invaders, and they stimulate and recruit rapidly other innate immune cells (Kim et al., 2015). When the bacterial count grows, macrophages demand and recruit neutrophils to the site through emitting pro-inflammatory cytokines including Interleukin-1 (IL-1) and Tumor necrosis factor alpha (TNF- α) (Kaufmann et al., 2016). The neutrophils reach the site

of infection 4-8 hours, and they increase rapidly to become the leader cell in the site (Strydom et al., 2013). A quick decrease in neutrophil population pursues their peak while in parallel derived monocytes arrive smoothly in 48 h after the virulence (Kaplanski et al., 2003a). The neutrophils which are faced with bacteria go through apoptosis what contribute to inflammation diminution and tissue healing (DeLeo, 2004; Summers et al., 2010). The monocytes activation is stimulated by some cytokines such as IL-6 and MCP-1, which are produced by macrophages and other cells (Cassatella, 1995; Deshmane et al., 2009; Kaplanski et al., 2003a).

2.3. Bacteria

2.3.1. Bacterial Growth Style and Characteristics

The acuity of bone infections is influenced by several factors, some of them are related to the bacteria themselves such as their virulence, colonization capability, pathogen type, and localization (Kahn et al., 1973). Bone and joint infections are mainly caused by bacteria called *Staphylococcus aureus* within 70% of infected cases (Grammatico-Guillon et al., 2012). One of the essential qualities of bacteria is the growth pattern where their reproduction process follows the binary fission function. While in some cases the daughter cells separate after division, in other cases they remain linked and divide into different planes as in *Staphylococcus*, which divide into random planes making a grapelike bunch (I. Edward Alcamo et al., 2009).

A typical in-vitro growth curve of the bacteria is represented as in (Figure 2.11), where it is divided into three phases (Harris et al., 2003). The first phase is the lag phase, which lasts a few hours, during which the bacteria are growing in size and keeping energy. The second phase is the log phase, through which the bacterial cells divide rapidly and increase exponentially. Following that the stationary phase, where the old cells die or spread to another site in the same rate as new cells division, and no increasing in population has happened.

The growth rate and generation time are determinant parameters to define the spread of bacteria. These parameters are dependent on the environment and microorganism type (POWELL, 1956). In a controlled culture condition, the bacterial count, growth rate, and generation time in the exponential phase are defined by the following equations (2.1-3) (Maier, 2009):

$$dX/dt = \mu X \quad (\text{Eq. 2.1})$$

$$X = 2^n X_0 \quad (\text{Eq. 2.1})$$

$$\mu = (\ln X - \ln X_0) / t \quad (\text{Eq. 2.2})$$

Where

X : The number of cells after n generations

X_0 : Cells initial number

n : Generations number

t : generation time

μ : Growth rate

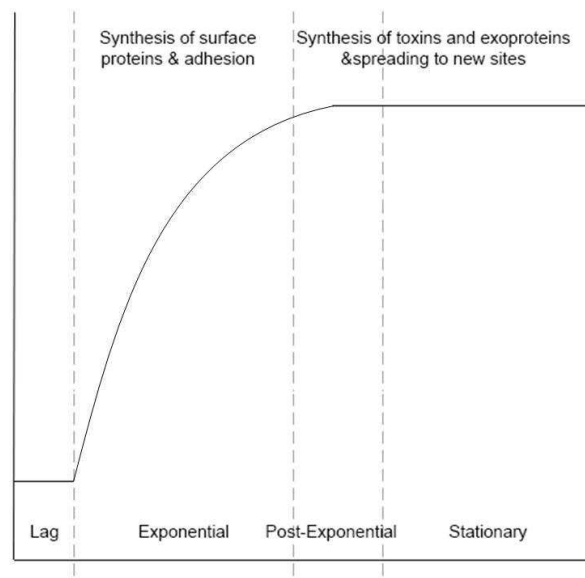


Figure 2.11. Ideal growth curve of bacteria with time. During the lag phase, the bacteria initiate the infection and get prepared to exponential phase, where they divide at a constant rate and make proteins that promote multiplying, growing and attaching to the host cells. In the stationary phase, the bacteria break away the localized infection to a new site.

Source (Harris et al., 2003)

However, the in-vivo bacterial growth is influenced by several factors that modulate the doubling time and the bacterial behavior such as the host condition and the immune defense (M R W Brown et al., 1985). Although the environment state such as pH, oxygen, and nutrition have a critical effect on bacterial growth, it is hard to define their impacts in the human body as same as an in-vitro culture (Smith, 1990, 1998, 2000; Walkup et al., 2015).

Bone and joint infections are harmful to the bone resulting in debilitated bones correlated with a gradual bone loss. Until present, complete and clear comprehension of the mechanisms of losing bone during this disease is still missing (Marriott, 2013; Nair et al., 1996). Several studies present insights into important interactions to understand these mechanisms. Claro et al. proposed that the *S. aureus* protein-A (SpA) attaches straight to osteoblasts cells what lead to stimulating the latter apoptosis, prohibit their reproduction, prevent ECM mineralization, and induce RANKL to increase the activation of bone degradation (Claro et al., 2011). Other experimental studies investigated the role of osteoblasts in the infection (Bost et al., 1999; Evans et al., 1998; Fullilove et al., 2000; Gillespie et al., 1990; Marriott et al., 2004). They state that osteoblasts release cytokines such as MCP-1, IL-6, and IL-12, which is normally expressed by immune cells, to stimulate an immune response. In turn, this response can contribute either in directing immune cells reaction or in rising severe inflammatory damage.

2.3.2. *Staphylococcus aureus* Resistance Mechanisms

Staphylococcus aureus (*S. aureus*) is the most demanding pathogens of BJI associated with disease chronicity development and frequent relapses (Tong et al., 2015). *S. aureus* BJIs are correlated with high treatment failure rate in both *S. aureus* methicillin-resistant and *S. aureus* methicillin-susceptible cases. The chronicity of BJI is estimated to reach 10-30% in hematogenous, and 1-20% in device associated infection (Marais et al., 2013; Valour et al., 2014). *S. aureus* BJIs can persist in the host tissue and reactivate months or years later (Brady et al., 2008; Panteli et al., 2016; Walter et al., 2012). *S. aureus* has several qualities that facilitate its function as the most frequent bacteria in BJI. It has the capability to cohere to bone extracellular matrix and biomaterial using their own adhesion proteins (Harris et al., 2003). It secretes specific toxins and enzymes that facilitate local bone destruction and

spreading between host cells (Lowy, 2000; Nair et al., 1995). *S. aureus* has several mechanisms to adapt to the human environment. Two principal bacterial mechanisms have been demonstrated to explain the persistence of *S. aureus* and the chronicization of BJI. These factors are biofilms formation, and intraosteoblastic persistence, correlated with bacterial phenotype transformation to small-colony variants (SCV) (Bjarnsholt, 2013; Ciampolini et al., 2000; Ellington et al., 2006; Gbejuade et al., 2015; Josse et al., 2015; Marais et al., 2013; Peeters et al., 2016; Valour et al., 2013). Both of these factors enable the bacteria to overcome the immune defense and become resistant to antibiotic treatment.

Biofilms are defined as surface-associated bacterial communities, which are embedded within an extracellular polymeric substance (Hall-Stoodley et al., 2009). The bacteria within biofilms introduce coordinated behaviors and heterogeneous functions to facilitate their formation and antibiotic resistance. These include nutritional starvation, high cell density, virulence suppression, and coordinated cell-cell communication behavior (Fux et al., 2005; Hall-Stoodley et al., 2004; Kong et al., 2018). In device-associated infections, other non-bacterial factors also play a role in bacterial adhesion and biofilms development. These include material surface properties, such as implant size, surface roughness, chemical composition, hydrophobicity, and material charge (Ribeiro et al., 2012).

S. aureus is able to incorporate within the osteoblasts and to grow intracellularly (Löffler et al., 2014; Tuchscher et al., 2016). The intracellular *S. aureus* demonstrates severe resistance to treatment if it has been formed for more than 12 hours, due to the structure change (Ellington et al., 2006). It also shows the ability to reactivate after the osteoblasts death and infect other osteoblasts (Dusane et al., 2018). When the bacteria form SCV, which is an indication to phenotypical adaptation, they display decreasing virulence, increasing immune defense escape, and antibiotic resistance (Trouillet-Assant et al., 2016; Tuchscher et al., 2010, 2016).

S. aureus has serious effects on destroying the bone by preventing osteoblasts activities and increasing RANKL expression (Sanchez et al., 2013). It directly influences the coupled activity of osteoblasts and osteoclasts (Marriott, 2013). Also, it causes an increase in the osteoblasts apoptosis and osteogenic differentiation (Sanchez et al., 2013).

3. Modeling Biological System Approaches

Understanding the behavior of a complex multi-scale biological system needs to use an efficient knowledge representation means. The computational modeling techniques represent an effective tool to integrate data from different sources and simulate the system behavior to test several existing patterns or even propose new ones. Choosing the best modeling technique is depending on the need of the investigators and on the capability of the technique to encompass different properties of the system at the purposed scale, here the spatiotemporal cellular and molecular mechanisms and interactions.

This chapter summarizes the limitation of the traditional (animal models) approach used for modeling biological systems. Then, it provides details about the different characteristics and scales of the biological systems that influence the modeling approach. It follows by a description of the different modeling approaches that could be used when shifting to model and simulate the biological systems on the cellular level. Finally, it highlights the agent-based modeling approach as it is the one we have adopted for this research.

3.1. Traditional Modeling Approach (Animal Models)

Studying the BJI through investigating its pathogenesis and treatment was the goal of abundant created animal models (Funao et al., 2012; Gaudin et al., 2011; Horst et al., 2012; Inzana et al., 2015; Kim et al., 2014; Li et al., 2008; de Mesy Bentley et al., 2017). These models have been designed to investigate the

effectiveness of new antibiotic treatment (Gaudin et al., 2011b), the diffusion of antibiotic into biofilms BJI (Inzana et al., 2015), or the antibiotic activity on intracellular bacteria (Valour et al., 2015).

Although these animal models provide an integral important part in the knowledge of BJI, several challenges and limitations accompany them (Reizner et al., 2014). There are several critical issues to take in the account when choosing the model depending on the explored disease type or stage since no single animal model could comprise all aspects of BJI (Patel et al., 2009). The small animals (rabbit, rat) are easy to be handled and are cost-effective, but they are limited by the incapacity to tolerate the antibiotic treatment and the numerous procedures. In contrast, the large animals (sheep, dogs) have more ability to sustain the antibiotic doses and multiple procedures, but they are limited by their availability, cost, and ability to be handled (Patel et al., 2009). Other important factors that influence the model selection are those related to the pathogen or the antibiotic such as the bacteria inoculum size, the location of the infection, the antibiotic family, concentration and diffusion (Tatara et al., 2015).

The physiological and anatomical variance in the infection progress or recovery between the model and human impose limitations in recapitulating the human conditions and further validating the model. For example, the infection initiation in an animal such as rabbit needs a high level of inoculum of bacteria (10^6 CFU), while the infection in human needs much less inoculum comparatively (Mader, 1985). In addition, the effects of the antibiotic on the animal are relatively different from human. For instance, rabbits are oversensitive to the toxicity of a broad-spectrum long-term treatment which leads to death (Greek et al., 2013). Moreover, there is no animal model could handle all the stages of the infection since the infection could span over a long duration (An et al., 2006).

These limitations besides the difficulties of interpreting results coming from the interaction between the host and pathogen promote the writers in (Lebeaux et al., 2013) to highlight the importance of the computational modeling in improving the biological system understanding. The need for facilitating the exploration and the prediction of system behavior on different scales make the computational modeling approaches a powerful alternative approach to the wet lab.

3.2. Characteristics of Complex Biological Systems

Human biological systems and diseases encompass different components which interplay with one another to develop complex and unforeseen attitudes (Cheema et al., 2016). Such systems have several characteristics to be taken in the account when choosing the modeling technique (Chiacchio et al., 2014; Gatti, M et al., 2007; Szallasi et al., 2006). These characteristics include the unpredictable behaviors, since they follow non-linear routines, in which a small disruption may have a big, comparable, or no effect on the system behavior. The relationships between the components are characterized by feedback loops in which the impact of a component's behavior influences the component itself. Moreover, the biological system is dynamic in that it is constantly changing over time. It is also characterized by having a memory, since previous system situations have impacts on the current situation. The biological system compounds of subsystems, which in their turns are built of several nested components. In addition, the biological system is a self-adaptive system, which reorganizes its components internally over time, space and function to enhance its attitude. In biological systems, the behavior patterns of a tissue emergent from the behaviors and interactions inter and intra cells (Alexander, 2013). These patterns have a contribution in the information about both the physiological and pathological process.

Another important characteristic of biological systems is the multi-scale property, which is clearly shown in the several functional structures over both temporal and spatial sphere that all results in the development, growth, and functionality of the organisms (Ji et al., 2017). The spatial multi-scales of the biological system ranges from the molecular scale to the organs or organisms scales (Figure 3.1) (Walpole et al., 2013).

3.3. Computational Modeling of Complex Biological Systems

3.3.1. Strength of Computational Modeling Approach

Studying and understanding the complex biological system through the dynamics and interactions of cells and signals, rather than studying these cells as isolated tissue in the experiments, represent a leap in shifting from this first basic knowledge to system-level understanding (Kitano, 2002a). In general, computational

biology aims at two different aspects (Kitano, 2002b). First, retrieving knowledge to take out the potential patterns from the pool of experimental data and use heuristics-based prediction. Second, conducting simulation-based analyses that make a prediction of the system dynamics upon in-silico experiments, and validating the result using experimental knowledge and further examination by in-vivo researches. In other words, it is essential to recognize the different resulting patterns of system behavior, why such patterns arise, and how to solve and control them (Evora et al., 2015).

The presence of the multiple levels of arrangement in the system puts up serious challenges in front of the information that produced from a certain study at a specific level to be applied and translated to a phenomenon that appeared in a higher level (Eissing et al., 2011). This interest in knowledge translation over multiple scales belongs to the consequences of connecting between the researches of the therapeutic objectives at cellular and molecular levels and their influences in tissue or organ levels. Computational modeling approaches are greatly fitting to recognize the link between the different scale of the biological system from molecular scale up to organ scale, using single or combined modeling methods (Figure 3.1) (Ghosh et al., 2011; Hambli, 2014; Pivonka et al., 2012).

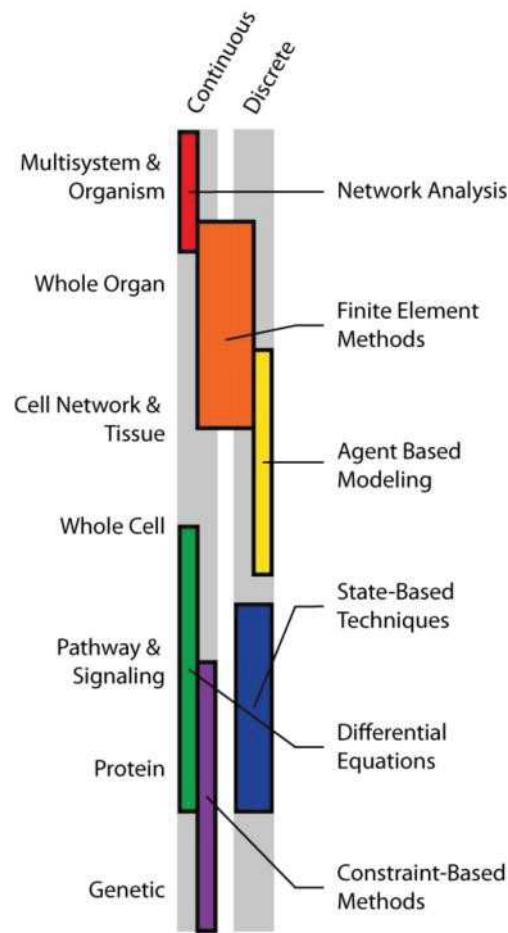


Figure 3.1. An abstract map of computational modeling methods classified according to the most fitting biological spatial scale within discrete and continuous classes.
Source (Walpole et al., 2013)

3.3.2. Computational Modeling Approaches

For a deeper understanding of complex biological systems, researchers have tended to model these systems using different mathematical and computational modeling approaches, which globally are classified into two main classes, the top-down approach and the bottom-up approach (Bianca et al., 2012; Borshchev et al., 2004; Chiacchio et al., 2014). The top-down approach aims at approximating the behaviors of the variable in the macroscopic level and modeling population instead of single entities. The most known methods of this class are the models based on the ordinary differential equations (ODE), the partial differential equations (PDE), and the stochastic differential equations (SDE), which have the ability to model a large

number of entities. Although the PDE take into consideration the topology and the SDE add some stochastic terms, all of these methods disregard the interactions of the individuals. Models built on these methods that address complex systems face the problem of difficulty along with approximations that cannot be ignored.

Using the equation-based modeling approach (EBM), two important models are proposed in the literature that study the bone mechanisms and they represent the basis of many following works that handle bone remodeling process in their researches using the EBM approach: the model of Komarova et al. and the model of Pivonka et al (Komarova, 2005; Komarova et al., 2003; Pivonka et al., 2008, 2010). These temporal mathematical models investigated the dynamics of bone cells and signals during the bone remodeling process.

The bottom-up approach deals with the individual agent and models the behaviors and interactions of the entities in the microscopic level. In this approach, the overall behavior of the system results from the accumulation of the local attitudes and interactions of the concerned agents. The most used methods of this approach are the agent-based models (ABM) and the cellular automata (CA) (Alemani et al., 2012; Motta et al., 2013; Pappalardo et al., 2012, 2013). By adopting these methods, the system can be characterized more accurately, through passing the negativity of large approximations in the top-down methods. That is because the bottom-up approach is already containing the stochastic feature and the spatial distribution consideration inside. However, these methods require high computational attempt since the agents are processed individually. However, these methods require more computational efforts for the analytical study because of their lack of strong mathematical tools behind.

3.4. Agent-Based Modeling (ABM) Approach

3.4.1. ABM in Modeling Biological System

The agent-based modeling (ABM) approach is a member of the discrete mathematical methods in which the global behavior of the system results from the behavior and interactions in entities level (Shi et al., 2014). The different features of ABM approach make it well fitting in biological system studies, especially when the goal is to verify the predefined mechanisms of the system rather than searching a

pattern from an existing data (An et al., 2009).

The built-in randomness and the naturally taking parallel mechanisms outcomes features make ABM display the hidden and multi-scale behavior of the biological system (Figure 3.2) (Folcik et al., 2007; Politopoulos, 2007). The ABM models could reproduce the complex behavior of the system with heterogeneous components and diverse essential rules, even if they are simple and not complete (Alexander, 2013; Hammond, 2015). The ABM also has an intuitive paradigm that considers the individual character, decision and propensity.

Another important feature of ABM is the capability to encompass the spatial organization and position of cells that have important influences on their behavior, proliferation, expansion, and signal secretion within a specific interval (Gilbert, 2008). As examples of this feature in the intra-cellular level, the *molecular gradients* that control intra-cellular signaling, and the *sub-cellular localization* that lead to different patterns of signaling pathways (Peter et al., 2012). In the cellular level, the spatial property of a process like *chemotaxis* directs the cell movement towards the high concentration chemotaxis or specific substances such as nutrients (Kholodenko, 2006). In addition, the cellular spatial distribution determines the scope of neighbors with whom they will interact (Fadiel et al., 2008).

The agent-based modeling approach is a promising tool that offers a peer in-silico experimental environment which could introduce a plausible dynamic representation of the achieved mechanistic knowledge from the literature or the laboratory experiments to examine the implicit hypotheses. It aims at getting more perception of the system behavior to produce and identify new behaviors and patterns through implementing the model using the essential rules and function. These new patterns could be further investigated as new hypotheses "generating hypotheses", or used as a means in enhancing the therapeutic design.

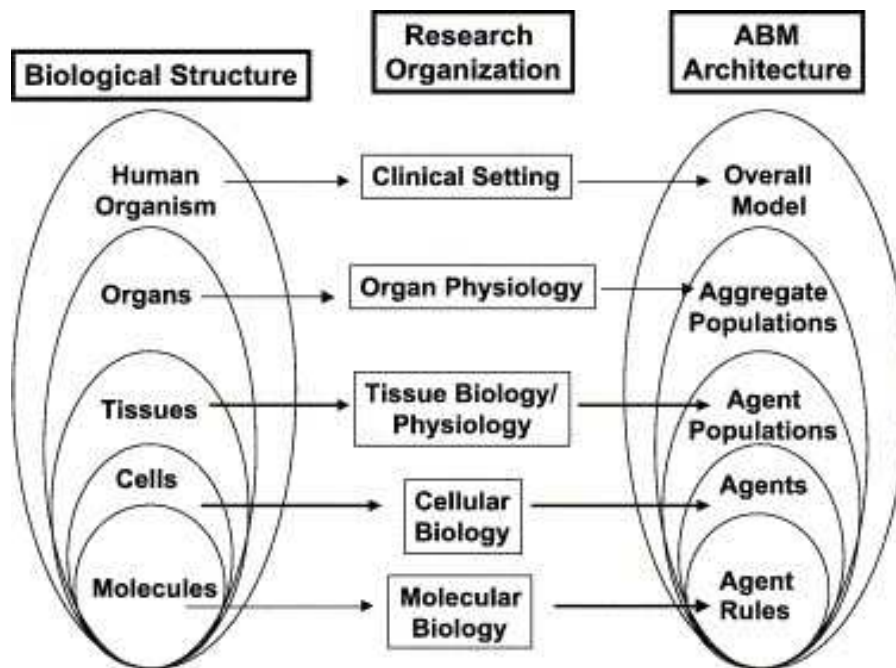


Figure 3.2. Mapping of the ABM approach to the research organization at each biological level of representation in multi-scale biological system structure, where the behavior in the upper level results from the sum of the behaviors at the bottom level. The proposed ABM model in this research of BJI is using the cellular level while the signaling mechanisms define the rule of these cells.

Source (An, 2006)

The advantages mentioned above of the ABM technique along with the improvement in computing processing power encouraged researchers to build numerous biomedical applications to investigate various subjects using the ABM approach. It has been used in investigating the intracellular pathways in the molecular levels in systems biology where it achieved advances especially with the ability of spatial characterization within ABM (An, 2009; Pogson et al., 2006, 2008; Ridgway et al., 2008).

However, ABM applications that consider cell-level as the principal level of representation are the most evident in modeling biological systems and the most common in the preliminary ABM biomedical applications (An, 2008; Hunt et al., 2006). That is because they could supply a connection between the laboratory experimental acquired information and the organization of ABM. Such applications either studied the dynamics of a disease process, or the changes in the spatial

physiology and function of tissues under pathological conditions, such as tumor growth, wound healing, and morphogenesis (An, 2001; Bauer et al., 2009; Engelberg et al., 2008; Folcik et al., 2007; Gary An, 2012; Grant et al., 2006; Segovia-Juarez et al., 2004; Zhang et al., 2009). These applications consider cell-cell interactions and spatial properties supported by ABM.

ABM approach in different applications has also been combined with other modeling approaches to integrate the various features and the acquired knowledge from the different system level. Examples of these hybrid models are integrating the dynamic system approach using differential equations with agent-based modeling of cell level (Athale et al., 2006; Vodovotz et al., 2009), and incorporating the agent-based modeling with finite elements analysis (Chincisan, 2016; Zahedmanesh et al., 2012). On another hand, combining the experiments with agent-based modeling approach was the focus of (Thorne et al., 2007), to give realistic and explanatory knowledge about the biological system work. This combination takes place in a cycle of work steps showed in (Figure 3.3).

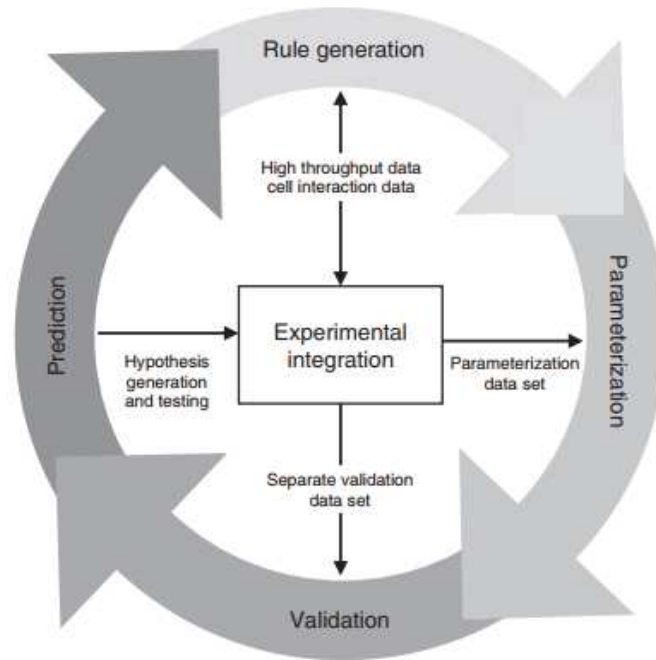


Figure 3.3. The cycle work of integrating the ABM model with experimental work, where first the rules of the agents in the ABM model and the interactions are obtained from the data in the literature or a parallel lab work such as in (Walker et al., 2006). Second, the parameterization step where the parameters should be set in a range that the model output matches the proper experimental data. Third, validating the ABM output using another group of experimental data that have not been used in the model building. The last step is the prediction from the validated models, which in turn fed the information of the experimental work and enhance the information used in building the model.

Source (Thorne et al., 2007).

3.4.2. Agent-Based Modeling Applications in Bone Biology and Infections

Several studies were done to investigate the cellular mechanisms of bone using the ABM approach in different contexts. For example, the work of (Ausk et al., 2006) investigated the role of osteocytes in stimulating bone remodeling process in response to mechanical strain using the agent-based modeling approach. Also in the research of (Schutte, 2012), an agent-based model was proposed to evaluate the dynamics of bone cells during the bone remodeling process. Another group studied the role of osteoclasts in bone resorption in BMU using a type of ABM, lattice-based model (Buenzli et al., 2012). A model of cell migration and proliferation in fracture healing using random-walk in lattice method was implemented by (Pérez et al., 2007).

A combination between shape calculus language and agent-based modeling was introduced by (Paoletti et al., 2012a) to study also the dynamics of the bone remodeling process.

In regards to our scope of interest, one group explored the dynamics of two types of bone cells: osteoclasts and osteoblasts, in addition to bone density in a comparison between the effect of bone infection and osteoporosis on bone remodeling process (Liò et al., 2012). The authors in this work proposed a hybrid mathematical modeling framework composed of a differential equation-based model that is based on the mentioned works of Komarova *et al.* and Pivonka *et al.* and probabilistic verification model of the stochastic system that used population-based approach. However, the model emerges from an equation-based approach which lacks the spatial distribution and micro-interactions of the components, and it ignores the interplay with the immune system.

In this study, we are focusing on how the cellular mechanisms and interactions influence the BJI development and give rise to the system-level behavior. In this thesis, we implemented the BJI system using ABM approach because of its inherent features and flexibility to investigate the system behavior as a result of the spatiotemporal dynamics and micro-scale interactions of BJI heterogeneous components (bone cells, bacteria, immune cells). The model proposed here is the first model of BJI that use the agent-based modeling technique and represent the infection as a comprehensive system that involves the interactions between the pathogen (bacteria) and the host tissue. This modeling framework has the power of facilitating the integration of information retrieved from different sources, and the application of different exploratory and predictive analyses methods.

3.4.3. Limitations of ABM approach

The features that were mentioned of the ABM approach make it a powerful technique to model the biological system. Nevertheless, it has several limitations (An et al., 2009). The accuracy and quality of the model are coupled with the reliability of the implicit hypotheses and the fineness of their implementation during the model building (Vodovotz et al., 2008). One of the challenges is that ABM models are built initially depending on some simplifying assumption because of the complexity (Xiang et al., 2005). However, the models should be refined in further work step where these

assumptions are re-examined. In addition, using the global analyses techniques to identify the relevance between the system behavior and the underlying agent's dynamics does not represent an easy task (Chiacchio et al., 2014). Another challenge is that the computing efficiency, however, handling a high number of agents and stochastic processes requires powerful computational processing effort (Bonabeau, 2002). Using parallel processors could be addressed to the large and complex ABMs; however, most exist agent-based modeling toolkits run on a single processor (Thorne et al., 2007).

4. Parameters Identification of BJI Model

Characterizing the system and its components in the cellular level represents the first step toward building the agent-based model of BJI. System characterization includes identifying the agent rules, interactions, and parameters. In Chapter 2, we presented the cellular and molecular attitudes of different components of BJI biological system during the first stage of infection; namely those cover the innate immune response, the bone remodeling cells and signals, and the bacteria development from the descriptive literature. These biological characteristics will be simplified and formulated as the agent rules in the next chapter.

In this chapter, we will identify the agent parameters, quantify their range of applicable values, and extract the different possible interactions between them from the literature using a systematic search. Different information in the literature exists handling the system components in different contexts. Identifying one component's parameter needed applying defined criteria, comparing these different studies and finding the relevant ones. This chapter provides the detailed methodology that we conducted to explore the literature and retrieve the needed information.

This characterization enhances our computational model by giving realistic values to the input parameters from the proven knowledge in the basic biology or experimental studies, by which the model could produce a meaningful prediction of the infection progression.

4.1. Bibliography Search Method

Relying on PubMed and ScienceDirect databases, we explored the related journal paper works from their inception to date, July 2017. In order to do that, we identified the search questions, the inclusion and the exclusion criteria for each investigated key term. We took benefits of quantitative and qualitative description in the related biology, physiology, computational and mathematical model along with the in-vivo and in-vitro experiments.

The queried terms are classified into four groups: bone cellular system group, the innate immune system group, bacterial system group, and the interactions between the components of these three systems group. In the following, we will itemize each group of terms with both inclusion and exclusion criteria.

1. For characterizing the bone cells, their lifespan, reproduction rate, main function: bone remodeling process, and the signals that involving in, we proposed the following questions and criteria:

a) The search questions were:

1. Osteoblast AND (half-life OR lifespan OR life-span OR (reproduc* rate))
2. Osteoclast* AND (half-life OR lifespan OR life-span OR (reproduc* rate))
3. Osteocyte* AND (half-life OR lifespan OR life-span OR (reproduc* rate) OR ratio OR density)
4. Bone remodeling process AND (signal* OR RANK OR RANKL OR OPG OR osteoprotegerin OR receptor activator of nuclear factor kappa*)

b) The inclusion criteria were human studies, articles on bone formation and bone resorption, bone biology and quantitative studies.

c) The exclusion criteria were excluding the article related to specific cases and diseases, the article related to genetic researches, pathway mediated, or specific treatment effects studies.

2. In order to identify the immune cells, quantify their lifespan, define the role of TGF signal on the immune response, and characterize the behavior of innate immune response, we proposed the following questions and criteria:

a) The search questions were:

1. Neutrophil* AND (half-life OR lifespan OR life-span OR (reproduc* rate))

2. Monocyte* AND (half-life OR lifespan OR life-span OR (reproduc* rate))
 3. (macrophage* OR (resident macrophage*))AND (half-life OR lifespan OR life-span OR (reproduc* rate))
 4. (innate immun* OR innate immun* system) AND ((math* OR computation*) model) AND (macrophage OR monocyte OR neutrophil)
 5. (tgf* OR Transforming growth factor) AND (regule* OR interact* OR signal*) AND (innate immunity OR innate immune system OR innate immune cells AND (macrophage* OR neutrophil* OR monocyte*))
- b) The inclusion criteria were: human studies, articles handling lifespan and regulation leukocytes, and innate immune response studies
- c) The exclusion criteria were: excluding the article related to specific cases and diseases, the article related to labeling methods, receptors patterns or gene expression studies.
3. In order to characterize the bacteria agents, their growth and population in the site of infection, we proposed the following questions and criteria:
- a) The search questions were:
 1. (*Staphylococcus aureus* AND bacteria) AND (count OR population) AND (osteomyelitis OR bone infection) AND animal model
 2. *Staphylococcus aureus* AND (reproduc* rate OR generat* time OR growth rate) AND (osteomyelitis OR bone infection)
 3. (computation* OR math*) AND model AND (osteomyelitis OR bone infection)
 - b) The inclusion criteria were *Staphylococcus aureus* population or rate, animal model of BJI for (1, 2).
 - c) The exclusion criteria were the implant material studies, in vitro studies, children osteomyelitis, antibodies studies, or image studies.
4. To investigate the interactions between the agents of the three previous systems, we proposed the following questions:
- a) The search questions were:
 1. (Macrophage* OR neutrophil* OR monocyte*) AND (bacteria OR *Staphylococcus aureus*) AND (bone infection* OR osteomyelitis)
 2. (Osteoclast* OR osteoblast* OR osteocyte*) AND (bacteria OR *Staphylococcus aureus*) AND (bone infection* OR osteomyelitis)

3. (RANK OR RANKL OR OPG OR osteoprotegerin OR receptor activator of nuclear factor kappa* OR TGF OR transforming growth factor) AND (bacteria OR *Staphylococcus aureus*) AND (bone infection* OR osteomyelitis)
 4. (macrophage* OR monocyte* OR neutrophil*) AND (osteoclast* OR osteoblast* OR osteocyte*) AND (osteomyelitis OR bone infection)
- b) The inclusion criteria were *Staphylococcus aureus* or osteomyelitis studies, animal model or human studies, signals and regulations studies, matching keywords articles.
- c) The exclusion criteria were the implant material studies, children osteomyelitis, antibodies, and gene expression studies, or image studies.

The Table 4.1 contains a summary of all research questions with the applied criteria.

Table 4.1. Table of research equations used in the literature review with corresponding inclusion and the exclusion criteria

Search Equations	Including Criteria	Excluding Criteria
Bone cells		
<ol style="list-style-type: none"> 1. Osteoblast* AND (half-life OR lifespan OR life-span OR (reproduc* rate)) 2. Osteoclast* AND (half-life OR lifespan OR life-span OR (reproduc* rate)) 3. Osteocyte* AND (half-life OR lifespan OR life-span OR (reproduc* rate) OR ratio OR density) 4. Bone remodeling process AND (signal* OR RANK OR RANKL OR OPG OR osteoprotegerin OR receptor activator of nuclear factor kappa*) 	human studies, articles on bone formation and bone resorption, quantitative studies, bone biology	the article related to specific cases and diseases, the article related to genetic researches, pathway mediated, or some treatment effects studies
Innate Immune Cells		
<ol style="list-style-type: none"> 1. Neutrophil* AND (half-life OR lifespan OR life-span OR (reproduc* rate)) 2. Monocyte* AND (half-life OR lifespan OR life-span OR (reproduc* rate)) 3. (macrophage* OR (resident macrophage*)) AND (half-life OR lifespan OR life-span OR (reproduc* rate)) 4. (innate immun* OR innate immun* system) AND ((math* OR computation*) model) AND (macrophage OR monocyte OR neutrophil) 5. (tgf* OR Transforming growth factor) AND (regule* OR interact* OR signal*) AND (innate immunity OR innate immune system OR innate immune cells AND (macrophage* OR neutrophil* OR monocyte*)) 	human studies, articles handling lifespan and regulation leukocytes, and innate immune response biology	excluding the article related to specific cases and diseases, the article related to labeling methods, receptors patterns or gene expression studies
Bacteria		
<ol style="list-style-type: none"> 1. (<i>Staphylococcus aureus</i> AND bacteria) AND (count OR population) AND (osteomyelitis OR bone infection) AND animal model 2. <i>Staphylococcus aureus</i> AND (reproduc* rate OR generat* time OR growth rate) AND (osteomyelitis OR bone infection) 3. (computation* OR math*) AND model AND (osteomyelitis OR bone infection) 	staphylococcus aureus population or rate, animal model of BJI for (1, 2)	implant material, in vitro studies, children osteomyelitis, antibodies studies, or image studies
Interactions		
<ol style="list-style-type: none"> 1. (Macrophage* OR neutrophil* OR monocyte*) AND (bacteria OR <i>Staphylococcus aureus</i>) AND (bone infection* OR osteomyelitis) 2. (Osteoclast* OR osteoblast* OR osteocyte*) AND (bacteria OR <i>Staphylococcus aureus</i>) AND (bone infection* OR osteomyelitis) 3. (RANK OR RANKL OR OPG OR osteoprotegerin OR receptor activator of nuclear factor kappa* OR TGF OR transforming growth factor) AND (bacteria OR <i>Staphylococcus aureus</i>) AND (bone infection* OR osteomyelitis) 4. (macrophage* OR monocyte* OR neutrophil*) AND (osteoclast* OR osteoblast* OR osteocyte*) AND (osteomyelitis OR bone infection) 	staphylococcus aureus or osteomyelitis studies, animal model or human studies, signals and regulations studies, matching keywords articles	implant material, children osteomyelitis, antibodies and gene expression studies, or image studies

4.2. Literature Review Results

Systematic search process identified 42 articles for bone cell characterizations, 48 articles for immune cell characterization, 12 articles for bacteria characterization, and 29 articles for interactions (Figure. 4.1-4.4). Following the systematic literature search, we identified the agent interactions and the parameter ranges from the retrieved articles (Table 4.1). The list of all articles used for the study is reported in the Appendix (Table A.1).

Table 4.2. Agent parameters and their values retrieved from the literature search.

Parameter	Summery Range In Literature	References
Bacteria production-rate	1-24 hour	(Ansari et al., 2015; Anwar et al., 2007b; Cramton et al., 2001; DosReis et al., 2001; Fux et al., 2005; Li et al., 2008b; Melter et al., 2010)
Bacteria inoculum size	—	Assumed
Osteocytes initial number	500-900 cell/mm ²	(Goggin et al., 2016; Vashishth et al., 2000)
Osteoblasts production-rate	4 cell/day	(Franchimont et al., 2000; Jilka et al., 2007; Ryser et al., 2009)
Osteoblasts lifespan	3 months	(Kollet et al., 2012; Komarova et al., 2003; Manolagas, 2000)
Osteoblasts initial number	~ 800 - 2000 cells/BMU	(Florenco-Silva et al., 2015; Komarova, 2005; Paoletti et al., 2012a; Ryser et al., 2009)
Osteoclasts production-rate	3 cell/day	(Bar-Shavit, 2007; Buenzli et al., 2011; Chambers, 2010; Charles et al., 2014; Del Fattore et al., 2008; Ryser et al., 2009)
Osteoclasts lifespan	~ 2 weeks	(Lemaire et al., 2004; Manolagas, 2000; Mellis et al., 2011; Roodman, 1999; Soysa et al., 2016; Tanaka et al., 2006)
Osteoclasts initial number	~ 5 - 20 cells/BMU	(Komarova, 2005; Paoletti et al., 2012a; Ryser et al., 2009)
RANKL concentration	10 ⁻⁶ mol/cell/day	(Anandarajah, 2009; Bahar et al., 2007; Boyce et al., 2008; Henriksen et al., 2009; Iolascon et al., 2011; Kardas et al., 2013; Ryser et al., 2009)
OPG concentration	3.10 ⁻⁶ mol/cell/day	(Nakashima, 2014; Paoletti et al., 2012b; Pivonka et al., 2008, 2010; Ryser et al., 2009; Scheiner et al., 2013; Sims et al., 2008; Zhao et al., 2010; Zumsande et al., 2011)
TGF-β concentration	150-500 pg/ml	(Ashcroft, 1999b; Bismar et al., 1999; Kelly et al., 2017; Knapp et al., 1998; Pivonka et al., 2008; Schmidt-Weber et al., 2004; Sheng et al., 2015)
TNF-α concentration	0-1000 pg/ml	(Corrado et al., 2016; Sharma et al., 2002; Szondy et al., 2017; Young et al., 2011)
MCP-1 concentration	0-2000 pg/ml	(Corrado et al., 2016; Kim et al., 2012; Ning et al., 2011)
Neutrophil production-rate	—	See text
Neutrophil lifespan tissue	24 - 120 hours	(Anwar et al., 2007a; Asensi et al., 2004; Bekkering, 2013; Kaplanski et al., 2003b; Kettritz et al., 1999; Kumar et al.,

		2010; Maianski et al., 2004; Rankin, 2010; Schröder, 2000; Summers et al., 2010; Whyte et al., 1999)
Monocyte lifespan	24 -120 hour	(Brunet de la Grange et al., 2013; Dale et al., 2008; Fehder et al., 2007; Ginhoux et al., 2014; Goasguen et al., 2009; Gonzalez-Mejia et al., 2009; Italiani et al., 2014; Parihar et al., 2010; Patel et al., 2017; Reuter et al., 2009; Whitelaw et al., 1966; Yona et al., 2013b)
Monocyte reproduction rate	—	See text
Macrophage lifespan	1-14 days	(Chazaud, 2014; Cole et al., 2014; Dancik et al., 2010; Dockrell et al., 2006; Epelman et al., 2014; Mulherin et al., 1996; Parwaresch et al., 1984; Smith et al., 2011a)
Macrophage reproduction rate	—	See text

Several determinant factors have impacts on the parameter identified in the literature. These include the conditions of the study; however cells parameters are not the same in health and during infection. The type of tissue and the labeling method also has an impact on cells parameters.

Moreover, some available cytokines concentration parameters existed in units which are difficult to be used in our ABM model, for which we made some approximations in order to use it. It is worth noting that since the parameters identification was based on varied studies, which in themselves were based on different conditions, the model calibration still to be carried out in order to ensure the parameters estimation accuracy.

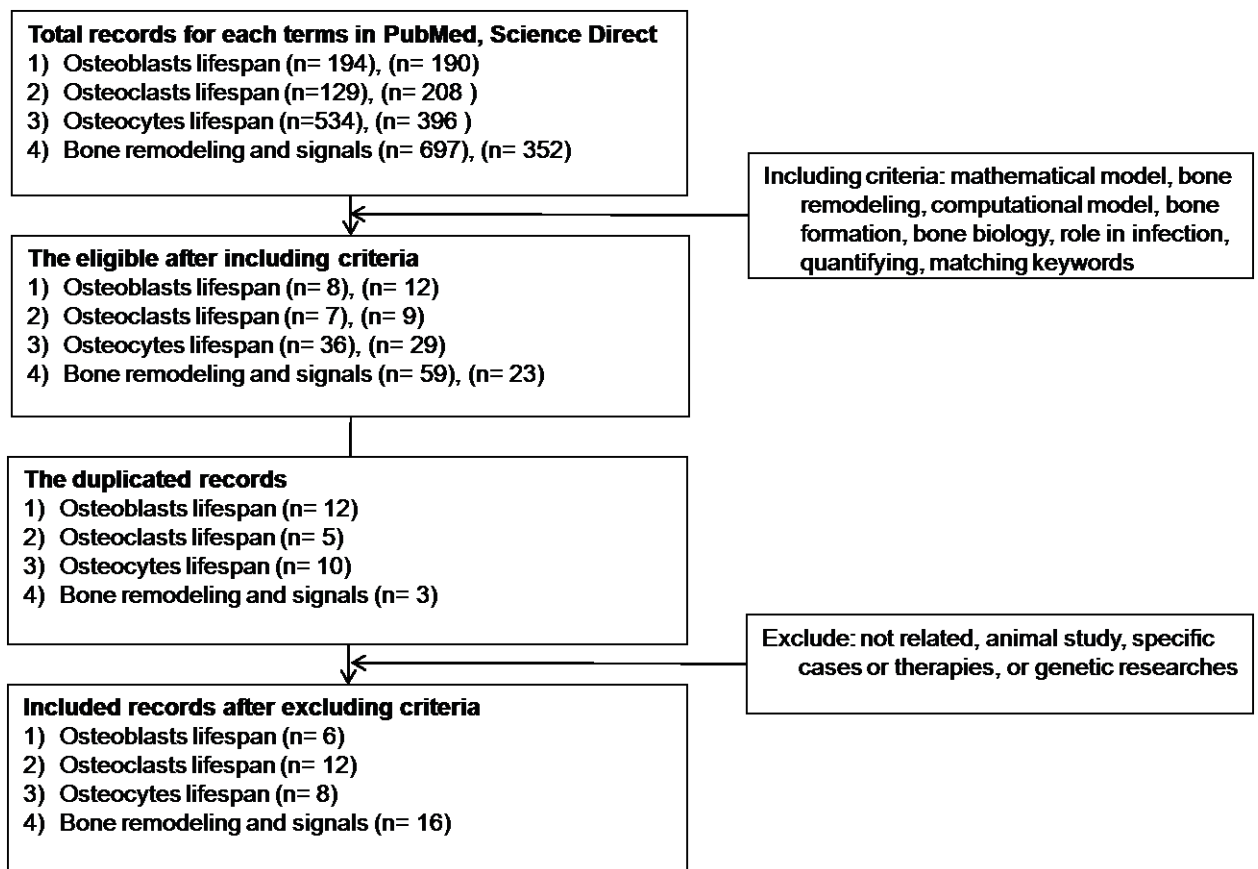


Figure 4.1. Flowchart of the review method steps to identify the parameters of bone cells and signals.

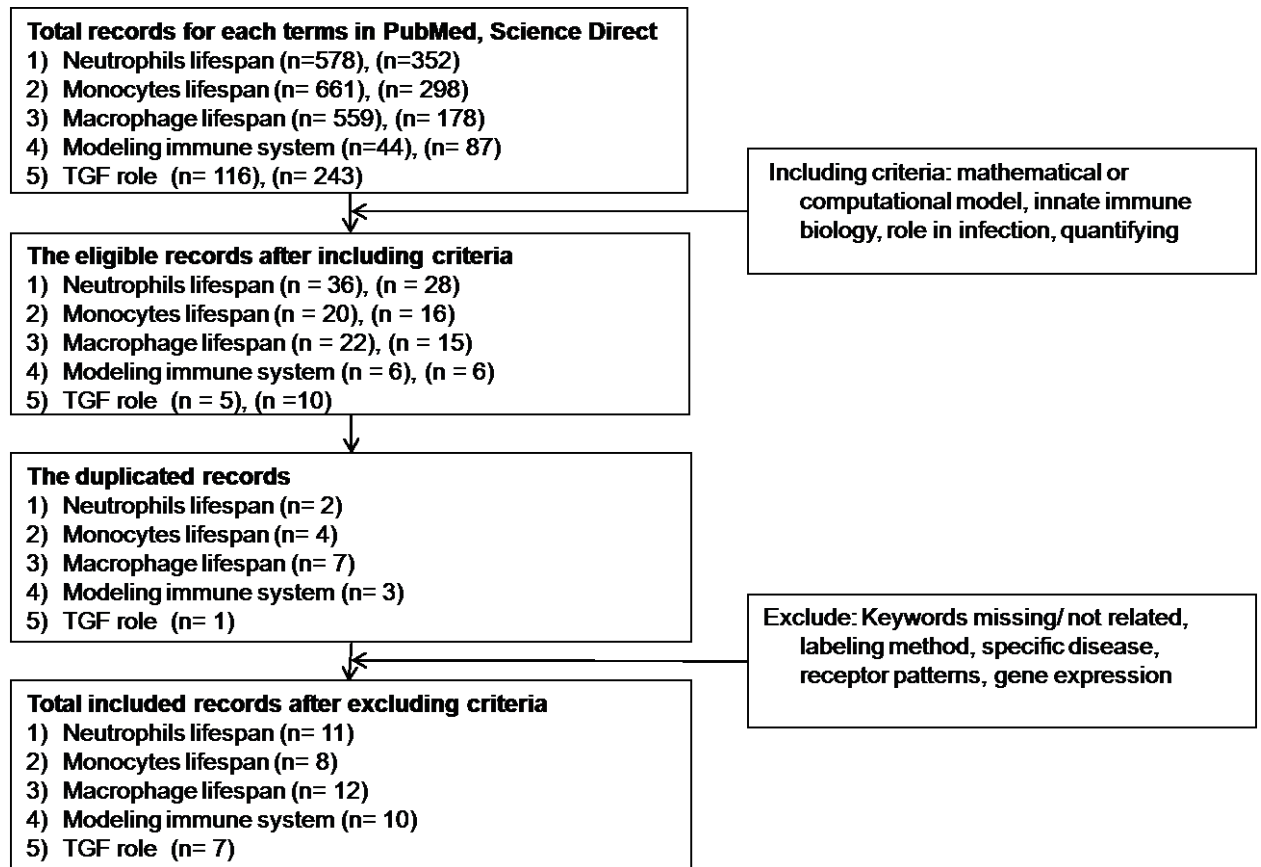


Figure 4.2. Flowchart of the review method steps to identify the parameters of innate immune cells and signals.

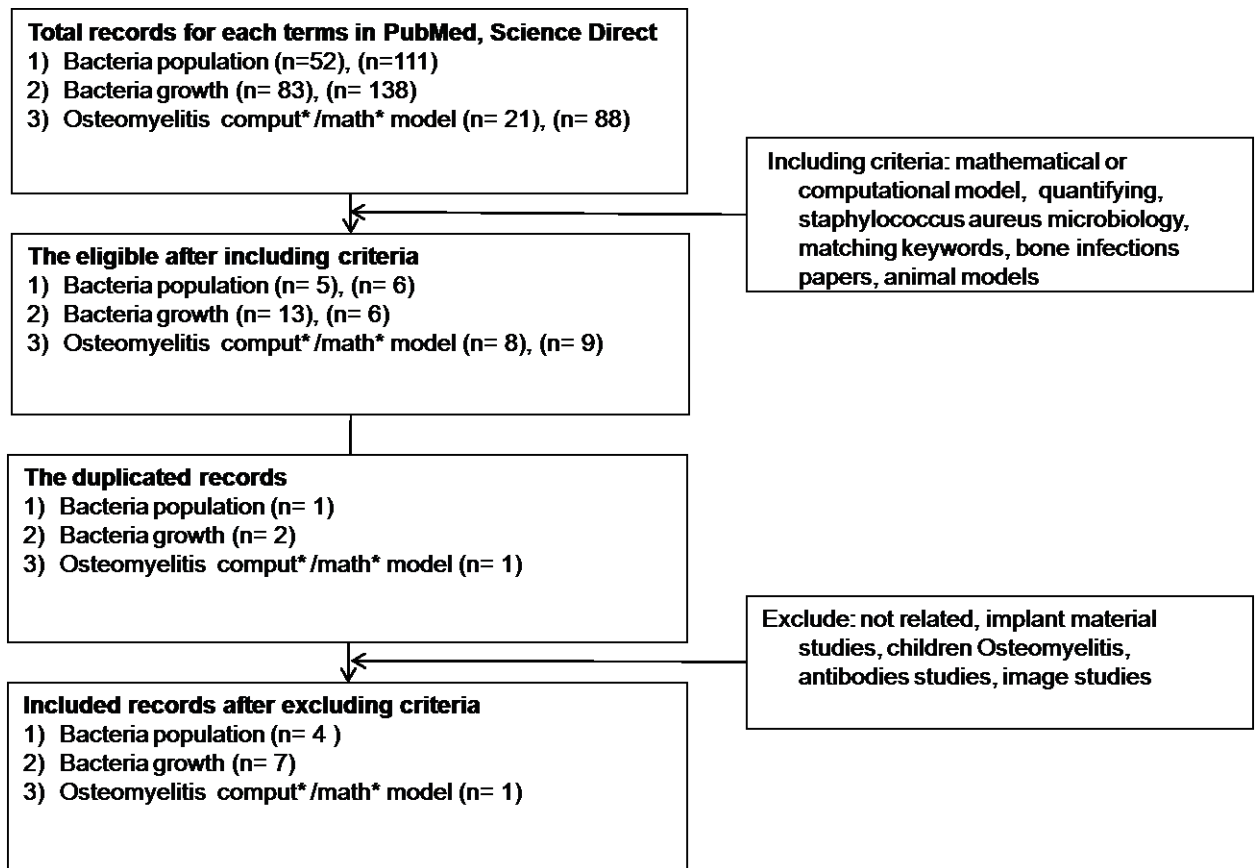


Figure 4.3. Flowchart of the review method steps to identify the parameters of bacteria (*S. aureus*).

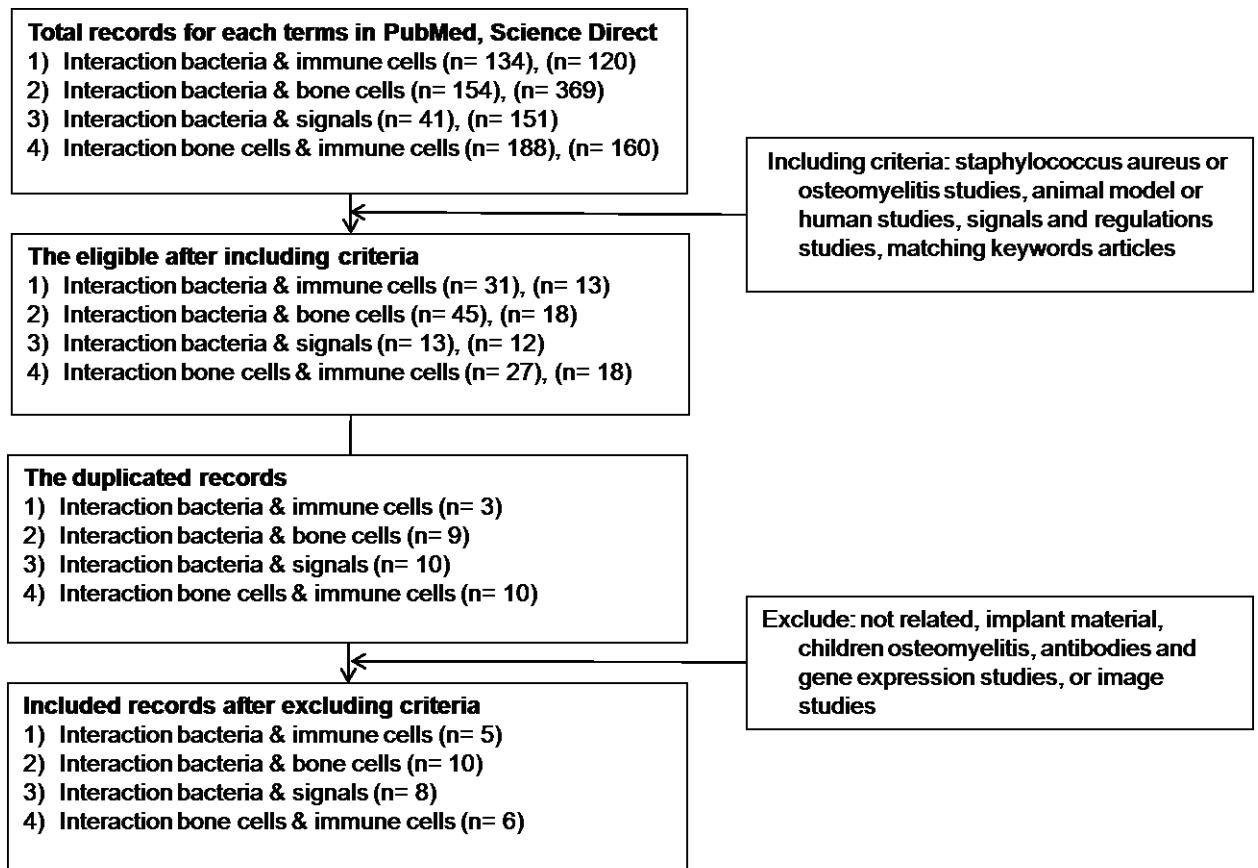


Figure 4.4. Flowchart of the review method steps to identify the interactions between agents.

5. Two-Dimensional Agent-Based Model of BJI

This chapter aims to present the ABM model of BJI that we propose. The model includes the main cells and signals that represent the system in the first stage of infection. The model involves the main cellular behaviors such as proliferation, recruitment, death, interactions between cells and between cells and their environment. We modeled the effect of the bacteria on both of bone remodeling process and innate immune response. We also modeled several signals, allowing the cells to evaluate bacteria progress and then adapt their behaviors accordingly.

This chapter is devoted to explaining step by step the workflow of the model development method (Fig. 5.1). The method is divided into two parts, first the model development process including platform selection, agents and rules identification, model implementation, and process overview. The second part describes the simulation design including steps and parameters used. After that, this chapter introduces the obtained results.

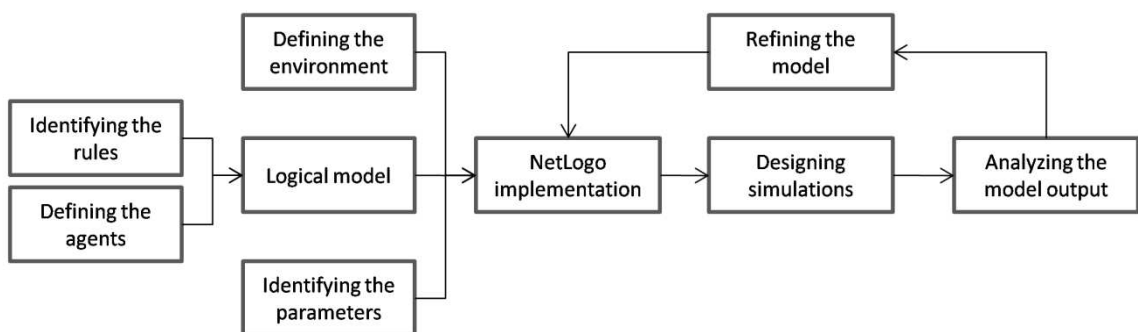


Figure 5.1. Method flow of the model development.

5.1. Model Development

5.1.1. The Model Platform

The BJI model was implemented using the freeware toolkit for agent-based modeling NetLogo 6.0.1 (Wilensky, 1999). NetLogo implementation was started in the Center of Connected Learning and Computer-Based Modeling (CCL) at Northwestern University, in 1999, which keeps improving and adding new functions henceforward (Grimm et al., 2010).

Even though ABM has object-oriented nature, several software matters are hard to be handled with traditional ones such as developing iterations scheduler, time synchronization, and processing parallel simulations. Therefore several agent-based modeling toolkits are developed with taking in the account the balance and trade-off between the representation capability, the computation competence, and the friendly user environment.

Among these toolkits, NetLogo introduces a promising tool to simulate the compound phenomena using a high-level multi-agent programming language and a robust, simple modeling platform. NetLogo was chosen for implementing the BJI model for its several features such as supporting investigating the agent behaviors over time and space and emerging the agents' heterogeneity within its framework. Among the most commonly used agent-based modeling toolkits: Repast, Swarm, Mason, and Flame, NetLogo is the less complex, best documented with the most professional appearance platform (Allan, 2009; Railsback et al., 2011; Shi et al., 2014).

NetLogo has a wide range of library models and a built-in graphical interface. It has built-in agents and features that facilitate programming process in terms of both time and effort, while in the same time it gives the ability to the modelers for adding their own functions (Sklar, 2007). NetLogo also has a set of extensions which contribute in adding additional features (Macal et al., 2005). NetLogo has many applications in several domains such as social science and biology, for both research and education purposes, in which it introduces the capability to simulate the complex system (Chiacchio et al., 2014; Macal et al., 2010). However, it has some limitations

such as the slowness in processing too many numbers of agents and patches, besides the fixed square shape for the grid's patches (Railsback et al., 2011).

Comparing to other most popular ABM platforms, Swarm has an advantage that it arranges multiple levels of ABM model's hierarchy and then combines these small models in an overall complex ABM model. Even this feature has a good application in systems biology; Swarm has remarkable limitations in both of the documentation and tutorial materials (Railsback et al., 2006).

On another hand, Repast is recognized by the ability to customize the behavior of the agents and develop the more complex functions. Nevertheless, Repast is more complex in modeling several simple behaviors of the agents, such as the reproduction and death function. In addition, it lacks the good documentation and the well-defined structure (Railsback et al., 2006).

Mason is also a common ABM platform, which is known as the faster alternative of those other toolkits. It has the minimal execution time, which is suitable to perform more iteration. However, Mason is the less mature platform (Shi et al., 2014).

Flame represents another powerful alternative tool due to the 3D modeling ability and the parallelism capability, for which it is suitable for large population models (Holcombe et al., 2012). Nevertheless, Flame has some constraints concerning the agents' communication and the impacts of the initial distribution on the processing efficiency, besides the limited documented examples (Kiran, 2014, 2017). A comparison between these different toolkits according to general features is summarized in (Table 5.1).

For this study, NetLogo offers a good platform and features with an acceptable execution time for the number of agents that we already have. Even without many structure details, NetLogo allows studying the agents' behaviors with a 2D representation of the cells. Through this environment, we can observe the dynamics over time and space for the set of agents working at the same time, executing their rules, and emerging the macro-level system behavior as a result of the micro-level behaviors and interactions.

Table 5.1. A comparison between ABM platforms according to general features. Reproduced from (Abar et al., 2017; Berryman, 2008; Madey, 2009; Railsback et al., 2006; Tissue et al., 2004)

Feature	NetLogo	FLAME	Repast	SWARM	MASON
Open-source	Yes	Yes	Yes	Yes	Yes
Programming Language	Logo-variant	C	C++ or Java	Objective-C or Java	Java
Built-in agents	Yes	NO	NO	NO	NO
Easy to use GUI	Yes	Needs to integrate tool	Yes	Yes	Yes
Modeling Strength/scalability	Medium ~ large scale	High/Large scale	High/Large scale	Extreme-scale	Medium ~ Large scale
Representation	2D/ 3D	2D/ 3D	2D/ 3D	2D/ 3D	2D/ 3D
Modeling effort	Medium/easy	Complex/Hard	Complex/Hard	Complex/Hard	Complex/Hard

5.1.2. The Agents in the Model

The three sub-systems that compose the BJI are represented through main cells which have initial roles in BJI development. The bone is modeled through the cells (osteoblasts, osteoclasts, osteocytes) and signals (RANK/RANKL/OPG signaling system), which are mainly involved in the bone remodeling process.

Osteoblasts and osteoclasts were chosen because of their direct function in forming and destroying the bone tissue when interacting with bacteria, while osteocytes represent the main tissue cells network. The bone-lining cells were not included to be represented in this stage of the model since their function is more involved in controlling the ECM mineral level and in stimulating with osteocytes the bone remodeling process in a specific site. Even other several molecules and hormones have effects on increasing or decreasing the bone formation, RANK/RANKL/OPG signaling pathway was chosen because it has the most essential and direct role on controlling osteoclasts/osteoblasts activity in BMU (Buenzli et al., 2011; Lemaire et al., 2004; Martin, 2004; Pivonka et al., 2008).

On the other hand, we considered as the innate immune cells those who play the major role in the first stage of infection including signaling cytokines between

them. These cells are the phagocytic cells which establish the first line of defense against the bacteria and activate other immune cells. The modeled agents and signals are macrophages, neutrophils, monocyte-derived macrophages, TNF- α , TGF- β and MCP-1 cytokines that mediate the interactions between these cells.

Although these cytokines are produced by various cell types and have multiple roles, here we considered a simple pathway that reflects the interactions between cells. Many other cytokines have a role in stimulating the innate immune cells. For this proposed model we considered the three mentioned types of cytokines for their importance to model the sequence in cell activation. Once the model is validated, other cytokines will be investigated.

This model is studying the important role of the innate immune defense in eliminating the bacteria in the first stage of infection when the innate immune cells are the only existing immune cells. The adaptive immune response normally is initiated 4-7 days after the invasion, for that none of the adaptive immune cells are counted here (Charles A Janeway et al., 2001).

With regard to the selection of the pathogen agent, we represented *Staphylococcus aureus*, which is the most common cause of BJI and the most investigated in the literature (Grammatico-Guillon et al., 2012).

At this stage of the study, we aimed at obtaining a robust feasible model with a reliable representation of the system. The model was based on the mentioned agent types which are the most relevant to BJI system in the first stage of infection. Once the model is validated and the parameters are well calibrated, another important agent types and functions will be included such as biofilms and developed ECM.

The different agents in the model which were implemented in NetLogo and the signals between them are represented in (Figure 5.2).

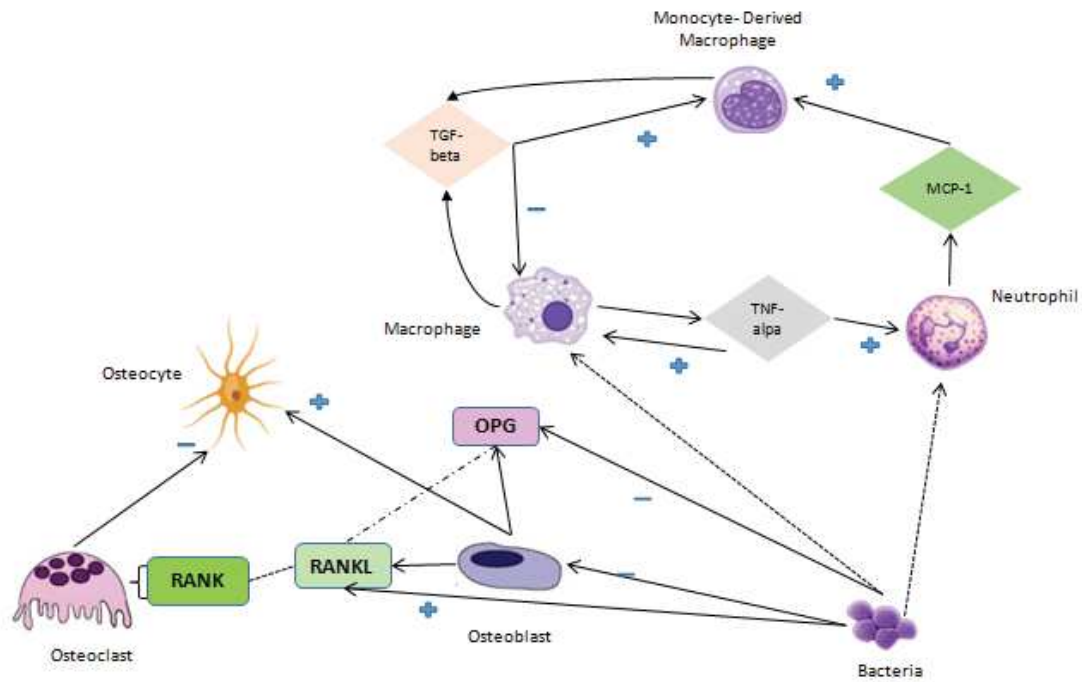


Figure 5.2. Schematic of the agents in the BJI model.

5.1.3. BJI Logical Model

The BJI system is modeled by considering the cells as embodies entities (agents) that interact with each other on micro-level (cellular and molecular level) and spread spatially as populations in the environment. The behaviors of cells were modeled embedding several functions and rules. This section describes how the biological functions of the agents are kept or simplified to be represented in this computational model as agent behaviors, which whole compose the logical model of the system. Summaries of agent and signals variables are included in (Table 5.2) and (Table 5.3), respectively.

First, the bone tissue is represented as three types of cell agents surrounded by an extracellular matrix (the non-cell agents). The RANK/RANKL/OPG signaling system is modeled in a way that RANKL and OPG are released by osteoblasts agents, while the osteoclasts react as RANK receptors. The osteoclast agents were modeled to perform bone resorption through destroying existing osteocyte agents, after being

activated by binding to RANKL. On the other hand, the osteoblast agents were modeled to move towards building new osteocyte agents within the cell matrix and to control the osteoclast agents' activation through RANKL/OPG signals. While RANKL was modeled to increase osteoclasts activation, OPG, in turn, is modeled to inhibit this activation by binding to RANKL. In a healthy state, the resorption and formation of new osteocytes are balanced. However, this process is modeled to be altered during the infection by increasing the RANKL concentration and subsequently the osteoclasts activity towards increasing bone destruction. Bone cells were modeled to have the following behavior rules and functions.

Osteocytes.

1. At the initial state, they are distributed in the bone tissue space taking in the account a minimum distance between them forming a network of osteocytes cells within the extracellular matrix of bone.
2. Because of their long lifespan, these cells agents will not go under apoptosis.
3. Instead, osteocyte population will be decreased by bone resorption phase and increased by bone formation phase.

Osteoclasts.

1. During initialization, they are distributed depending on their count in one bone remodeling unit.
2. They go through apoptosis when their ages, which are increased by each time step, reach the lifespan parameter.
3. New osteoclasts are reproduced every day depending on their reproduction rate parameter.
4. The osteoclasts have RANK receptors on their surfaces (Roodman, 1999), which cause osteoclasts activation through binding to RANKL molecules.
5. Activated osteoclasts move towards destroying neighboring osteocytes cells.

Osteoblasts.

1. Their initial distribution is based on their count in one bone multicellular unit.
2. When their ages reach their lifespan parameter, they change their status to new osteocytes.

3. New osteoblasts are reproduced every day depending on their reproduction rate parameter.
4. Osteoblasts agents are considered as the source of releasing RANKL. Releasing RANKL is depending on both the production rate parameter and the existence of the bacteria. RANKL modeled to bind to RANK and activate osteoclasts.
5. OPG molecules are also released by osteoblasts agents using their reproduction rate and modeled to bind to RANKL in order to inhibit osteoclasts activation.
6. Osteoblasts agents migrate toward forming new osteocytes, after searching for a place where no osteocyte occupies a nearby location to maintain a minimum distance between two osteocytes (Repp et al., 2017).

Table 5.2. List of the agents in the bone and joint infections agent-based model, their rules, and behaviors.

Agent type	Agent Parameters	Agent' rules in bond and joint infections ABM
Bacteria	Inoculum size Reproduction rate	Increase rapidly and spread spatially to invade the bone tissue, stimulate releasing RANKL and activating OC, stimulate immune defense and engulfed by them, stimulate OB death
Neutrophils (PMN)	Count, Lifespan Reproduction rate	Undergo reproduction and death function, recruited due to the presence of bacteria and try to ingest them, recruit MDM
Macrophages (MA)	Count, Lifespan Reproduction rate	Undertake reproduction and death function, stimulated by the presence of bacteria and attack them, regulate macrophages and MDM recruitment through TGF-beta, stimulating neutrophils
Monocytes (MDM)	Count, Lifespan Reproduction rate	Undergo reproduction and death function, stimulated by the presence of bacteria, PMN, and MA after T hours, phagocytosis the bacteria, release TGF-beta to regulate macrophages and MDM recruitment
Osteoblasts (OB)	Count, Lifespan Reproduction rate	Go through reproduction and death cycle, spatial localization, releasing RANKL and OPG, take a role in bone remodeling process: form new osteocytes
Osteoclasts (OC)	Count, Lifespan Reproduction rate	Go through reproduction and death cycle, spatial localization, bind with RANKL to be activated, take a role in bone remodeling process: destroying osteocytes
Osteocytes (OS)	Count, percentage	Form bone osteocytes cells network with respecting the minimum distance between them, derived from mature osteoblasts, destroyed by active osteoclasts

TGF- β : Transforming growth factor beta, RANKL: Receptor activator of nuclear factor kappa-B ligand, OPG: Osteoprotegerin.

Second, the innate immune cells were modeled to respond to the presence of bacteria on sequence according to the biological events that were described in chapter 2. This sequence is modeled on two steps. First, the macrophage and neutrophil agents, which are created at the initialization of the model, are modeled to react directly against the bacteria and phagocytose them. In addition, their stimulation is increased by the proliferating of bacteria and regulated by the tumor necrosis factor alpha $TNF-\alpha$ and transforming growth factor-beta $TGF-\beta$ cytokines.

The second step of defense is modeled to take place if both of macrophages and neutrophils cells could not succeed in eliminating the bacteria by the first 48 hours, through recruiting the monocyte-derived macrophages cells to the site of infection. The MDM cells were modeled to be stimulated by the Monocyte chemoattractant protein-1 (MCP-1) cytokine that is released by neutrophil agents. MDM population is also regulated by the $TGF-\beta$ signal through a positive feedback loop. The functions and rules behind the innate immune cells' work follow.

Macrophages

1. At initialization, macrophages agents are distributed randomly in the model space depending on their initial number, and they are stimulated by the presence of the bacteria.
2. Macrophages go through apoptosis depending on their lifespan parameter, while their ages increase at each time step.
3. New macrophages are reproduced depending on their production rate. The reproduction process follows the uniform distribution function in which the probability of reproducing new macrophages in an one time interval is the same for the whole reproduction time.
4. The macrophages agents move around the space and are attracted to the presence of bacteria to phagocytosis them. When one macrophage engulfs a bacterial agent, it dies.
5. The macrophages reproduce $TGF-\beta$ cytokine that has a double role. They decrease the reproduction of macrophages through a negative feedback loop, while on the second hand, they increase the monocyte production.

6. The macrophages also increase the inflammation by releasing the TNF- α cytokine as an associated variable that used to interact with neutrophils agents to increase their recruitments.

Neutrophils

1. Neutrophils agents are created with the initialization of the model and randomly distributed in the modeled area with an initial concentration.
2. Neutrophils go during their life cycle by increasing their age and then apoptosis which determined by the lifespan parameter.
3. New neutrophils agents are reproduced each day depending on their reproduction rate. Agents' reproduction is also equally distributed over the time of reproduction.
4. Neutrophils agents follow a random walk towards phagocytosis the bacteria. They die after engulfing the bacteria.
5. They are stimulated by the presence of bacteria and by the pro-inflammatory cytokine TNF- α that are released by the macrophages. In addition, they are considered as the source of MCP-1, through which the monocytes are recruited.

Monocyte-Derived Macrophages (MDM)

1. They are recruited to the site 48 hours post the bacterial invasion, stimulated by macrophages and neutrophils through MCP-1 and TGF- β cytokines.
2. They have a life cycle that goes through increasing the age and ends by the apoptosis depending on the lifespan parameter (Ginhoux et al., 2014; Italiani et al., 2014; Whitelaw et al., 1966).
3. Each day, new MDM agents are modeled to reproduce following the uniform distribution function.
4. They move randomly over the area towards phagocytosis bacteria, and they die after doing their mission.
5. They also release TGF- β cytokines and regulated by them through a positive feedback loop.

Table 5.3. List of mediators and their effects that are represented in BJI model.

Mediator Variable	Mediator Parameter	Source	Role in BJI agent-based model
RANKL	Concentration	Osteoblasts	Diffusion, activate osteoclasts by binding to them or inhibit their activation by binding with OPG
OPG	Concentration	Osteoblasts	Diffusion, bind with RANKL to inhibit activating osteoclasts
TGF-beta	Concentration	Macrophages Monocytes	Released by both monocyte and macrophages to increase monocytes recruitment and decrease macrophage recruitment
MCP-1	Concentration	Neutrophils	Released by neutrophils to stimulate monocytes recruitment
TNF-alpha	Concentration	Macrophages	Released by macrophages to enlist neutrophils to the site

TGF- β : Transforming growth factor beta, RANKL: Receptor activator of nuclear factor kappa-B ligand, OPG: Osteoprotegerin, MCP-1: Monocyte chemoattractant protein-1, TNF- α : Tumor necrosis factor alpha

Third, the bacteria in the model are affected by several factors; some of them are related to the bacteria themselves, such as the concentration which is represented by the initial inoculum size, and the reproduction rate. The other types of factors are those related to the strength of immune cells defense and their ability to eliminate the bacteria. In their turn, the bacteria dynamics affect the bone tissue health represented by decreasing the number of osteocytes or ECM agents. The modeled bacterial behaviors rules follow.

Bacteria

1. Bacteria agents are randomly distributed depending on their initial inoculum number.
2. Their life cycle goes first through the growing phase or reproduction phase, which follows the binary fission of bacteria. The distribution of reproduction modeled to follow the normal distribution function. At the time of reproduction, the agents that have to divide search for an empty place around it, otherwise, they will not divide.
3. The bacteria spread and move towards invading the bone tissue.
4. The bacteria go through death rate which symbolizes the run out of their resources for survival.
5. The existence of bacteria stimulates the immune cells to react against the invasion starting by macrophages and neutrophils agents.

6. The bacteria are modeled to work on destroying and weaken the bone tissue by increasing the release of RANKL and thereby increasing osteoclasts activity. They also increase the osteoblasts apoptosis.

An overall schematic of the agents, their functions and interactions, and the signals mechanisms included in the BJI model can be seen in (Figure 5.3).

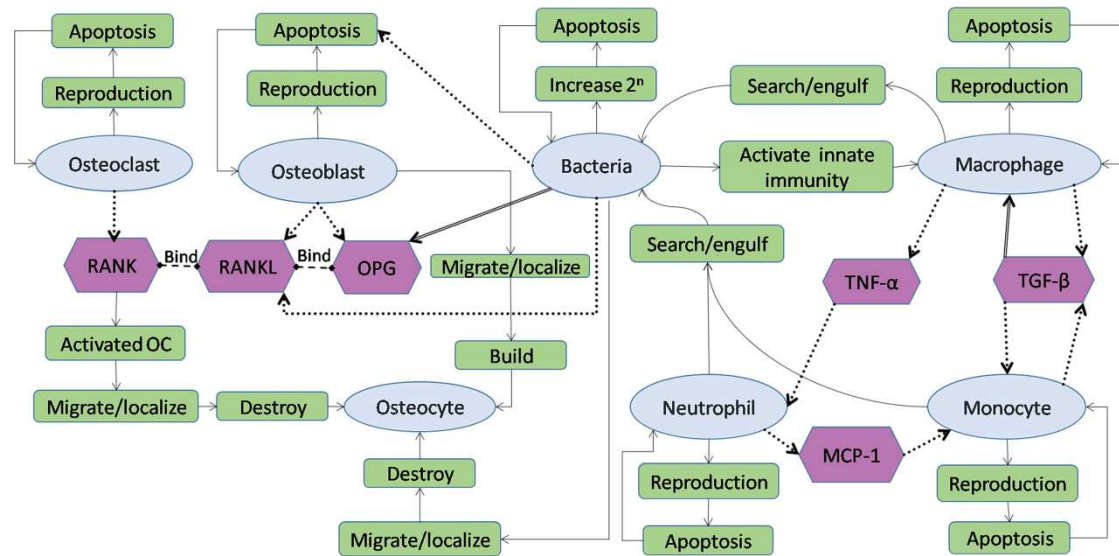


Figure 5.3. Schematic diagram showing agents used in the model, interactions between them, and governing functions for each of them. The oval shapes represent cell agents; hexagons represent signals in the model. The rectangle boxes represent the main functions and roles of each agent. A solid arrow indicates the flow of agent functions, a dotted arrow characterizes stimulation from source to target (destination), while a double lined arrow reflects the opposite effect (source leads to reduce the destination object).

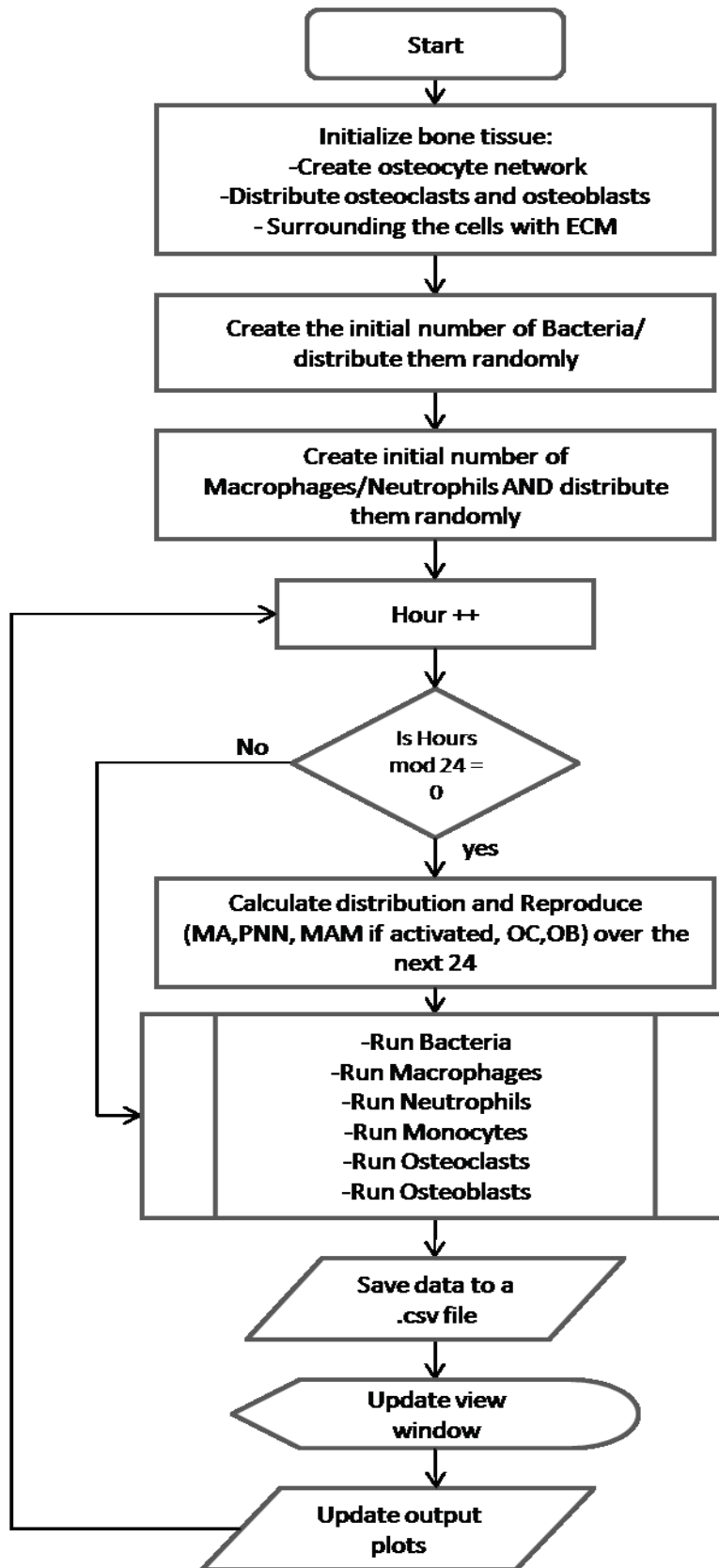


Figure 5.4. A flowchart of the main body of the ABM code.

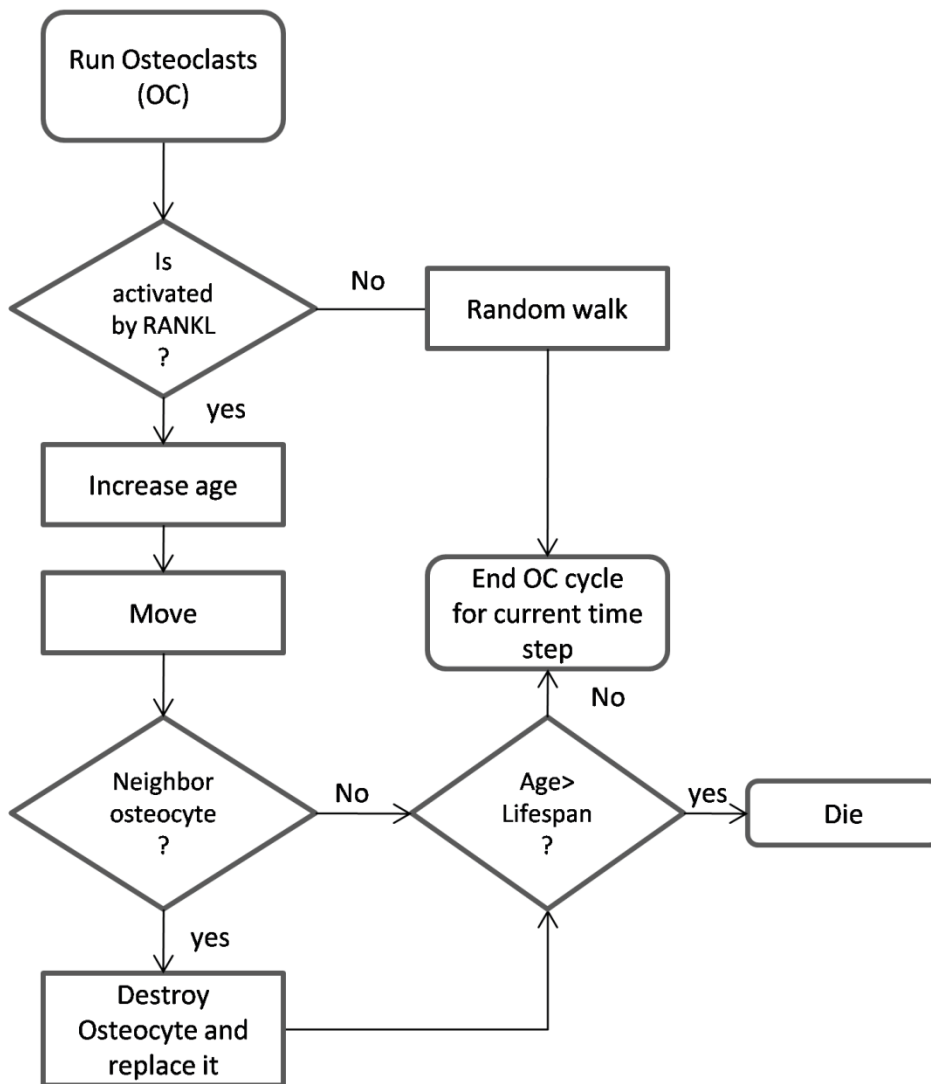


Figure 5.5. Logical flowcharts of the code run by the osteoclasts agents.

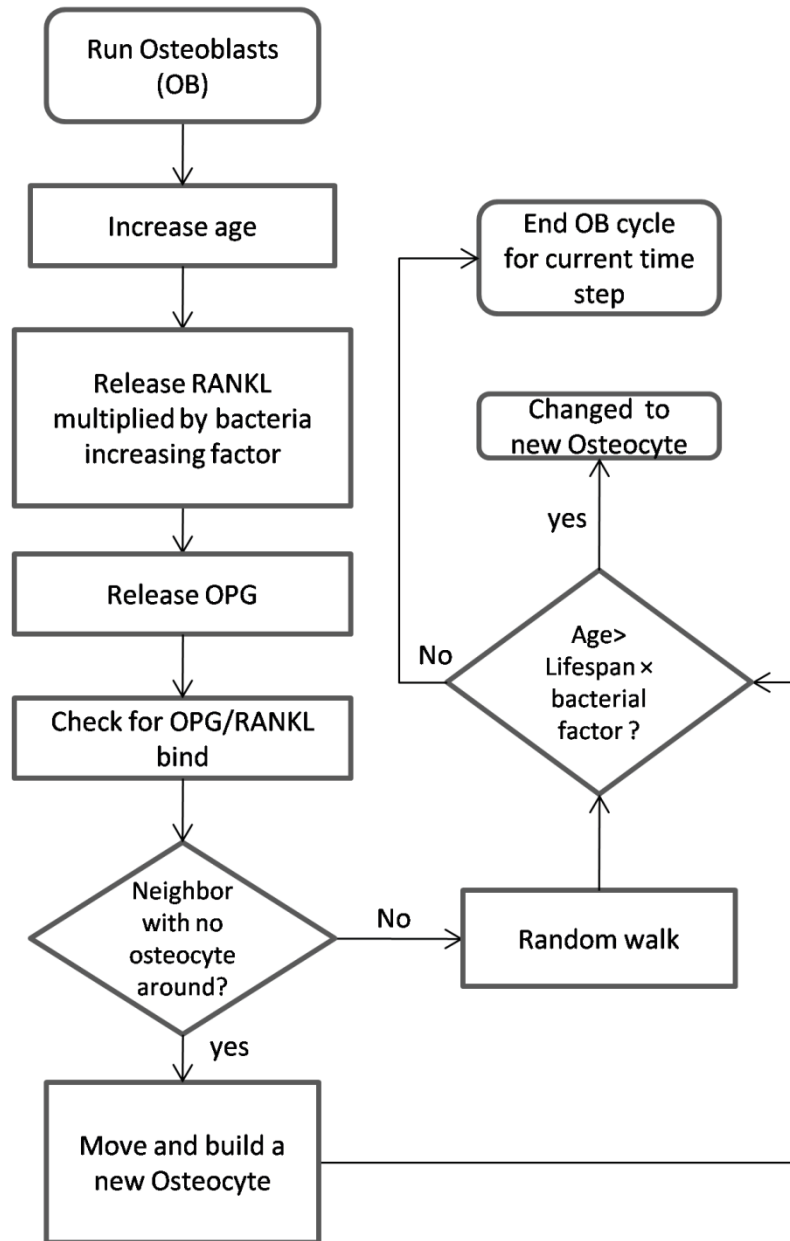


Figure 5.6. Logical flowcharts of the code run by the osteoblasts agents.

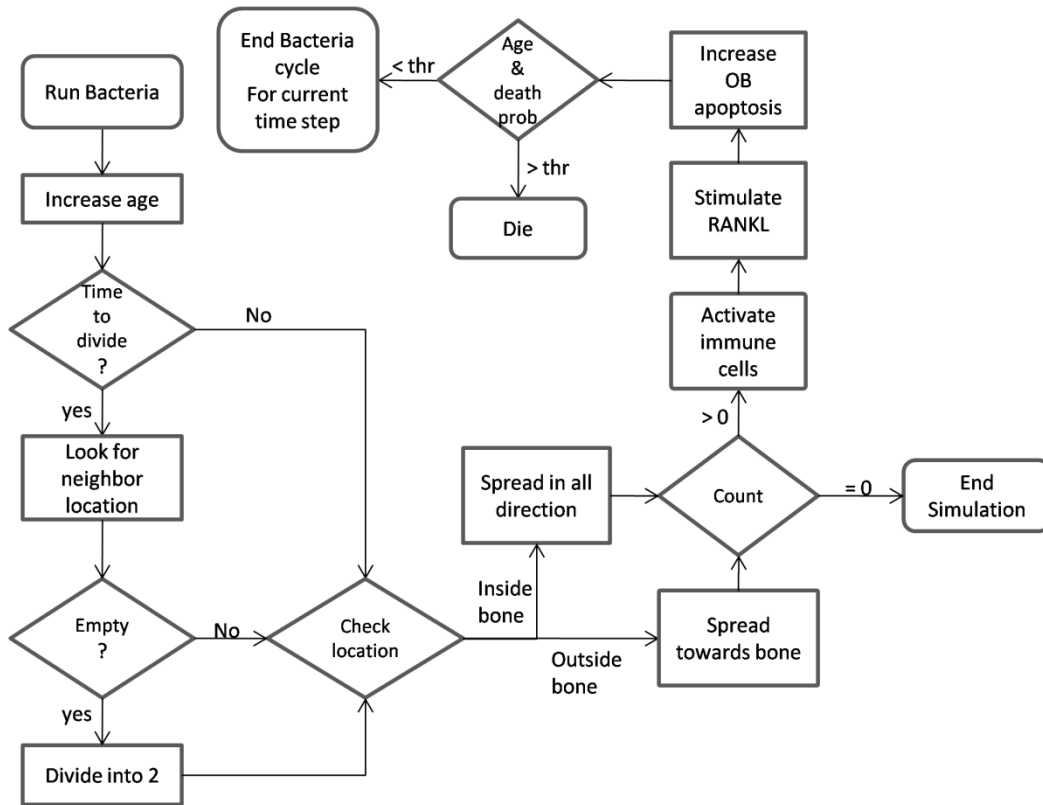


Figure 5.7. Logical flowcharts of the code run by the bacteria agents.

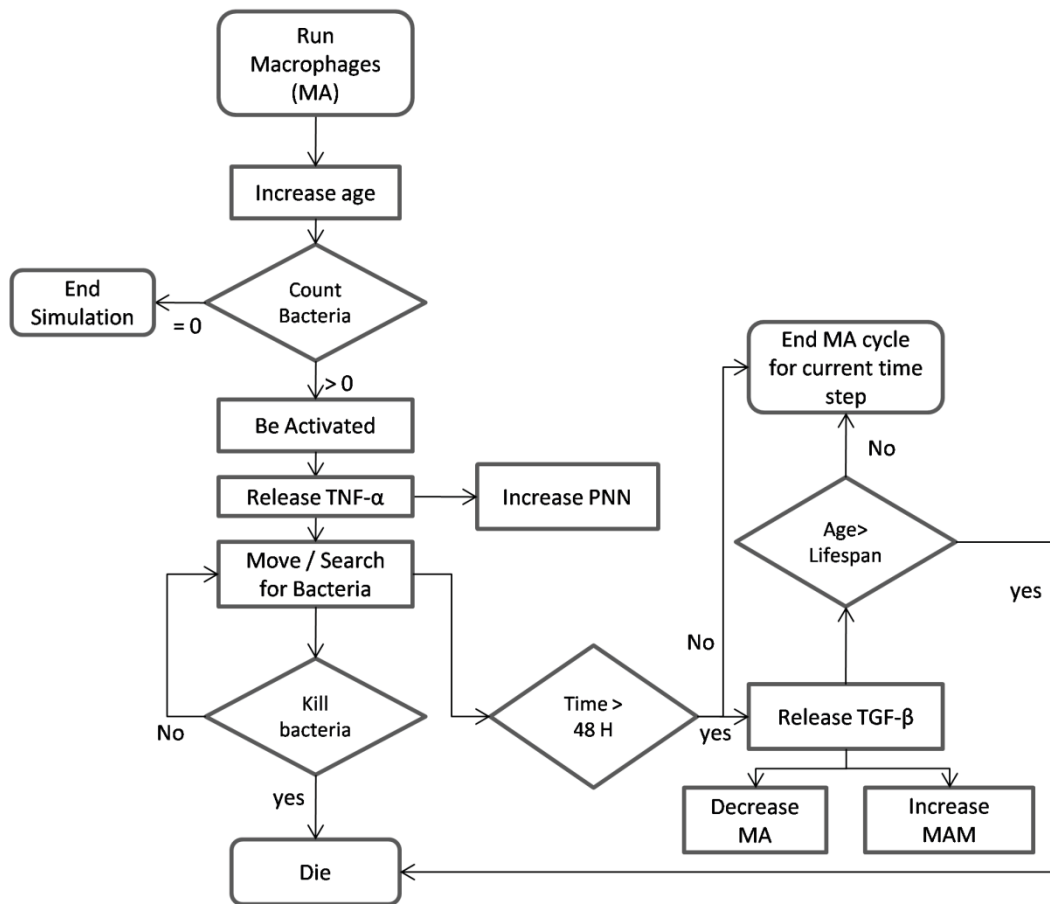


Figure 5.8. Logical flowcharts of the code run by the macrophage agents.

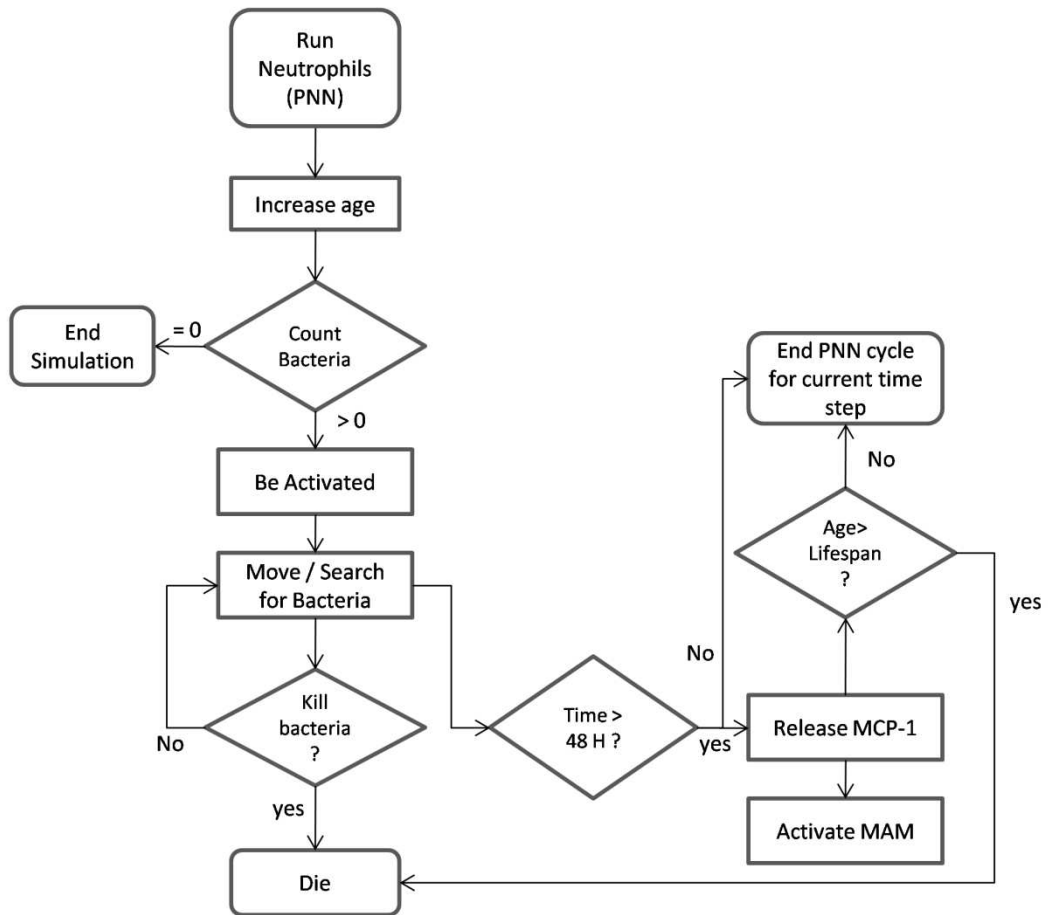


Figure 5.9. Logical flowcharts of the code run by the neutrophil agents.

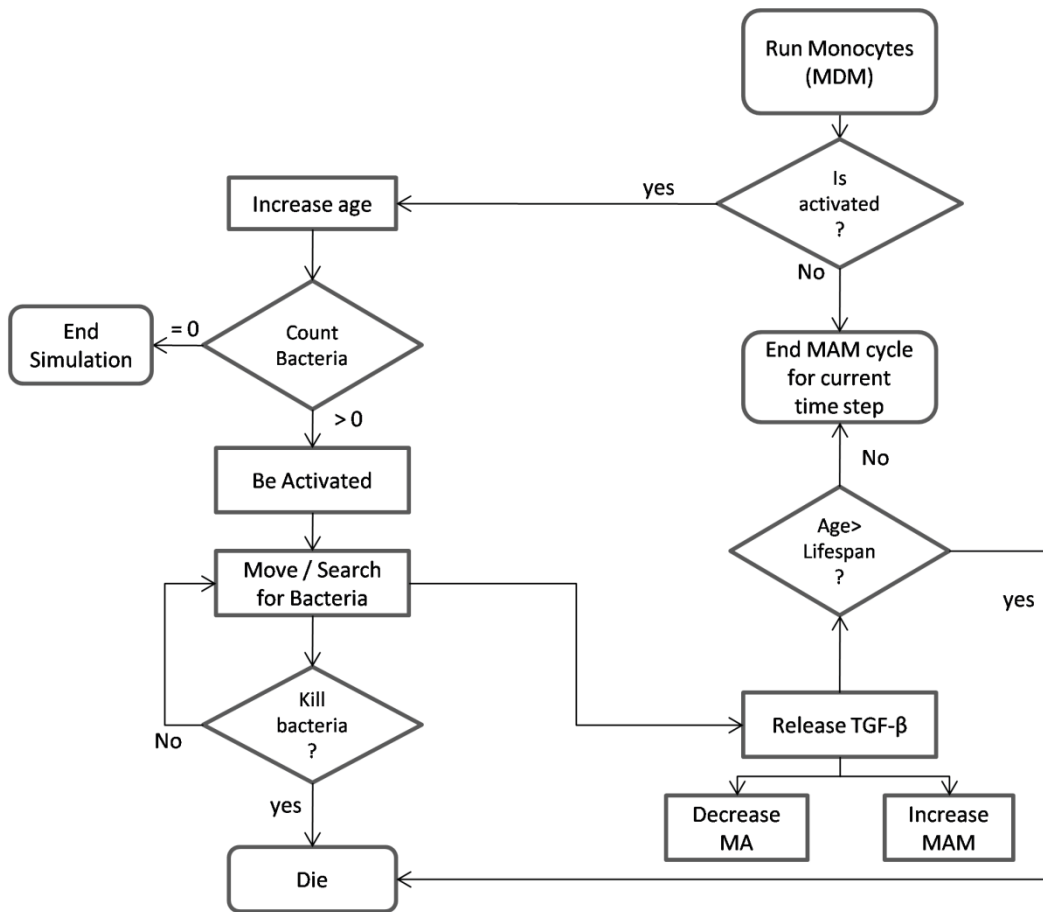


Figure 5.10. Logical flowcharts of the code run by the monocyte agents.

5.1.4. Model Implementation in NetLogo and Parameters Identification

The (Figure 5.11) shows the overall architecture of the BJI model implemented in NetLogo involves the representation of the 2-dimensional section of bone tissue and the adjacent section. Parameter values that used in the model and their applicable ranges that were identified from the literature are given in (Table 5.4). The simulator enables visualizing the location of the different agents in the model, the osteocyte density, the immune cells distribution, the damage occurs in bone tissue, the spreading of bacteria, and the spatial diffusion of RANK and OPG signals. In addition, it supports time-course plots of the cells and signals in the model to display their dynamics. It provides a user-friendly interface that facilitates the system simulation under different initial conditions using sliders that enable changing the value of parameters in order to test several hypotheses

Time Step

Given that the growth of bacteria could happen within hours, and the reproduction and apoptosis of the immune cells can vary between hours to days, we assume that each tick (the virtual time in NetLogo) is equal to one hour of real time.

Projections

The spatial domain of the BJI model is a discrete space of 2D grid of overall dimension 151×101 patch (patch is the NetLogo grid unit). We considered the grid as two adjacent surfaces: the bone tissue on the right, where each bone cell is mapped to a patch on the grid composing together the osteocytes cells network and the bone remodeling cells. This space has a dimension of 2 mm^2 (101×101 patches). The left space is the adjacent tissue where the bacteria start from and spread towards the bone tissue. The dimension of this space is 50×101 patches.

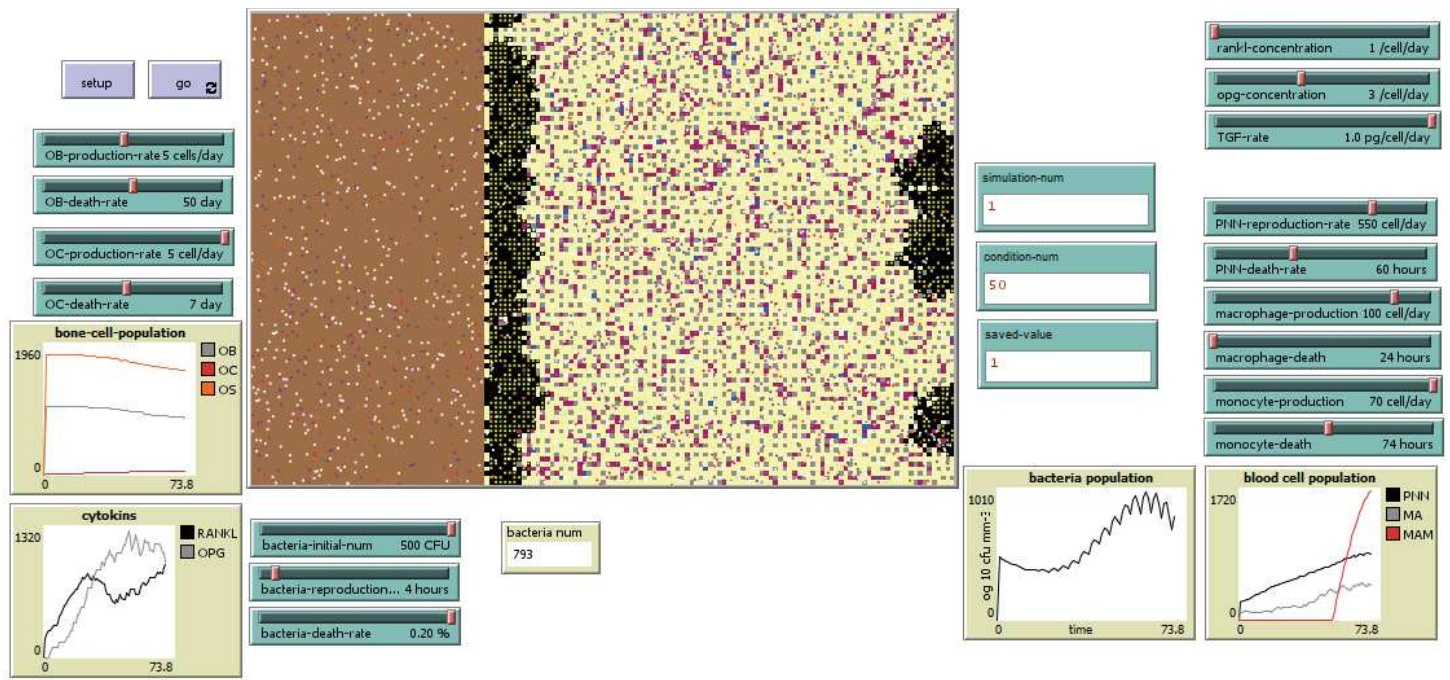


Figure 5.11. Snapshot BJI model interface using NetLogo platform. The projection shows the bone tissue cells (right space), and the adjacent tissue (left space). The sliders enable adjusting parameter ranges. The output time course represents the different agents' dynamics.

Bone Tissue

The two-dimensional cell layer of bone tissue structured as a network of osteocytes cells and a set of osteoclasts and osteoblasts cells that all are distributed randomly and surrounded by the extracellular matrix (non-cell agents). The random distribution of the bone cells respects the allocation conditions. These conditions include representing each cell type according to its percentage in the surface unit and having a minimum distance between two osteocytes, which is represented by one patch. The osteocytes are represented by patches on the grid (the non-mobile agent in NetLogo). Each osteocyte occupies a place where there is no another osteocyte in the eight surrounding neighbors.

We assumed that this area of bone tissue contains one active bone multicellular unit (BMU) represented by osteoclasts and osteoblasts cells, the responsible for bone destruction and formation phases. Both types are also represented as patches in the model, and they change their location to execute their functions.

The initial number of osteoclasts and osteoblasts is corresponding to their count in one BMU. They are defined from the literature to be 5–20 osteoclasts and 800–2000 osteoblasts per BMU (Table 5.4) (Florencio-Silva et al., 2015; Komarova et al., 2003; Liò et al., 2012; Paoletti et al., 2012a; Ryser et al., 2009).

The age variable of each of osteoclasts and osteoblasts agents increases with each time step until reaching their lifespan value. While aged osteoclasts undergo apoptosis, the aged osteoblasts change their status to new osteocytes. The lifespan parameter of each cell type was identified from the literature as ~2 weeks for osteoclasts, and ~3 months for osteocytes (Manolagas, 2000). The lifespan of osteoblasts is affected by the bacteria in the direction of increasing their apoptosis. On the other hand, the lifespan of the osteocytes determines by the resorption and formation activities of osteoclasts and osteoblasts cells (Dallas et al., 2013). During the simulation, new osteocytes originate from active or mature osteoblasts and are destroyed by active osteoclasts.

New osteoclasts and osteoblasts cells are created in the site each day depending on their reproduction rate which also was taken from the mathematical model of Ryser and Komarova (Ryser et al., 2009). The reproduction rate for osteoclasts is identified as 3 cells per day, and for osteoblasts as 4 cells per day.

The osteoblasts cells are the source of releasing RANKL and OPG signals that are responsible for mediating the bone formation and resorption. This function is accomplished using the "sprout" function in NetLogo. Both of RANKL and OPG are represented in the model as mobile agents. We assumed that RANK is located on the surface of osteoclasts, so they are not modeled as separate agents. Instead, the osteoclasts act as receptors of RANKL, and the osteoclasts activation occurs when collisions are detected between osteoclasts agents and RANKL signals. When an osteoclast is activated, it searches for a neighbor osteocyte and moves towards destroying it. When one osteocyte is destroyed, it changes its state to "empty" state. The osteoblasts cells in their turn change their location randomly searching for an empty place with no osteocytes around it and fill it by forming a new osteocyte. The osteocytes are also destroyed by the bacteria, which attack the tissue and spread through it.

The OPG molecules are in competition to bind to RANKL in order to inhibit activating the osteoclasts. While this process is balanced in the healthy condition, the bacteria alter this balance by increasing RANKL releasing and therefore osteoclasts activity and bone destruction. RANKL and OPG production parameters are defined from the literature as 10^{-6} mol/cell/day and $3 \cdot 10^{-6}$ mol/cell/day respectively, which is equal to 1 μ mol/cell/day and 3 μ mol/cell/day (Table 5.4) (Ryser et al., 2009). We assumed in the model that each RANKL and OPG agent released by an osteoblast is representing 1 μ mol of concentration.

Innate Immune Cells

The innate immune cells in the model were represented as mobile agents (turtles) in NetLogo. At initialization, the macrophages and neutrophils agents are distributed randomly in the modeling space according to their initial condition. To my knowledge, information about the count of innate immune cells at steady state in bone tissue is not available in the literature, so we estimated these numbers from studies on lung tissue. The initial number of macrophages is estimated to have a value between 20–100 cells per mm^2 (Table 5.4). Since we have a surface of 2 mm^2 in the model, this range becomes 40–200 macrophages (Wallace et al., 1993). The initial number of neutrophils was also estimated from lung tissue and inflammatory response studies to have a value between 70–150 cell/ mm^2 (150–300 neutrophils in the model) (Akbarshahi et al., 2012; Schirm et al., 2016; Wang et al., 2005). Regarding the monocytes cells, they do not exist during the initialization. Instead, they are recruited to the site after 48 hours of the infection by the stimulation of macrophages and neutrophils.

During their life cycle, each of modeled immune cells searches for the bacteria to engulf it. When a collision between an immune cell and a bacterium is detected, the phagocytosis is accrued. These cells go through apoptosis when they reach their lifespan value. Each cell's agent has age variable that increases with each time step during the simulation. The lifespan for the three cells types was defined from the literature review (Table 5.4). The lifespan of each type was identified as following: 1–2 weeks for macrophages, 5 days for neutrophils, and 4–5 days for monocytes (Bekkering, 2013; Ginhoux et al., 2014; Italiani et al., 2014; Parwaresch et al., 1984; Patel et al., 2017; Rankin, 2010; Whitelaw et al., 1966).

While the aged immune cells die, new cells are created each day according to the reproduction rate parameter for each type of cells. The production rate of each of these cells was estimated using the method used in the mathematical model of Smith et al. (Smith et al., 2011b). We assumed that the steady state N is given by $N = s/d$, where s is the production rate of cells per day and d is the clearance rate per day. The clearance rate of macrophages, which is taken from their identified lifespan, is in the range $d = 7-14 \times 10^{-2} \text{ day}^{-1}$, implying $s = 28-115 \text{ cell/day}$, for a steady state $200-800 \text{ cell/mm}^3$ (Wallace et al., 1993). In the same way, the production rate for each of neutrophils and monocytes was estimated for steady values taken from an animal model of bone infections (Corrado et al., 2016). The production rate of neutrophils was calculated as $120-700 \text{ cell/day}$ for steady state $250-700 \text{ cell/mm}^3$ and $d = 0.2-1 \text{ day}^{-1}$. When the monocytes are activated, they will reproduce in a rate of $4-70 \text{ cell/day}$ that estimated for $d = 0.2-1 \text{ day}^{-1}$ and steady state $20-70 \text{ cell/mm}^3$.

The immune cells use signals or cytokines for intercellular communication to regulate the cells recruitments. MCP-1 and TNF- α cytokines were represented as associated variables of the source cells that release them using the "diffuse" function in NetLogo, while TGF- β was modeled as mobile agents released by the monocytes and macrophages cells to regulate their activities through feedback loops. The concentration value of these cytokines was investigated in the literature in several conditions. For instance, TNF- α take value as $0-1000 \text{ pg/ml}$, MCP-1 as $0-2000 \text{ pg/ml}$ in Corrado model (Corrado et al., 2016), and TGF- β has a value of $150-500 \text{ pg/ml}$ in (Knapp et al., 1998). In our model, and for simplifying the releasing value of these cytokines was assumed to be $1 \times 10^{-3} \text{ pg}$ per the source cell per day.

Bacteria

The bacteria are modeled as mobile agents (turtle in NetLogo), each of them occupies one patch on the grid. The initial inoculum size could be chosen from a range of values ($0-500 \text{ CFU/mm}^2$). Having this range enables testing several hypotheses for different bacteria inoculums to see their effects on the system dynamics, in addition to test the efficiency of the immune cells to eliminate the different bacteria population. At initializing the simulation, the initial bacterial agents are modeled to distribute randomly in the adjacent tissue or space, which is

represented by the left model space of size 50×101 patches, and then they spread towards the bone tissue.

The bacteria reduplicate when reaching their generation time, following the binary fission function. Their age variable increases during the simulation with each time step. When a bacterium reaches the generation time, it searches for the non-bacterial neighbor patch in the grid to propagate; otherwise it will not divide. The generation time of bacteria differs in the controlled culture from it in the human body. This time is difficult to be determined in the human body because of the different factors that have impacts on the bacterial growth in the infected bone such as the location, vascularization, pH, nutrition, and type of prosthesis, if exist. The bacteria characteristics, such as SCV, also have an impact on the growth rate towards decreasing it (Bui et al., 2015). The generation time in the model was identified by the range of 1-24 hours to cover several proposed values (Anwar et al., 2007b; Fux et al., 2005).

The existence of bacteria activates and stimulates several activities in the model, the immune response on one side, and the bone destruction on the other side. The factors that impact the bacteria growth represented as decline parameter taking a value in the range (0–20%) per day.

In addition, since we don't have information about the bacteria count in human, we took some knowledge about the count range from the animal models. In the study of C.Jacqueline (Gaudin et al., 2011a), the count of bacteria could rise to 10^7 – 10^8 CFU/g of bone ($\sim 1.85 \times 10^4$ – 10^5 CFU/mm³). For simplifying reason, and because we are using the 2D representation, we considered this value in the mm² unit. Even though the inoculum size of bacteria in the animal model should be high to start an infection, this inoculum is much smaller in human (Mader, 1985). To give the initial number of bacteria a domain to divide and proliferate, we assumed that the inoculum range between 5–500 CFU, so it can reach the count of power 10^4 in some hours (that depends on the reproduction rate and the immune defense).

Table 5.4. Table of agent's parameters, their range of applicable values, the references, the corresponding ranges used in the model, the step size of each range slider, and the values used in the simulation for each parameter.

Parameter	Summery Range In literature	Range in the model	Step size	Simulation value
Bacteria production-rate	1-24 hour	[1-24] hour	1 hour	12 hours
Bacteria inoculum size	0-500 CFU/mm ³	[0-500] CFU/mm ²	10 CFU/mm ²	5, 50, 500 CFU
Osteocytes initial number	500-900 cell/mm ²	1500-2000 cells		1790 cells
Osteoblasts production-rate	4 cell/day	[1-10] cell/day	1 cell/day	4 cell/day
Osteoblasts lifespan	3 months	[10-90] day	5 days	50 days
Osteoblasts initial number	800-2000 cell/BMU	800-200 cells	—	1000 cells
Osteoclasts production-rate	3 cell/day	[1-5] cell/day	1 cell/day	3 cell/day
Osteoclasts lifespan	~ 2 weeks	[1-14] day	1 day	7 days
Osteoclasts initial number	5 - 20 cell/BMU	5-20 cells	—	8 cells
RANKL concentration	10 ⁻⁶ mol/cell/day	1 µmol/cell/day	1 µmol/cell/day	1 µmol/cell/day
OPG concentration	3.10 ⁻⁶ mol/cell/day	3 µmol/cell/day	1 µmol/cell/day	3 µmol/cell/day
TGF-β concentration	150-500 pg/ml	1×10 ⁻³ pg/cell/day	—	1×10 ⁻³ pg/cell/day
TNF-α concentration	0-1000 pg/ml	1×10 ⁻³ pg/cell/day	—	1×10 ⁻³ pg/cell/day
MCP-1 concentration	0-2000 pg/ml	1×10 ⁻³ pg/cell/day	—	1×10 ⁻³ pg/cell/day
Neutrophil initial number	70–150 cell/mm ²	250 cell	—	250 cell
Neutrophil production-rate	See text	[120–700] cell/hour	50 cells	550 cell/day
Neutrophil lifespan tissue	24 - 120 hours	[24 – 120] hour	6 hours	60 hours
Monocyte lifespan	24 -120 hour	[24-120] hour	5 hours	60 hours
Monocyte reproduction rate	See text	[4–70] cell/day	50 cell/day	150 cell/day
Macrophage initial number	20–100 cell/mm ²	100 cell	—	100 cell
Macrophage lifespan	1-14 days	[24-300] hours	6 hours	24 hours
Macrophage reproduction rate	See text	[28–115] cell/day	10 cell/day	550 cell/day

5.1.5. Process Review and Event Series

The model algorithm starts with an initial state, and then it is followed by a set of rules and functions (described in 5.1.3) that are repeated up to the end of simulation either by eliminating the bacteria or reaching the determined simulation time.

Set-up: Initiating all model variables and set all parameters to their initial value,

- creating the basic grid of (151×101) square patches,
- initiating the bone cells patches according to their percentage of bone cells count and allocate them randomly respecting the allocation conditions,
- creating a number of macrophages and neutrophils agents corresponds to their initial value, and distributing them randomly,
- creating a number of bacteria agents resembles their chosen initial value and allocate each cell to one patch on the left part of the grid randomly,
- and set hour = 1.

Moving: The agents update their location and move upon their functions,

- the bacteria move towards invading the bone tissue,
- the immune cells move towards engulfing the bacteria,
- and the osteoclasts and osteoblasts update their location towards resorbing and forming new osteocytes.

Life cycle: The population and distribution of each type of agent are calculated at each time step,

- if some agents reach their lifespan, they undergo apoptosis, otherwise increase the age.
- If it is the time to reproduce, new agents are created upon their reproduction rate and allocation conditions,
- During their life, each type of agents performs its rules and functions that described in 5.1.3.

Saving data: At each time step, the population of a defined set of agents was saved to ".csv" file. These output files are identified by the initial conditions of the simulation. Multiple runs of the same simulation are saved to the same output file in order to analyze the model outcomes for the same initial conditions.

Update the view: The progress of the infection over time and space during the simulation is shown in the simulator interface (Figure 5.12).

Output plots: We can monitor the changes in the agents' counts through time courses graph for each type of agent in the NetLogo interface; these populations are summarized in (Table 5.5).

The code used for saving the data of the model output follows.

```
//In Set-up function creates and identifies the file
Let file (word "Model" bacteria-initial-num "-Rate" bacteria-reproduction-rate ".csv")
  if is-string? file [
    file-open file]
// In Run function call the write-to-file function in each time step
write-to-file
// The writ-to-file function where the population of set of agents is saved
to write-to-file
  ifelse (ticks <simulation time)[
    file-print ( word ticks "," Bacteria-population "," PMN-population "," Osteocytes-population ) ]
    [ file-print ( word ticks "," "NA," "NA," "NA" ) ]
  ]
  file-flush
end
```

Code Snippet 1: Saving the data to .CSV file in NetLogo

Table 5.5. List of the observed variables through the BJI model time courses

Observed variable changes	
1)	Bacteria population
2)	Immune cells' population <ul style="list-style-type: none"> a. Neutrophils' population b. Macrophages' population c. Monocyte-derived-macrophage population
3)	Bone cells' population <ul style="list-style-type: none"> a. Osteocytes' population b. Osteoblasts' population c. Osteoclasts' population
4)	Bone remodeling mediators <ul style="list-style-type: none"> a. RANKL concentration b. OPG concentration

5.2. Simulation Design

The goal of the simulation is to illustrate the relationships between the variation in bone cells' populations and the evolution of the infectious process. The goal is also to investigate the efficiency of the innate immune system in defending the bacteria during the first stage of BJI. Moreover, the simulation is designed to experience several scenarios of the system progress without treatment intervention and to detect the impact of several parameters on the dynamics of the system.

To investigate the effect of bacteria initial concentration on the system dynamics, the initial inoculum of bacteria was adjusted to three different values (5, 5×10 , 5×10^2 CFU/mm²). These values were assumed to represent three different infected states, low (5 CFU/mm²), medium (5×10 CFU/mm²), and high (5×10^2 CFU/mm²). The values of the other parameters in the model for this simulation were set to their given value in (Table 5.4). As we mentioned before, the virtual time in the platform was assumed as 1 tick = 1 hour of real time.

We verified the model reliability and performance by running the simulation several iterations under the same initial conditions and examined how much the model responses varied. We ran the simulation (n= 100) iterations for each value of bacteria initial inoculum size (5, 5×10 , 5×10^2 CFU/mm²) and for time duration of 300 hours (t = 300 ticks). For each iteration and at each time click (one hour), the dynamics of the population of each of bacteria, osteocyte, and neutrophil agents was tracked and saved to an output data file (.csv). Subsequently, the mean and standard deviation (SD) for the population at each time step and for each type of these agents was quantified and used to analyze the system response for these agents. The osteocyte population will express the bone density since any increase or decrease in bone remodeling process activity in responding to the infection will be reflected on the osteocyte population along with ECM density.

Further, the relation between two agents over time under the same initial conditions for each of bacteria and neutrophil populations, bacteria and osteocyte populations, and neutrophil and osteocyte populations was analyzed using 3D surface graphs.

5.3. Results

5.3.1. The Developed Agent-Based Model of BJI

In the (Figure 5.12), snapshots of the model were taken at different times during a single simulation. (A) At $t = 0$: represents the initial state of the model, where the bacteria (yellow circles) is randomly distributed in the adjacent surface, the left rectangle, with low presence of immune cells macrophages (red circles) and neutrophils (violet circles). The right rectangle represents 2 mm^2 of bone tissue where the bone cells, osteoblasts (magenta square patches), osteoclasts (blue square patches) and osteocytes (gray square patches), are randomly allocated respecting their percentage and allocation condition.

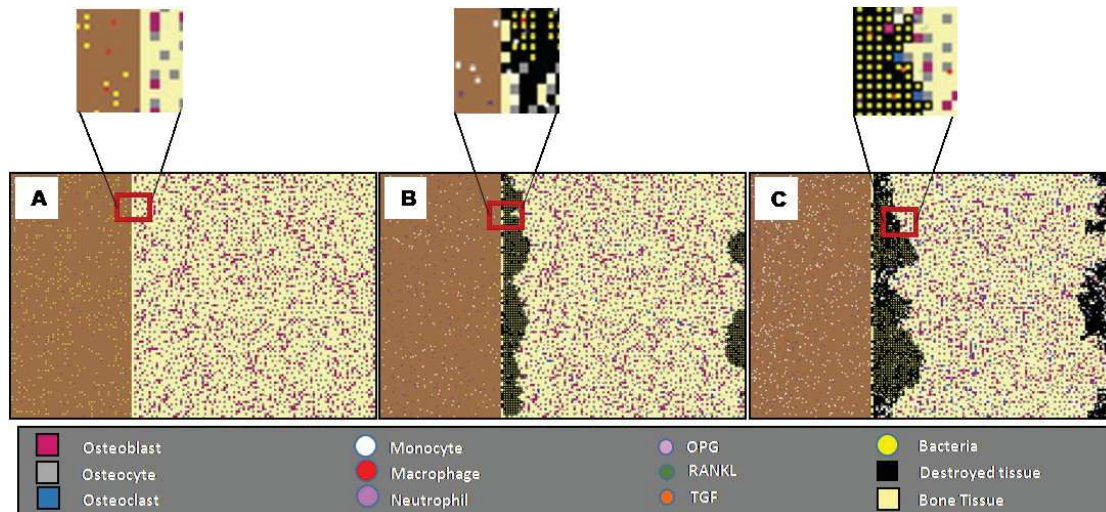


Figure 5.12. Snapshots of the ABM space at three different time steps for inoculum infection state of ($5 \times 10^2 \text{ CFU/mm}^2$). The left rectangle in each sub-figure represents bacteria population, and the right rectangle represents 2 mm^2 of bone tissue where the cells, osteoclasts, osteoblasts, and osteocytes are randomly allocated respecting their percentage and the minimum distance between osteocyte agents. (A) Shows the initial state of the model at $t = 0 \text{ h}$, where the bacteria are randomly distributed in the adjacent surface, the left rectangle, with low presence of immune cells especially macrophages. (B) Shows the state at time $t = 60 \text{ h}$, where the bacteria entered the bone tissue and started destroying it. (C) Shows the model state at $t = 150 \text{ h}$, where the damage happens to the bone tissue, the black patches within bone tissue reflect this destruction, while at the same time the bacteria count was decreased because of engulfing by immune cells.

(B) At $t = 60$: shows the state after two and a half days, where the bacteria have already entered the bone tissue and started destroying it. The monocytes (white square) also have been activated in this step besides the other immune cells.

(C) At $t = 150$: shows the model state after 6 days, where the damage happens to the bone tissue. The black patches within bone tissue reflect this destruction. While at the same time the bacteria count was decreased because of the engulfing by the immune cells.

The implemented ABM model is qualitatively representing several aspects of bone and joint infections evolution dynamics, such as the impact of bacteria proliferation on the bone cells in the site, and the induction and activation of several innate immune cells, accompany with the stimulation of various cytokines and signal that lead to alteration in bone remodeling process.

5.3.2. Simulation Result

The mean and the standard deviation of the dynamics of the population for 100 iterations under different infection inoculum states (low, medium, high) revealed different behavior for each of bacterial, neutrophil (PMN), and osteocyte population is given in (Figure 5.13-5.15).

The bacterial population inclined towards the same steady non-null counts regardless of the inoculum state (Figure 5.13, A-C). In addition, the population intensity of the first stage of infection was proportional to inoculum state. It was also observed that the behavior of the bacteria varied compared to the mean behavior with a small variance magnitude. The bacterial outcomes illustrated rapid variations within population behavior represented by the high-frequency oscillation. At the same time, it showed a lower frequency fluctuation in the context of the general trend of the bacteria population. It was also observed that the bacterial population faced quasi-extinction, followed by re-growth for the medium and high infection state.

On the other hand, the PMN dynamics followed the evolution of the bacteria with a slight delay, reaching a non-null stable level on the 12th day (Figure 5.14, A-

C). In addition, it illustrated that PMN population did not subject to rapid variations represented by the low-frequency oscillations, which are comparatively smoother than those introduced by the bacteria. Asymptotic behavior of PMN population for the three-inoculum size seemed to be a non null mean value with fixed frequency oscillations and decreasing magnitude with time.

Concerning the bone tissue loss (Figure 5.15, A-C), the osteocyte population dynamics were similar in mean population intensity for the three inoculum states. On the other hand, the outcomes of the osteocytes differ from the mean behavior with important variance magnitudes whatever the inoculum. The bone cells' population predicted a trend of unexpected high-frequency oscillations after $t= 200$ h.

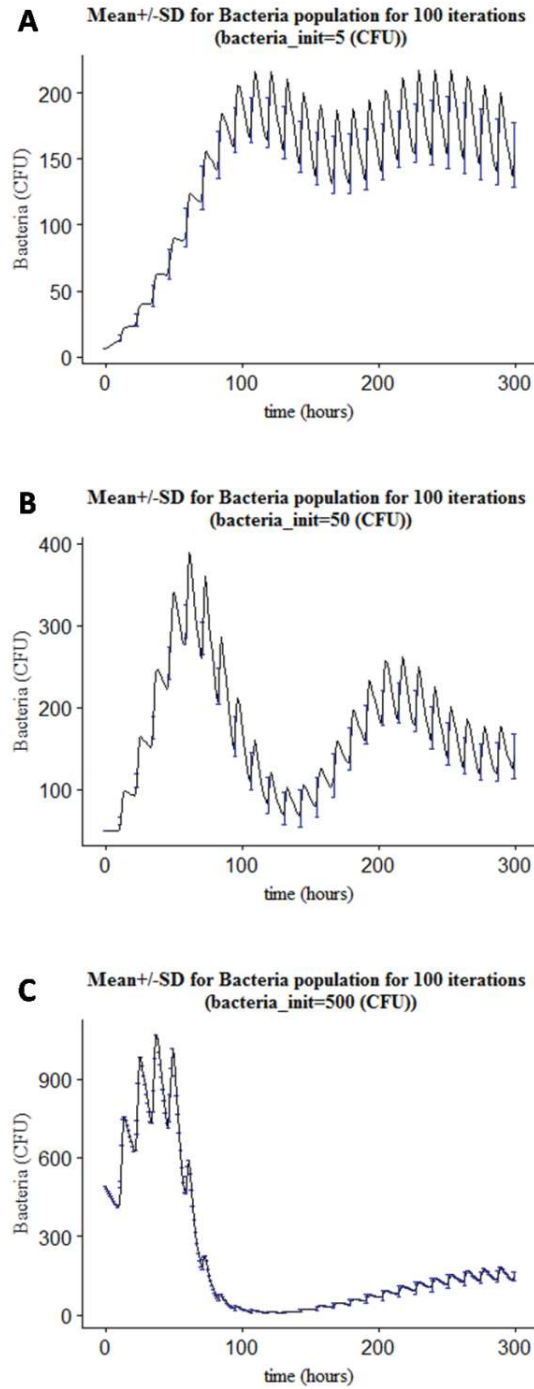


Figure 5.13. The mean and standard deviation (SD) for 100 iterations for bacterial populations over time, $t = 300$ hours, at three different initial inoculum state of bacteria. (A) represents the outcomes for low inoculum state ($5 \text{ CFU}/\text{mm}^2$), (B) the outcomes for medium inoculum state ($50 \text{ CFU}/\text{mm}^2$), and (C) the outcomes for high inoculum state ($500 \text{ CFU}/\text{mm}^2$).

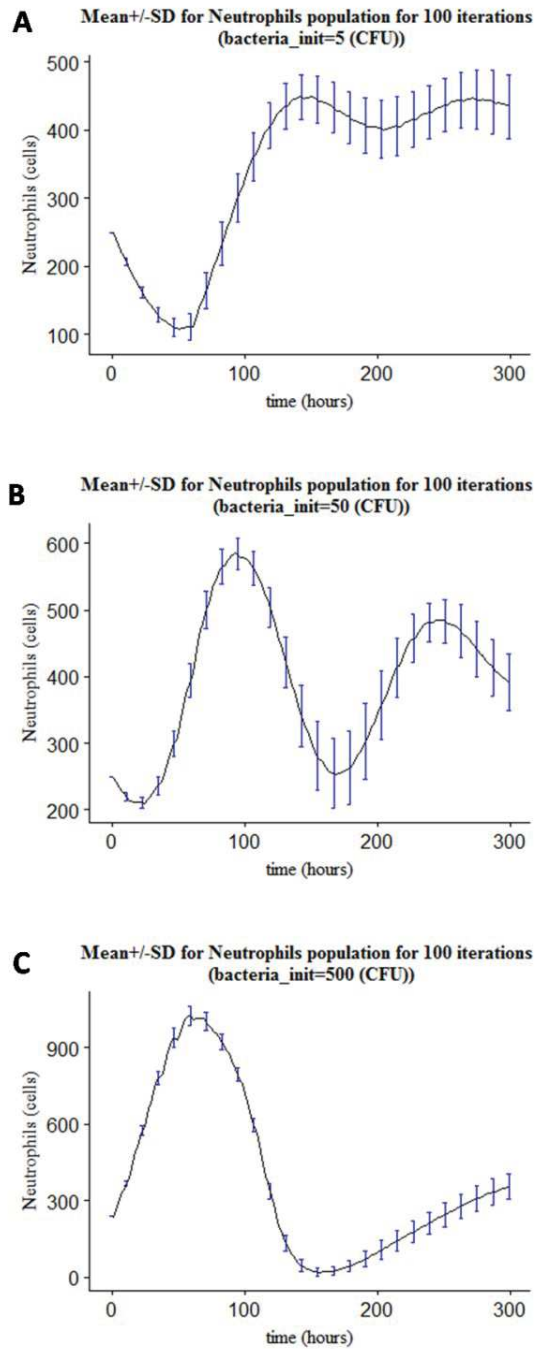


Figure 5.14. The mean and standard deviation (SD) for 100 iterations for neutrophil populations over time, $t = 300$ hours, at three different initial inoculum state of bacteria. (A) represents the outcomes for low inoculum state ($5 \text{ CFU}/\text{mm}^2$), (B) the outcomes for medium inoculum state ($50 \text{ CFU}/\text{mm}^2$), and (C) the outcomes for high inoculum state ($500 \text{ CFU}/\text{mm}^2$).

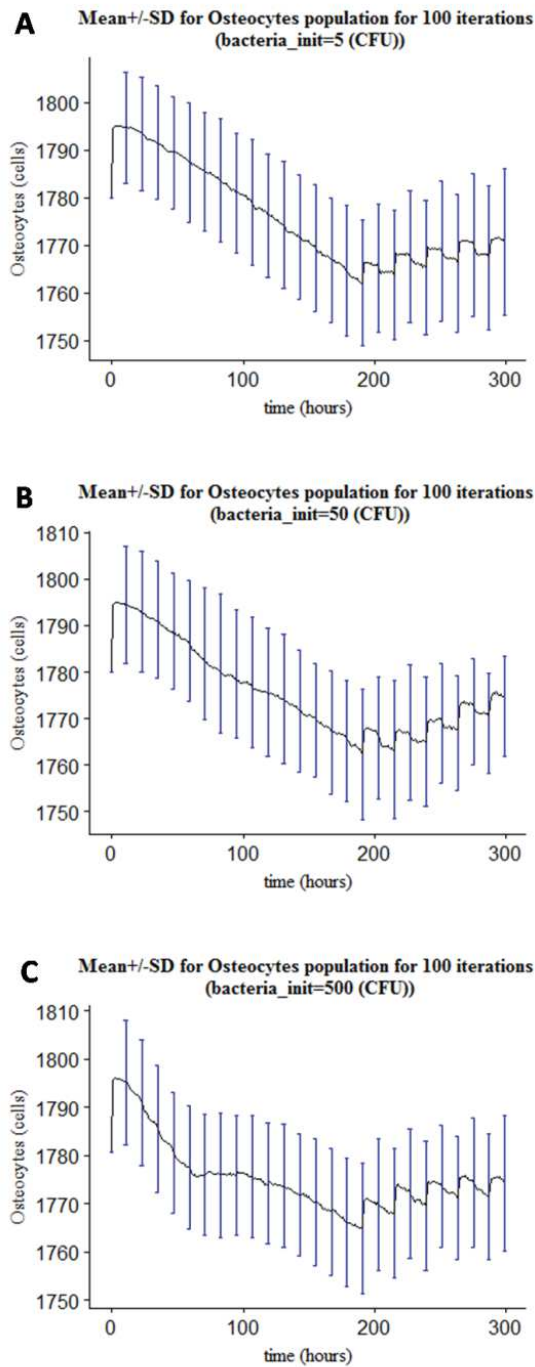


Figure 5.15. The mean and standard deviation (SD) for 100 iterations for osteocyte populations overtime, $t=300$ hours, at three different initial inoculum state of bacteria. (A) represents the outcomes for low inoculum state ($5 \text{ CFU}/\text{mm}^2$), (B) the outcomes for medium inoculum state ($50 \text{ CFU}/\text{mm}^2$), and (C) the outcomes for high inoculum state ($500 \text{ CFU}/\text{mm}^2$).

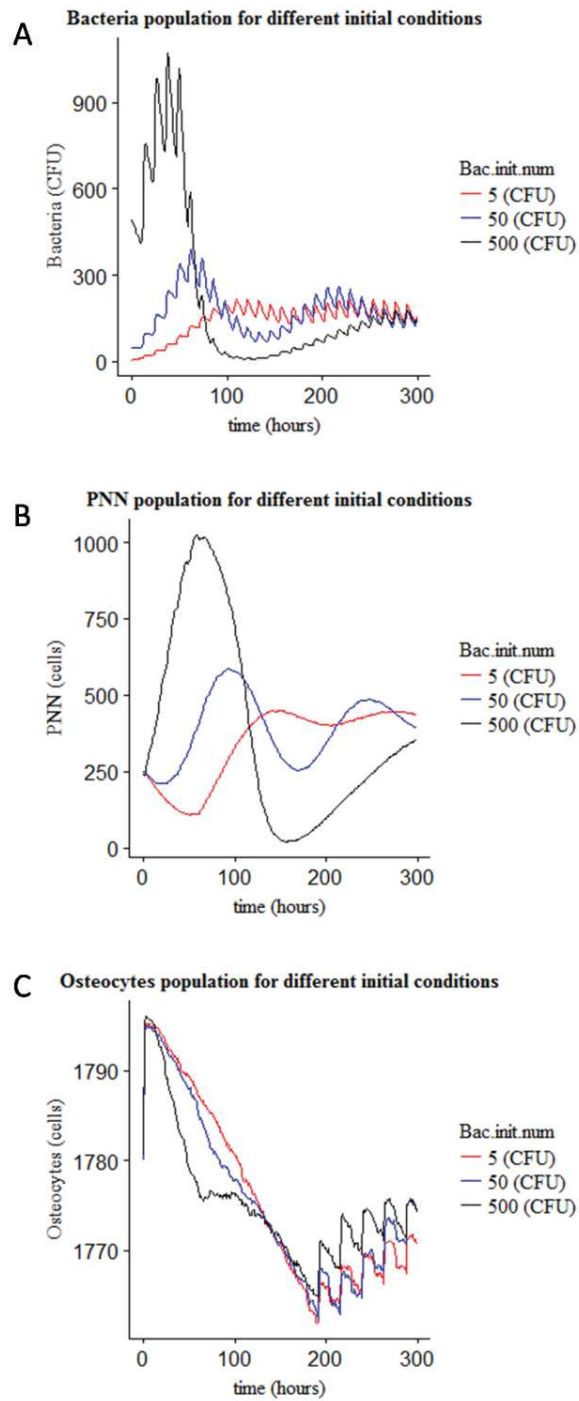


Figure 5.16. Comparisons of system response for three inoculum infection state of bacteria (5, 50, 500 CFU/ mm²). (A) System response for bacteria population over time, (B) System response for PMN population over time, and (C) System response for osteocyte population over time.

Comparisons of system response for different inoculum sizes of bacteria over time for the same type of agent population suggested that the higher inoculum infection state was associated with close to full elimination of bacteria and PMN population (Figure 5.16, A-B). It was also associated with the highest population counts for both agent types in the first few days of the infection. The results presented that bacteria and PMN tended towards a steady asymptotic non-null state, regardless of the inoculum infection state.

As regards to bone tissue damage, the first response stage had a similar degradation phase represented by decreasing count of osteocytes for all three-inoculum size, while the recovery phase that followed was inversely proportional to the inoculum, with sub optimum recovery at 300 hours. It was noted that osteocytes passed by a common minimum level by the 7th- 8th day for all three-inoculum size, representing 2% of the loss in the infected site mass. During the recovery phase, it was observed that the smallest infection state caused more severe and relatively stable loss on bone cells by the 12th day, the medium infection state showed better progressive recovery, and the high infection state displayed an intermediate recovery. The displayed loss of bone tissue compared to baseline for each inoculum size was 1.4%, 1.2% and 1%, respectively.

The 3D representation of the relation between two types of agents over time suggested minimum levels of bacteria and PMN population count around the fourth day of infection, while it suggested a delay in minimum levels of population in osteocytes count, with regard to the minimum levels of bacteria and PMN (Figure 5.17-5.19).

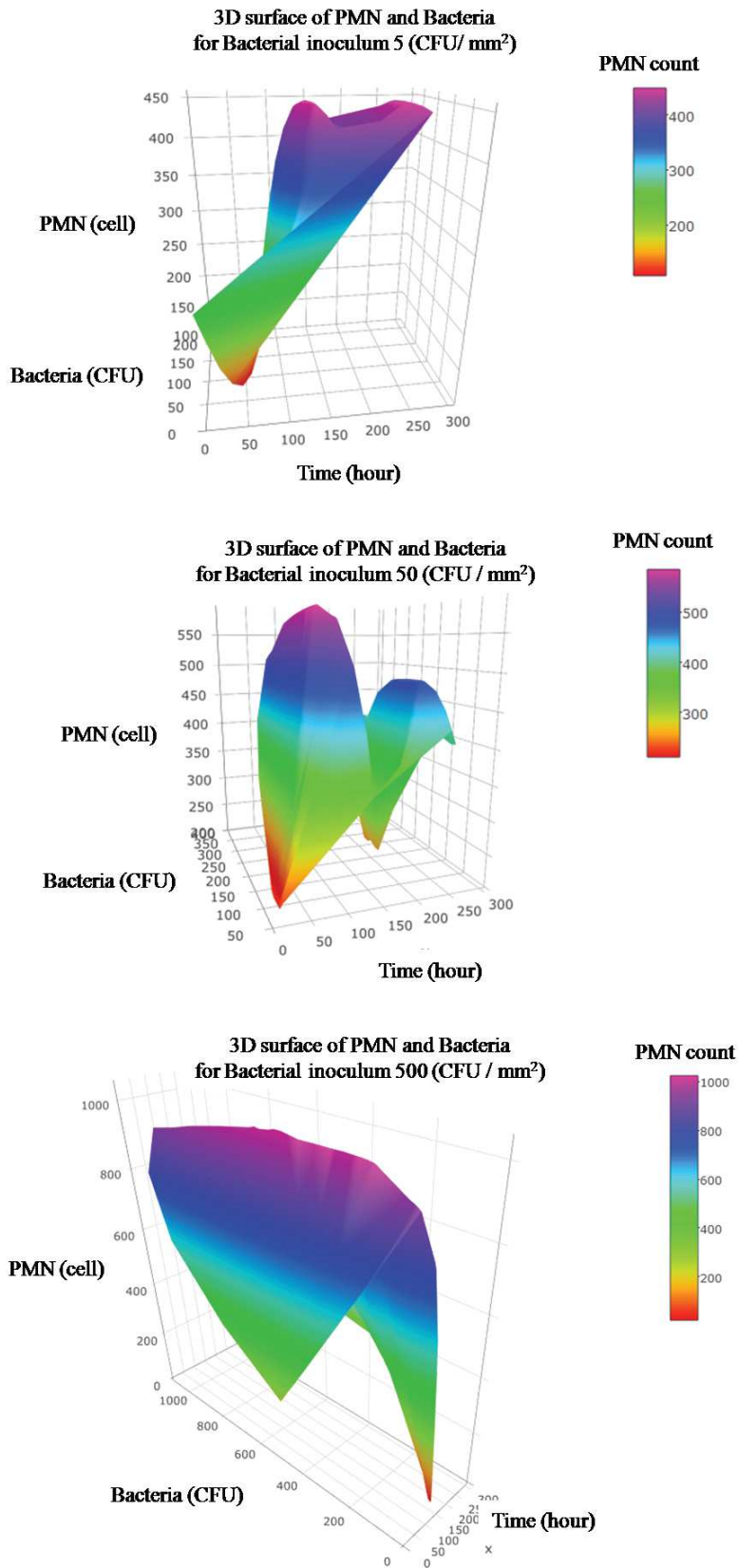


Figure 5.17. 3D surface graphs to analyze the relationship between the bacteria vs. neutrophils (PMN) over time at three inoculum infection state of bacteria (5, 50, 500 (CFU/mm²)).

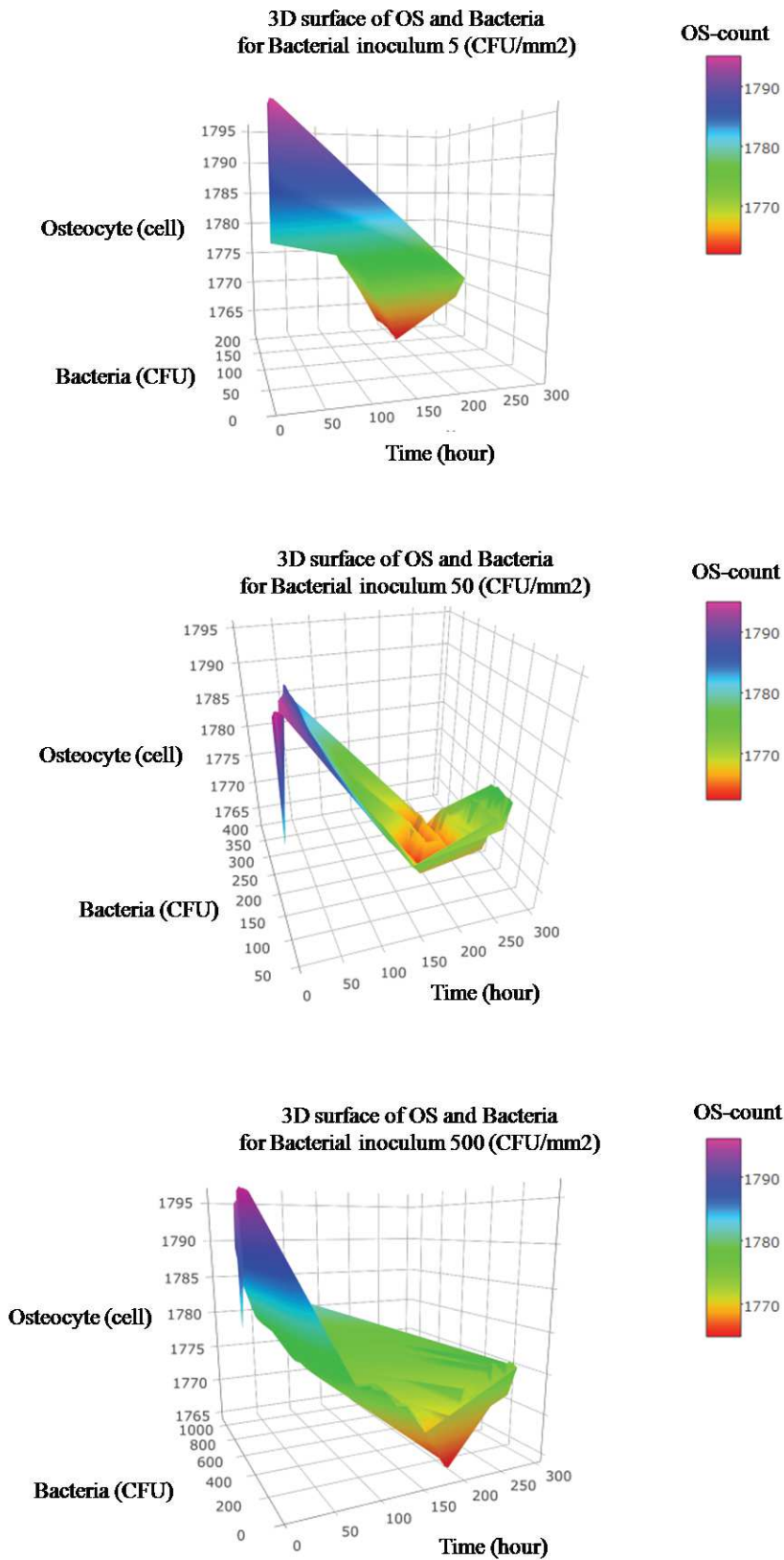


Figure 5.18. 3D surface graphs to analyze the relationship between the bacteria vs. osteocytes (OS) over time at three inoculum infection state of bacteria (5, 50 500 (CFU/mm²)).

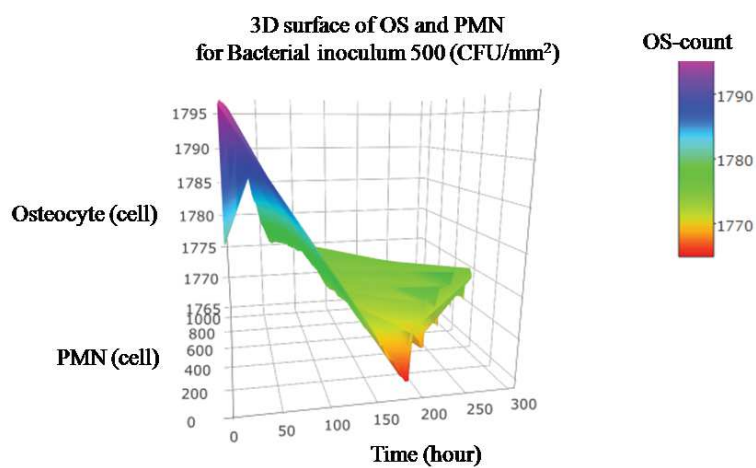
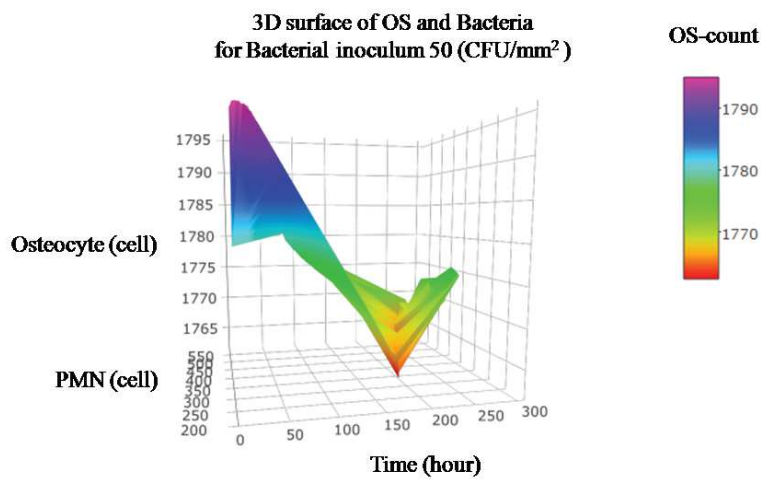
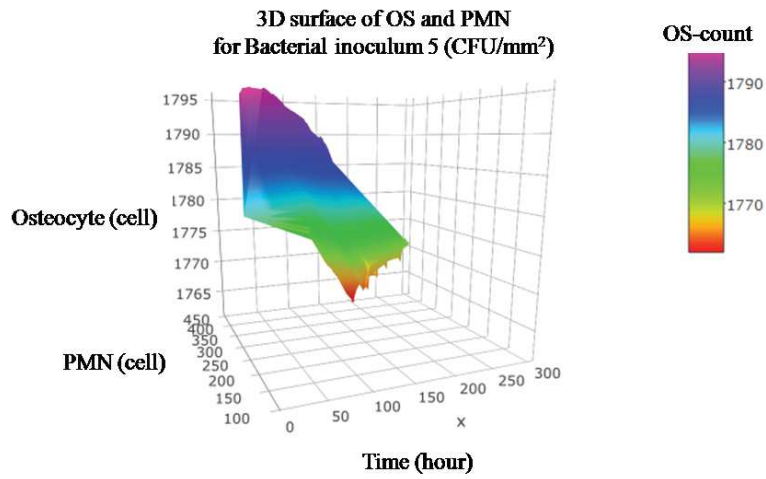


Figure 5.19. 3D surface graphs to analyze the relationship between the neutrophils (PMN) vs. osteocytes (OS) over time at three inoculum infection state of bacteria (5, 50, 500 (CFU/mm²)).

5.4. Discussion

By integrating the ABM modeling technique along with the experimental knowledge from the literature review, this study introduces an innovative in-silico experimental environment to explore the BJI dynamics qualitatively and comprehensively. The interactions between the agents and signals provide an exhaustive ability to analyze the system considering the spatial characteristics and the inter-agent variability. The developed model offers a means to test the impact of several factors on the infected tissue. Through this model, this study illustrated the role of initial bacterial concentration and host defense state as important factors that identify the consequences of bacterial invasion to the bone.

The outcomes of the simulation proposed several observations that could be used to explain different infection cases. For "realistic" inoculum ranges in human, on the 12th day, the observed bacterial population for the inoculum of the order of 100 was stable, and not extinct, which could be considered as an indication for the latent infection. Since the PMN populations followed, in the same manner, the bacteria populations but in a slight delay to reach the stable non-null levels at the 12th day, it could also be used as a pointer to the latent infection. If so, it should be validated in terms of PMN count in the biological laboratory test.

In addition, the outcomes of the osteocyte populations that revealed an inverse proportional relationship between the osteocyte population and the bacteria inoculum size raise the question of whether it refers to a *restitutio ad integrum* state.

Further, it was notable that the bacterial population during the three bacteria inoculum states could not be completely eliminated by the innate immune cells, but it remained at stable levels. This behavior shows the imperative role of further defense methods: the adaptive immune response and the therapeutic intervention.

In the term of population fluctuations (intra-simulation), the observed small variance within the bacterial population dynamics highlighted their stable behavior even with the rapid, strong oscillation, which the latter could be an artifact of the time characteristic. The fluctuations observed in PMN population had a less important effect compared to the inoculum state, which reflects a spatial impact. In fact, the

greater the probability that a PMN encountered a bacterium, the more likely it would have reacted, which ultimately reduced the fluctuations.

On the other hand, the predicted high-frequency oscillating trend of the osteocyte population after $t = 200$ h was unexpected. It was expected to display a rapid decreasing phase, and then a slower increasing phase. This considerable fluctuations in osteocyte population appeared interesting as it could partially explain the inter-individual variability. Further, these fluctuations increased in intensity over time, raising the question if it could be explained as a pre-chaotic behavior "positive feedback". It was also noted that the PMN and the bacteria populations reach their minimum level simultaneously before rising again. This weakness in the innate immune response could provide a best possible window to start the therapeutic treatment.

From another point of view, the model showed the ability to reproduce the infection with resulting patterns of system behavior that are close to what is observed clinically and microbiologically (Wagner et al., 2003). It has also shown its predictive ability for the evolution of bone mass with respect to the bacterial inoculum size and time.

Despite the model features, several limitations emerged during the work and need to be enhanced. The first limitation is the model validation due to the lack of experimental data, which might be acquired at a later stage (e.g., the bone mass). Actually, the available patient data are the blood count and the images which are far from been used in validating this model.

The 2D representation represents a limitation with regards to the ability of agents to interact in 3D space. However, we adopted the simplicity in building this first model aiming at developing a feasible modeling framework and understanding the complex integration of available physiological data with the ABM modeling framework. For future work, other ABM platforms aimed to be discovered in order to choose the best one for the 3D implementation of bone tissue architecture including the ECM. We aimed at enhancing the model by a more realistic architecture using patient-specific data.

The current model did not take in the account the second stage of the immune response, the adaptive immune response, which is necessary to investigate further progression of the infection. The current model also lacks of presenting the bacteria biofilms, which play an important role in identifying the behavior of the bacteria themselves and the system response due to their resistance to immune defense and antibiotic agents. Since biofilms are important in *S. aureus* pathogenesis during BJI, it is worthwhile to model them in the future. Other agents including implants and bacterial survival factors have a significant contribution in introducing an additional approximation to mimic the real system, which aimed at being integrated in the future. This work highlights the progression of the simulation environment that generates data which would be used in the extraction and synthesis of the model in the form of dynamical systems.

6. Analyzing BJI Model Simulation Output Data Using System Dynamics Approach

Analyzing the model output is an essential part of the modeling process to describe, explore, and predict the model outcomes. The BJI model simulations result in different patterns of cell population changes for different initial conditions. Since one simulation is not enough to study properly and rigorously the model, many simulations are needed with a lot of key parameters testing. Therefore, so many simulation data cannot be analyzed easily by a human. There is a need for some information extraction techniques that summarize the overall model through its simulations. Differential equations (DEs) are a possibility that allows both numerical solution and structural analysis for a qualitative investigation of the system.

In this study, we modeled a complex system with a meta-analysis-like approach, by which we characterized the model's agents and quantified its parameters. Then, we ran several simulations with a variety of parameters values and tried to summarize this complex system with the most possible compact and useful representation, here the differential equations. This chapter explains the method used to analyze the BJI model simulation data using nonlinear differential equations and the obtained results.

6.1. System Dynamics Approach

We relied on the system dynamics approach and data-driven methodology to model the BJI model simulation output data with nonlinear, polynomial differential equations. We extracted the nonlinear DE system from data rather than testing predefined models against data. We identified the DE models that fit the agent's dynamics time series data and include interactions terms of these variables. We used the method and the developed R package proposed by Ranganathan and colleagues, namely Bayesian Dynamical Systems Modeling " *bdynsys*" (Ranganathan et al., 2014a). The Bayesian framework is used in this method to identify the shape of the systems and to select the best fit model among other plausible models that have a different number of terms.

We used models that identify relationships in cell population level to understand the data patterns that emerged from bottom level interactions (cells and signals) in order to answer questions about the causes of the infection progression and identify potential relationships between the components. This method uses the nonlinear polynomial differential equations to fulfill its purpose since they identify the changes in one variable at time t and $t+1$ as a function of the other variables in the system at time t .

The methodology of the approach is first described for two variables, and then it is generalized (Ranganathan et al., 2014a). It is applied on longitudinal dataset containing changes in M entities and N variables over time of length T to fit them with the corresponding ordinary differential equations (ODE) system that can be represented as:

$$\frac{dX_1}{dt} = f_1(X_1, X_2) \quad (\text{eq. 6.1})$$

$$\frac{dX_2}{dt} = f_2(X_1, X_2) \quad (\text{eq. 6.2})$$

The degree of the polynomial $f_i(\cdot)$ is chosen considering two principal constraints. First, to be of sufficient degree to allow modeling enough non-linearity that reflects sufficient complexity of the model. Second, to keep the number of estimated models acceptable, and keep allowing capturing the interactions between variables.

For computational purposes, it is assumed that the function $f_i(\cdot)$ contains the terms that result from the different combinations of the variables each of power -1, 0, and 1:

$$a_0 + \frac{a_1}{X_1} + \frac{a_2}{X_2} + a_3 X_1 + a_4 X_2 + \frac{a_5}{X_1 X_2} + \frac{a_6 X_2}{X_1} + \frac{a_7 X_1}{X_2} + a_8 X_1 X_2$$

It is also allowed for the quadratic and cubic terms in the variables or their reciprocals, which allow capturing the nonlinear impact of the variables themselves:

$$a_9 X_1^2 + a_{10} X_2^2 + \frac{a_{11}}{X_1^2} + \frac{a_{12}}{X_2^2} + a_{13} X_1^3 + a_{14} X_2^3 + \frac{a_{15}}{X_1^3} + \frac{a_{16}}{X_2^3}$$

The method starts the standard performance of two variables model by studying models of the form:

$$\begin{aligned} f_i(X_1, X_2) = & a_0 + \frac{a_1}{X_1} + \frac{a_2}{X_2} + a_3 X_1 + a_4 X_2 + \frac{a_5}{X_1 X_2} + \frac{a_6 X_2}{X_1} + \frac{a_7 X_1}{X_2} + a_8 X_1 X_2 + a_9 X_1^2 \\ & + a_{10} X_2^2 + \frac{a_{11}}{X_1^2} + \frac{a_{12}}{X_2^2} + a_{13} X_1^3 + a_{14} X_2^3 + \frac{a_{15}}{X_1^3} + \frac{a_{16}}{X_2^3} \quad (eq. 6.3) \end{aligned}$$

A model is identified by a set of coefficients $\{a_0, \dots, a_{16}\}$ that were acquired from the best fit regression of the corresponding polynomial terms.

For the previous general model of 17 terms (eq.6.3), different models with different number of terms m can result from the possible combinations. Thus, the number of models that have m terms is the result of $\binom{17}{m}$.

The fitting method is applied to select the best models that fit the data among all those possible models using two steps. The first step is to detect the maximum-likelihood model for each possible number of terms m , by fitting the variation in the indicator variables employing multiple linear regression over the $2^{17} = 131072$ possible models. The log-likelihood value is calculated for all models:

$$\log P(dx_1 | x_1, x_2, \Phi) \quad (eq. 6.4)$$

Where Φ is representing the parameter set of each specific model. Thus, the best fit model with the maximum-likelihood $L_i(m)$ for each number of terms is obtained in this step, $f_i^*(X_1, X_2; \Phi_i^*(m)), i = 1, 2$.

In the second step of the selection algorithm, the Bayesian marginal-likelihood or the *Bayes factor* $B_i(m)$ is calculated for the models obtained from the first step (MacKay, 2002; Skilling, 2006). Bayesian marginal-likelihood is used to compare between a set of models and to choose the one with the largest $B_i(m)$ value as the best overall model. Since the models acquired by the first step are those with the highest log-likelihood for each possible number of terms, the *Bayes factor* will be applied to select through these models the one with the best number of terms.

$$B_i(m) = \int_{\Phi_i(m)} P(dx_i | x_1, x_2, \Phi_i(m)) \pi(\Phi_i(m)) d\Phi_i(m) \quad (eq. 6.5)$$

where $i = 1, 2$, and $\pi(\Phi_i(m))$ is the prior distribution of the parameters, which is assumed as uniform over the parameters' range (Bishop, 2006). This process is done for the both function $f_1^*(X_1, X_2; \Phi_1^*(m))$ and $f_2^*(X_1, X_2; \Phi_2^*(m))$.

In the absence of prior knowledge about the system, we choose as the best fit model the one with the highest Bayes factor.

For systems with more than two variables, as in our case, the described method for two variables is expanded to get the best models by calculating $f_i^*(X_1, X_2, \dots, X_N; \phi_i^*(m_i))$, $i = 1, \dots, N$, and both of $L_i(m)$ and $B_i(m)$. Since the number of models that will be explored increases exponentially with the number of variables, and due to computational issue, the model space is explored for models with up to five terms in this state (Ranganathan et al., 2014a).

6.2. Methods

6.2.1. Software

We used "bdynsys" package in R, that could be reached on CRAN (<https://cran.r-project.org>), and which implemented by Ranganathan and colleagues (Ranganathan et al., 2014b). This package integrates methods to modeling the dynamics in up to four variables in longitudinal data over time as a function of the variables themselves and up to three predictor variables using the ordinary differential equations and polynomial terms. Within this package, the described Bayesian model selection method is implemented to choose the best fit models for each number of terms. The package includes tools to visualize phase portraits of the variables in the systems or to compare the Bayes factors of different models. The main tool in this package is "bdynsys" function that performs the Bayesian dynamical system modeling process. It is given by:

$$\text{bdynsys}(\text{dataset}, \text{indnr}, \text{paramnr}, x, y, z, v) \quad (\text{fun 6.1})$$

The function's arguments include:

dataset: panel data frame.

indnr: number of the indicator variables to be included in the modeling process.

paramnr: maximum number of polynomial terms included.

x , y , z , v : references of the variables from the dataset to be included as indicators 1, 2, 3, and 4, respectively.

The result of this function is the best first three models for the defined variables and for each number of terms, up to the maximum number defined in the function. The calculated Bayes factor is also obtained from this function for each selected model.

6.2.2. Methods of analysis

We applied Bayesian dynamical systems modeling approach on the output data of the proposed agent-based model of BJI system, aiming at two objectives: (a) verifying the simulation coherence when running for the same initial conditions, and (b) identifying relationships between model's agents. We investigated the relationship between bacteria dynamics and the host tissue cells dynamics, more specifically the relationships between bacteria, neutrophils, and osteocyte populations under different initial conditions. This method is able to capture the nonlinear and complex behaviors of the variables using differential equation models.

However, this method is applied on a longitudinal data, so we produced the output data of BJI model simulations for agent population changes over time in the form of panel data and saved them to ".csv" file. The time step between the time t and $t+1$ was 1 tick which is equal to 1 hour.

a. Exploring System Behavior for the Same Initial Conditions

Since the BJI model uses random seeds, the coherence behavior of the system for the same initial conditions during different iterations should be confirmed. In other words, the independent simulations should reproduce similar outputs for the same input data, and this is considered as one of the verification faces of an agent-based model (Xiang et al., 2005).

We explored the different behaviors of the system through comparing the resulting differential equations models of different iterations in order to confirm the model internal validity. The R-squared value for each model was calculated and compared with the other models. R-squared value is a measure of how close the data are from the fitted model and its value ranges between 0 and 100%.

We followed the following steps.

- 1- Fixing the initial conditions (input parameters) as given in (Table 6.1).
- 2- Running the simulation 20 iterations and generating one corresponding output file that contains the variables changes for the 20 iterations (first group).
- 3- Calculating the differential equations corresponding to this first group of iterations, that represents the first dynamical system (Code snippet 2).
- 4- Rerunning the simulation for another 20 iterations (second group) under the same initial conditions, generating the corresponding output file and calculating the new DE system.
- 5- Redo the process until having 10 different groups of DE systems each one is for 20 iterations.
- 6- For each iterations group, the DE systems are obtained for two terms models, and as a function of two variables. We get the models for the relationship between bacteria and neutrophil population, then the relationship between bacteria and osteocyte population.
- 7- Comparing the resulting DE systems.

Table 6.1. The parameters' values at the initial state during 200 iterations of BJI model simulation for testing the system behavior coherence

Bacteria inoculum size = 10 CFU	osteoblasts reproduction rate = 5 cell/day
bacteria reproduction rate = 12 h	osteoblasts death rate = 90 days
macrophages reproduction rate = 250 cell/day	osteoclasts reproduction rate = 3 cell/day
macrophages death rate = 24 h	osteoblasts death rate = 12 days
neutrophils reproduction rate = 250 cell/day	monocytes reproduction rate = 150 cell/day
neutrophils death rate = 48 h	monocytes death rate = 120 h

```

library("bdynsys", lib.loc="~/R/win-library/3.3")

# loading the csv file for the first group of 20 iterations (redoing this code for the whole groups)

myData <- read.csv("group01.csv",header=TRUE, sep=",", stringsAsFactors=FALSE)

# converting dataframe to panel dataframe

myPanelData<-pdata.frame (myData, index = "ID", drop.index = FALSE, row.names=TRUE)

# calculating the DE models of two terms for bacteria and neutrophils (PMN) dynamics

bdynsys(myPanelData, 2, 2, myPanelData$BACTERIA, myPanelData$PMN)

# calculating the DE models of two terms for bacteria and osteocyte (OS) dynamics

bdynsys(myPanelData, 2, 2, myPanelData$BACTERIA, myPanelData$OS)

```

Code Snippet 2: R code for calculating the DE systems using *bdynsys* function

b. Analyzing Variable Relationships

In this step, we used the Bayesian dynamical system method to analyze the relationships between the model variables under different initial conditions. This analysis enables studying the model dynamics in responding to the input variations and exploring different patterns of the system's behavior. The system was investigated using varying values of inoculum size, and bacteria reproduction rate. The initial values of other parameters were fixed. The effects of these varied inputs were observed on the dynamics of each of bacteria, neutrophils, and osteocytes cells. The steps follow.

1- Setting the model parameters to their initial values that given in (Table 6.1), except the value of bacteria inoculum size which was set to value 50 (CFU/mm³) and the bacteria reproduction rate to value 2 h.

2- Running the simulation 20 iterations under the same initial conditions and generating the output file that contains the outcomes for bacteria, neutrophil, and osteocyte populations for each time step and for all iterations (.csv file).

3- Changing the initial inoculum size of bacteria between the values (50, 100, 150, 250 CFU/mm²), and for each of these inoculum values we changed the reproduction rate of bacteria between the values (2, 4, 6, 12, 18, 24 h) (Table 6.2).

4- Running the simulation n= 20 iterations for each group of initial conditions and calculating the corresponding differential equation systems for each output file. We calculated the DEs using *bdynsys* function for 3 terms and 2 variables, first for bacteria and PMN, then for bacteria and osteocyte populations.

5- Comparing the output of the dynamical system model with the output of the BJI model simulation.

6- Combining the simulation data for the different initial conditions of bacteria inoculum size, while the same reproduction rate of 6 hours in one (.csv) file and calculating the corresponding dynamical system models for each possible number of terms of bacteria, neutrophils, and osteocytes variables.

7- Choosing the best overall dynamical system models by comparing the Bayes factor for the different number of terms models.

Table 6.2. The initial conditions used to identify relationships between variables. The table represents values of bacterial inoculum size (CFU/mm²) and reproduction rate (h) parameters for the 24 groups of simulations, for which each run for 20 iterations.

Bacteria inoculum size	50 (CFU/mm²)					
Bacteria reproduction rate	2 h	4 h	6 h	12 h	18 h	24 h
Bacteria inoculum size	100 (CFU/mm²)					
Bacteria reproduction rate	2 h	4 h	6 h	12 h	18 h	24 h
Bacteria inoculum size	150 (CFU/mm²)					
Bacteria reproduction rate	2 h	4 h	6 h	12 h	18 h	24 h
Bacteria inoculum size	250 (CFU/mm²)					
Bacteria reproduction rate	2 h	4 h	6 h	12 h	18 h	24 h

6.3. Results

a. Exploring System Behavior for the Same Initial Conditions

The two terms differential equation systems for the population of bacteria, neutrophils, and osteocytes for the 10 groups of iterations under the same initial conditions with their R-squared values are shown in (Table 6.3). Each group was calculated for 20 iterations of the BJI model simulation.

Table 6.3. The two terms DE systems that result from the Bayesian dynamical system modeling method with their R-squared values. These systems were calculated for 10 groups of simulation data that were generated under the same initial conditions. The first column presents the DE systems for the bacteria population (x) and the neutrophil population (y), and the second column presents the DE systems for the bacteria population (x) and the osteocyte population (y).

Group	2 terms DE system of bacteria (x) (CFU) and neutrophils (y) (cells)		2 terms DE system of bacteria (x) (CFU) and osteocytes (y) (cells)	
	dx =	R ² =	dx =	R ² =
group 1	$dx = + 69 x/y - 2.4 \times 10^{-7} y^3$ $dy = + 0.18 x - 0.00038 y^2$	R ² = 0.71 R ² = 0.70	$dx = + 0.00045 xy - 4 \times 10^{-4} x^2$ $dy = + 0.10 y - 6.9 \times 10^{-8} y^3$	R ² = 0.61 R ² = 0.19
group 2	$dx = + 73 x/y - 2.7 \times 10^{-7} y^3$ $dy = + 0.18 x - 0.00039 y^2$	R ² = 0.82 R ² = 0.70	$dx = + 0.00047 xy - 4 \times 10^{-4} x^2$ $dy = + 0.13 y - 5.8 \times 10^{-8} y^3$	R ² = 0.62 R ² = 0.19
group 3	$dx = + 71 x/y - 2.5 \times 10^{-7} y^3$ $dy = + 0.17 x - 0.00036 y^2$	R ² = 0.79 R ² = 0.69	$dx = + 0.00047 xy - 4 \times 10^{-4} x^2$ $dy = + 0.11 y - 5.9 \times 10^{-8} y^3$	R ² = 0.62 R ² = 0.11
group 4	$dx = + 70 x/y - 2.7 \times 10^{-7} y^3$ $dy = + 0.18 x - 0.00039 y^2$	R ² = 0.75 R ² = 0.66	$dx = + 0.00045 xy - 0.00039 x^2$ $dy = + 0.083 y - 6.9 \times 10^{-8} y^3$	R ² = 0.58 R ² = 0.19
group 5	$dx = + 71 x/y - 2.7 \times 10^{-7} y^3$ $dy = + 0.17 x - 0.00037 y^2$	R ² = 0.79 R ² = 0.68	$dx = + 0.00047 xy - 0.00041 x^2$ $dy = + 0.083 y - 5.9 \times 10^{-8} y^3$	R ² = 0.63 R ² = 0.19
group 6	$dx = + 69 x/y - 2.6 \times 10^{-7} y^3$ $dy = + 0.17 x - 0.00038 y^2$	R ² = 0.77 R ² = 0.62	$dx = + 0.00043 xy - 0.00037 x^2$ $dy = + 0.091 y - 6.4 \times 10^{-8} y^3$	R ² = 0.65 R ² = 0.12
group 7	$dx = + 69 x/y - 2.6 \times 10^{-7} y^3$ $dy = + 0.16 x - 0.00035 y^2$	R ² = 0.78 R ² = 0.67	$dx = + 0.00046 xy - 4 \times 10^{-4} x^2$ $dy = + 0.11 y - 7.9 \times 10^{-8} y^3$	R ² = 0.65 R ² = 0.15
group 8	$dx = + 71 x/y - 2.6 \times 10^{-7} y^3$ $dy = + 0.18x - 0.00037 y^2$	R ² = 0.78 R ² = 0.67	$dx = + 0.00045 xy - 0.00039 x^2$ $dy = + 0.093y - 5.9 \times 10^{-8} y^3$	R ² = 0.57 R ² = 0.15
group 9	$dx = + 70 x/y - 2.6 \times 10^{-7} y^3$ $dy = + 0.17 x - 0.00036 y^2$	R ² = 0.79 R ² = 0.66	$dx = + 0.00045 xy - 0.00039 x^2$ $dy = + 0.11 y - 7.6 \times 10^{-8} y^3$	R ² = 0.63 R ² = 0.16
group 10	$dx = + 68 x/y - 2.6 \times 10^{-7} y^3$ $dy = + 0.18 x - 0.00039 y^2$	R ² = 0.76 R ² = 0.68	$dx = + 0.00041 xy - 0.00035 x^2$ $dy = + 0.094 y - 6.6 \times 10^{-8} y^3$	R ² = 0.52 R ² = 0.13

The system dynamics in the first column are calculated for the bacteria and neutrophil population. The (x) variable in the equations represents the bacteria population, while the (y) variable represents the neutrophil population. The second column presents the system dynamics models for the bacteria population (x) and the osteocyte population (y). The resulting equations are the best fit 2-term models with the highest log-likelihood for the defined initial conditions.

Then, we compared the shape of the differential equations in the 10 groups and for each variable that shown in (Table 6.3). We then calculated the mean (M) and the standard deviation (SD) of the equations' coefficients of those 10 models for each variable (Table 6.4).

Table 6.4. The form, coefficient values and R-squared values for each variables' models that are represented in (Table 6.3).

System	DE form	Mean Coefficient	SD Coefficient	Mean R ²	SD R ²
Bacteria (x) and PMN (y) dynamics system	$\frac{dx}{dt} = a x/y + b y^3$	$a = 70.1$	1.4	0.78	0.02
		$b = -2.6 \times 10^{-7}$	0.09×10^{-7}		
	$\frac{dy}{dt} = c x + d y^2$	$c = 0.174$	0.007	0.67	0.02
		$d = -3.8 \times 10^{-4}$	0.14×10^{-4}		
Bacteria (x) and OS (y) dynamics system	$\frac{dx}{dt} = a xy + b x^2$	$a = 4.5 \times 10^{-4}$	0.2×10^{-4}	0.61	0.04
		$b = -3.9 \times 10^{-4}$	0.17×10^{-4}		
	$\frac{dy}{dt} = c y + d y^3$	$c = 0.1$	0.015	0.16	0.03
		$d = -6.7 \times 10^{-8}$	0.7×10^{-8}		

PMN: neutrophils, OS: osteocytes, Coeff: Coefficient

These results show that the DE models of different groups of BJI model given data under the same initial conditions have a similar form for each set of variable equations and small variances between the coefficient values of that set. That could be translated as an indicator for the similar behaviors of the system using the same initial conditions.

In addition, the different calculated models under the same initial conditions show a similar R-squared value for the same variable in one equation system. This value might also indicate the similarity in the behaviors of the system under the same initial conditions. It is noted that the R-squared measurements have good values for the bacteria and neutrophils models in the first system, which means that the calculated models are well fitting the BJI model simulation data. Regarding the bacteria and osteocytes system, the R-squared values are good for the bacteria dynamics models while their values for osteocytes dynamics model are remarkably low. This result is coupled with the observation that the calculated osteocyte dynamics models are autonomous, in which they only depend on y . That leads to the need for including more terms in the calculated equations and more variables to study the ability to enhance the model fitting goodness.

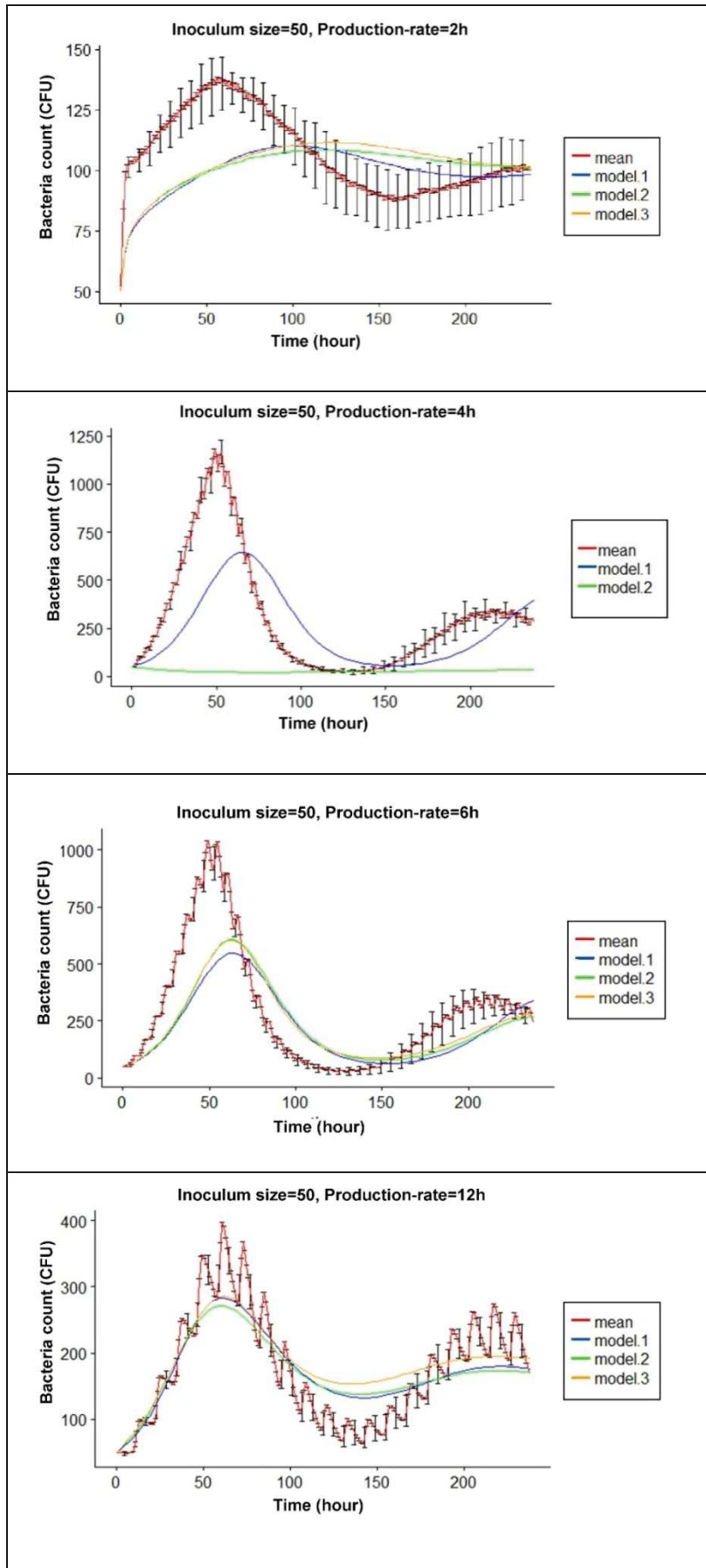
b. Identifying Variable Relationships

The impact of the bacterial inoculum size and the reproduction rate was investigated over different values and retrieved a set of differential equations. In (Table 6.5) we listed the calculated models for the initial condition of inoculum size (50 CFU/mm^2) and different values of reproduction rate of bacteria (2, 4, 6, 12, 18, 24 h). These resulting models are calculated for two variables, bacteria (x) and neutrophil (y) populations, and for three terms equations.

We compared these best fit models with the means of 20 iterations of the BJI model simulation outputs in (Figure 6.1-6.2). Additional calculated dynamical models with the DE systems for inoculum size of ($100, 150, 250 \text{ CFU/mm}^2$) along with different reproduction rate, for bacteria, neutrophil, and osteocyte populations are represented in the Appendix (Figure B.1-B.11) and (Table B.1-B-2).

Table 6.5. The calculated three terms differential equations systems for bacteria (x) and neutrophils (y) dynamics when bacteria inoculum size= 50 (CFU/mm²) and for different bacteria reproduction rates= 2, 4, 6, 12, 18, 24 (h).

GROUP	3 terms DE systems of 2 variables: Bacteria population (x) and Neutrophil population (y) R function: bdynsys(mydata, 2, 3, mydata\$Bacteria, mydata\$PMN)
Condition 1: Bacteria inoculum size= 50 CFU/mm ² , Bacteria reproduction rate= 2h	$dx = -249212/(xy) + 406455/y^2 + 3423620/x^3$ $dx = -526/x + 6.1 x/y + 2807177/x^3$ $dx = +606/y - 77185/x^2 + 5305618/x^3$ <hr/> $dy = +0.038 x - 1.8 y/x + 6 \times 10^{+5}/x^3$ $dy = -0.026 y + 5.7 x/y + 0.00016 xy$ $dy = +0.042 x - 0.026y + 8.1 \times 10^{-5} xy$
Condition 2: Bacteria inoculum size = 50 CFU/mm ² , Bacteria reproduction rate= 4h	$dx = + 0.086 x - 0.00016 xy + 2.8 \times 10^{-5} x^2$ $dx = - 0.00015 xy + 0.00029 x^2 - 1.7 \times 10^{-7} x^3$ $dx = -3.9 + 0.11 x - 0.00015 xy$ <hr/> $dy = - 987/y + 13 x/y - 0.79 y/x$ $dy = + 0.041 x - 0.9 y/x - 3.1 \times 10^{-5} xy$ $dy = -284/x + 0.028 x - 1.2 \times 10^{-5} y^2$
Condition 3: Bacteria inoculum size = 50 CFU/mm ² , Bacteria reproduction rate= 6h	$dx = +0.085x - 0.00016 xy + 2.5 \times 10^{-5} x^2$ $dx = +0.13x - 8.2 x/y - 0.00018 xy$ $dx = +0.092x - 0.00016 xy + 1.5 \times 10^{-8} x^3$ <hr/> $dy = -1015/y + 14 x/y - 0.8y/x$ $dy = +0.04 x - 0.93 y/x - 2.9 \times 10^{-5} xy$ $dy = +0.027 x - 0.75 y/x - 8.2 \times 10^{-6} y^2$
Condition 4: Bacteria inoculum size = 50 CFU/mm ² , Bacteria reproduction rate= 12h	$dx = +0.073 x - 0.00015 xy - 1.8 \times 10^{-7} x^3$ $dx = +0.082 x - 0.00015 xy - 8.5 \times 10^{-5} x^2$ $dx = +0.063x + 0.0065 y - 0.00018 xy$ <hr/> $dy = +0.033x - 2y/x + 519329/x^3$ $dy = +0.033 x - 2.1y/x + 11689/x^2$ $dy = +0.059x - 0.038 y + 3 \times 10^{-5} y^2$
Condition 5: Bacteria inoculum size= 50 CFU/mm ² , Bacteria reproduction rate= 18h	$dx = +9.5 - 351/x - 0.00014 xy$ $dx = +0.075x - 0.00014 xy - 0.00016 x^2$ $dx = +0.063x - 0.00015 xy - 4.6 \times 10^{-7} x^3$ <hr/> $dy = +0.037x - 2 y/x + 555997/x^3$ $dy = +0.037 x - 2.1 y/x + 11999/x^2$ $dy = +0.087x - 0.025 y - 7.4 x/y$
Condition 6: Bacteria inoculum size= 50 CFU/mm ² , Bacteria reproduction rate= 24h	$dx = +5.6 - 0.00015 xy - 373021/x^3$ $dx = +6.3 - 0.00015 xy - 8976/x^2$ $dx = +8.2 - 259/x - 0.00016 xy$ <hr/> $dy = +0.092 x - 0.026 y - 6.9 x/y$ $dy = +0.064 x - 0.023 y - 1.1e+07/y^3$ $dy = -0.016 y + 5 \times 10^{-4} x^2 - 1.2 \times 10^{-6} x^3$



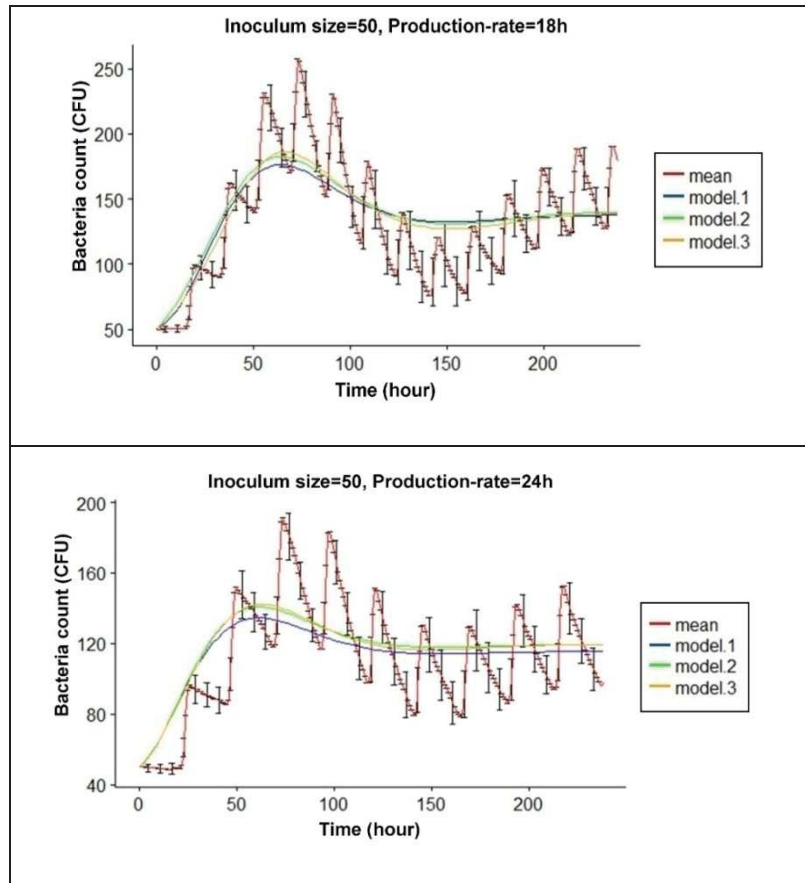
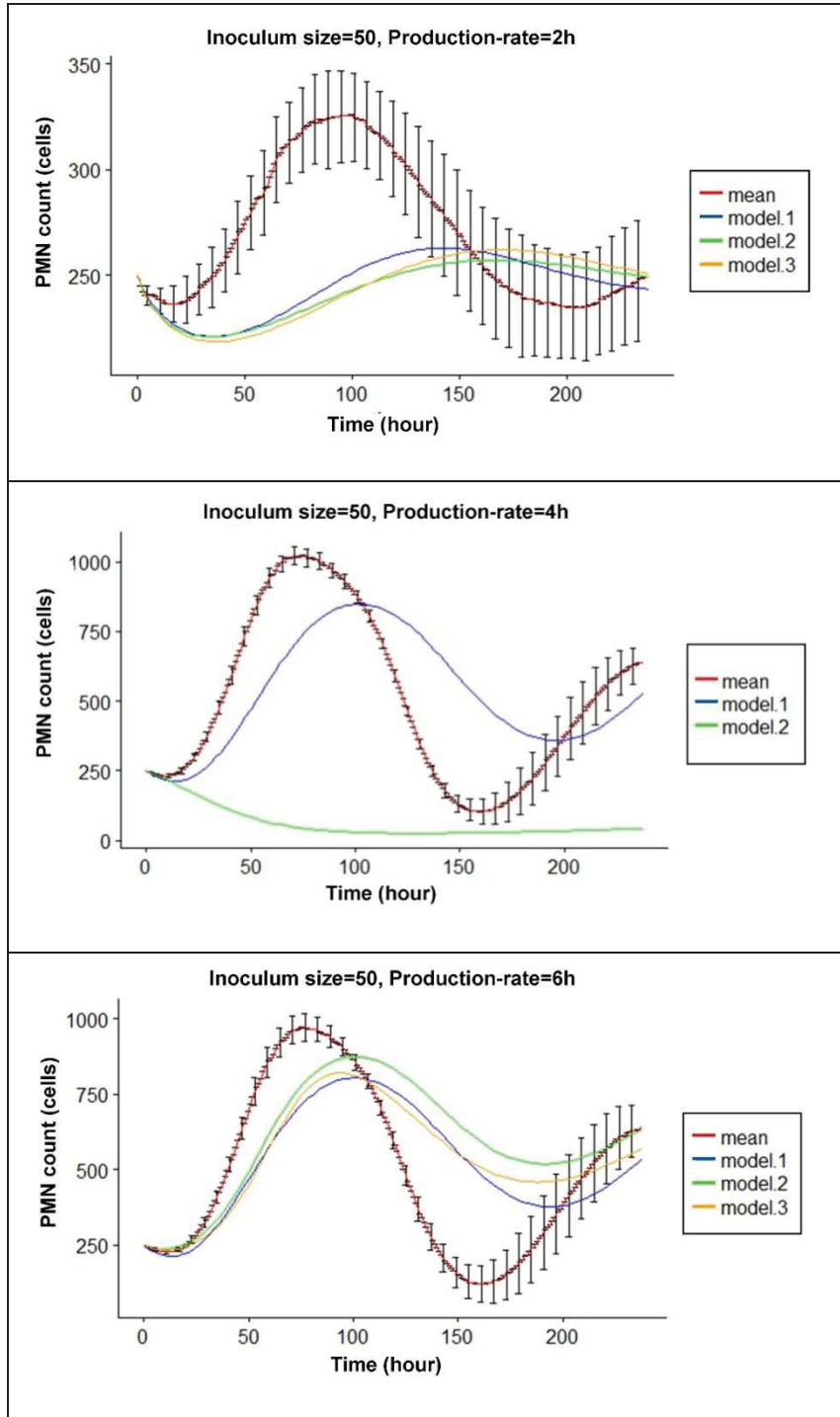


Figure 6.1. Comparison between the BJI model simulation outputs and the system dynamics model outputs of bacteria population over time. The outputs were calculated for bacteria inoculum size= 50 (CFU/mm²) and for different values of bacterial reproduction rate= 2, 4, 6, 12, 18, 24 hours, respectively. The red line represents the mean of 20 iterations of simulation output. The other lines represent the three best-fit models calculated by Bayesian dynamical system approach for the same data. The blue line represents the first best fit calculated model. The green line represents the second best fit calculated model. The orange line represents the third best fit calculated model.

As we mentioned before, the function "*bdynsys*" calculates the best three models according to the Bayes factor. We represented here the three resulting models within these figures, except in some cases where the calculated models are non-reasonable and out of range. It is noted that the calculated models of bacteria change for the values 2, 4, and 6 hours of bacteria reproduction rate differ from the simulation output, especially in the maximum and minimum values with a time offset in some cases. Nevertheless, the calculated models for the bacteria reproduction rate values equal to 12, 18 and 24 hours are very close to the simulation outputs. These observations were also noted for the models calculated for the inoculum size of 100, 150, while with more variation for 250 (CFU/mm²) (Figure B.1-B.3 in the Appendix).



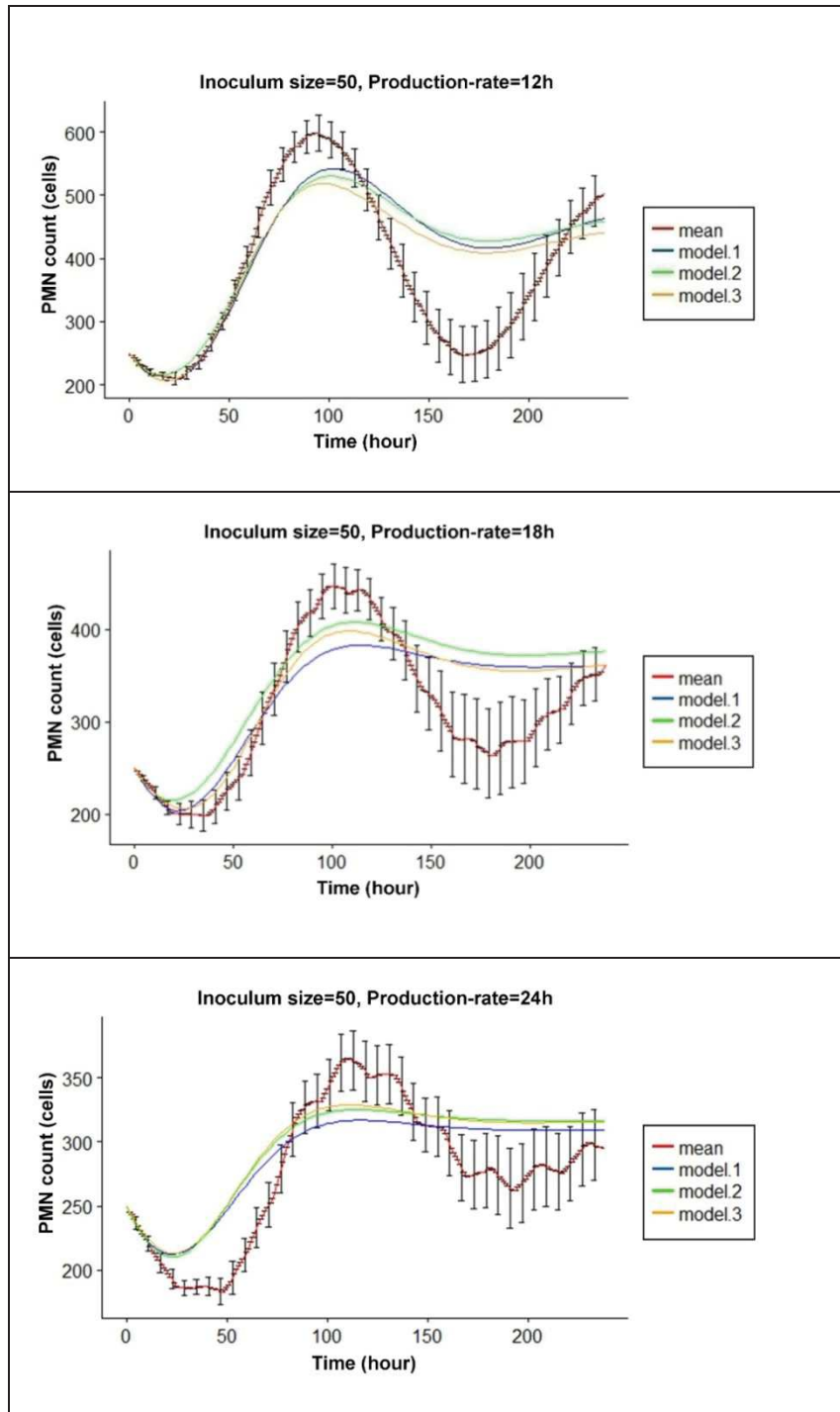


Figure 6.2. Comparison between BJI model simulation outputs and the system dynamics model outputs of the neutrophil (PMN) population over time. The outputs were calculated for bacteria inoculum size= 50 (CFU/mm³), and for different values of bacterial reproduction rate= 2,4,6,12,18 and 24 hours, respectively. The red line represents the mean of 20 iterations of simulation output. The other lines represent the three best-fit models calculated by Bayesian dynamical system approach for the same data. The blue line represents the first best calculated model. The green line represents the second best calculated model. The orange line represents the third best fit calculated model.

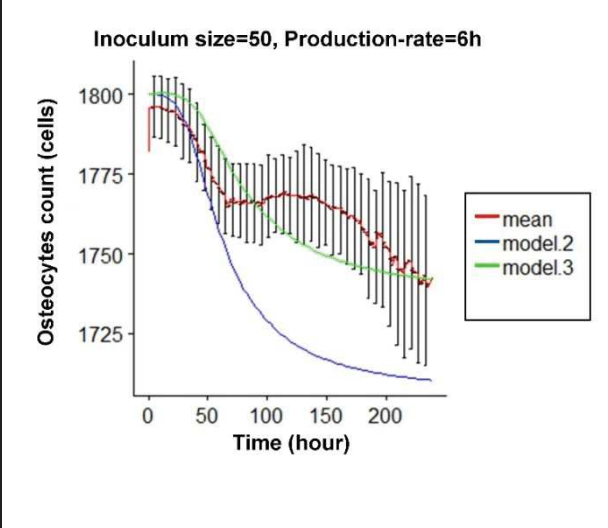
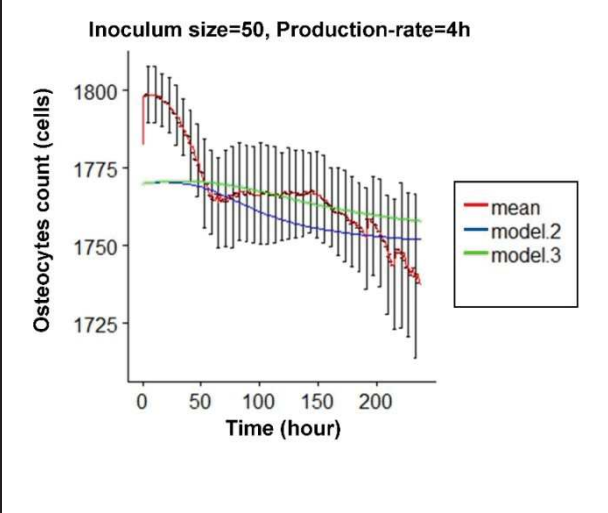
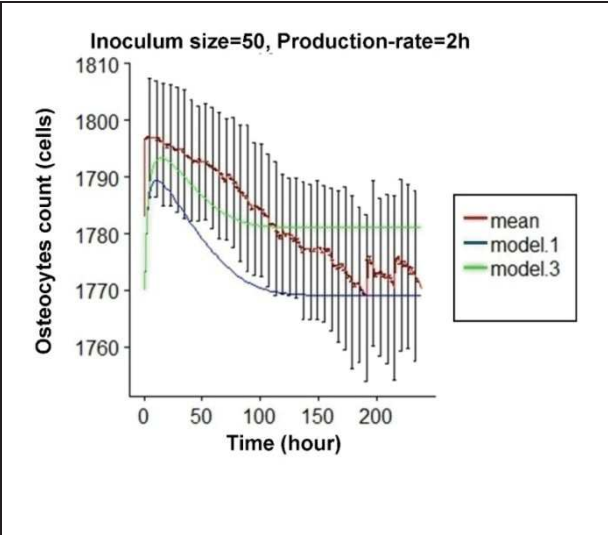
The calculated models for the neutrophils populations introduced differences between the simulation models and the dynamical systems models with the values 2, 4, and 6 hours of reproduction rates (Figure 6.2). For the results of the values 12, 18 and 24 hours of reproduction rates, the dynamical systems could capture the dynamics of the neutrophil population in the first phase (up to $t=120$ hours), after that, it showed big differences between the dynamical models and the simulation. Similar behaviors were noted for models calculated for inoculum size = 100 (CFU/mm²), while more differences were noted in the models calculated for the inoculum size= 150, 250 (CFU/mm²) (Figure B.4-B.6 in the Appendix).

Similarly, the dynamical models of osteocytes cells as a function of themselves and bacteria was calculated for the longitudinal data generated from the ABM model of BJI. The best three fit models of three terms for bacteria initial inoculum equal to 50 (CFU/mm²) and different bacteria reproduction rate (2, 4, 6, 12, 18, 24 hours), are given in (Table 6.6), where x variables represents the bacteria population and y variable represents the osteocyte population. We displayed the resulting best-selected models with the output of BJI model simulation as a mean of 20 iterations for the same initial conditions in (Figure 6.3).

By comparing the result, it is notable that the calculated dynamic models were able to capture the dynamics of the osteocytes cells in the given time ($t=0-240$ hours) for the different reproduction rate of bacteria with a little more differences for the reproduction rate of 2, 4, 6 hours. It is noted that in all cases, the high-frequency oscillation within the agent dynamics could not be considered in the dynamical models. For the inoculum size= 100, 150 (CFU/mm²), the dynamic models showed differences from the simulation output, while they were closer for the inoculum size= 250 (CFU/mm²) and reproduction rate = 12, 18, 24 hours (Figure B.9-B-11).

Table 6.6. The calculated three terms differential equations systems for bacteria population (x) and osteocyte population (y) dynamics for bacteria inoculum size = 50 (CFU/mm²) and for different bacteria reproduction rates (2, 4, 6, 12, 18, 24 h).

GROUP	3 terms DE systems of 2 variables: Bacteria population (x) and Osteocyte population (y) R function: bdynsys(mydata, 2, 3, mydata\$Bacteria, mydata\$Osteocyte)
Condition 1: Bacteria inoculum size= 50 CFU/mm ² , Bacteria reproduction rate= 2h	$\begin{aligned} dx &= -6295/x + 3.4y/x + 1813531/x^3 \\ dx &= -5581341/(xy) + 1.7y/x + 1812667/x^3 \\ dx &= +5893/x - 1.1 \times 10^{+7}/(xy) + 1811915/x^3 \\ dy &= +1196593/(xy) - 135970/x^2 + 6563221/x^3 \\ dy &= +618/x - 127079/x^2 + 6222056/x^3 \\ dy &= -74810/x^2 + 4809727/x^3 + 1.3 \times 10^{+10}/y^3 \end{aligned}$
Condition 2: Bacteria inoculum size= 50 CFU/mm ² , Bacteria reproduction rate= 4h	$\begin{aligned} dx &= -1.9x + 0.0011xy - 3.9 \times 10^{-5} x^2 \\ dx &= -1.9x + 0.0011xy - 2.6 \times 10^{-8} x^3 \\ dx &= -1670x/y + 0.00055 xy - 3.9 \times 10^{-5} x^2 \\ dy &= +1.9x - 1695x/y - 0.00056 xy \\ dy &= +3.5/x + 0.021x - 1.2 \times 10^{-05} xy \\ dy &= +0.021x + 0.002y/x - 1.2 \times 10^{-05} xy \end{aligned}$
Condition 3: Bacteria inoculum size= 50 CFU/mm ² , Bacteria reproduction rate= 6h	$\begin{aligned} dx &= -108x + 93757x/y + 0.031xy \\ dx &= -1.5x + 0.00089xy - 4.6 \times 10^{-5} x^2 \\ dx &= -1.5x + 0.00087xy - 3.4 \times 10^{-8} x^3 \\ dy &= +0.022x - 1.3 \times 10^{-5} xy + 1.8 \times 10^{-11} y^3 \\ dy &= +0.022x - 1.3 \times 10^{-5} xy + 3.1 \times 10^{-8} y^2 \\ dy &= +20x/y - 6.7 \times 10^{-6} xy + 1.8 \times 10^{-11} y^3 \end{aligned}$
Condition 4: Bacteria inoculum size= 50 CFU/mm ² , Bacteria reproduction rate= 12h	$\begin{aligned} dx &= -0.4x + 0.00025xy - 0.00014x^2 \\ dx &= -357x/y + 0.00013xy - 0.00014x^2 \\ dx &= +0.47x - 776x/y - 0.00014x^2 \\ dy &= -4.5 \times 10^{+7}/y^2 + 88860/x^3 + 7.9 \times 10^{+10}/y^3 \\ dy &= -12716/y + 88914/x^3 + 3.9 \times 10^{+10}/y^3 \\ dy &= -4.8 + 88968/x^3 + 2.6 \times 10^{+10}/y^3 \end{aligned}$
Condition 5: Bacteria inoculum size= 50 CFU/mm ² , Bacteria reproduction rate= 18h	$\begin{aligned} dx &= -0.41x + 0.00026xy - 0.00024x^2 \\ dx &= -368x/y + 0.00014xy - 0.00024x^2 \\ dx &= -729994/(xy) - 100x/y + 2.1 \times 10^{-9} y^3 \\ dy &= -2663/x + 4676659/(xy) + 218842/x^3 \\ dy &= +2298545/(xy) - 0.75y/x + 218760/x^3 \\ dy &= +2573/x - 1.5y/x + 218676/x^3 \end{aligned}$
Condition 6: Bacteria inoculum size= 50 CFU/mm ² , Bacteria reproduction rate= 24h	$\begin{aligned} dx &= +2740359/(xy) - 51647/x^2 - 5.1 \times 10^{+10}/y^3 \\ dx &= +1551/x - 52496/x^2 - 2.9 \times 10^{+7}/y^2 \\ dx &= +1548/x - 52595/x^2 - 5.1 \times 10^{+10}/y^3 \\ dy &= -2827/x + 4923928/(xy) + 4963/x^2 \\ dy &= +2397612/(xy) - 0.79y/x + 4956/x^2 \\ dy &= +2683/x - 1.5y/x + 4949/x^2 \end{aligned}$



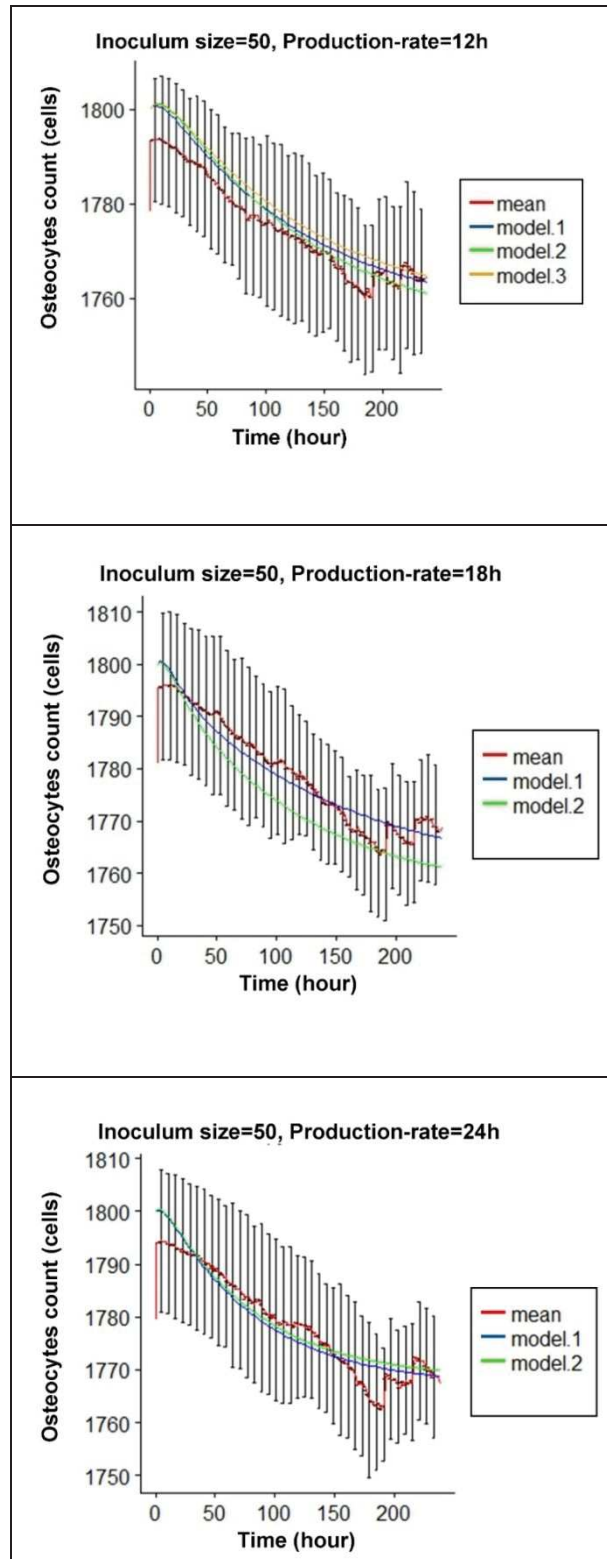


Figure 6.3. Comparison between BJI model simulation outputs and the system dynamics model outputs of the osteocyte population over time. The outputs were calculated for bacteria inoculum size= 50 (CFU/mm²), and for different values of bacterial reproduction rate= 2,4,6,12,18 and 24 hours, respectively. The red line represents the mean of 20 iterations of simulation output. The other lines represent the three best-fit models calculated by Bayesian dynamical system approach for the same data. The blue line represents the first acceptable best model. The green line represents the second acceptable best calculated model. The orange line represents the third acceptable best fit calculated model.

6.4. Analysis of Results: Optimal Selection of System Dynamics Model

The calculated models resulted from applying the steps described in 6.2.2.b by considering the model simulation data for all initial conditions of bacteria inoculum size (50, 100, 150, 250 CFU/mm²) and the same reproduction rates of 12 hours are shown in (Table 6.7). The table shows the system dynamics models with the maximum log-likelihood (MLL) and R-squared value for each number of terms models.

Table 6.7. System dynamics models of up to four terms with their maximum log-likelihood (MLL) calculated for data that combines the simulation output for different initial conditions of bacteria inoculum size (CFU/mm²). The models are calculated for bacteria (CFU), neutrophil (cells) and osteocyte population (cells).

Models of Bacteria (x) with PMN (y) dynamics	MLL	R²
$\frac{dx}{dt} = -1.9 \times 10^{-8} y^3$	-9256.74	0.03
$\frac{dx}{dt} = +0.058 x - 0.00012 x y$	-8922.96	0.07
$\frac{dx}{dt} = +0.054 x - 0.00014 x y + 3.6 \times 10^{-5} x^2$	-8874.54	0.08
$\frac{dx}{dt} = +0.041 x - 0.00014 x y + 0.00011 x^2 - 8.5 \times 10^{-8} x^3$	-8858.02	0.08
Models of PMN (y) with Bacteria (x) dynamics		
$\frac{dy}{dt} = +3.8 \times 10^{-5} x^2$	-6749.3	0.29
$\frac{dy}{dt} = +0.023 x - 0.81 y/x$	-2731.6	0.7
$\frac{dy}{dt} = +0.034 x - 0.0085 y - 0.56 y/x$	-2373.88	0.75
$\frac{dy}{dt} = -148/x + 0.057 x - 0.016 y - 0.29 y/x - 3.3 \times 10^{-5} x^2$	-2116.6	0.77
Models of Bacteria (x) with OS (y) dynamics		
$\frac{dx}{dt} = -2.4 \times 10^{-8} x^3$	-9532.99	0.006
$\frac{dx}{dt} = +4 \times 10^{-6} x y - 4.4 \times 10^{-8} x^3$	-9504.43	0.010
$\frac{dx}{dt} = -0.79 x + 0.00045 x y - 4.7 \times 10^{-5} x^2$	-9439.81	0.016
$\frac{dx}{dt} = -54 x + 47536 x/y + 0.015 x y - 4.9 \times 10^{-8} x^3$	-9429.03	0.018
Models of OS (y) with Bacteria (x) dynamics		
$\frac{dy}{dt} = -8.8 \times 10^{-7} x^2$	-9585.18	0.002
$\frac{dy}{dt} = -0.067 x + 118 x/y$	-9557.27	0.004
$\frac{dy}{dt} = -5.2 x + 4706 x/y + 0.0014 x y$	-9549.32	0.005
$\frac{dy}{dt} = -6952/x y - 8.6 \times 10^{-7} x^2 - 4.9 \times 10^{+7}/y^2 + 8.7 \times 10^{+10}/y^3 x^3$	-9546.3	0.006

PMN: neutrophils, OS: osteocytes

We can see that the MLL value increases with each addition of a new term. Since the Bayesian dynamical system modeling method first calculates the best fit models that have the MLL value for each number of terms, the Bayes factor is used then to choose the best overall model. For reducing the computational complexity, the Bayes factors in this method are calculated in their logarithmic value ($\log B_f$). (Figure 6.4) shows the Bayes factor for each number of terms (m) models of bacteria and neutrophils changes.

The Bayes factor for (a) bacteria dynamics significantly increased when we add a second term, increased slightly for $m = 3$, and $m = 4$. The best fit selected model is the model with the highest Bayes factor (the four terms model). Since complex models with a high number of terms overfitting the data and are more difficult to be interpreted, we can choose the model of three terms whose Bayes factor is only a little smaller. Considering the Bayes factor of neutrophils changes models (b), the best overall model is the model with three terms.

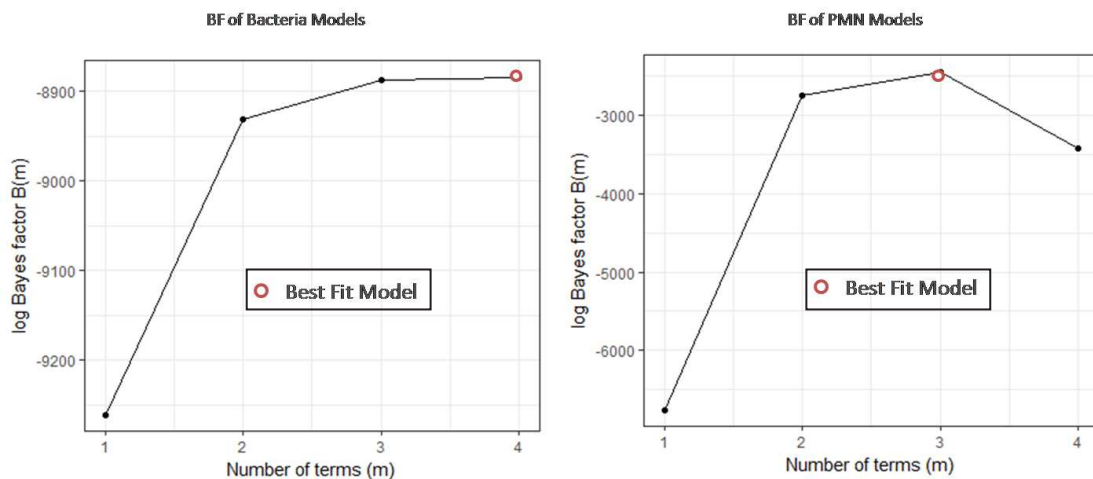


Figure 6.4. Log Bf for the bacteria and neutrophils system dynamics models. On the left: Log Bayes factor for each number of terms models for the changes in bacteria models as a function of bacteria and PMN. On the right: Log Bayes factor for each number of terms models for the changes in PMN models as a function of bacteria and PMN.

For the model systems of bacteria and osteocyte, the Bayes factor for each number of terms model given in (Figure 6.5). The overall best-selected model of (a) bacteria dynamics was also chosen as the model of four terms. While the two terms model was selected as the best model of (b) osteocytes changes models, the three terms model might be more informative with a little smaller value of Bayes factor.

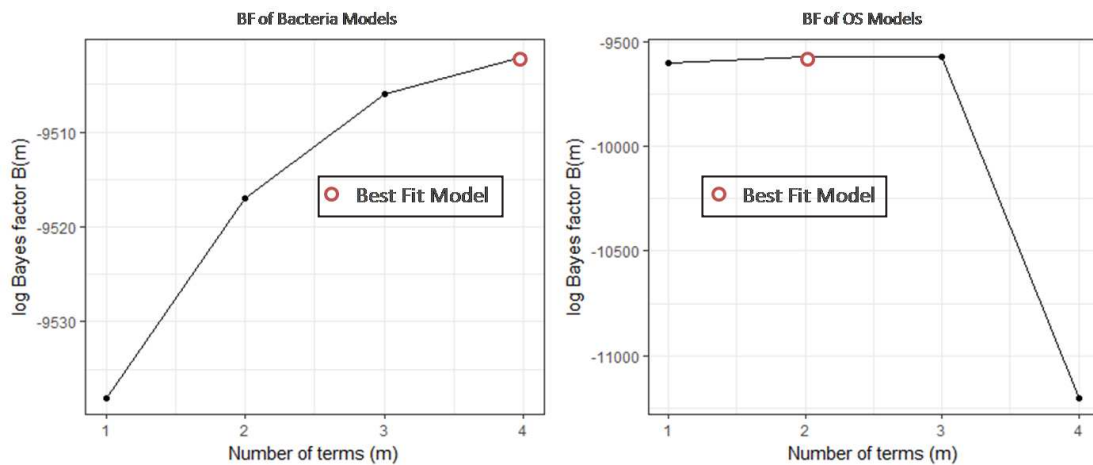


Figure 6.5. Log Bf for bacteria and osteocytes system dynamics model. (a) log Bayes factor for each number of terms models for the changes in bacteria models as a function of bacteria and osteocytes. (b) log Bayes factor for each number of terms models for the changes in osteocytes (OS) models as a function of bacteria and osteocytes.

The dynamical models that result for each of bacteria, neutrophils and osteocytes agents give more information about the behaviors of these variables over time. They show complex interactions and identify different relationships between them.

The dynamical system model of two variables bacteria (x) and neutrophils (y) is given by the equations (eq.6.6-6.8). The (Eq.6.6) gives the best fit model of bacteria population changes as a function of themselves and neutrophil population:

$$\frac{dx}{dt} = + 0.041 x - 0.00014 x y + 0.00011 x^2 - 8.5 \times 10^{-8} x^3 \quad (eq. 6.6)$$

This equation shows that the bacteria population increases by the rise in their count (in the first and third terms). The model shows in the second term a decreasing effect of the growth of neutrophils on the increase in bacteria. This effect is more stimulated by the bacteria themselves. The fourth term shows the secondary effect of the bacteria population on themselves, which slows the percentage increase in their population when it is very high due to the $-x^3$. This effect will be neglected for the small value of the bacteria population because of the very small coefficient: 8.5×10^{-8} .

By comparing this four terms model (eq 6.6) with the three terms model (eq 6.7) that have a very close Bayes factor and which is given by:

$$\frac{dx}{dt} = + 0.054 x - 0.00014 x y + 3.6 \times 10^{-5} x^2 \quad (eq. 6.7)$$

We find that the three terms model could be considered as a good candidate as the best fit model of bacteria population changes since it is less complex, similar to the first three terms in the four terms model, and since the fourth term in (eq.6.6) has a very small effect. And according to Occam's Razors, a model with less complexity (fewer terms) is preferable.

The best fit model of neutrophil population changes as a function of bacteria (x) and neutrophils (y) themselves is shown by:

$$\frac{dy}{dt} = + 0.034 x - 0.0085 y - 0.56 y/x \quad (eq. 6.8)$$

This model shows that the recruitment of neutrophil cells increases by the growth of bacteria once they amount to a specific value that determined by the count

of neutrophils themselves. The model also shows a self-limiting effect in the second term that is representing the clearance of neutrophils.

The selected best fit model system of bacteria and osteocyte population changes is given by the equations (eq.6.9-6.10). The (eq. 6.9) shows the bacteria dynamics model as a function of osteocytes and bacteria themselves:

$$\frac{dx}{dt} = -54 x + 47536 x/y + 0.015 x y - 4.9 \times 10^{-8} x^3 \quad (\text{eq. 6.9})$$

This model shows bacteria clearance in the first and fourth negative feedback terms. It also shows that the bacteria growth rate increases by the rising in bacteria themselves. This growth is slowed if the number of osteocytes is high. It is noted that the third term shows the exact opposite effect of osteocyte population on the increase of bacteria. This result has to be more verified and investigated with more data and different terms.

The best overall model of osteocyte population changes as a function of bacteria and osteocytes themselves is given by (eq. 6.10):

$$\frac{dy}{dt} = -0.067 x + 118 x/y \quad (\text{eq. 6.10})$$

This model shows that the osteocyte population decreases by the growth of bacteria until reaching a specific threshold. This decrease is determined by the count of osteocytes themselves. The greater the number of osteocytes in the site, the greater the induction of resorption. That might refer to the role of osteocytes in controlling the bone remodeling process.

The result also showed that the models of bacteria in the bacteria and neutrophils DE system have low R-squared values, while the neutrophils models have good values especially in the models with more than one term. The results also

showed R-squared values are very low for the models in bacteria and osteocytes DE system. However, the R-squared value is not an indicator of the goodness of the model, unfitted model could have good R-squared value¹. The low R-squared value could result from the generalization of the model. The complexity of the investigated system could result in a low R-squared value too. More investigation of the model in comparison with other possible terms and data set is needed.

6.5. Discussion

Although the Bayesian dynamical system approach was first proposed to study social systems (Ranganathan et al., 2014a), we have benefited from it here to study the behavior of a complex biological systems. Integrating the Bayesian dynamical system modeling approach with the ABM simulation model has introduced an exploratory method that supports identifying novel and unforeseen patterns and explication of the model outputs data (Beyer H., 2007; Gelman, 2004; Ranganathan et al., 2014c, 2014a). This method has used the data to tell us about the mathematical relationships between the variables.

We used this method to verify the system response to the same initial conditions of BJI model simulation. The resulting DEs showed small variance values in terms of coefficients and R-squared values, and similar form of the DEs. Bayesian system dynamics modeling method represented a good solution to compare and explore the BJI model behaviors. In addition, it was used to identify relationships between different variables of the system. It produced a set of differential equation systems which express the dynamics of each of bacteria, neutrophil and osteocyte populations as a function of the variables themselves and the other indicators. Even the obtained models do not solve definitely the system; it could be a starting point for explaining the relationship between the variables. It was shown that the Bayesian dynamical system modeling method could propose models that well fit the simulation data for different initial conditions, especially for the reproduction rate of bacteria 12, 18, 24 h. Nonetheless, other calculated models introduced some differences for other condition of reproduction rate (2, 4, 6 h).

¹ <http://blog.minitab.com>

Since the method output a set of dynamical models with a different number of terms, choosing the best informative and correct model represents a challenge. As more than one model could be plausible, comparing the Bayes factor of the selected models gives insight and facilitates choosing the best model and making a tradeoff between the model complexity and informativity. On the other hand, using the DEs will contribute in enriching the further analysis with more explanation of the system behavior and how the variables influence each other, with the ability to make a prediction of system progression.

Although comparing the models of the BJI system using the Bayes factor facilitates choosing the best fit model, other factors have an impact on the model selection such as our knowledge about the system. Additional comparison with other theoretical or mathematical models, if exist, could give another insight on the model selection. More comparison between the calculated models for different initial conditions or with more indicators could help in finding more relationships between variables. Integrating the knowledge of the mechanisms in macro and micro-level will give a better understanding of the system.

Moreover, it was noted that the calculated models were limited by the conditions of the simulated experiments, in which more investigation is required to generalize the models by integrating the data of all initial conditions in the modeling process. Validating the models in terms of the real system behavior introduces a challenge and requires integrating more information and variables.

7. Conclusion

7.1. Brief Summary of the Study

Management and diagnosis of bone and joint infections is a challenging task due to more frequent paucisymptomatic cases, and increasing rate of developing chronicity. It represents a complex multi-environment biological system that is characterized by not well understood possible cellular interactions that control BJI pathogenesis.

Developing a model that captures the emergent behavior of the disease development from the cellular interactions, in this stage without therapeutic intervention, allows exploring the natural evolution of the infection and characterizing the potential role of different system elements such as innate immune cells, and the consequences on the micro-structure of bone tissue. Thus, it can provide a novel insight into the bacterial development and the system response.

In this dissertation, we implemented a novel computational framework aiming at introducing a simulated experimental environment to investigate the BJI dynamics in an integral qualitative manner. We successfully developed an agent-based model of BJI that focused on studying the emergent behaviors of the system result from the spatiotemporal mechanisms of cellular interactions between BJI components during the first stage of infection.

In this thesis, the BJI model was built on the diverse descriptive knowledge from the literature, through which we provided the specifications of the agent behaviors, interactions, and parameter. It was built on a set of agent rules and

interactions, which result from simplifying the biological behaviors of the components, to mimic their response to the local environment.

We then analyzed the different patterns generated by the developed ABM of BJI by the Bayesian dynamical system modeling approach to find the best differential equations that identify relationships between BJI agents. Applying this method on the ABM output resulted in proposing a set of plausible dynamical system models of the agent behaviors. We employed the Bayes factor to choose the best fit model through those all proposed solutions. We as well used this method to verify the BJI model reliability. The BJI model displayed small variances of system behavior when comparing the different dynamical models calculated for the same input of the different model iterations.

7.2. Contribution

The implemented framework in this study is the first model of BJI that comprehends different heterogeneous variables of the system using ABM approach and explores the different patterns of the agent dynamics and the system behavior using Bayesian dynamical system method; thus it can be the basis of upcoming developing work. Even Liò et al. (Liò et al., 2012) proposed a computational model of BJI, they rely on EBM models, and they miss the integration of immune system role.

The model succeeded in mimicking the dynamics of bacteria, the innate immune cells (macrophages, neutrophils, monocyte-derived macrophages), and the bone cells (osteocytes, osteoblasts, osteoclasts) during the first stage of infection and for different inoculum levels in a compatible manner. The developed model offers a tool to investigate the influence of several variables on the dynamics of the infection. Through this model, we tested the effect of the bacteria inoculum size on the dynamics of innate immune cell and bone cells. The simulation showed that the innate immune cells followed the increasing of bacteria with the inability to eliminate them totally for the suggested inoculum size. The simulation suggested a minimum level of bacteria around the fourth day of infection. However, it highlighted the need for another type of defense such as the adaptive immune response or treatment intervention. The simulation also showed that the bone mass reached a common minimum level by the 7th day of infection representing 2% of loss in bone mass. It

suggested a reverse proportional relation between the inoculum size and the osteocyte population. Although the simulations are at the preliminary levels with regards to their accuracy and validity, several interesting outcomes were observed that would certainly provide insights into the BJI dynamics.

However, the mathematical models of biological systems are not considered as the mathematical solutions of these systems, they are considered as a systematic representation of the systems to test several hypotheses or further to predict the outcomes of the model under several therapeutic intervention conditions (An, 2005).

In this context, the proposed model framework introduces a flexible and interactive virtual laboratory to test and explain several existing hypotheses or knowledge or even to explore new ones. It gives rise to new perceptions to research and facilitate studying the biological system and processes under the different scenario that could not be realized in the laboratory, besides saving in terms of time and cost.

By using the ABM approach, the complex model behavior results from integrating the entities behaviors which also predict the collective behavior of cells. It well fits in the biomedical application where there are no predefined patterns of data. Instead, it uses a set of rules and the computational representation of the agent mechanisms to rebuild the observed patterns.

7.3. Limitation and Future Work

However, there is no complete model, but there is the model which give a best approximate representation that supply practical knowledge about the addressed system (An, 2005). The model proposed in this thesis is a simplified representation of the real system since several assumptions and simplifications have been made while implementing this model for several reasons such as missing information and the limited number of agents. We aimed at this stage of work to construct this first basic BJI model with plausible type of agents that represent the system in the first stage of infection and to build upon it later. In general, the assumptions and extractions lead to differences between the phenomena and the models' behaviors.

As all simulation modeling works, testing the model accuracy and reliability comparing to the original real system is a main task in the modeling work. However

several difficulties faced the validation task in this work, such as the absence of historical data concerning the cellular scale during BJI, which could be used either for building the model or for examining it. In addition, the real system proceeds differently following several factors and patient personal state, which have not been taken in the account in this basic model.

Nevertheless, more work could be done for future work to validate this developed model following proposed validation schemes or methods in the literature (Guerini et al., 2017; Kleijnen, 1999; Sanchez, 1999; Sargent, 2007; Windrum et al., 2007; Xiang et al., 2005).

Future work will include making more comparisons with different patterns of the bone mass and signals changes to make the ABM able to reproduce it in accurate time. It also will integrate important agents and variables such as bacteria biofilms, implants, and adaptive immune cells, to increase the correlation between the ABM model and the real BJI system. The future work also aims to represent three-dimensional ECM taking in the account the patient variability. This integration will lead to more confidence in the ability of BJI model to describe the real system and represent the cells spatial localization (Figure 2.2) in order to predict the pathology outcomes. As further data is made available, the model would be refined to better estimate an in-depth comprehension of BJI pathophysiology.

Although this model showed the ability to incorporated varied data from the literature, it is still in its early stages and has not integrated enough of knowledge and variables to predict the output of patient-specific treatment. This model is meant to be integrated with a decision support system called (Spot-Risc) as a hybrid approach between the modeling and the exploitation of real data. This global framework aims to use the population data stored in the electronic health record (EHR), the patient-specific clinical, biological and imaging data, and then execute exploratory and explanatory analysis to understand and predict the infection outcomes.

Several prediction methods could be used to enhance the prediction process such as machine learning techniques and Bayesian network. It would also be useful to get benefit from an advanced technique such as *mass cytometric* to better validate the cell behaviors and dynamics in different states.

Such a framework can be a starting point for future works that could have direct influences on multiple directions in the way of progress against the disease. These impacts include choosing the best diagnostic criteria, treatment protocol, and efficient follow-up parameters, besides simulating clinical trials and predicting patient-specific response. In other words, if we realize how to control the infection progress in the model, we can infer feasible counsel for the real infection management.

Publication and Communication

The work presented in this manuscript has been the subject of poster communications, and provide the material for a journal publication that is already submitted

- Alsassa S, Lefèvre T, Laugier V, Ansart S, Stindel E. "Simulating bone and joint infections using a combined agent-based modeling framework and Bayesian dynamic systems approach", (journal paper being written)
- Alsassa S, Lefèvre T, Laugier V, Ansart S, Stindel E. "Modeling Early Stages of Bone and Joint Infections Dynamics in Humans: a Multi-Agents, Multi Systems Based Model", (submitted to *Frontiers* journal)
- E-Health Research International Congress, 2016. "A First Simple Two-Dimensional Agent-Based Model Of Bone And Joint Infections To Simulate The Behavior Of The System". (abstract & poster)
- IEEE International Conference on Healthcare Informatics (ICHI), Doctoral consortium session, 2016. "Individualizing Treatment of Patients With Bone And Joint Infections: The Use of Embedded Agent-Based Modeling and Analytical Methods In Clinical Framework". (abstract & poster)

References

- Abar, S., Theodoropoulos, G.K., Lemariniere, P., and O'Hare, G.M.P. (2017). Agent Based Modelling and Simulation tools: A review of the state-of-art software. *Computer Science Review* 24, 13–33.
- Akbarshahi, H., Menzel, M., Bauden, M.P., Rosendahl, A., and Andersson, R. (2012). Enrichment of Murine CD68+CCR2+ and CD68+CD206+ Lung Macrophages in Acute Pancreatitis-Associated Acute Lung Injury. *PLOS ONE* 7, e42654.
- Alberts, B., Johnson, A., Lewis, J., Raff, M., Roberts, K., and Walter, P. (2002). *Innate Immunity*.
- Aleman, D., Pappalardo, F., Pennisi, M., Motta, S., and Brusica, V. (2012). Combining cellular automata and lattice Boltzmann method to model multiscale avascular tumor growth coupled with nutrient diffusion and immune competition. *Journal of Immunological Methods* 376, 55–68.
- Alexander, G. (2013). The biology of interacting things: the intuitive power of agent-based models. *Biomed. Comput. Rev* 2013, 20–27.
- Allan, R.J. (2009). Survey of Agent Based Modelling and Simulation Tools.
- An, G. (2001). Agent-based computer simulation and SIRS: Building a bridge between basic science and clinical trials. *Shock (Augusta, Ga.)* 16, 266–273.
- An, G. (2005). Mathematical modeling in medicine: A means, not an end*. *Critical Care Medicine* 33, 253.
- An, G. (2006). Concepts for developing a collaborative in silico model of the acute inflammatory response using agent-based modeling. *Journal of Critical Care* 21, 105–110.
- An, G. (2008). Introduction of an agent-based multi-scale modular architecture for dynamic knowledge representation of acute inflammation. *Theoretical Biology and Medical Modelling* 5, 11.
- An, G. (2009). A model of TLR4 signaling and tolerance using a qualitative, particle-event-based method: Introduction of spatially configured stochastic reaction chambers (SCSRC). *Mathematical Biosciences* 217, 43–52.
- An, G., Mi, Q., Dutta-Moscato, J., and Vodovotz, Y. (2009). Agent-based models in translational systems biology. *Wiley Interdiscip Rev Syst Biol Med* 1, 159–171.
- An, Y.H., Kang, Q.K., and Arciola, C.R. (2006). Animal models of osteomyelitis. *Int J Artif Organs* 29, 407–420.

- Anandarajah, A.P. (2009). Role of RANKL in bone diseases. *Trends in Endocrinology & Metabolism* 20, 88–94.
- Ansari, S., Nepal, H.P., Gautam, R., Shrestha, S., Chhetri, M.R., and Chapagain, M.L. (2015). Staphylococcus Aureus: Methicillin Resistance and Small Colony Variants from Pyogenic Infections of Skin, Soft Tissue and Bone. *J.Nepal Health.Res.Counc.* 13, 126–132.
- Anwar, S., and Whyte, M.K. (2007a). Neutrophil apoptosis in infectious disease. *Exp.Lung Res.* 33, 519–528.
- Anwar, H.A., Aldam, C.H., Visuvanathan, S., and Hart, A.J. (2007b). The effect of metal ions in solution on bacterial growth compared with wear particles from hip replacements. *Bone & Joint Journal* 89-B, 1655–1659.
- Argenson, J.-N., Boisgard, S., Parratte, S., Descamps, S., Bercovy, M., Bonneville, P., Briard, J.-L., Brilhault, J., Chouteau, J., Nizard, R., et al. (2013). Survival analysis of total knee arthroplasty at a minimum 10 years' follow-up: A multicenter French nationwide study including 846 cases. *Orthopaedics & Traumatology: Surgery & Research* 99, 385–390.
- Asensi, V., Valle, E., Meana, A., Fierer, J., Celada, A., Alvarez, V., Paz, J., Coto, E., Carton, J.A., Maradona, J.A., et al. (2004). In vivo interleukin-6 protects neutrophils from apoptosis in osteomyelitis. *Infect.Immun.* 72, 3823–3828.
- Ashcroft, G.S. (1999a). Bidirectional regulation of macrophage function by TGF- β . *Microbes and Infection* 1, 1275–1282.
- Ashcroft, G.S. (1999b). Bidirectional regulation of macrophage function by TGF- β . *Microbes and Infection* 1, 1275–1282.
- Athale, C.A., and Deisboeck, T.S. (2006). The effects of EGF-receptor density on multiscale tumor growth patterns. *Journal of Theoretical Biology* 238, 771–779.
- Ausk, B.J., Gross, T.S., and Srinivasan, S. (2006). An agent based model for real-time signaling induced in osteocytic networks by mechanical stimuli. *Journal of Biomechanics* 39, 2638–2646.
- Bahar, H., Benayahu, D., Yaffe, A., and Binderman, I. (2007). Molecular signaling in bone regeneration. *Crit.Rev.Eukaryot.Gene Expr.* 17, 87–101.
- Bar-Shavit, Z. (2007). The osteoclast: A multinucleated, hematopoietic-origin, bone-resorbing osteoimmune cell. *J. Cell. Biochem.* 102, 1130–1139.
- Bauer, A.L., Beauchemin, C.A., and Perelson, A.S. (2009). Agent-based modeling of host–pathogen systems: The successes and challenges. *Information Sciences* 179, 1379–1389.
- Bejon, P., and Robinson, E. (2017). Bone and joint infection. *Medicine* 45, 711–714.
- Bekkering, S. (2013). Another look at the life of a neutrophil. *World Journal of Hematology* 2, 44.

- Berryman, M. (2008). Review of Software Platforms for Agent Based Models.
- Beutler, B. (2004). Innate immunity: an overview. *Molecular Immunology* 40, 845–859.
- Beyer H. (2007). Tukey, John W.: Exploratory Data Analysis. Addison- Wesley Publishing Company Reading, Mass. — Menlo Park, Cal., London, Amsterdam, Don Mills, Ontario, Sydney 1977, XVI, 688 S. *Biometrical Journal* 23, 413–414.
- Bianca, C., and Pennisi, M. (2012). Immune system modelling by top-down and bottom-up approaches. *INTERNATIONAL MATHEMATICAL FORUM* 7, 109–128.
- Bilezikian, J.P., Raisz, L.G., and Rodan, G.A. (2002). Principles of Bone Biology, Two-Volume Set (Academic Press).
- Bishop, C.M. (2006). Pattern Recognition and Machine Learning (Information Science and Statistics) (Secaucus, NJ, USA: Springer-Verlag New York, Inc.).
- Bismar, H., Klöppinger, T., Schuster, E.M., Balbach, S., Diel, I., Ziegler, R., and Pfeilschifter, J. (1999). Transforming growth factor β (TGF- β) levels in the conditioned media of human bone cells: relationship to donor age, bone volume, and concentration of TGF- β in human bone matrix in vivo. *Bone* 24, 565–569.
- Bjarnsholt, T. (2013). The role of bacterial biofilms in chronic infections. *APMIS* 121, 1–58.
- Bogdan, C., and Nathan, C. (1993). Modulation of macrophage function by transforming growth factor beta, interleukin-4, and interleukin-10. *Ann. N. Y. Acad. Sci.* 685, 713–739.
- Bonabeau, E. (2002). Agent-based modeling: Methods and techniques for simulating human systems. *PNAS* 99, 7280–7287.
- Bonewald, L.F. (2002). Osteocytes: a proposed multifunctional bone cell. *J Musculoskelet Neuronal Interact* 2, 239–241.
- Bonewald, L.F. (2011). The amazing osteocyte. *J Bone Miner Res* 26, 229–238.
- Bonewald, L.F., and Johnson, M.L. (2008). Osteocytes, mechanosensing and Wnt signaling. *Bone* 42, 606–615.
- Borshchev, A., and Filippov, A. (2004). From system dynamics and discrete event to practical agent based modeling: reasons, techniques, tools. In Proceedings of the 22nd International Conference of the System Dynamics Society, (Citeseer), p.
- Bost, K.L., Ramp, W.K., Nicholson, N.C., Bento, J.L., Marriott, I., and Hudson, M.C. (1999). Staphylococcus aureus Infection of Mouse or Human Osteoblasts Induces High Levels of Interleukin-6 and Interleukin-12 Production. *J Infect Dis* 180, 1912–1920.

- Boyce, B.F. (2013). Advances in the Regulation of Osteoclasts and Osteoclast Functions. *J Dent Res* 92, 860–867.
- Boyce, B.F., and Xing, L. (2008). Functions of RANKL/RANK/OPG in bone modeling and remodeling. *Archives of Biochemistry and Biophysics* 473, 139–146.
- Boyce, B., Yao, Z., and Xing, L. (2009). Osteoclasts Have Multiple Roles in Bone in Addition to Bone Resorption. *CRE* 19.
- Boyce, B.F., Rosenberg, E., de Papp, A.E., and Duong, L.T. (2012). The osteoclast, bone remodelling and treatment of metabolic bone disease. *Eur.J.Clin.Invest.* 42, 1332–1341.
- Brady, R.A., Leid, J.G., Calhoun, J.H., Costerton, J.W., and Shirtliff, M.E. (2008). Osteomyelitis and the role of biofilms in chronic infection. *FEMS Immunology & Medical Microbiology* 52, 13–22.
- Brunet de la Grange, P., Vlaski, M., Duchez, P., Chevaleyre, J., Lapostolle, V., Boiron, J.-M., Praloran, V., and Ivanovic, Z. (2013). Long-term repopulating hematopoietic stem cells and “side population” in human steady state peripheral blood. *Stem Cell Research* 11, 625–633.
- Buckwalter, J.A., Glimcher, M.J., Cooper, R.R., and Recker, R. (1995). Bone biology. Part I: Structure, blood supply, cells, matrix, and mineralization. *Journal of Bone and Joint Surgery - American Volume, The Journal of Bone and Joint Surgery. American Volume, The Journal of Bone and Joint Surgery. American Volume.* 77, 1256–1275.
- Buenzli, P.R., Pivonka, P., and Smith, D.W. (2011). Spatio-temporal structure of cell distribution in cortical Bone Multicellular Units: A mathematical model. *Bone* 48, 918–926.
- Buenzli, P.R., Jeon, J., Pivonka, P., Smith, D.W., and Cummings, P.T. (2012). Investigation of bone resorption within a cortical basic multicellular unit using a lattice-based computational model. *Bone* 50, 378–389.
- Bui, L.M.G., Hoffmann, P., Turnidge, J.D., Zilm, P.S., and Kidd, S.P. (2015). Prolonged Growth of a Clinical *Staphylococcus aureus* Strain Selects for a Stable Small-Colony-Variant Cell Type. *Infect. Immun.* 83, 470–481.
- Carek, P.J., Dickerson, L.M., and Sackier, J.M. (2001). Diagnosis and Management of Osteomyelitis. *AFP* 63, 2413.
- Cassat, J.E., Hammer, N.D., Campbell, J.P., Benson, M.A., Perrien, D.S., Mrak, L.N., Smeltzer, M.S., Torres, V.J., and Skaar, E.P. (2013). A Secreted Bacterial Protease Tailors the *Staphylococcus aureus* Virulence Repertoire to Modulate Bone Remodeling during Osteomyelitis. *Cell Host & Microbe* 13, 759–772.
- Cassatella, M.A. (1995). The production of cytokines by polymorphonuclear neutrophils. *Immunology Today* 16, 21–26.
- Chambers, T. j. (2010). The birth of the osteoclast. *Annals of the New York Academy of Sciences* 1192, 19–26.

- Charles, J.F., and Aliprantis, A.O. (2014). Osteoclasts: more than ‘bone eaters.’ *Trends in Molecular Medicine* 20, 449–459.
- Charles A Janeway, J., Travers, P., Walport, M., and Shlomchik, M.J. (2001). *Principles of innate and adaptive immunity*.
- Chazaud, B. (2014). Macrophages: Supportive cells for tissue repair and regeneration. *Immunobiology* 219, 172–178.
- Cheatle, J., Aldrich, A., Thorell, W.E., Boska, M.D., and Kielian, T. (2013). Compartmentalization of Immune Responses during Staphylococcus aureus Cranial Bone Flap Infection. *The American Journal of Pathology* 183, 450–458.
- Cheema, A.K., Fiandaca, M.S., Mapstone, M., and Federoff, H.J. (2016). Systems biology: unravelling molecular complexity in health and disease. In *The Value of Systems and Complexity Sciences for Healthcare*, (Springer), pp. 21–28.
- Chiacchio, F., Pennisi, M., Russo, G., Motta, S., and Pappalardo, F. (2014). Agent-Based Modeling of the Immune System: NetLogo, a Promising Framework. *BioMed Research International* 2014, 907171.
- Chincisan, A.-I.-M. (2016). Analysis of 3d knee joint deformation using a multiscale modelling approach. University of Geneva.
- Ciampolini, J., and Harding, K.G. (2000). Pathophysiology of chronic bacterial osteomyelitis. Why do antibiotics fail so often? *Postgraduate Medical Journal* 76, 479–483.
- Clarke, B. (2008). Normal bone anatomy and physiology. *Clin.J.Am.Soc.Nephrol.* 3 *Suppl* 3, S131-9.
- Claro, T., Widaa, A., O’Seaghdha, M., Miajlovic, H., Foster, T.J., O’Brien, F.J., and Kerrigan, S.W. (2011). Staphylococcus aureus Protein A Binds to Osteoblasts and Triggers Signals That Weaken Bone in Osteomyelitis. *PLOS ONE* 6, e18748.
- Cobelli, N., Scharf, B., Crisi, G., Hardin, J., and Santambrogio, L. (2011). Mediators of the inflammatory response to joint replacement devices. *Nature Reviews. Rheumatology* 7, 600–608.
- Coenye, T., and Nelis, H.J. (2010). In vitro and in vivo model systems to study microbial biofilm formation. *Journal of Microbiological Methods* 83, 89–105.
- Cohen, M.C., and Cohen, S. (1996). Cytokine Function: A Study in Biologic Diversity. *Am J Clin Pathol* 105, 589–598.
- Cohen, G., Lager, S., Cece, D., and Rubel, I.F. (2004). The Social Impact Associated with Chronic Osteomyelitis. A Grading System for the Most Frequent Complication. *Osteo Trauma Care* 12, 74–76.
- Colas, S., Ocean, B.-V., Rudnichi, A., Dray-Spira, R., and Zureik, M. (2016). Nationwide Knee Arthroplasty in France Between 2008 and 2013: Characteristics of the Patients, Implants and Procedures. In *PHARMACOEPIDEMIOLOGY AND*

DRUG SAFETY, (WILEY-BLACKWELL 111 RIVER ST, HOBOKEN 07030-5774, NJ USA), pp. 127–127.

Cole, J., Aberdein, J., Jubrail, J., and Dockrell, D.H. (2014). Chapter Four - The Role of Macrophages in the Innate Immune Response to *Streptococcus pneumoniae* and *Staphylococcus aureus*: Mechanisms and Contrasts. *Adv.Microb.Physiol.* 65, 125–202.

Corrado, A., Donato, P., Maccari, S., Cecchi, R., Spadafina, T., Arcidiacono, L., Tavarini, S., Sammicheli, C., Laera, D., Manetti, A.G.O., et al. (2016). *Staphylococcus aureus*-dependent septic arthritis in murine knee joints: local immune response and beneficial effects of vaccination. *Scientific Reports* 6, srep38043.

Cram, P., Lu, X., Kaboli, P.J., Vaughan-Sarrazin, M.S., Cai, X., Wolf, B., and Li, Y. (2011). Clinical characteristics and outcomes of Medicare patients undergoing total hip arthroplasty, 1991–2008. *JAMA* 305, 1560–1567.

Cramton, S.E., Gerke, C., and Götz, F. (2001). In vitro methods to study staphylococcal biofilm formation. *Meth.Enzymol.* 336, 239–255.

Dale, D.C., Boxer, L., and Liles, W.C. (2008). The phagocytes: neutrophils and monocytes. *Blood* 112, 935–945.

Dallas, S.L., Prideaux, M., and Bonewald, L.F. (2013). The Osteocyte: An Endocrine Cell ... and More. *Endocr Rev* 34, 658–690.

Dancik, G.M., Jones, D.E., and Dorman, K.S. (2010). Parameter estimation and sensitivity analysis in an agent-based model of *Leishmania major* infection. *Journal of Theoretical Biology* 262, 398–412.

Dapunt, U., Hänsch, G.M., and Arciola, C.R. (2016). Innate Immune Response in Implant-Associated Infections: Neutrophils against Biofilms. *Materials (Basel)* 9.

Davies, L.C., Jenkins, S.J., Allen, J.E., and Taylor, P.R. (2013). Tissue-resident macrophages. *Nat Immunol* 14, 986–995.

Del Fattore, A., Teti, A., and Rucci, N. (2008). Osteoclast receptors and signaling. *Arch.Biochem.Biophys.* 473, 147–160.

DeLeo, F.R. (2004). Modulation of phagocyte apoptosis by bacterial pathogens. *Apoptosis* 9, 399–413.

Delves, P.J., and Roitt, I.M. (2000). The Immune System. *New England Journal of Medicine* 343, 37–49.

Deshmane, S.L., Kremlev, S., Amini, S., and Sawaya, B.E. (2009). Monocyte Chemoattractant Protein-1 (MCP-1): An Overview. *Journal of Interferon & Cytokine Research* 29, 313–326.

Dockrell, D.H., and Whyte, M.K. (2006). Regulation of phagocyte lifespan in the lung during bacterial infection. *J.Leukoc.Biol.* 79, 904–908.

- DosReis, G.A., and Barcinski, M.A. (2001). Apoptosis and parasitism: from the parasite to the host immune response. *Adv.Parasitol.* 49, 133–161.
- Dusane, D.H., Kyrouac, D., Petersen, I., Bushrow, L., Calhoun, J.H., Granger, J.F., Phieffer, L.S., and Stoodley, P. (2018). Targeting intracellular *Staphylococcus aureus* to lower recurrence of orthopaedic infection. *J. Orthop. Res.* 36, 1086–1092.
- Eissing, T., Kuepfer, L., Becker, C., Block, M., Coboeken, K., Gaub, T., Goerlitz, L., Jaeger, J., Loosen, R., Ludewig, B., et al. (2011). A Computational Systems Biology Software Platform for Multiscale Modeling and Simulation: Integrating Whole-Body Physiology, Disease Biology, and Molecular Reaction Networks. *Front. Physiol.* 2.
- Ellington, J.K., Harris, M., Hudson, M.C., Vishin, S., Webb, L.X., and Sherertz, R. (2006). Intracellular *Staphylococcus aureus* and antibiotic resistance: implications for treatment of staphylococcal osteomyelitis. *J. Orthop. Res.* 24, 87–93.
- Engelberg, J.A., Ropella, G.E., and Hunt, C.A. (2008). Essential operating principles for tumor spheroid growth. *BMC Systems Biology* 2, 110.
- Epelman, S., Lavine, K.J., and Randolph, G.J. (2014). Origin and Functions of Tissue Macrophages. *Immunity* 41, 21–35.
- Eriksen, E.F. (2010). Cellular mechanisms of bone remodeling. *Rev Endocr Metab Disord* 11, 219–227.
- Evans, C.A.W., Jellis, J., Hughes, S.P.F., Remick, D.G., and Friedland, J.S. (1998). Tumor Necrosis Factor- α , Interleukin-6, and Interleukin-8 Secretion and the Acute-Phase Response in Patients with Bacterial and Tuberculous Osteomyelitis. *The Journal of Infectious Diseases* 177, 1582–1587.
- Everts, V., Delaissé, J.M., Korper, W., Jansen, D.C., Tigchelaar-Gutter, W., Saftig, P., and Beertsen, W. (2002). The Bone Lining Cell: Its Role in Cleaning Howship's Lacunae and Initiating Bone Formation. *J Bone Miner Res* 17, 77–90.
- Evora, J., Hernandez, J.J., and Hernandez, M. (2015). Advantages of Model Driven Engineering for studying complex systems. *Nat Comput* 14, 129–144.
- Fadiel, A., Eichenbaum, K., and Xia, Y. (2008). Cell Interactome: Good Neighbors or Bad Neighbors. *Biosci Hypotheses* 1, 255–257.
- Fearon, D.T. (1999). Innate immunity and the biological relevance of the acquired immune response. *QJM* 92, 235–237.
- Fearon, D.T., and Locksley, R.M. (1996). The Instructive Role of Innate Immunity in the Acquired Immune Response. *Science* 272, 50–54.
- Fehder, W.P., Tuluc, F., Ho, W.-Z., and Douglas, S.D. (2007). Macrophages*. In *Encyclopedia of Stress (Second Edition)*, G. Fink, ed. (New York: Academic Press), pp. 634–639.

- Florencio-Silva, R., Sasso, G.R. da S., Sasso-Cerri, E., Simões, M.J., Cerri, P.S., and Rigio (2015). Biology of Bone Tissue: Structure, Function, and Factors That Influence Bone Cells.
- Folcik, V.A., An, G.C., and Orosz, C.G. (2007). The Basic Immune Simulator: An agent-based model to study the interactions between innate and adaptive immunity. *Theoretical Biology and Medical Modelling* 4, 39.
- Forsberg, J.A., Potter, B.K., Cierny, G., and Webb, L. (2011). Diagnosis and management of chronic infection. *J Am Acad Orthop Surg* 19 Suppl 1, S8–S19.
- Franchimont, N., Rydziel, S., and Canalis, E. (2000). Transforming growth factor- β increases interleukin-6 transcripts in osteoblasts. *Bone* 26, 249–253.
- Franz-Odenaal, T.A., Hall, B.K., and Witten, P.E. (2006). Buried alive: How osteoblasts become osteocytes. *Dev. Dyn.* 235, 176–190.
- Fritz, J.M., and McDonald, J.R. (2008). Osteomyelitis: Approach to Diagnosis and Treatment. *Phys Sportsmed* 36, nihpa116823.
- Fullilove, S., Jellis, J., Hughes, S.P.F., Remick, D.G., and Friedland, J.S. (2000). Local and systemic concentrations of tumour necrosis factor- α , interleukin-6 and interleukin-8 in bacterial osteomyelitis. *Trans.R.Soc.Trop.Med.Hyg.* 94, 221–224.
- Funao, H., Ishii, K., Nagai, S., Sasaki, A., Hoshikawa, T., Aizawa, M., Okada, Y., Chiba, K., Koyasu, S., Toyama, Y., et al. (2012). Establishment of a Real-Time, Quantitative, and Reproducible Mouse Model of Staphylococcus Osteomyelitis Using Bioluminescence Imaging. *Infect. Immun.* 80, 733–741.
- Furth, R. van, and Cohn, Z.A. (1968). The Origin and Kinetics of Mononuclear Phagocytes. *Journal of Experimental Medicine* 128, 415–435.
- Furze, R.C., and Rankin, S.M. (2008). Neutrophil mobilization and clearance in the bone marrow. *Immunology* 125, 281–288.
- Fux, C.A., Costerton, J.W., Stewart, P.S., and Stoodley, P. (2005). Survival strategies of infectious biofilms. *Trends in Microbiology* 13, 34–40.
- Galli, S.J., Borregaard, N., and Wynn, T.A. (2011). Phenotypic and functional plasticity of cells of innate immunity: macrophages, mast cells and neutrophils. *Nat Immunol* 12, 1035–1044.
- Gary An, V.G. (2012). Using an Agent-Based Model to Examine the Role of Dynamic Bacterial Virulence Potential in the Pathogenesis of Surgical Site Infection. *ADVANCES IN WOUND CARE, NUMBER 9 VOLUME 2.*
- Gatti, M, and C. Lucena (2007). An Agent-Based Approach for Building Biological Systems: Improving The Software Engineering for Complex and Adaptative Multi-Agent Systems. *Monografias de Ciências Da Computação PUC-Rio.*
- Gaudin, A., Amador Del Valle, G., Hamel, A., Le Mabecque, V., Miegerville, A.-F., Potel, G., Caillon, J., and Jacqueline, C. (2011a). A new experimental model of acute

osteomyelitis due to methicillin-resistant *Staphylococcus aureus* in rabbit. *Letters in Applied Microbiology* 52, 253–257.

Gaudin, A., Amador Del Valle, G., Hamel, A., Le Mabecque, V., Miegerville, A.-F., Potel, G., Caillon, J., and Jacqueline, C. (2011b). A new experimental model of acute osteomyelitis due to methicillin-resistant *Staphylococcus aureus* in rabbit. *Letters in Applied Microbiology* 52, 253–257.

Gbejuade, H.O., Lovering, A.M., and Webb, J.C. (2015). The role of microbial biofilms in prosthetic joint infections. *Acta Orthop* 86, 147–158.

Gelman, A. (2004). Exploratory Data Analysis for Complex Models. *Journal of Computational and Graphical Statistics* 13, 755–779.

Ghosh, S., Matsuoka, Y., Asai, Y., Hsin, K.-Y., and Kitano, H. (2011). Software for systems biology: from tools to integrated platforms. *Nat Rev Genet* 12, 821–832.

Gilbert, N. (2008). *Agent-Based Models* (SAGE).

Gillespie, W.J., and Allardyce, R.A. (1990). Mechanisms of Bone Degradation in Infection: A Review of Current Hypotheses. *ORTHOPEDICS* 13, 407–410.

Ginhoux, F., and Jung, S. (2014). Monocytes and macrophages: Developmental pathways and tissue homeostasis. *Nature Reviews. Immunology* 14, 392–404.

Goasguen, J.E., Bennett, J.M., Bain, B.J., Vallespi, T., Brunning, R., Mufti, G.J., and International Working Group on Morphology of Myelodysplastic Syndrome (2009). Morphological evaluation of monocytes and their precursors. *Haematologica* 94, 994–997.

Goggin, P., Zygalkis, K., Oreffo, R., and Schneider, P. (2016). High-resolution 3D imaging of osteocytes and computational modelling in mechanobiology: Insights on bone development, ageing, health and disease. *European Cells & Materials* 1–86.

Gong, D., Shi, W., Yi, S., Chen, H., Groffen, J., and Heisterkamp, N. (2012). TGF β signaling plays a critical role in promoting alternative macrophage activation. *BMC Immunology* 13, 31.

Gonzalez-Mejia, M.E., and Doseff, A.I. (2009). Regulation of monocytes and macrophages cell fate. *Front.Biosci.(Landmark Ed)* 14, 2413–2431.

Gordon, S., and Plüddemann, A. (2017). Tissue macrophages: heterogeneity and functions. *BMC Biol* 15.

Grammatico-Guillon, L., Baron, S., Gettner, S., Lecuyer, A.-I., Gaborit, C., Rosset, P., Rusch, E., and Bernard, L. (2012). Bone and joint infections in hospitalized patients in France, 2008: clinical and economic outcomes. *Journal of Hospital Infection* 82, 40–48.

Grant, M.R., Mostov, K.E., Tlsty, T.D., and Hunt, C.A. (2006). Simulating Properties of In Vitro Epithelial Cell Morphogenesis. *PLOS Computational Biology* 2, e129.

- Greek, R., and Hansen, L.A. (2013). The Strengths and Limits of Animal Models as Illustrated by the Discovery and Development of Antibacterials. *Biological Systems: Open Access* 2, 1–15.
- Grimm, V., Berger, U., DeAngelis, D.L., Polhill, J.G., Giske, J., and Railsback, S.F. (2010). The ODD protocol: A review and first update. *Ecological Modelling* 221, 2760–2768.
- Guerini, M., and Moneta, A. (2017). A method for agent-based models validation. *Journal of Economic Dynamics and Control* 82, 125–141.
- Hadjidakis, D.J., and Androulakis, I.I. (2006). Bone Remodeling. *Annals of the New York Academy of Sciences* 1092, 385–396.
- Hall-Stoodley, L., and Stoodley, P. (2009). Evolving concepts in biofilm infections. *Cell. Microbiol.* 11, 1034–1043.
- Hall-Stoodley, L., Costerton, J.W., and Stoodley, P. (2004). Bacterial biofilms: from the Natural environment to infectious diseases. *Nature Reviews Microbiology* 2, 95–108.
- Hambli, R. (2014). Connecting Mechanics and Bone Cell Activities in the Bone Remodeling Process: An Integrated Finite Element Modeling. *Frontiers in Bioengineering and Biotechnology* 2, 6.
- Hammond, R.A. (2015). *Considerations and Best Practices in Agent-Based Modeling to Inform Policy* (National Academies Press (US)).
- Harris, L., J Foster, S., and Richards, R. (2003). An introduction to *Staphylococcus aureus*, and techniques for identifying and quantifying *S. aureus* adhesins in relation to adhesion to biomaterials: Review. *European Cells & Materials* 4, 39–60.
- Hashimoto, D., Chow, A., Noizat, C., Teo, P., Beasley, M.B., Leboeuf, M., Becker, C.D., See, P., Price, J., Lucas, D., et al. (2013). Tissue-Resident Macrophages Self-Maintain Locally throughout Adult Life with Minimal Contribution from Circulating Monocytes. *Immunity* 38, 792–804.
- Hatzenbuehler, J., and Pulling, T.J. (2011). Diagnosis and management of osteomyelitis. *Am Fam Physician* 84, 1027–1033.
- Henriksen, K., Neutzsky-Wulff, A.V., Bonewald, L.F., and Karsdal, M.A. (2009). Local communication on and within bone controls bone remodeling. *Bone* 44, 1026–1033.
- Holcombe, M., Adra, S., Bicak, M., Chin, S., Coakley, S., I. Graham, A., Green, J., Greenough, C., Jackson, D., Kiran, M., et al. (2012). Modelling complex biological systems using an agent-based approach. *Integrative Biology* 4, 53–64.
- Horst, S.A., Hoerr, V., Beineke, A., Kreis, C., Tuchscher, L., Kalinka, J., Lehne, S., Schleicher, I., Köhler, G., Fuchs, T., et al. (2012). A Novel Mouse Model of *Staphylococcus aureus* Chronic Osteomyelitis That Closely Mimics the Human

- Infection: An Integrated View of Disease Pathogenesis. *The American Journal of Pathology* 181, 1206–1214.
- Hunt, C.A., Ropella, G.E.P., Yan, L., Hung, D.Y., and Roberts, M.S. (2006). Physiologically Based Synthetic Models of Hepatic Disposition. *J Pharmacokinet Pharmacodyn* 33, 737–772.
- I. Edward Alcamo, and Jennifer Warner (2009). *Schaum's Outline of Microbiology, Second Edition* (McGraw-Hill).
- Inzana, J.A., Schwarz, E.M., Kates, S.L., and Awad, H.A. (2015). A novel murine model of established Staphylococcal bone infection in the presence of a fracture fixation plate to study therapies utilizing antibiotic-laden spacers after revision surgery. *Bone* 72, 128–136.
- Iolascon, G., Resmini, G., and Tarantino, U. (2011). Inhibition of RANK ligand: a new option for preventing fragility fractures. *Aging Clin.Exp.Res.* 23, 28–29.
- Italiani, P., and Boraschi, D. (2014). From Monocytes to M1/M2 Macrophages: Phenotypical vs. Functional Differentiation. *Front Immunol* 5.
- Ji, Z., Yan, K., Li, W., Hu, H., and Zhu, X. (2017). *Mathematical and Computational Modeling in Complex Biological Systems*.
- Jilka, R.L. (2003). Biology of the basic multicellular unit and the pathophysiology of osteoporosis. *Med. Pediatr. Oncol.* 41, 182–185.
- Jilka, R.L., Weinstein, R.S., Bellido, T., Parfitt, A.M., and Manolagas, S.C. (1998). Osteoblast Programmed Cell Death (Apoptosis): Modulation by Growth Factors and Cytokines. *J Bone Miner Res* 13, 793–802.
- Jilka, R.L., Weinstein, R.S., Parfitt, A.M., and Manolagas, S.C. (2007). Quantifying osteoblast and osteocyte apoptosis: challenges and rewards. *J.Bone Miner.Res.* 22, 1492–1501.
- Jorge, L.S., Chueire, A.G., and Rossit, A.R.B. (2010). Osteomyelitis: a current challenge. *Brazilian Journal of Infectious Diseases* 14, 310–315.
- Josse, J., Velard, F., and Gangloff, S.C. (2015). Staphylococcus aureus vs. Osteoblast: Relationship and Consequences in Osteomyelitis. *Front.Cell.Infect.Microbiol.* 5, 85.
- Jr, C.A.J., Travers, P., Walport, M., Shlomchik, M.J., Jr, C.A.J., Travers, P., Walport, M., and Shlomchik, M.J. (2001). *Immunobiology* (Garland Science).
- Junka, A., Szymczyk, P., Ziółkowski, G., Karuga-Kuzniewska, E., Smutnicka, D., Bil-Lula, I., Bartoszewicz, M., Mahabady, S., and Sedghizadeh, P.P. (2017). Bad to the Bone: On In Vitro and Ex Vivo Microbial Biofilm Ability to Directly Destroy Colonized Bone Surfaces without Participation of Host Immunity or Osteoclastogenesis. *PLOS ONE* 12, e0169565.
- Kahn, D.S., and Pritzker, K.P. (1973). The pathophysiology of bone infection. *Clin Orthop Relat Res* 12–19.

- Kaplanski, G., Marin, V., Montero-Julian, F., Mantovani, A., and Farnarier, C. (2003a). IL-6: a regulator of the transition from neutrophil to monocyte recruitment during inflammation. *Trends in Immunology* 24, 25–29.
- Kaplanski, G., Marin, V., Montero-Julian, F., Mantovani, A., and Farnarier, C. (2003b). IL-6: a regulator of the transition from neutrophil to monocyte recruitment during inflammation. *Trends in Immunology* 24, 25–29.
- Kardas, D., Nackenhorst, U., and Balzani, D. (2013). Computational model for the cell-mechanical response of the osteocyte cytoskeleton based on self-stabilizing tensegrity structures. *Biomech.Model.Mechanobiol* 12, 167–183.
- Kaufmann, S.H.E., and Dorhoi, A. (2016). Molecular Determinants in Phagocyte-Bacteria Interactions. *Immunity* 44, 476–491.
- Kehrl, J.H. (1991). Transforming growth factor-beta: an important mediator of immunoregulation. *Int. J. Cell Cloning* 9, 438–450.
- Kelly, A., Houston, S.A., Sherwood, E., Casulli, J., and Travis, M.A. (2017). Chapter Four - Regulation of Innate and Adaptive Immunity by TGF β . *Adv.Immunol.* 134, 137–233.
- Kettritz, R., Xu, Y.X., Kerren, T., Quass, P., Klein, J.B., Luft, F.C., and Haller, H. (1999). Extracellular matrix regulates apoptosis in human neutrophils. *Kidney Int.* 55, 562–571.
- Kholodenko, B.N. (2006). Cell-signalling dynamics in time and space. *Nature Reviews Molecular Cell Biology* 7, nrm1838.
- Kierdorf, K., Prinz, M., Geissmann, F., and Perdiguero, E.G. (2015). Development and function of tissue resident macrophages in mice. *Semin Immunol* 27, 369–378.
- Kim, N.D., and Luster, A.D. (2015). The role of tissue resident cells in neutrophil recruitment. *Trends Immunol* 36, 547–555.
- Kim, H.K., Thammavongsa, V., Schneewind, O., and Missiakas, D. (2012). Recurrent infections and immune evasion strategies of *Staphylococcus aureus*. *Curr.Opin.Microbiol.* 15, 92–99.
- Kim, H.K., Missiakas, D., and Schneewind, O. (2014). Mouse models for infectious diseases caused by *Staphylococcus aureus*. *Journal of Immunological Methods* 410, 88–99.
- Kiran, M. (2014). Using FLAME Toolkit for Agent-Based Simulation: Case Study Sugarscape Model. ArXiv:1408.3441 [Cs].
- Kiran, M. (2017). *X-Machines for Agent-Based Modeling: FLAME Perspectives* (CRC Press).
- Kitano, H. (2002a). Systems Biology: A Brief Overview. *Science* 295, 1662–1664.
- Kitano, H. (2002b). Computational systems biology. *Nature* 420, 206–210.

Kleijnen, J.P.C. (1999). Validation of models: statistical techniques and data availability. In *Simulation Conference Proceedings, 1999 Winter*, pp. 647–654 vol.1.

Knapp, S., Thalhammer, F., Locker, G.J., Laczika, K., Hollenstein, U., Frass, M., Winkler, S., Stoiser, B., Wilfing, A., and Burgmann, H. (1998). Prognostic Value of MIP-1 α , TGF- β 2, sELAM-1, and sVCAM-1 in Patients with Gram-Positive Sepsis. *Clinical Immunology and Immunopathology* 87, 139–144.

Knothe Tate, M.L., Adamson, J.R., Tami, A.E., and Bauer, T.W. (2004). The osteocyte. *The International Journal of Biochemistry & Cell Biology* 36, 1–8.

Kollet, O., Canaani, J., Kalinkovich, A., and Lapidot, T. (2012). Regulatory cross talks of bone cells, hematopoietic stem cells and the nervous system maintain hematopoiesis. *Inflamm.Allergy Drug Targets* 11, 170–180.

Komarova, S.V. (2005). Mathematical Model of Paracrine Interactions between Osteoclasts and Osteoblasts Predicts Anabolic Action of Parathyroid Hormone on Bone. *Endocrinology* 146, 3589–3595.

Komarova, S.V., Smith, R.J., Dixon, S.J., Sims, S.M., and Wahl, L.M. (2003). Mathematical model predicts a critical role for osteoclast autocrine regulation in the control of bone remodeling. *Bone* 33, 206–215.

Kong, C., Chee, C.-F., Richter, K., Thomas, N., Rahman, N.A., and Nathan, S. (2018). Suppression of *Staphylococcus aureus* biofilm formation and virulence by a benzimidazole derivative, UM-C162. *Scientific Reports* 8, 2758.

Kremers, H.M., Nwojo, M.E., Ransom, J.E., Wood-Wentz, C.M., Melton, L.J., and Huddleston, P.M. (2015). Trends in the epidemiology of osteomyelitis: a population-based study, 1969 to 2009. *J Bone Joint Surg Am* 97, 837–845.

Kumar, V., and Sharma, A. (2010). Neutrophils: Cinderella of innate immune system. *Int.Immunopharmacol.* 10, 1325–1334.

Kurtz, S., Ong, K., Lau, E., Mowat, F., and Halpern, M. (2007a). Projections of primary and revision hip and knee arthroplasty in the United States from 2005 to 2030. *J Bone Joint Surg Am* 89, 780–785.

Kurtz, S.M., Ong, K.L., Schmier, J., Mowat, F., Saleh, K., Dybvik, E., Ksrrholm, J., Garellick, G., Havelin, L.I., Furnes, O.M., et al. (2007b). Future Clinical and Economic Impact of Revision Total Hip and Knee Arthroplasty. *JBJS* 89, 144.

Kurtz, S.M., Lau, E., Ong, K., Zhao, K., Kelly, M., and Bozic, K.J. (2009). Future Young Patient Demand for Primary and Revision Joint Replacement: National Projections from 2010 to 2030. *Clin Orthop Relat Res* 467, 2606–2612.

Kurtz, S.M., Ong, K.L., Lau, E., Widmer, M., Maravic, M., Gómez-Barrena, E., de Fátima de Pina, M., Manno, V., Torre, M., Walter, W.L., et al. (2011). International survey of primary and revision total knee replacement. *Int Orthop* 35, 1783–1789.

Laurent, E., Gras, G., Druon, J., Rosset, P., Baron, S., Le-Louarn, A., Rusch, E., Bernard, L., and Grammatico-Guillon, L. (2018). Key features of bone and joint

infections following the implementation of reference centers in France. *Med Mal Infect* 48, 256–262.

Lebeaux, D., Chauhan, A., Rendueles, O., and Beloin, C. (2013). From in vitro to in vivo Models of Bacterial Biofilm-Related Infections. *Pathogens* 2, 288–356.

Lee, Y.-W., Chung, Y., Juhn, S.K., Kim, Y., and Lin, J. (2011). Activation of the Transforming Growth Factor Beta Pathway in Bacterial Otitis Media. *Ann Otol Rhinol Laryngol* 120, 204–213.

Lemaire, V., Tobin, F.L., Greller, L.D., Cho, C.R., and Suva, L.J. (2004). Modeling the interactions between osteoblast and osteoclast activities in bone remodeling. *Journal of Theoretical Biology* 229, 293–309.

Lew, D.P., and Waldvogel, F.A. (2004). Osteomyelitis. *The Lancet* 364, 369–379.

Li, D., Gromov, K., Søballe, K., Puzas, J.E., O’Keefe, R.J., Awad, H., Drissi, H., and Schwarz, E.M. (2008a). Quantitative mouse model of implant-associated osteomyelitis and the kinetics of microbial growth, osteolysis, and humoral immunity. *J. Orthop. Res.* 26, 96–105.

Li, D., Gromov, K., Soballe, K., Puzas, J.E., O’Keefe, R.J., Awad, H., Drissi, H., and Schwarz, E.M. (2008b). Quantitative mouse model of implant-associated osteomyelitis and the kinetics of microbial growth, osteolysis, and humoral immunity. *J.Orthop.Res.* 26, 96–105.

Liò, P., Paoletti, N., Moni, M.A., Atwell, K., Merelli, E., and Viceconti, M. (2012). Modelling osteomyelitis. *BMC Bioinformatics* 13, S12.

Löffler, B., Tuchscher, L., Niemann, S., and Peters, G. (2014). Staphylococcus aureus persistence in non-professional phagocytes. *International Journal of Medical Microbiology* 304, 170–176.

Lorenzo, J., Horowitz, M., and Choi, Y. (2008). Osteoimmunology: Interactions of the Bone and Immune System. *Endocr Rev* 29, 403–440.

Losina, E., Thornhill, T.S., Rome, B.N., Wright, J., and Katz, J.N. (2012). The dramatic increase in total knee replacement utilization rates in the United States cannot be fully explained by growth in population size and the obesity epidemic. *J Bone Joint Surg Am* 94, 201–207.

Lowy, F.D. (2000). Is Staphylococcus aureus an intracellular pathogen? *Trends in Microbiology* 8, 341–343.

M R W Brown, and Williams, and P. (1985). The Influence of Environment on Envelope Properties Affecting Survival of Bacteria in Infections. *Annual Review of Microbiology* 39, 527–556.

Macal, C.M., and North, M.J. (2005). Tutorial on agent-based modeling and simulation. In *Proceedings of the Winter Simulation Conference, 2005.*, pp. 14 pp.-.

- Macal, C.M., and North, M.J. (2010). Tutorial on agent-based modelling and simulation. *J Simulation* 4, 151–162.
- MacKay, D.J.C. (2002). *Information Theory, Inference & Learning Algorithms* (New York, NY, USA: Cambridge University Press).
- Mackie, E.J. (2003). Osteoblasts: novel roles in orchestration of skeletal architecture. *Int.J.Biochem.Cell Biol.* 35, 1301–1305.
- Mader, J.T. (1985). Animal models of osteomyelitis. *The American Journal of Medicine* 78, 213–217.
- Madey, C.N. and G. (2009). *Tools of the Trade: A Survey of Various Agent Based Modeling Platforms*.
- Maianski, N.A., Maianski, A.N., Kuijpers, T.W., and Roos, D. (2004). Apoptosis of neutrophils. *Acta Haematol.* 111, 56–66.
- Maier, R.M. (2009). Chapter 3 - Bacterial Growth. In *Environmental Microbiology* (Second Edition), (San Diego: Academic Press), pp. 37–54.
- Manolagas, S.C. (2000). Birth and Death of Bone Cells: Basic Regulatory Mechanisms and Implications for the Pathogenesis and Treatment of Osteoporosis. *Endocr Rev* 21, 115–137.
- Marais, L.C., Ferreira, N., Aldous, C., and le Roux, T.L.B. (2013). The pathophysiology of chronic osteomyelitis. *SA Orthopaedic Journal* 12, 14–18.
- Marriott, I. (2013). Apoptosis-associated uncoupling of bone formation and resorption in osteomyelitis. *Front.Cell.Infect.Microbiol.* 3, 101.
- Marriott, I., Gray, D.L., Tranguch, S.L., Fowler, V.G., Stryjewski, M., Scott Levin, L., Hudson, M.C., and Bost, K.L. (2004). Osteoblasts Express the Inflammatory Cytokine Interleukin-6 in a Murine Model of *Staphylococcus aureus* Osteomyelitis and Infected Human Bone Tissue. *The American Journal of Pathology* 164, 1399–1406.
- Marriott, I., Gray, D.L., Rati, D.M., Fowler, V.G., Stryjewski, M.E., Levin, L.S., Hudson, M.C., and Bost, K.L. (2005). Osteoblasts produce monocyte chemoattractant protein-1 in a murine model of *Staphylococcus aureus* osteomyelitis and infected human bone tissue. *Bone* 37, 504–512.
- Martin, T.J. (2004). Paracrine regulation of osteoclast formation and activity: milestones in discovery. *J Musculoskelet Neuronal Interact* 4, 243–253.
- Mass, E., Ballesteros, I., Farlik, M., Halbritter, F., Günther, P., Crozet, L., Jacome-Galarza, C.E., Händler, K., Klughammer, J., Kobayashi, Y., et al. (2016). Specification of tissue-resident macrophages during organogenesis. *Science* 353, aaf4238.
- Mathews, C.J., Weston, V.C., Jones, A., Field, M., and Coakley, G. (2010). Bacterial septic arthritis in adults. *Lancet* 375, 846–855.

McHenry, M.C., Easley, K.A., and Locker, G.A. (2002). Vertebral osteomyelitis: long-term outcome for 253 patients from 7 Cleveland-area hospitals. *Clin. Infect. Dis.* *34*, 1342–1350.

Medzhitov, R., and Janeway, C.A. (1997). Innate immunity: impact on the adaptive immune response. *Current Opinion in Immunology* *9*, 4–9.

Mellis, D.J., Itzstein, C., Helfrich, M.H., and Crockett, J.C. (2011). The skeleton: a multi-functional complex organ: the role of key signalling pathways in osteoclast differentiation and in bone resorption. *J.Endocrinol.* *211*, 131–143.

Melter, O., and Radojevic, B. (2010). Small colony variants of *Staphylococcus aureus*--review. *Folia Microbiol.(Praha)* *55*, 548–558.

Merelli, E. (2013). FORMAL COMPUTATIONAL MODELLING OF BONE PHYSIOLOGY AND DISEASE PROCESSES. UNIVERSITY OF CAMERINO.

Miller, S.C., Jee, W.S.S., and Jee, W.S.S. (1987). The bone lining cell: A distinct phenotype? *Calcif Tissue Int* *41*, 1–5.

Mori, G., D'Amelio, P., Faccio, R., and Brunetti, G. (2013). The Interplay between the Bone and the Immune System.

Motta, S., and Pappalardo, F. (2013). Mathematical modeling of biological systems. *Brief Bioinform* *14*, 411–422.

Mousa, A., and Bakhiet, M. (2013). Role of Cytokine Signaling during Nervous System Development. *Int J Mol Sci* *14*, 13931–13957.

Mulherin, D., Fitzgerald, O., and Bresnihan, B. (1996). Synovial tissue macrophage populations and articular damage in rheumatoid arthritis. *Arthritis & Rheumatism* *39*, 115–124.

Mullender, M.G., and Huiskes, R. (1997). Osteocytes and bone lining cells: Which are the best candidates for mechano-sensors in cancellous bone? *Bone* *20*, 527–532.

Nair, S., Song, Y., Meghji, S., Reddi, K., Harris, M., Ross, A., Poole, S., Wilson, M., and Henderson, B. (1995). Surface-associated proteins from *Staphylococcus aureus* demonstrate potent bone resorbing activity. *J. Bone Miner. Res.* *10*, 726–734.

Nair, S.P., Meghji, S., Wilson, M., Reddi, K., White, P., and Henderson, B. (1996). Bacterially induced bone destruction: mechanisms and misconceptions. *Infect. Immun.* *64*, 2371–2380.

Nakashima, T. (2014). Coupling and communication between bone cells. *Clin.Calcium* *24*, 853–861.

Niemeläinen, M.J., Mäkelä, K.T., Robertsson, O., W-Dahl, A., Furnes, O., Fenstad, A.M., Pedersen, A.B., Schröder, H.M., Huhtala, H., and Eskelinen, A. (2017). Different incidences of knee arthroplasty in the Nordic countries. *Acta Orthopaedica* *88*, 173–178.

- Ning, R., Zhang, X., Guo, X., and Li, Q. (2011). Staphylococcus aureus regulates secretion of interleukin-6 and monocyte chemoattractant protein-1 through activation of nuclear factor kappaB signaling pathway in human osteoblasts. *Braz.J.Infect.Dis.* *15*, 189–194.
- Olson, M.E., and Horswill, A.R. (2013). Staphylococcus aureus Osteomyelitis: Bad to the Bone. *Cell Host & Microbe* *13*, 629–631.
- Osmon, D.R., Berbari, E.F., Berendt, A.R., Lew, D., Zimmerli, W., Steckelberg, J.M., Rao, N., Hanssen, A., and Wilson, W.R. (2013). Diagnosis and Management of Prosthetic Joint Infection: Clinical Practice Guidelines by the Infectious Diseases Society of America. *Clin Infect Dis* *56*, e1–e25.
- Panteli, M., and Giannoudis, P.V. (2016). Chronic osteomyelitis: what the surgeon needs to know. *EFORT Open Rev* *1*, 128–135.
- Paoletti, N., Lio, P., Merelli, E., and Viceconti, M. (2012a). Multilevel computational modeling and quantitative analysis of bone remodeling. *IEEE/ACM Trans.Comput.Biol.Bioinform* *9*, 1366–1378.
- Paoletti, N., Liò, P., Merelli, E., and Viceconti, M. (2012b). Multilevel Computational Modeling and Quantitative Analysis of Bone Remodeling. *IEEE/ACM Transactions on Computational Biology and Bioinformatics* *9*, 1366–1378.
- Pappalardo, F., Chiacchio, F., and Motta, S. (2012). Cancer vaccines: state of the art of the computational modeling approaches. *BioMed Research International* *2013*.
- Pappalardo, F., Pennisi, M., Chiacchio, F., Musumeci, S., and Motta, S. (2013). iAtheroSim: Atherosclerosis Process Simulator on Smart Devices. In *Proceedings of the International Conference on Bioinformatics, Computational Biology and Biomedical Informatics*, (New York, NY, USA: ACM), pp. 815:815–815:817.
- Parfitt, A.M. (1994). Osteonal and hemi-osteonal remodeling: The spatial and temporal framework for signal traffic in adult human bone. *J. Cell. Biochem.* *55*, 273–286.
- Parihar, A., Eubank, T.D., and Doseff, A.I. (2010). Monocytes and macrophages regulate immunity through dynamic networks of survival and cell death. *J.Innate Immun.* *2*, 204–215.
- Parvizi, J., Pawasarat, I.M., Azzam, K.A., Joshi, A., Hansen, E.N., and Bozic, K.J. (2010). Periprosthetic joint infection: the economic impact of methicillin-resistant infections. *J Arthroplasty* *25*, 103–107.
- Parwaresch, M.R., and Wacker, H.H. (1984). Origin and kinetics of resident tissue macrophages. Parabiosis studies with radiolabelled leucocytes. *Cell Tissue Kinet* *17*, 25–39.
- Patel, A., Pavlou, G., Mújica-Mota, R.E., and Toms, A.D. (2015). The epidemiology of revision total knee and hip arthroplasty in England and Wales. *The Bone & Joint Journal* *97-B*, 1076–1081.

- Patel, A.A., Zhang, Y., Fullerton, J.N., Boelen, L., Rongvaux, A., Maini, A.A., Bigley, V., Flavell, R.A., Gilroy, D.W., Asquith, B., et al. (2017). The fate and lifespan of human monocyte subsets in steady state and systemic inflammation. *Journal of Experimental Medicine* 214, 1913–1923.
- Patel, M., Rojavin, Y., Jamali, A.A., Wasielewski, S.J., and Salgado, C.J. (2009). Animal Models for the Study of Osteomyelitis. *Seminars in Plastic Surgery* 23, 148–154.
- Peeters, O., Ferry, T., Ader, F., Boibieux, A., Braun, E., Bouaziz, A., Karsenty, J., Forestier, E., Laurent, F., Lustig, S., et al. (2016). Teicoplanin-based antimicrobial therapy in *Staphylococcus aureus* bone and joint infection: tolerance, efficacy and experience with subcutaneous administration. *BMC Infect. Dis.* 16, 622.
- Pérez, M.A., and Prendergast, P.J. (2007). Random-walk models of cell dispersal included in mechanobiological simulations of tissue differentiation. *Journal of Biomechanics* 40, 2244–2253.
- Peter, I.S., Faure, E., Davidson, E.H., Faure, E., and Peter, I.S. (2012). Predictive computation of genomic logic processing functions in embryonic development. *PNAS* 109, 16434–16442.
- Pillay, J., Braber, I. den, Vrisekoop, N., Kwast, L.M., Boer, R.J. de, Borghans, J.A.M., Tesselaar, K., and Koenderman, L. (2010). In vivo labeling with ²H₂O reveals a human neutrophil lifespan of 5.4 days. *Blood* 116, 625–627.
- Pinchuk, G. (2001). *Schaum's Outline of Immunology* (McGraw Hill Professional).
- Pineda, C., Vargas, A., and Rodríguez, A.V. (2006). Imaging of Osteomyelitis: Current Concepts. *Infectious Disease Clinics* 20, 789–825.
- Pineda, C., Espinosa, R., and Pena, A. (2009). Radiographic Imaging in Osteomyelitis: The Role of Plain Radiography, Computed Tomography, Ultrasonography, Magnetic Resonance Imaging, and Scintigraphy. *Semin Plast Surg* 23, 80–89.
- Pivonka, P., and Dunstan, C.R. (2012). Role of mathematical modeling in bone fracture healing. *BoneKEY Rep* 1, 221.
- Pivonka, P., Zimak, J., Smith, D.W., Gardiner, B.S., Dunstan, C.R., Sims, N.A., John Martin, T., and Mundy, G.R. (2008). Model structure and control of bone remodeling: A theoretical study. *Bone* 43, 249–263.
- Pivonka, P., Zimak, J., Smith, D.W., Gardiner, B.S., Dunstan, C.R., Sims, N.A., John Martin, T., and Mundy, G.R. (2010). Theoretical investigation of the role of the RANK–RANKL–OPG system in bone remodeling. *Journal of Theoretical Biology* 262, 306–316.
- Pogson, M., Smallwood, R., Qwarnstrom, E., and Holcombe, M. (2006). Formal agent-based modelling of intracellular chemical interactions. *Biosystems* 85, 37–45.

- Pogson, M., Holcombe, M., Smallwood, R., and Qwarnstrom, E. (2008). Introducing Spatial Information into Predictive NF- κ B Modelling – An Agent-Based Approach. *PLOS ONE* 3, e2367.
- Politopoulos, I. (2007). Review and analysis of agent-based models in biology. University of Liverpool.
- POWELL, E.O. (1956). Growth Rate and Generation Time of Bacteria, with Special Reference to Continuous Culture. *Microbiology* 15, 492–511.
- Prideaux, M., Findlay, D.M., and Atkins, G.J. (2016). Osteocytes: The master cells in bone remodelling. *Current Opinion in Pharmacology* 28, 24–30.
- Raggatt, L.J., and Partridge, N.C. (2010). Cellular and Molecular Mechanisms of Bone Remodeling. *J. Biol. Chem.* 285, 25103–25108.
- Railsback, S.F., and Grimm, V. (2011). Agent-Based and Individual-Based Modeling: A Practical Introduction (Princeton University Press).
- Railsback, S.F., Lytinen, S.L., and Jackson, S.K. (2006). Agent-based Simulation Platforms: Review and Development Recommendations. *SIMULATION* 82, 609–623.
- Raisz, L.G. (1999). Physiology and Pathophysiology of Bone Remodeling. *Clinical Chemistry* 45, 1353–1358.
- Ranganathan, S., Spaiser, V., Mann, R.P., and Sumpter, D.J.T. (2014a). Bayesian Dynamical Systems Modelling in the Social Sciences. *PLOS ONE* 9, e86468.
- Ranganathan, S., Spaiser, V., Mann, R.P., and Sumpter, D.J.T. (2014b). bdynsys: Bayesian Dynamical System Model.
- Ranganathan, S., Bali Swain, R., and Sumpter, D. (2014c). A Dynamical Systems Approach To Modeling Human Development (Uppsala University, Department of Economics).
- Rankin, S.M. (2010). The bone marrow: a site of neutrophil clearance. *J Leukoc Biol* 88, 241–251.
- Ravi, B., Croxford, R., Reichmann, W.M., Losina, E., Katz, J.N., and Hawker, G.A. (2012). The changing demographics of total joint arthroplasty recipients in the United States and Ontario from 2001 to 2007. *Best Pract Res Clin Rheumatol* 26, 637–647.
- Reed, S.G. (1999). TGF- β in infections and infectious diseases. *Microbes and Infection* 1, 1313–1325.
- Reizner, W., Hunter, J.G., O'Malley, N.T., Southgate, R.D., Schwarz, E.M., and Kates, S.L. (2014). A systematic review of animal models for Staphylococcus aureus osteomyelitis. *Eur Cell Mater* 27, 196–212.

- Renner, U., Paez-Pereda, M., Arzt, E., and Stalla, G.K. (2004). Growth factors and cytokines: function and molecular regulation in pituitary adenomas. *Front Horm Res* 32, 96–109.
- Repp, F., Kollmannsberger, P., Roschger, A., Kerschnitzki, M., Berzlanovich, A., Gruber, G.M., Roschger, P., Wagermaier, W., and Weinkamer, R. (2017). Spatial heterogeneity in the canalicular density of the osteocyte network in human osteons. *Bone Reports* 6, 101–108.
- Reuter, S., and Lang, D. (2009). Life span of monocytes and platelets: importance of interactions. *Front.Biosci.(Landmark Ed)* 14, 2432–2447.
- Ribeiro, M., Monteiro, F.J., and Ferraz, M.P. (2012). Infection of orthopedic implants with emphasis on bacterial adhesion process and techniques used in studying bacterial-material interactions. *Biomatter* 2, 176–194.
- Ridgway, D., Broderick, G., Lopez-Campistrous, A., Ru'aini, M., Winter, P., Hamilton, M., Boulanger, P., Kovalenko, A., and Ellison, M.J. (2008). Coarse-Grained Molecular Simulation of Diffusion and Reaction Kinetics in a Crowded Virtual Cytoplasm. *Biophysical Journal* 94, 3748–3759.
- Roberts, W.E., Roberts, J.A., Epker, B.N., Burr, D.B., and Hartsfield, J.K. (2006). Remodeling of Mineralized Tissues, Part I: The Frost Legacy. *Seminars in Orthodontics* 12, 216–237.
- Rochford, E.T.J., Sabaté Brescó, M., Zeiter, S., Kluge, K., Poulsson, A., Ziegler, M., Richards, R.G., O'Mahony, L., and Moriarty, T.F. (2016). Monitoring immune responses in a mouse model of fracture fixation with and without *Staphylococcus aureus* osteomyelitis. *Bone* 83, 82–92.
- Rodan, G.A. (1992). Introduction to bone biology. *Bone* 13, S3–S6.
- Roodman, G.D. (1999). Cell biology of the osteoclast. *Exp.Hematol.* 27, 1229–1241.
- Rucci, N. (2008). Molecular biology of bone remodelling. *Clin Cases Miner Bone Metab* 5, 49–56.
- Ryser, M.D., Nigam, N., and Komarova, S.V. (2009). Mathematical Modeling of Spatio-Temporal Dynamics of a Single Bone Multicellular Unit. *J Bone Miner Res* 24, 860–870.
- Sanchez, S.M. (1999). ABC's of output analysis. In *Simulation Conference Proceedings, 1999 Winter*, pp. 24–32 vol.1.
- Sanchez, C.J., Ward, C.L., Romano, D.R., Hurtgen, B.J., Hardy, S.K., Woodbury, R.L., Trevino, A.V., Rathbone, C.R., and Wenke, J.C. (2013). *Staphylococcus aureus* biofilms decrease osteoblast viability, inhibits osteogenic differentiation, and increases bone resorption in vitro. *BMC Musculoskeletal Disorders* 14, 187.
- Sargent, R.G. (2007). Verification and validation of simulation models. In *2007 Winter Simulation Conference*, pp. 124–137.

- Sarko, J. (2005). Bone and Mineral Metabolism. *Emergency Medicine Clinics* 23, 703–721.
- Savina, A., and Amigorena, S. (2007). Phagocytosis and antigen presentation in dendritic cells. *Immunological Reviews* 219, 143–156.
- Schaffler, M.B., and Kennedy, O.D. (2012). Osteocyte Signaling in Bone. *Curr Osteoporos Rep* 10, 118–125.
- Schaffler, M.B., Cheung, W.-Y., Majeska, R., and Kennedy, O. (2014). Osteocytes: Master Orchestrators of Bone. *Calcif Tissue Int* 94, 5–24.
- Scheiner, S., Pivonka, P., and Hellmich, C. (2013). Coupling systems biology with multiscale mechanics, for computer simulations of bone remodeling. *Comput.Methods Appl.Mech.Eng.* 254, 181–196.
- Schirm, S., Ahnert, P., Wienhold, S., Mueller-Redetzky, H., Nouailles-Kursar, G., Loeffler, M., Witzernath, M., and Scholz, M. (2016). A Biomathematical Model of Pneumococcal Lung Infection and Antibiotic Treatment in Mice. *PLOS ONE* 11, e0156047.
- Schmidt-Weber, C.B., and Blaser, K. (2004). Regulation and role of transforming growth factor- β in immune tolerance induction and inflammation. *Curr.Opin.Immunol.* 16, 709–716.
- Schneider, P., Meier, M., Wepf, R., and Müller, R. (2010). Towards quantitative 3D imaging of the osteocyte lacuno-canalicular network. *Bone* 47, 848–858.
- Schröder, J.-M. (2000). Chemoattractants as mediators of neutrophilic tissue recruitment. *Clin.Dermatol.* 18, 245–263.
- Schroer, W.C., Berend, K.R., Lombardi, A.V., Barnes, C.L., Bolognesi, M.P., Berend, M.E., Ritter, M.A., and Nunley, R.M. (2013). Why are total knees failing today? Etiology of total knee revision in 2010 and 2011. *J Arthroplasty* 28, 116–119.
- Schutte, L. (2012). An Agent-based Model for Evaluating Cellular Mechanisms of Bone Remodeling. *Dissertations*.
- Segovia-Juarez, J.L., Ganguli, S., and Kirschner, D. (2004). Identifying control mechanisms of granuloma formation during *M. tuberculosis* infection using an agent-based model. *Journal of Theoretical Biology* 231, 357–376.
- Shapiro, F. (2008). Bone development and its relation to fracture repair. The role of mesenchymal osteoblasts and surface osteoblasts. *Eur Cell Mater* 15, 53–76.
- Sharma, R., and Anker, S.D. (2002). Cytokines, apoptosis and cachexia: the potential for TNF antagonism. *Int.J.Cardiol.* 85, 161–171.
- Sheng, J., Chen, W., and Zhu, H.J. (2015). The immune suppressive function of transforming growth factor-beta (TGF-beta) in human diseases. *Growth Factors* 33, 92–101.

- Shi, C., and Pamer, E.G. (2011). Monocyte recruitment during infection and inflammation. *Nature Reviews Immunology* 11, 762–774.
- Shi, Z.Z., Wu, C.-H., and Ben-Arieh, D. (2014). Agent-Based Model: A Surging Tool to Simulate Infectious Diseases in the Immune System. *Open Journal of Modelling and Simulation* 02, 12.
- Sia, I.G., and Berbari, E.F. (2006). Osteomyelitis. *Best Practice & Research Clinical Rheumatology* 20, 1065–1081.
- Silva, M.T. (2011). Macrophage phagocytosis of neutrophils at inflammatory/infectious foci: a cooperative mechanism in the control of infection and infectious inflammation. *J Leukoc Biol* 89, 675–683.
- Simon, S.I., and Kim, M.-H. (2010). A day (or 5) in a neutrophil's life. *Blood* 116, 511–512.
- Sims, N.A., and Gooi, J.H. (2008). Bone remodeling: Multiple cellular interactions required for coupling of bone formation and resorption. *Semin.Cell Dev.Biol.* 19, 444–451.
- Sims, N.A., and Martin, T.J. (2014). Coupling the activities of bone formation and resorption: a multitude of signals within the basic multicellular unit. *BoneKEy Rep* 3, 481.
- Sims, N.A., and Martin, T.J. (2015). Coupling Signals between the Osteoclast and Osteoblast: How are Messages Transmitted between These Temporary Visitors to the Bone Surface? *Front. Endocrinol.* 6.
- Skilling, J. (2006). Nested sampling for general Bayesian computation. *Bayesian Anal.* 1, 833–859.
- Sklar, E. (2007). NetLogo, a multi-agent simulation environment. *Artif Life* 13, 303–311.
- Smith, H. (1990). Pathogenicity and the Microbe in vivo: The 1989 Fred Griffith Review Lecture. *Microbiology* 136, 377–383.
- Smith, H. (1998). What happens to bacterial pathogens in vivo? *Trends in Microbiology* 6, 239–243.
- Smith, H. (2000). Host factors that influence the behaviour of bacterial pathogens in vivo. *International Journal of Medical Microbiology* 290, 207–213.
- Smith, A.M., McCullers, J.A., and Adler, F.R. (2011a). Mathematical model of a three-stage innate immune response to a pneumococcal lung infection. *J.Theor.Biol.* 276, 106–116.
- Smith, A.M., McCullers, J.A., and Adler, F.R. (2011b). Mathematical model of a three-stage innate immune response to a pneumococcal lung infection. *Journal of Theoretical Biology* 276, 106–116.

- Smith, I.M., Austin, O.M.B., and Batchelor, A.G. (2006). The treatment of chronic osteomyelitis: A 10 year audit. *Journal of Plastic, Reconstructive & Aesthetic Surgery* 59, 11–15.
- Soysa, N.S., and Alles, N. (2016). Osteoclast function and bone-resorbing activity: An overview. *Biochem.Biophys.Res.Commun.* 476, 115–120.
- Spellberg, B., and Lipsky, B.A. (2012). Systemic Antibiotic Therapy for Chronic Osteomyelitis in Adults. *Clin Infect Dis* 54, 393–407.
- Steele, D.G., and Bramblett, C.A. (1988). *The Anatomy and Biology of the Human Skeleton* (Texas A&M University Press).
- Stone, K.D., Prussin, C., and Metcalfe, D.D. (2010). IgE, mast cells, basophils, and eosinophils. *Journal of Allergy and Clinical Immunology* 125, S73–S80.
- Strydom, N., and Rankin, S.M. (2013). Regulation of Circulating Neutrophil Numbers under Homeostasis and in Disease. *JIN* 5, 304–314.
- Suda, T., Nakamura, I., Jimi, E., and Takahashi, N. (1997). Regulation of Osteoclast Function. *J Bone Miner Res* 12, 869–879.
- Summers, C., Rankin, S.M., Condliffe, A.M., Singh, N., Peters, A.M., and Chilvers, E.R. (2010). Neutrophil kinetics in health and disease. *Trends Immunol.* 31, 318–324.
- Szallasi, Z., Stelling, J., and Periwal, V. (2006). *System Modeling in Cellular Biology: From Concepts to Nuts and Bolts* (The MIT Press).
- Szondy, Z., and Pallai, A. (2017). Transmembrane TNF-alpha reverse signaling leading to TGF-beta production is selectively activated by TNF targeting molecules: Therapeutic implications. *Pharmacological Research* 115, 124–132.
- Takayanagi, H. (2007). Osteoimmunology: shared mechanisms and crosstalk between the immune and bone systems. *Nat Rev Immunol* 7, 292–304.
- Tanaka, S., Miyazaki, T., Fukuda, A., Akiyama, T., Kadono, Y., Wakeyama, H., Kono, S., Hoshikawa, S., Nakamura, M., Ohshima, Y., et al. (2006). Molecular mechanism of the life and death of the osteoclast. *Ann.N.Y.Acad.Sci.* 1068, 180–186.
- Tande, A.J., and Patel, R. (2014). Prosthetic Joint Infection. *Clin. Microbiol. Rev.* 27, 302–345.
- Tatara, A.M., Shah, S.R., Livingston, C.E., and Mikos, A.G. (2015). Infected Animal Models for Tissue Engineering. *Methods* 84, 17–24.
- Teti, A. (2013). Mechanisms of osteoclast-dependent bone formation. *BoneKEY Rep* 2, 449.
- Thorne, B.C., Bailey, A.M., and Peirce, S.M. (2007). Combining experiments with multi-cell agent-based modeling to study biological tissue patterning. *Brief Bioinform* 8, 245–257.

- Tisue, S., and Wilensky, U. (2004). NetLogo: A simple environment for modeling complexity. In *International Conference on Complex Systems*, pp. 16–21.
- Tong, S.Y.C., Davis, J.S., Eichenberger, E., Holland, T.L., and Fowler, V.G. (2015). Staphylococcus aureus infections: epidemiology, pathophysiology, clinical manifestations, and management. *Clin. Microbiol. Rev.* 28, 603–661.
- Trouillet-Assant, S., Lelièvre, L., Martins-Simões, P., Gonzaga, L., Tasse, J., Valour, F., Rasigade, J.-P., Vandenesch, F., Muniz Guedes, R.L., Ribeiro de Vasconcelos, A.T., et al. (2016). Adaptive processes of Staphylococcus aureus isolates during the progression from acute to chronic bone and joint infections in patients. *Cell. Microbiol.* 18, 1405–1414.
- Tuscherr, L., Heitmann, V., Hussain, M., Viemann, D., Roth, J., von Eiff, C., Peters, G., Becker, K., and Löffler, B. (2010). Staphylococcus aureus Small-Colony Variants Are Adapted Phenotypes for Intracellular Persistence. *J Infect Dis* 202, 1031–1040.
- Tuscherr, L., Kreis, C.A., Hoerr, V., Flint, L., Hachmeister, M., Geraci, J., Bremer-Streck, S., Kiehntopf, M., Medina, E., Kribus, M., et al. (2016). Staphylococcus aureus develops increased resistance to antibiotics by forming dynamic small colony variants during chronic osteomyelitis. *J. Antimicrob. Chemother.* 71, 438–448.
- Turner, M.D., Nedjai, B., Hurst, T., and Pennington, D.J. (2014). Cytokines and chemokines: At the crossroads of cell signalling and inflammatory disease. *Biochimica et Biophysica Acta (BBA) - Molecular Cell Research* 1843, 2563–2582.
- Valour, F., Trouillet-Assant, S., Rasigade, J.-P., Lustig, S., Chanard, E., Meugnier, H., Tigaud, S., Vandenesch, F., Etienne, J., Ferry, T., et al. (2013). Staphylococcus epidermidis in Orthopedic Device Infections: The Role of Bacterial Internalization in Human Osteoblasts and Biofilm Formation. *PLOS ONE* 8, e67240.
- Valour, F., Trouillet-Assant, S., Riffard, N., Tasse, J., Flammier, S., Rasigade, J.-P., Chidiac, C., Vandenesch, F., Ferry, T., and Laurent, F. (2015). Antimicrobial activity against intraosteoblastic Staphylococcus aureus. *Antimicrob. Agents Chemother.* 59, 2029–2036.
- Van der Meide, P.H., and Schellekens, H. (1996). Cytokines and the immune response. *Biotherapy* 8, 243–249.
- Vashishth, D., Verborgt, O., Divine, G., Schaffler, M.B., and Fyhrie, D.P. (2000). Decline in osteocyte lacunar density in human cortical bone is associated with accumulation of microcracks with age. *Bone* 26, 375–380.
- Vasselon, T., and Detmers, P.A. (2002). Toll Receptors: a Central Element in Innate Immune Responses. *Infect. Immun.* 70, 1033–1041.
- Vodovotz, Y., Csete, M., Bartels, J., Chang, S., and An, G. (2008). Translational Systems Biology of Inflammation. *PLOS Computational Biology* 4, e1000014.

- Vodovotz, Y., Constantine, G., Rubin, J., Csete, M., Voit, E.O., and An, G. (2009). Mechanistic simulations of inflammation: Current state and future prospects. *Mathematical Biosciences* 217, 1–10.
- Wagner, C., Kondella, K., Bernschneider, T., Heppert, V., Wentzensen, A., and Hänsch, G.M. (2003). Post-Traumatic Osteomyelitis: Analysis of Inflammatory Cells Recruited into the Site of Infection. *Shock* 20, 503.
- Walker, D., Sun, T., Macneil, S., and Smallwood, R. (2006). Modeling the Effect of Exogenous Calcium on Keratinocyte and HaCat Cell Proliferation and Differentiation Using an Agent-Based Computational Paradigm. *Tissue Engineering* 12, 2301–2309.
- Walkup, G.K., You, Z., Ross, P.L., Allen, E.K.H., Daryaei, F., Hale, M.R., O'Donnell, J., Ehmann, D.E., Schuck, V.J.A., Buurman, E.T., et al. (2015). Translating slow-binding inhibition kinetics into cellular and in vivo effects. *Nat Chem Biol* 11, 416–423.
- Wallace, W.A., Gillooly, M., and Lamb, D. (1993). Age related increase in the intra-alveolar macrophage population of non-smokers. *Thorax* 48, 668–669.
- Walpole, J., Papin, J.A., and Peirce, S.M. (2013). Multiscale Computational Models of Complex Biological Systems. *Annual Review of Biomedical Engineering* 15, 137–154.
- Walter, G., Kemmerer, M., Kappler, C., and Hoffmann, R. (2012). Treatment Algorithms for Chronic Osteomyelitis. *Dtsch Arztebl Int* 109, 257–264.
- Wang, Y., and Thorlacius, H. (2005). Mast cell-derived tumour necrosis factor- α mediates macrophage inflammatory protein-2-induced recruitment of neutrophils in mice. *Br J Pharmacol* 145, 1062–1068.
- Whitelaw, D.M., and Bell, M. (1966). The Intravascular Lifespan of Monocytes. *Blood* 28, 455–464.
- Whyte, M., Renshaw, S., Lawson, R., and Bingle, C. (1999). Apoptosis and the regulation of neutrophil lifespan. *Biochem.Soc.Trans.* 27, 802–807.
- Wilensky, U. (1999). NetLogo.
- Williams, R.C., and Fudenberg, H.H. (1972). Phagocytic mechanisms in health and disease (Intercontinental Medical Book Corp.).
- Windrum, P., Fagiolo, G., and Moneta, A. (2007). Empirical Validation of Agent-Based Models: Alternatives and Prospects. *Journal of Artificial Societies and Social Simulation* 10, 1–8.
- Witko-Sarsat, V., Rieu, P., Descamps-Latscha, B., Lesavre, P., and Halbwachs-Mecarelli, L. (2000). Neutrophils: Molecules, Functions and Pathophysiological Aspects. *Laboratory Investigation* 80, 617.

- Xiang, X., Kennedy, R., Madey, G., and Cabaniss, S. (2005). Verification and Validation of Agent-based Scientific Simulation Models. In 2005 Agent-Directed Simulation Symposium ADS'05, p.
- Yamashita, T., Takahashi, N., and Udagawa, N. (2012). New roles of osteoblasts involved in osteoclast differentiation. *World J Orthop* 3, 175–181.
- Yona, S., Kim, K.-W., Wolf, Y., Mildner, A., Varol, D., Breker, M., Strauss-Ayali, D., Viukov, S., Guilliams, M., Misharin, A., et al. (2013a). Fate Mapping Reveals Origins and Dynamics of Monocytes and Tissue Macrophages under Homeostasis. *Immunity* 38, 79–91.
- Yona, S., Kim, K.W., Wolf, Y., Mildner, A., Varol, D., Breker, M., Strauss-Ayali, D., Viukov, S., Guilliams, M., Misharin, A., et al. (2013b). Fate mapping reveals origins and dynamics of monocytes and tissue macrophages under homeostasis. *Immunity* 38, 79–91.
- Yoshii, T., Magara, S., Miyai, D., Nishimura, H., Kuroki, E., Furudoi, S., Komori, T., and Ohbayashi, C. (2002). LOCAL LEVELS OF INTERLEUKIN-1 β , -4, -6, AND TUMOR NECROSIS FACTOR α IN AN EXPERIMENTAL MODEL OF MURINE OSTEOMYELITIS DUE TO STAPHYLOCOCCUS AUREUS. *Cytokine* 19, 59–65.
- Young, A.B., Cooley, I.D., Chauhan, V.S., and Marriott, I. (2011). Causative agents of osteomyelitis induce death domain-containing TNF-related apoptosis-inducing ligand receptor expression on osteoblasts. *Bone* 48, 857–863.
- Zahedmanesh, H., Lally, C., and Lally, C. (2012). A multiscale mechanobiological modelling framework using agent-based models and finite element analysis: application to vascular tissue engineering. *Biomech Model Mechanobiol* 11, 363–377.
- Zhang, L., Wang, Z., Sagotsky, J.A., and Deisboeck, T.S. (2009). Multiscale agent-based cancer modeling. *Journal of Mathematical Biology* 58, 545–559.
- Zhao, Y., Cai, Y., and Wang, Y.N. (2010). RANKL and OPG regulation on bone remodeling. *Shanghai Kou Qiang Yi Xue* 19, 443–446.
- Zhou, H., Lu, S.S., and Dempster, D.W. (2010). Chapter 2 - Bone Remodeling: Cellular Activities in Bone. In *Osteoporosis in Men (Second Edition)*, E.S. Orwoll, J.P. Bilezikian, and D. Vanderschueren, eds. (San Diego: Academic Press), pp. 15–24.
- Zimmerli, W., Trampuz, A., and Ochsner, P.E. (2004). Prosthetic-Joint Infections. *New England Journal of Medicine* 351, 1645–1654.
- Zumsande, M., Stiefs, D., Siegmund, S., and Gross, T. (2011). General analysis of mathematical models for bone remodeling. *Bone* 48, 910–917.

Appendix

Appendix A. Literature systematic search retrieved article

Table A.1. Table of the resulting articles of the literature review

<u>Osteocyte lifespan</u>
Alliston, T. "Biological Regulation of Bone Quality." <i>Current osteoporosis reports</i> 12.3 (2014): 366–375. Web.
Buenzli, P. R. "Osteocytes as a Record of Bone Formation Dynamics: A Mathematical Model of Osteocyte Generation in Bone Matrix." <i>Journal of theoretical biology</i> 364. Journal Article (2015): 418–427. Web.
Buenzli, P. R., and N. A. Sims. "Quantifying the Osteocyte Network in the Human Skeleton." <i>Bone</i> 75. Journal Article (2015): 144–150. Web.
Capulli, Mattia, Riccardo Paone, and Nadia Rucci. "Osteoblast and Osteocyte: Games without Frontiers." <i>Bone: A dynamic and integrating tissue</i> 561. Journal Article (2014): 3–12. Web.
Florencio-Silva, Rinaldo et al. "Biology of Bone Tissue: Structure, Function, and Factors That Influence Bone Cells." <i>BioMed Research International</i> 2015 (2015): n. pag. <i>PubMed Central</i> . Web. 14 Aug. 2017.
Prideaux, M., D. M. Findlay, and G. J. Atkins. "Osteocytes: The Master Cells in Bone Remodelling." <i>Current opinion in pharmacology</i> 28. Journal Article (2016): 24–30. Web.
Qiu, S. et al. "Relationships between Osteocyte Density and Bone Formation Rate in Human Cancellous Bone." <i>Bone</i> 31.6 (2002): 709–711. Print.
Teti, Anna, and Alberta Zallone. "Do Osteocytes Contribute to Bone Mineral Homeostasis? Osteocytic Osteolysis Revisited." <i>Bone</i> 44.1 (2009): 11–16. <i>ScienceDirect</i> . Web.
<u>Osteoclast lifespan & reproduction rate</u>
Bar-Shavit, Zvi. "The Osteoclast: A Multinucleated, Hematopoietic-Origin, Bone-Resorbing Osteoimmune Cell." <i>Journal of Cellular Biochemistry</i> 102.5 (2007): 1130–1139. <i>Wiley Online Library</i> . Web.
Buenzli, P. R., P. Pivonka, and D. W. Smith. "Spatio-Temporal Structure of Cell Distribution in Cortical Bone Multicellular Units: A Mathematical Model." <i>Bone</i> 48.4 (2011): 918–926. <i>ScienceDirect</i> . Web.
Chambers, T.j. "The Birth of the Osteoclast." <i>Annals of the New York Academy of Sciences</i> 1192.1 (2010): 19–26. <i>Wiley Online Library</i> . Web.
Charles, Julia F., and Antonios O. Aliprantis. "Osteoclasts: More than 'Bone Eaters.'" <i>Trends in Molecular Medicine</i> 20.8 (2014): 449–459. <i>ScienceDirect</i> . Web.
Del Fattore, A., A. Teti, and N. Rucci. "Osteoclast Receptors and Signaling." <i>Archives of Biochemistry and Biophysics</i> 473.2 (2008): 147–160. Web.
Lemaire, Vincent et al. "Modeling the Interactions between Osteoblast and Osteoclast Activities in Bone Remodeling." <i>Journal of Theoretical Biology</i> 229.3 (2004): 293–309. <i>ScienceDirect</i> . Web.
Mellis, D. J. et al. "The Skeleton: A Multi-Functional Complex Organ: The Role of Key Signalling Pathways in Osteoclast Differentiation and in Bone Resorption." <i>The Journal of endocrinology</i> 211.2 (2011): 131–143. Web.
Roodman, G. David. "Cell Biology of the Osteoclast." <i>Experimental hematology</i> 27.8 (1999): 1229–1241. Web.
Ryser, Marc D., Nilima Nigam, and Svetlana V. Komarova. "Mathematical modeling of spatio-temporal dynamics of a single bone multicellular unit." <i>Journal of bone and mineral research</i> 24.5 (2009): 860-870.
Soysa, Niroshani Surangika, and Neil Alles. "Osteoclast Function and Bone-Resorbing Activity: An Overview." <i>Biochemical and biophysical research communications</i> 476.3 (2016): 115–120. Web.
Tanaka, S. et al. "Molecular Mechanism of the Life and Death of the Osteoclast." <i>Annals of the New York Academy of Sciences</i> 1068. Journal Article (2006): 180–186. Print.
Manolagas, Stavros C. "Birth and death of bone cells: basic regulatory mechanisms and implications for the pathogenesis and

treatment of osteoporosis." *Endocrine reviews* 21.2 (2000): 115-137.

Osteoblast lifespan & reproduction rate

Franchimont, N., S. Rydziel, and E. Canalis. "Transforming Growth Factor- β Increases Interleukin-6 Transcripts in Osteoblasts." *Bone* 26.3 (2000): 249–253. Web.

Jilka, R. L. et al. "Quantifying Osteoblast and Osteocyte Apoptosis: Challenges and Rewards." *Journal of bone and mineral research : the official journal of the American Society for Bone and Mineral Research* 22.10 (2007): 1492–1501. Web.

Kollet, O. et al. "Regulatory Cross Talks of Bone Cells, Hematopoietic Stem Cells and the Nervous System Maintain Hematopoiesis." *Inflammation & allergy drug targets* 11.3 (2012): 170–180. Print.

Komarova, Svetlana V. et al. "Mathematical Model Predicts a Critical Role for Osteoclast Autocrine Regulation in the Control of Bone Remodeling." *Bone* 33.2 (2003): 206–215. *ScienceDirect*. Web.

Manolagas, Stavros C. "Birth and Death of Bone Cells: Basic Regulatory Mechanisms and Implications for the Pathogenesis and Treatment of Osteoporosis." *Endocrine Reviews* 21.2 (2000): 115–137. *academic.oup.com*. Web.

Ryser, Marc D, Nilima Nigam, and Svetlana V Komarova. "Mathematical Modeling of Spatio-Temporal Dynamics of a Single Bone Multicellular Unit." *Journal of Bone and Mineral Research* 24.5 (2009): 860–870. *Wiley Online Library*. Web.

Bone Remodeling and signals

Anandarajah, Allen P. "Role of RANKL in Bone Diseases." *Trends in Endocrinology & Metabolism* 20.2 (2009): 88–94. Web.

Bahar, H. et al. "Molecular Signaling in Bone Regeneration." *Critical reviews in eukaryotic gene expression* 17.2 (2007): 87–101. Print.

Boyce, Brendan F., and Lianping Xing. "Functions of RANKL/RANK/OPG in Bone Modeling and Remodeling." *Archives of Biochemistry and Biophysics* 473.2 (2008): 139–146. *ScienceDirect*. Web. Highlight Issue: Bone Remodeling: Facts and Perspectives.

Henriksen, Kim et al. "Local Communication on and within Bone Controls Bone Remodeling." *Bone* 44.6 (2009): 1026–1033. Web.

Iolascon, G., G. Resmini, and U. Tarantino. "Inhibition of RANK Ligand: A New Option for Preventing Fragility Fractures." *Aging clinical and experimental research* 23.2 Suppl (2011): 28–29. Print.

Kardas, D., U. Nackenhurst, and D. Balzani. "Computational Model for the Cell-Mechanical Response of the Osteocyte Cytoskeleton Based on Self-Stabilizing Tensegrity Structures." *Biomechanics and modeling in mechanobiology* 12.1 (2013): 167–183. Web.

Ryser, Marc D., Nilima Nigam, and Svetlana V. Komarova. "Mathematical modeling of spatio-temporal dynamics of a single bone multicellular unit." *Journal of bone and mineral research* 24.5 (2009): 860-870.

Nakashima, T. "Coupling and Communication between Bone Cells." *Clinical calcium* 24.6 (2014): 853–861. Print.

Paoletti, N. et al. "Multilevel Computational Modeling and Quantitative Analysis of Bone Remodeling." *IEEE/ACM Transactions on Computational Biology and Bioinformatics* 9.5 (2012): 1366–1378. *IEEE Xplore*. Web.

Pivonka, Peter et al. "Model Structure and Control of Bone Remodeling: A Theoretical Study." *Bone* 43.2 (2008): 249–263. *ScienceDirect*. Web.

---. "Theoretical Investigation of the Role of the RANK–RANKL–OPG System in Bone Remodeling." *Journal of Theoretical Biology* 262.2 (2010): 306–316. *ScienceDirect*. Web.

Scheiner, Stefan, Peter Pivonka, and Christian Hellmich. "Coupling Systems Biology with Multiscale Mechanics, for Computer Simulations of Bone Remodeling." *Computer Methods in Applied Mechanics and Engineering* 254. Journal Article (2013): 181–196. Web.

Sims, N. A., and J. H. Gooi. "Bone Remodeling: Multiple Cellular Interactions Required for Coupling of Bone Formation and Resorption." *Seminars in cell & developmental biology* 19.5 (2008): 444–451. Web.

Zhao, Y., Y. Cai, and Y. N. Wang. "RANKL and OPG Regulation on Bone Remodeling." *Shanghai kou qiang yi xue = Shanghai journal of stomatology* 19.4 (2010): 443–446. Print.

Zumsande, Martin et al. "General Analysis of Mathematical Models for Bone Remodeling." *Bone* 48.4 (2011): 910–917. *ScienceDirect*. Web.

Macrophage lifespan

Chazaud, Bénédicte. "Macrophages: Supportive Cells for Tissue Repair and Regeneration." *Immunobiology* 219.3 (2014): 172–178.

Print.

Cole, Joby et al. "Chapter Four - The Role of Macrophages in the Innate Immune Response to Streptococcus Pneumoniae and Staphylococcus Aureus: Mechanisms and Contrasts." *Advances in Bacterial Pathogen Biology* 65. Journal Article (2014): 125–202. Print.

Dancik, Garrett M., Douglas E. Jones, and Karin S. Dorman. "Parameter Estimation and Sensitivity Analysis in an Agent-Based Model of Leishmania Major Infection." *Journal of Theoretical Biology* 262.3 (2010): 398–412. *ScienceDirect*. Web.

Dockrell, D. H., and M. K. Whyte. "Regulation of Phagocyte Lifespan in the Lung during Bacterial Infection." *Journal of leukocyte biology* 79.5 (2006): 904–908. Print.

Epelman, Slava, Kory J Lavine, and Gwendalyn J Randolph. "Origin and Functions of Tissue Macrophages." *Immunity* 41.1 (2014): 21–35. Print.

Mulherin, Diarmuid, Oliver Fitzgerald, and Barry Bresnihan. "Synovial Tissue Macrophage Populations and Articular Damage in Rheumatoid Arthritis." *Arthritis & Rheumatism* 39.1 (1996): 115–124. *Wiley Online Library*. Web.

Smith, Amber M., Jonathan A. McCullers, and Frederick R. Adler. "Mathematical Model of a Three-Stage Innate Immune Response to a Pneumococcal Lung Infection." *Journal of Theoretical Biology* 276.1 (2011): 106–116. *ScienceDirect*. Web.

Parwaresch, M. R., and H-H. Wacker. "Origin and kinetics of resident tissue macrophages: parabiosis studies with radiolabelled leucocytes." *Cell Proliferation* 17.1 (1984): 25-39.

Monocyte lifespan

Brunet de la Grange, Philippe et al. "Long-Term Repopulating Hematopoietic Stem Cells and 'Side Population' in Human Steady State Peripheral Blood." *Stem Cell Research* 11.1 (2013): 625–633. Print.

Dale, D. C., L. Boxer, and W. C. Liles. "The Phagocytes: Neutrophils and Monocytes." *Blood* 112.4 (2008): 935–945. Print.

Fehder, W. P. et al. "Macrophages*." *Encyclopedia of Stress (Second Edition)*. Ed. George Fink. Book, Section. New York: Academic Press, 2007. 634–639. Web.

Ginhoux, Florent, and Steffen Jung. "Monocytes and Macrophages: Developmental Pathways and Tissue Homeostasis." *Nature Reviews Immunology* 14.6 (2014): 392–404. *www.nature.com*. Web.

Goasguen, J. E. et al. "Morphological Evaluation of Monocytes and Their Precursors." *Haematologica* 94.7 (2009): 994–997. Print.

Gonzalez-Mejia, M. E., and A. I. Doseff. "Regulation of Monocytes and Macrophages Cell Fate." *Frontiers in bioscience (Landmark edition)* 14. Journal Article (2009): 2413–2431. Print.

Italiani, Paola, and Diana Boraschi. "From Monocytes to M1/M2 Macrophages: Phenotypical vs. Functional Differentiation." *Frontiers in Immunology* 5 (2014): n. pag. *PubMed Central*. Web. 10 Aug. 2017.

Parihar, A., T. D. Eubank, and A. I. Doseff. "Monocytes and Macrophages Regulate Immunity through Dynamic Networks of Survival and Cell Death." *Journal of innate immunity* 2.3 (2010): 204–215. Print.

Patel, A. A. et al. "The Fate and Lifespan of Human Monocyte Subsets in Steady State and Systemic Inflammation." *The Journal of experimental medicine* 214.7 (2017): 1913–1923. Print.

Reuter, S., and D. Lang. "Life Span of Monocytes and Platelets: Importance of Interactions." *Frontiers in bioscience (Landmark edition)* 14. Journal Article (2009): 2432–2447. Print.

Whitelaw, D. M., and Maureen Bell. "The Intravascular Lifespan of Monocytes." *Blood* 28.3 (1966): 455–464. Print.

Yona, S. et al. "Fate Mapping Reveals Origins and Dynamics of Monocytes and Tissue Macrophages under Homeostasis." *Immunity* 38.1 (2013): 79–91. Print.

Neutrophil lifespan

Anwar, S., and M. K. Whyte. "Neutrophil Apoptosis in Infectious Disease." *Experimental lung research* 33.10 (2007): 519–528. Print.

Asensi, V. et al. "In Vivo Interleukin-6 Protects Neutrophils from Apoptosis in Osteomyelitis." *Infection and immunity* 72.7 (2004): 3823–3828. Web.

Kaplanski, Gilles et al. "IL-6: A Regulator of the Transition from Neutrophil to Monocyte Recruitment during Inflammation." *Trends in Immunology* 24.1 (2003): 25–29. *ScienceDirect*. Web.

Kettritz, R. et al. "Extracellular Matrix Regulates Apoptosis in Human Neutrophils." *Kidney international* 55.2 (1999): 562–571. Web.

Kumar, V., and A. Sharma. "Neutrophils: Cinderella of Innate Immune System." *International immunopharmacology* 10.11 (2010):

1325–1334. Web.

Maianski, N. A. et al. "Apoptosis of Neutrophils." *Acta Haematologica* 111.1–2 (2004): 56–66. Web.

Rankin, S. M. "The Bone Marrow: A Site of Neutrophil Clearance." *Journal of leukocyte biology* 88.2 (2010): 241–251. Web.

Schröder, J. -M. "Chemoattractants as Mediators of Neutrophilic Tissue Recruitment." *Clinics in dermatology* 18.3 (2000): 245–263. Web.

Rankin, Sara M. "The bone marrow: a site of neutrophil clearance." *Journal of leukocyte biology* 88.2 (2010): 241–251.

Summers, C. et al. "Neutrophil Kinetics in Health and Disease." *Trends in immunology* 31.8 (2010): 318–324. Web.

Whyte, M. et al. "Apoptosis and the Regulation of Neutrophil Lifespan." *Biochemical Society transactions* 27.6 (1999): 802–807. Print.

TGF

Ashcroft, Gillian S. "Bidirectional Regulation of Macrophage Function by TGF- β ." *Microbes and Infection* 1.15 (1999): 1275–1282. *ScienceDirect*. Web.

Bismar, H et al. "Transforming Growth Factor β (TGF- β) Levels in the Conditioned Media of Human Bone Cells: Relationship to Donor Age, Bone Volume, and Concentration of TGF- β in Human Bone Matrix in Vivo." *Bone* 24.6 (1999): 565–569. *ScienceDirect*. Web.

Kelly, Aoife et al. "Chapter Four - Regulation of Innate and Adaptive Immunity by TGF β ." *Advances in Immunology* 134. Journal Article (2017): 137–233. Print.

Pivonka, Peter et al. "Model Structure and Control of Bone Remodeling: A Theoretical Study." *Bone* 43.2 (2008): 249–263. *ScienceDirect*. Web.

Schmidt-Weber, Carsten B., and Kurt Blaser. "Regulation and Role of Transforming Growth Factor- β in Immune Tolerance Induction and Inflammation." *Current opinion in immunology* 16.6 (2004): 709–716. Print.

Sheng, J., W. Chen, and H. J. Zhu. "The Immune Suppressive Function of Transforming Growth Factor-Beta (TGF-Beta) in Human Diseases." *Growth factors (Chur, Switzerland)* 33.2 (2015): 92–101. Print.

Knapp, Sylvia, et al. "Prognostic value of MIP-1 α , TGF- β 2, sELAM-1, and sVCAM-1 in patients with gram-positive sepsis." *Clinical immunology and immunopathology* 87.2 (1998): 139–144.

Immune system mathematical or computational model

Afacan, Nicole J., Christopher D. Fjell, and Robert E. W. Hancock. "A Systems Biology Approach to Nutritional Immunology – Focus on Innate Immunity." *Nutritional Immunology* 33.1 (2012): 14–25. Print.

Herald, M. C. "General Model of Inflammation." *Bulletin of mathematical biology* 72.4 (2010): 765–779. Print.

Kalita, J. K. et al. "Computational Modelling and Simulation of the Immune System." *International journal of bioinformatics research and applications* 2.1 (2006): 63–88. Print.

Lehnert, T. et al. "Bottom-up Modeling Approach for the Quantitative Estimation of Parameters in Pathogen-Host Interactions." *Frontiers in microbiology* 6. Journal Article (2015): 608. Print.

Marino, S., E. Beretta, and D. E. Kirschner. "The Role of Delays in Innate and Adaptive Immunity to Intracellular Bacterial Infection." *Mathematical biosciences and engineering : MBE* 4.2 (2007): 261–288. Print.

Nakaoka, Shinji. "Mathematical Modeling and Simulation for a Coupled Communication System of Immune Cells*." *4th IFAC Conference on Analysis and Control of Chaotic Systems CHAOS 2015 Tokyo, Japan, 26–28 August 2015* 48.18 (2015): 41–46. Print.

Tegner, J. et al. "Systems Biology of Innate Immunity." *Cellular immunology* 244.2 (2006): 105–109. Print.

Woelke, Anna Lena, Manuela S. Murgueitio, and Robert Preissner. "Theoretical Modeling Techniques and Their Impact on Tumor Immunology." *Clinical and Developmental Immunology* 2010 (2010): n. pag. *PubMed Central*. Web. 11 Aug. 2017.

Wolf, Katarina, and Peter Friedl. "Extracellular Matrix Determinants of Proteolytic and Non-Proteolytic Cell Migration." *Trends in cell biology* 21.12 (2011): 736–744. Print.

Zhang, Yue, and James B. Bliska. "Mathematical Relationship between Cytokine Concentrations and Pathogen Levels during Infection." *Cytokine* 53.2 (2011): 158–162. Print.

Bacteria count

Gaudin, A. et al. "A New Experimental Model of Acute Osteomyelitis Due to Methicillin-Resistant Staphylococcus Aureus in

Rabbit." *Letters in applied microbiology* 52.3 (2011): 253–257. Web.

Jarrett, A. M., N. G. Cogan, and M. E. Shirtliff. "Modelling the Interaction between the Host Immune Response, Bacterial Dynamics and Inflammatory Damage in Comparison with Immunomodulation and Vaccination Experiments." *Mathematical medicine and biology: a journal of the IMA* 32.3 (2015): 285–306. Web.

Paharik, Alexandra E., and Alexander R. Horswill. "The Staphylococcal Biofilm: Adhesins, Regulation, and Host Response." *Microbiology Spectrum* 4.2 (2016): n. pag. www.asmscience.org. Web.

Søe, Niels H. et al. "A Novel Knee Prosthesis Model of Implant-Related Osteo- Myelitis in Rats." *Acta Orthopaedica* 84.1 (2013): 92–97. *Taylor and Francis+NEJM*. Web.

Bacteria production rate

Ansari, S. et al. "Staphylococcus Aureus: Methicillin Resistance and Small Colony Variants from Pyogenic Infections of Skin, Soft Tissue and Bone." *Journal of Nepal Health Research Council* 13.30 (2015): 126–132. Print.

Cramton, Sarah E., Christiane Gerke, and Friedrich Götz. "In Vitro Methods to Study Staphylococcal Biofilm Formation." *Microbial Growth in Biofilms - Part A: Developmental and Molecular Biological Aspects* 336. Journal Article (2001): 239–255. Web.

DosReis, George A., and Marcello A. Barcinski. "Apoptosis and Parasitism: From the Parasite to the Host Immune Response." *Advances in Parasitology* 49. Journal Article (2001): 133–161. Web.

Li, D. et al. "Quantitative Mouse Model of Implant-Associated Osteomyelitis and the Kinetics of Microbial Growth, Osteolysis, and Humoral Immunity." *Journal of orthopaedic research: official publication of the Orthopaedic Research Society* 26.1 (2008): 96–105. Web.

Melter, O., and B. Radojevic. "Small Colony Variants of Staphylococcus Aureus--Review." *Folia microbiologica* 55.6 (2010): 548–558. Web.

Anwar, H. A., et al. "The effect of metal ions in solution on bacterial growth compared with wear particles from hip replacements." *The Journal of bone and joint surgery. British volume* 89.12 (2007): 1655-1659.

Fux, C. A., et al. "Survival strategies of infectious biofilms." *Trends in microbiology* 13.1 (2005): 34-40.

BJI computational model

Liò, P., Paoletti, N., Moni, M.A., Atwell, K., Merelli, E., and Viceconti, M. (2012). Modelling osteomyelitis. *BMC Bioinformatics* 13, S12.

Interaction Bacteria and Bone cells

Akdis, Mübeccel et al. "Interleukins (from IL-1 to IL-38), Interferons, Transforming Growth Factor β , and TNF- α : Receptors, Functions, and Roles in Diseases." *Journal of Allergy and Clinical Immunology* 138.4 (2016): 984–1010. Web.

Bost, K. L. et al. "Staphylococcus Aureus Infection of Mouse or Human Osteoblasts Induces High Levels of Interleukin-6 and Interleukin-12 Production." *The Journal of infectious diseases* 180.6 (1999): 1912–1920. Print.

Chen, Q. et al. "Involvement of Toll-like Receptor 2 and pro-Apoptotic Signaling Pathways in Bone Remodeling in Osteomyelitis." *Cellular physiology and biochemistry: international journal of experimental cellular physiology, biochemistry, and pharmacology* 34.6 (2014): 1890–1900. Web.

Claro, T. et al. "Staphylococcus Aureus Protein A Binding to Osteoblast Tumour Necrosis Factor Receptor 1 Results in Activation of Nuclear Factor Kappa B and Release of Interleukin-6 in Bone Infection." *Microbiology (Reading, England)* 159.Pt 1 (2013): 147–154. Web.

Ellington, John K. et al. "Mechanisms Of Staphylococcus Aureus invasion of Cultured Osteoblasts." *Microbial Pathogenesis* 26.6 (1999): 317–323. *ScienceDirect*. Web.

Josse, J., F. Velard, and S. C. Gangloff. "Staphylococcus Aureus vs. Osteoblast: Relationship and Consequences in Osteomyelitis." *Frontiers in cellular and infection microbiology* 5. Journal Article (2015): 85. Web.

Junka, A. et al. "Bad to the Bone: On In Vitro and Ex Vivo Microbial Biofilm Ability to Directly Destroy Colonized Bone Surfaces without Participation of Host Immunity or Osteoclastogenesis." *PLoS one* 12.1 (2017): e0169565. Web.

Marriott, I. "Apoptosis-Associated Uncoupling of Bone Formation and Resorption in Osteomyelitis." *Frontiers in cellular and infection microbiology* 3. Journal Article (2013): 101. Web.

---. "Osteoblast Responses to Bacterial Pathogens: A Previously Unappreciated Role for Bone-Forming Cells in Host Defense and Disease Progression." *Immunologic research* 30.3 (2004): 291–308. Print.

---. "Osteoblasts Express the Inflammatory Cytokine Interleukin-6 in a Murine Model of Staphylococcus Aureus Osteomyelitis and

Infected Human Bone Tissue.” *The American journal of pathology* 164.4 (2004): 1399–1406. Print.

Interaction bacteria and immune cells

Asensi, V. et al. “In Vivo Interleukin-6 Protects Neutrophils from Apoptosis in Osteomyelitis.” *Infection and immunity* 72.7 (2004): 3823–3828. Web.

Carmichael, Andrew, and Mark Wills. “The Immunology of Infection.” *Infections Part 1 of 3* 41.11 (2013): 611–618. Web.

Kim, Hwan Keun et al. “Recurrent Infections and Immune Evasion Strategies of Staphylococcus Aureus.” *Host–microbe interactions: bacteria* 15.1 (2012): 92–99. Web.

Ning, R. et al. “Staphylococcus Aureus Regulates Secretion of Interleukin-6 and Monocyte Chemoattractant Protein-1 through Activation of Nuclear Factor KappaB Signaling Pathway in Human Osteoblasts.” *The Brazilian journal of infectious diseases : an official publication of the Brazilian Society of Infectious Diseases* 15.3 (2011): 189–194. Print.

Corrado, Alessia, et al. “Staphylococcus aureus-dependent septic arthritis in murine knee joints: local immune response and beneficial effects of vaccination.” *Scientific reports* 6 (2016): 38043.

Interaction bacteria and signals

Aggarwal, Bharat B. “Nuclear Factor-KB: The Enemy Within.” *Cancer Cell* 6.3 (2004): 203–208. Web.

Cassat, J. E. et al. “A Secreted Bacterial Protease Tailors the Staphylococcus Aureus Virulence Repertoire to Modulate Bone Remodeling during Osteomyelitis.” *Cell host & microbe* 13.6 (2013): 759–772. Web.

Ning, R. et al. “Attachment of Staphylococcus Aureus Is Required for Activation of Nuclear Factor Kappa B in Human Osteoblasts.” *Acta biochimica et biophysica Sinica* 42.12 (2010): 883–892. Web.

Ning, R. D. et al. “Activation of Nuclear Factor KappaB Signaling Pathway in Human Osteoblasts Responses to Staphylococcus Aureus in Vitro.” *Zhonghua wai ke za zhi [Chinese journal of surgery]* 50.3 (2012): 264–267. Print.

Sharma, Rakesh, and Stefan D. Anker. “Cytokines, Apoptosis and Cachexia: The Potential for TNF Antagonism.” *Cachexia* 85.1 (2002): 161–171. Web.

Szondy, Zsuzsa, and Anna Pallai. “Transmembrane TNF-Alpha Reverse Signaling Leading to TGF-Beta Production Is Selectively Activated by TNF Targeting Molecules: Therapeutic Implications.” *Pharmacological Research* 115. Journal Article (2017): 124–132. Web.

Young, A. B. et al. “Causative Agents of Osteomyelitis Induce Death Domain-Containing TNF-Related Apoptosis-Inducing Ligand Receptor Expression on Osteoblasts.” *Bone* 48.4 (2011): 857–863. Web.

Corrado, Alessia, et al. “Staphylococcus aureus-dependent septic arthritis in murine knee joints: local immune response and beneficial effects of vaccination.” *Scientific reports* 6 (2016): 38043.

Interaction bone cells and immune cells

Allaelys, Isabelle et al. “Osteoblast Retraction Induced by Adherent Neutrophils Promotes Osteoclast Bone Resorption: Implication for Altered Bone Remodeling in Chronic Gout.” *Laboratory Investigation* 91.6 (2011): 905–920. www.nature.com.scd-proxy.univ-brest.fr. Web.

El-Jawhari, Jehan J., Elena Jones, and Peter V. Giannoudis. “The Roles of Immune Cells in Bone Healing; What We Know, Do Not Know and Future Perspectives.” *Injury* 47.11 (2016): 2399–2406. Web.

Ferrari-Lacraz, S., and S. Ferrari. “Do RANKL Inhibitors (Denosumab) Affect Inflammation and Immunity?” *Osteoporosis international : a journal established as result of cooperation between the European Foundation for Osteoporosis and the National Osteoporosis Foundation of the USA* 22.2 (2011): 435–446. Web.

Michalski, Megan N., and Laurie K. McCauley. “Macrophages and Skeletal Health.” *Pharmacology & therapeutics* 174. Journal Article (2017): 43–54. Web.

Nakashima, Tomoki, and Hiroshi Takayanagi. “The Dynamic Interplay between Osteoclasts and the Immune System.” *Archives of Biochemistry and Biophysics* 473.2 (2008): 166–171. *ScienceDirect*. Web. Highlight Issue: Bone Remodeling: Facts and Perspectives.

Takayanagi, Hiroshi. “Osteoimmunology: Shared Mechanisms and Crosstalk between the Immune and Bone Systems.” *Nature Reviews Immunology* 7.4 (2007): 292–304. www.nature.com.scd-proxy.univ-brest.fr. Web.

Appendix B. Differential equation systems of different initial conditions of BJI model simulation

The equation systems for different initial condition of bacteria inoculum size and reproduction rate along with the corresponding figures follows.

Table B.1. The calculated three terms differential equations systems for the bacteria(x) and neutrophils (y) population for different initial conditions: for bacteria inoculum size = 100, 150, 250 CFU/mm² and reproduction rates = 2, 4, 6, 12, 18, 24 hour

The initial condition of BJI model simulation	The resulting three terms models of bacteria (x) and neutrophils (y) population
Bacteria inoculum size = 100 CFU/mm² reproduction rate= 2 h	$\begin{aligned} dx &= +0.00051x^2 - 3e-05y^2 - 2.1e-06 x^3 \\ dx &= -0.00014 xy + 0.00063x^2 - 1.9e-06 x^3 \\ dx &= +0.00034x^2 - 1.4e-06 x^3 - 5.3e-08 y^3 \end{aligned}$ <hr/> $\begin{aligned} dy &= + 5.4 - 2.3 y/x + 2.7e-07 x^3 \\ dy &= + 5.1 - 2.3 y/x + 6e-05 x^2 \\ dy &= + 225 /x + 0.032 x - 2.3 y/x \end{aligned}$
Bacteria inoculum size = 100 CFU/mm² reproduction rate= 4 h	$\begin{aligned} dx &= -0.00014 xy + 0.00023x^2 - 1e-07x^3 \\ dx &= +0.094x - 0.00015 xy + 2.7e-05x^2 \\ dx &= +0.1x - 0.00011 xy - 9.6e-09 y^3 \end{aligned}$ <hr/> $\begin{aligned} dy &= -122/x + 0.024x - 1.2e-05 y^2 \\ dy &= +0.04x - 0.36y/x - 3e-05 xy \\ dy &= -130/x + 0.022x - 1e-08 y^3 \end{aligned}$
Bacteria inoculum size = 100 CFU/mm² reproduction rate= 6 h	$\begin{aligned} dx &= -0.00015 xy + 0.00026x^2 - 1.3e-07 x^3 \\ dx &= +0.093x - 0.00016 xy + 2.9e-05x^2 \\ dx &= -5.3 + 0.12x - 0.00015 xy \end{aligned}$ <hr/> $\begin{aligned} dy &= +0.041x - 0.44y/x - 3.1e-05 xy \\ dy &= +0.022x - 0.38y/x - 7.5e-09 y^3 \\ dy &= +0.023x - 0.36y/x - 8.2e-06 y^2 \end{aligned}$
Bacteria inoculum size = 100 CFU/mm² reproduction rate= 12 h	$\begin{aligned} dx &= +0.12x - 9.7x/y - 0.00022 xy \\ dx &= -251/y + 0.079x - 0.00017 xy \\ dx &= +0.074x - 0.00016 xy - 23840/y^2 \end{aligned}$ <hr/> $\begin{aligned} dy &= -756/x + 12x/y + 11088 /x^2 \\ dy &= -589/x + 11x/y + 159801 /x^3 \\ dy &= -961/y + 14x/y - 0.89 y/x \end{aligned}$
Bacteria inoculum size = 100 CFU/mm² reproduction rate= 18 h	$\begin{aligned} dx &= +0.055x - 0.00014 xy - 1.3e-07 x^3 \\ dx &= +0.06x - 0.00014 xy - 5e-05x^2 \\ dx &= +0.051x + 0.0035y - 0.00016 xy \end{aligned}$ <hr/> $\begin{aligned} dy &= +0.04x - 1.7y/x - 1.9e-05 xy \\ dy &= +0.034x - 1.6y/x - 7.7e-09 y^3 \\ dy &= +0.035x - 1.6y/x - 4.9e-06 y^2 \end{aligned}$
Bacteria inoculum size = 100 CFU/mm² reproduction rate= 24 h	$\begin{aligned} dx &= +0.06x - 0.00015 xy - 1e-04x^2 \\ dx &= +0.053x - 0.00015 xy - 3.2e-07 x^3 \\ dx &= +1.8 + 0.032x - 0.00015 xy \end{aligned}$ <hr/> $\begin{aligned} dy &= +0.042x - 1.6y/x - 4.7e-05 x^2 \\ dy &= +0.038x - 1.6y/x - 1.3e-07 x^3 \\ dy &= +1.1 + 0.028 x - 1.6y/x \end{aligned}$

Bacteria inoculum size = 150 CFU/mm2 reproduction rate= 2 h	$\begin{aligned} dx &= -2e-04xy + 0.001x^2 - 2.5e-06 x^3 \\ dx &= +0.00081x^2 - 4.4e-05 y^2 - 2.5e-06 x^3 \\ dx &= +0.00065x^2 - 2e-06x^3 - 6.9e-08 y^3 \end{aligned}$ <hr/> $\begin{aligned} dy &= +4.8 - 2.1y/x + 1.8e-07 x^3 \\ dy &= +4.5 - 2.1y/x + 5.5e-05 x^2 \\ dy &= +194/x + 0.03 x - 2.2 y/x \end{aligned}$
Bacteria inoculum size = 150 CFU/mm2 reproduction rate= 4 h	$\begin{aligned} dx &= -0.00013 xy + 2e-04x^2 - 7.9e-08 x^3 \\ dx &= +0.1x - 0.00011 xy - 9.4e-09 y^3 \\ dx &= +0.11x - 0.00011 xy - 9.4e-06 y^2 \end{aligned}$ <hr/> $\begin{aligned} dy &= -104/x + 0.022x - 1.1e-05 y^2 \\ dy &= -112/x + 0.021x - 8.9e-09 y^3 \\ dy &= -90/x + 0.023x - 0.012 y \end{aligned}$
Bacteria inoculum size = 150 CFU/mm2 reproduction rate= 6 h	$\begin{aligned} dx &= -0.00014 xy + 0.00021x^2 - 8.8e-08 x^3 \\ dx &= +0.1x - 0.00011 xy - 9.7e-09 y^3 \\ dx &= +0.096x - 0.00015 xy + 2.5e-05x^2 \end{aligned}$ <hr/> $\begin{aligned} dy &= +0.04x - 0.3y/x - 2.9e-05 xy \\ dy &= +0.02x - 0.26y/x - 7.2e-09 y^3 \\ dy &= +0.021x - 0.25y/x - 8.4e-06 y^2 \end{aligned}$
Bacteria inoculum size = 150 CFU/mm2 reproduction rate= 12 h	$\begin{aligned} dx &= -0.00015 xy + 0.00041x^2 - 4.6e-07 x^3 \\ dx &= +0.11x - 8.1x/y - 0.00019 xy \\ dx &= -2.3 + 0.084x - 0.00015 xy \end{aligned}$ <hr/> $\begin{aligned} dy &= -743/y + 13x/y - 0.78 y/x \\ dy &= -625 /x + 11x/y + 6542 /x^2 \\ dy &= +0.038x - 0.92y/x - 2.7e-05 xy \end{aligned}$
Bacteria inoculum size = 150 CFU/mm2 reproduction rate= 18 h	$\begin{aligned} dx &= +0.12x - 11x/y - 0.00023 xy \\ dx &= -226/y + 0.063x - 0.00015 xy \\ dx &= +0.06x - 0.00015 xy - 30038/y^2 \end{aligned}$ <hr/> $\begin{aligned} dy &= +0.041x - 1.4y/x - 2.8e-05 xy \\ dy &= +0.021 x + 3x/y - 1.4y/x \\ dy &= -796 /y + 13x/y - 1.1 y/x \end{aligned}$
Bacteria inoculum size = 150 CFU/mm2 reproduction rate= 24 h	$\begin{aligned} dx &= +6e-05y^2 - 1.3e-07 x^3 - 1.5e-07 y^3 \\ dx &= +0.13x - 15x/y - 0.00026 xy \\ dx &= +0.01y - 1.2e-07 x^3 - 6.9e-08 y^3 \end{aligned}$ <hr/> $\begin{aligned} dy &= +0.033x - 1.4y/x - 1.3e-08 y^3 \\ dy &= +0.034x - 1.3y/x - 7.6e-06 y^2 \\ dy &= +239/y + 0.028 x - 1.6y/x \end{aligned}$
Bacteria inoculum size = 250 CFU/mm2 reproduction rate= 2 h	$\begin{aligned} dx &= -0.00031 xy + 0.0014x^2 - 2.5e-06 x^3 \\ dx &= +0.00058x^2 - 1.2e-06 x^3 - 6.4e-08 y^3 \\ dx &= -8.5 + 23x/y - 2e-07 x^3 \end{aligned}$

	$dy=+0.033x -1.1y/x -1e-05 y^2$ $dy=+0.037x -0.0095 y -0.85y/x$ $dy=+0.031x -1.2y/x -1.3e-08 y^3$
Bacteria inoculum size = 250 CFU/mm2 reproduction rate= 2 h	$dx= -0.00012 xy+0.00018x^2 -6.8e-08 x^3$ $dx=+0.1x -9.7e-05 xy -9.8e-09 y^3$ $dx=+0.1x -1e-04 xy -1e-05 y^2$
	$dy= -62/x+0.021x -1.2e-05 y^2$ $dy= -67/x+0.02x -9.6e-09 y^3$ $dy= -52/x+0.021x -0.014 y$
Bacteria inoculum size = 250 CFU/mm2 reproduction rate= 6 h	$dx= -0.00013 xy+0.00019x^2 -7e-08x^3$ $dx=+0.1x -1e-04xy -9.4e-09 y^3$ $dx=+0.11x -0.00011 xy -9.6e-06 y^2$
	$dy=+0.04x -0.26y/x -2.8e-05 xy$ $dy=+0.018x -0.23y/x -6.9e-09 y^3$ $dy=+0.019x -0.21y/x -8.4e-06 y^2$
Bacteria inoculum size = 250 CFU/mm2 reproduction rate= 12 h	$dx= -0.00014 xy+0.00032x^2 -2.9e-07 x^3$ $dx=+0.062x -9.7e-05 xy -1.1e-08 y^3$ $dx= -2.8 + 0.085x -0.00014 xy$
	$dy=+0.03x -0.0078 y -0.48y/x$ $dy=+0.026x -0.55y/x -7.8e-06 y^2$ $dy=+0.025x -0.58y/x -8.4e-09 y^3$
Bacteria inoculum size = 250 CFU/mm2 reproduction rate= 18 h	$dx=+6.7e-05 y^2-4.3e-08 x^3 -1.2e-07 y^3$ $dx=-1.5e-05 x^2 +6.7e-05 y^2-1.2e-07 y^3$ $dx=-0.00011 xy +0.00034x^2 -5.2e-07 x^3$
	$dy=+0.039 x -1.3 y/x -2.8e-05 xy$ $dy=+0.018 x + 3.4 x/y -1.3 y/x$ $dy=+0.029 x -1.2 y/x -8.1e-09 y^3$
Bacteria inoculum size = 250 CFU/mm2 reproduction rate= 24 h	$dx=+5.2e-05 y^2 -7.4e-08 x^3 -1.2e-07 y^3$ $dx=-2.2e-05 x^2 +5.5e-05 y^2 -1.2e-07 y^3$ $dx=-1.7e-05 xy + 5.5e-05 y^2 -1.2e-07 y^3$
	$dy=+ 0.031 x -1.2 y/x -1.4e-08 y^3$ $dy=+ 0.033 x -1.1 y/x -9.2e-06 y^2$ $dy=+ 0.041 x -1.3 y/x -3.4e-05 xy$

Table B.2. The calculated three terms differential equations systems for the bacteria(x) and osteocytes (y) population for different initial conditions: for bacteria inoculum size = 100, 150, 250 CFU/mm² and reproduction rates = 2, 4, 6, 12, 18, 24 hour.

The initial condition of BJI model simulation	The resulting three terms models of bacteria (x) and osteocytes (y) population
Bacteria inoculum size = 100 CFU/mm² reproduction rate= 2 h	$\begin{aligned} dx &= -0.36x + 2e-04xy - 2.2e-07x^3 \\ dx &= -318x/y + 1e-04xy - 2.3e-07x^3 \\ dx &= +0.37x - 647x/y - 2.3e-07x^3 \\ dy &= +2438646/y - 8.8e+09/y^2 + 7.9e+12/y^3 \\ dy &= +453 - 4.4e+09/y^2 + 5.3e+12/y^3 \\ dy &= +0.13y - 2.9e+09/y^2 + 4e+12/y^3 \end{aligned}$
Bacteria inoculum size = 100 CFU/mm² reproduction rate= 4 h	$\begin{aligned} dx &= -1.6x + 0.00092xy - 1e-08x^3 \\ dx &= -1428x/y + 0.00046xy - 1e-08x^3 \\ dx &= +1.6x - 2864x/y - 1e-08x^3 \\ dy &= -0.028x + 48x/y + 7.3e+08/y^3 \\ dy &= -0.028x + 49x/y + 413913/y^2 \\ dy &= +234/y - 0.028x + 49x/y \end{aligned}$
Bacteria inoculum size = 100 CFU/mm² reproduction rate= 6 h	$\begin{aligned} dx &= +1.6x - 2775x/y - 1.5e-08x^3 \\ dx &= -1372x/y + 0.00044xy - 1.5e-08x^3 \\ dx &= -1.5x + 0.00088xy - 1.5e-08x^3 \\ dy &= +2.2x/y - 4.5e-06x^2 + 2.5e-09x^3 \\ dy &= +0.0012x - 4.4e-06x^2 + 2.5e-09x^3 \\ dy &= +6.3e-07xy - 4.3e-06x^2 + 2.4e-09x^3 \end{aligned}$
Bacteria inoculum size = 100 CFU/mm² reproduction rate= 12 h	$\begin{aligned} dx &= -1.2x + 0.00068xy - 1.4e-07x^3 \\ dx &= -1061x/y + 0.00034xy - 1.4e-07x^3 \\ dx &= +1.2x - 2140x/y - 1.4e-07x^3 \\ dy &= -0.13x + 225x/y - 1.7e-06x^2 \\ dy &= +113x/y - 3.5e-05xy - 1.8e-06x^2 \\ dy &= +0.13x - 7.1e-05xy - 1.8e-06x^2 \end{aligned}$
Bacteria inoculum size = 100 CFU/mm² reproduction rate= 18 h	$\begin{aligned} dx &= -0.41x + 0.00024xy - 0.00013x^2 \\ dx &= -361x/y + 0.00013xy - 0.00013x^2 \\ dx &= +0.46x - 764x/y - 0.00013x^2 \\ dy &= +1731167/y - 6.2e+09/y^2 + 5.6e+12/y^3 \\ dy &= +324 - 3.1e+09/y^2 + 3.8e+12/y^3 \\ dy &= +0.091y - 2.1e+09/y^2 + 2.8e+12/y^3 \end{aligned}$

Bacteria inoculum size = 100 CFU/mm² reproduction rate= 24 h	$dx = -0.21x + 0.00013xy - 0.00018x^2$ $dx = -184x/y + 7.3e-05xy - 0.00018x^2$ $dx = +0.26x - 412x/y - 0.00018x^2$
	$dy = -8.9x + 8062x/y + 0.0025xy$ $dy = -0.12x + 224x/y - 8.5e-06x^2$ $dy = +112x/y - 3.5e-05xy - 8.5e-06x^2$
Bacteria inoculum size = 150 CFU/mm² reproduction rate= 2 h	$dx = -54x + 48480x/y + 0.015xy$ $dx = +2.7y - 0.003y^2 + 8.5e-07y^3$ $dx = +1596 - 0.0015y^2 + 5.7e-07y^3$
	$dy = -52046/(xy) - 9.5e+07/y^2 + 1.7e+11/y^3$ $dy = -29/x - 9.4e+07/y^2 + 1.7e+11/y^3$ $dy = -0.016y/x - 9.3e+07/y^2 + 1.7e+11/y^3$
Bacteria inoculum size = 150 CFU/mm² reproduction rate= 4 h	$dx = +2.6x - 4631x/y - 8.4e-09x^3$ $dx = -2302x/y + 0.00074xy - 8.4e-09x^3$ $dx = -2.6x + 0.0015xy - 8.3e-09x^3$
	$dy = -0.037x + 65x/y - 2.9e-07x^2$ $dy = +32x/y - 1e-05xy - 2.9e-07x^2$ $dy = +0.036x - 2.1e-05xy - 2.9e-07x^2$
Bacteria inoculum size = 150 CFU/mm² reproduction rate= 6 h	$dx = -2311x/y + 0.00074xy - 8e-09x^3$ $dx = +2.6x - 4641x/y - 8e-09x^3$ $dx = -2.6x + 0.0015xy - 8e-09x^3$
	$dy = -0.034x + 58x/y + 7.7e+08/y^3$ $dy = -0.034x + 59x/y + 434262/y^2$ $dy = +28x/y - 9.4e-06xy + 7.7e+08/y^3$
Bacteria inoculum size = 150 CFU/mm² reproduction rate= 12 h	$dx = -1.1x + 0.00065xy - 8.3e-08x^3$ $dx = -1017x/y + 0.00033xy - 8.3e-08x^3$ $dx = +1.2x - 2054x/y - 8.3e-08x^3$
	$dy = -9.8x + 8808x/y + 0.0027xy$ $dy = +1356633/y - 4.9e+09/y^2 + 4.4e+12/y^3$ $dy = +254 - 2.5e+09/y^2 + 3e+12/y^3$
Bacteria inoculum size = 150 CFU/mm² reproduction rate= 18 h	$dx = -0.54x + 0.00031xy - 1.9e-07x^3$ $dx = -479x/y + 0.00016xy - 1.9e-07x^3$ $dx = +0.55x - 969x/y - 1.9e-07x^3$

	$dy = -31576/(xy) - 8.4e+07 /y^2 + 1.5e+11/y^3$ $dy = -18/x - 8.3e+07 /y^2 + 1.5e+11/y^3$ $dy = -0.01y/x - 8.3e+07 /y^2 + 1.5e+11/y^3$
Bacteria inoculum size = 150 CFU/mm2 reproduction rate= 24 h	$dx = -0.11x + 7.2e-05xy - 0.00011 x^2$ $dx = +3e-06xy - 2.5e-07 x^3 + 143300/x^3$ $dx = -99x/y + 4e-05xy - 0.00011 x^2$
	$dy = -1595/x + 2844595 /xy - 1140/x^2$ $dy = +1430343 /xy - 0.45y/x - 1146/x^2$ $dy = +1613/x - 0.9y/x - 1151 /x^2$
Bacteria inoculum size = 250 CFU/mm2 reproduction rate= 2 h	$dx = -25x + 21690 x/y + 0.007 xy$ $dx = -0.38x + 0.00021 xy + 307/x^2$ $dx = -0.39x + 17202/(xy) + 0.00021 xy$
	$dy = -19029/y - 15612/(xy) + 6.1e+10 /y^3$ $dy = -15579/(xy) - 6.8e+07 /y^2 + 1.2e+11/y^3$ $dy = -38274/y - 15645/(xy) + 6.8e+07 /y^2$
Bacteria inoculum size = 250 CFU/mm2 reproduction rate= 2 h	$dx = -2.6x + 0.0015xy - 7.3e-09 x^3$ $dx = -2341x/y + 0.00076xy - 7.3e-09 x^3$ $dx = +2.7x - 4699x/y - 7.4e-09 x^3$
	$dy = +4.2x/y - 4.7e-06 x^2 + 1.7e-09x^3$ $dy = +0.0022x - 4.5e-06 x^2 + 1.7e-09x^3$ $dy = -0.031x + 54x/y + 7.9e+08 /y^3$
Bacteria inoculum size = 250 CFU/mm2 reproduction rate= 6 h	$dx = -2.1x + 0.0012xy - 7.1e-09 x^3$ $dx = -1836x/y + 0.00059xy - 7.1e-09 x^3$ $dx = +2.1x - 3684x/y - 7.2e-09 x^3$
	$dy = -3.4e-07 x^2 - 8e+07/y^2 + 1.4e+11/y^3$ $dy = -22701/y - 3.4e-07 x^2 + 7.2e+10/y^3$ $dy = -8.6 - 3.4e-07 x^2 + 4.8e+10/y^3$
Bacteria inoculum size = 250 CFU/mm2 reproduction rate= 12 h	$dx = +0.76x - 1329x/y - 5.1e-08 x^3$ $dx = -652x/y + 0.00021xy - 5.1e-08 x^3$ $dx = -0.73x + 0.00042xy - 5.1e-08 x^3$
	$dy = -3.7e+07 /y^2 - 7.3e-10 x^3 + 6.6e+10/y^3$ $dy = -10468/y - 7.3e-10 x^3 + 3.3e+10/y^3$ $dy = -3.9 - 7.3e-10 x^3 + 2.2e+10/y^3$
Bacteria inoculum size = 250 CFU/mm2 reproduction rate= 18 h	$dx = -0.53 x + 3e-04 xy - 1e-07 x^3$ $dx = -468 x/y + 0.00015 xy - 1e-07 x^3$ $dx = + 0.54 x - 945 x/y - 1e-07 x^3$

$$\begin{aligned} dy &= + 10 - 14720 / (xy) - 3.2e-06 y^2 \\ dy &= + 20 - 0.011 y - 14679 / (xy) \\ dy &= + 8973 / y - 14720 / (xy) - 8.9e-10 y^3 \end{aligned}$$

Bacteria inoculum size = $dx = -1723 / x + 3096524 / (xy) - 1e-07 x^3$
250 CFU/mm2 $dx = + 1568274 / (xy) - 0.49 y/x - 1e-07 x^3$
reproduction rate= 24 h $dx = + 1768 / x - 0.98 y/x - 1e-07 x^3$

$$\begin{aligned} dy &= + 3.8 x/y + 9.2e-06 y^2 - 5.3e-09 y^3 \\ dy &= + 0.0082 y + 3.8 x/y - 2.7e-09 y^3 \\ dy &= + 0.017 y + 3.8 x/y - 9.4e-06 y^2 \end{aligned}$$

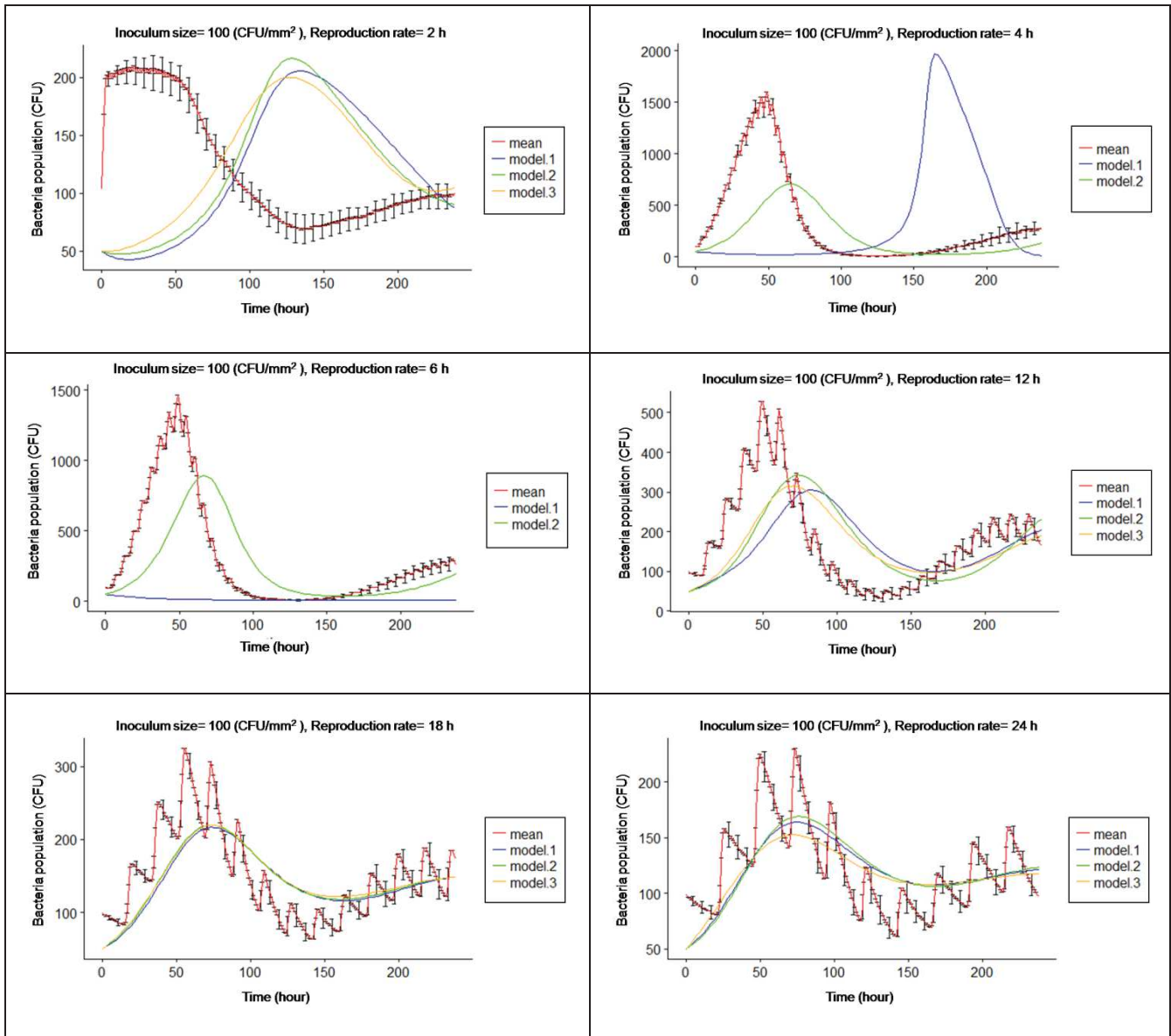


Figure B.1. Comparison between the BJI model simulation outputs and the system dynamics model outputs of bacteria population over time. The outputs were calculated for bacteria inoculum size= 100 (CFU/mm²) and for different values of bacterial reproduction rate= 2, 4, 6, 12, 18, 24 hours, respectively. The red line represents the mean of 20 iterations of simulation output. The other lines represent the three best fit models calculated by Bayesian dynamical system approach for the same data. Blue line represents the first best fit calculated model. Green line represents the second best fit calculated model. Orange line represents the third best fit calculated model.

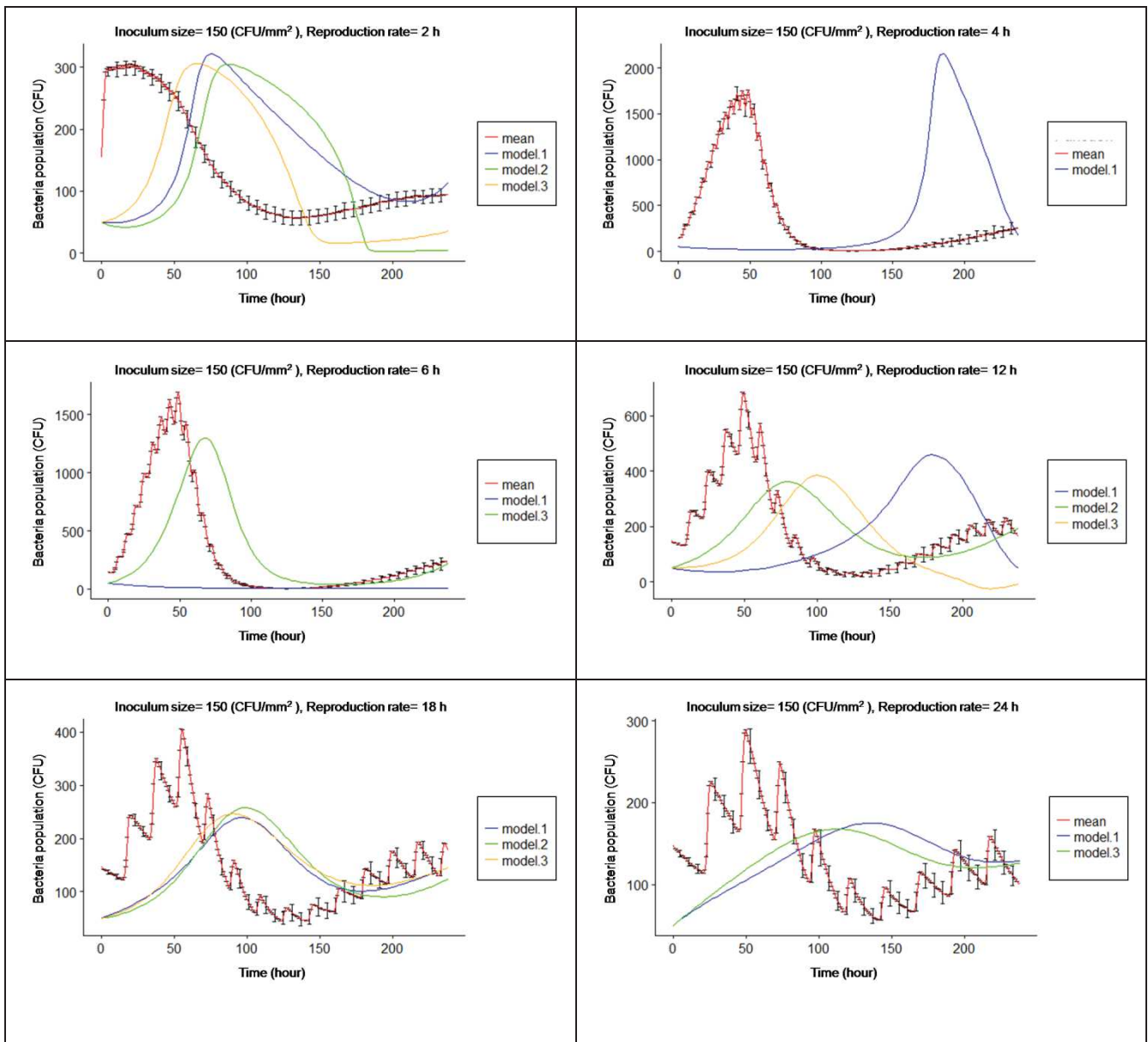


Figure B.2. Comparison between the BJI model simulation outputs and the system dynamics model outputs of bacteria population over time. The outputs were calculated for bacteria inoculum size= 150 (CFU/mm²) and for different values of bacterial reproduction rate= 2, 4, 6, 12, 18, 24 hours, respectively. The red line represents the mean of 20 iterations of simulation output. The other lines represent the three best fit models calculated by Bayesian dynamical system approach for the same data. Blue line represents the first best fit calculated model. Green line represents the second best fit calculated model. Orange line represents the third best fit calculated model.

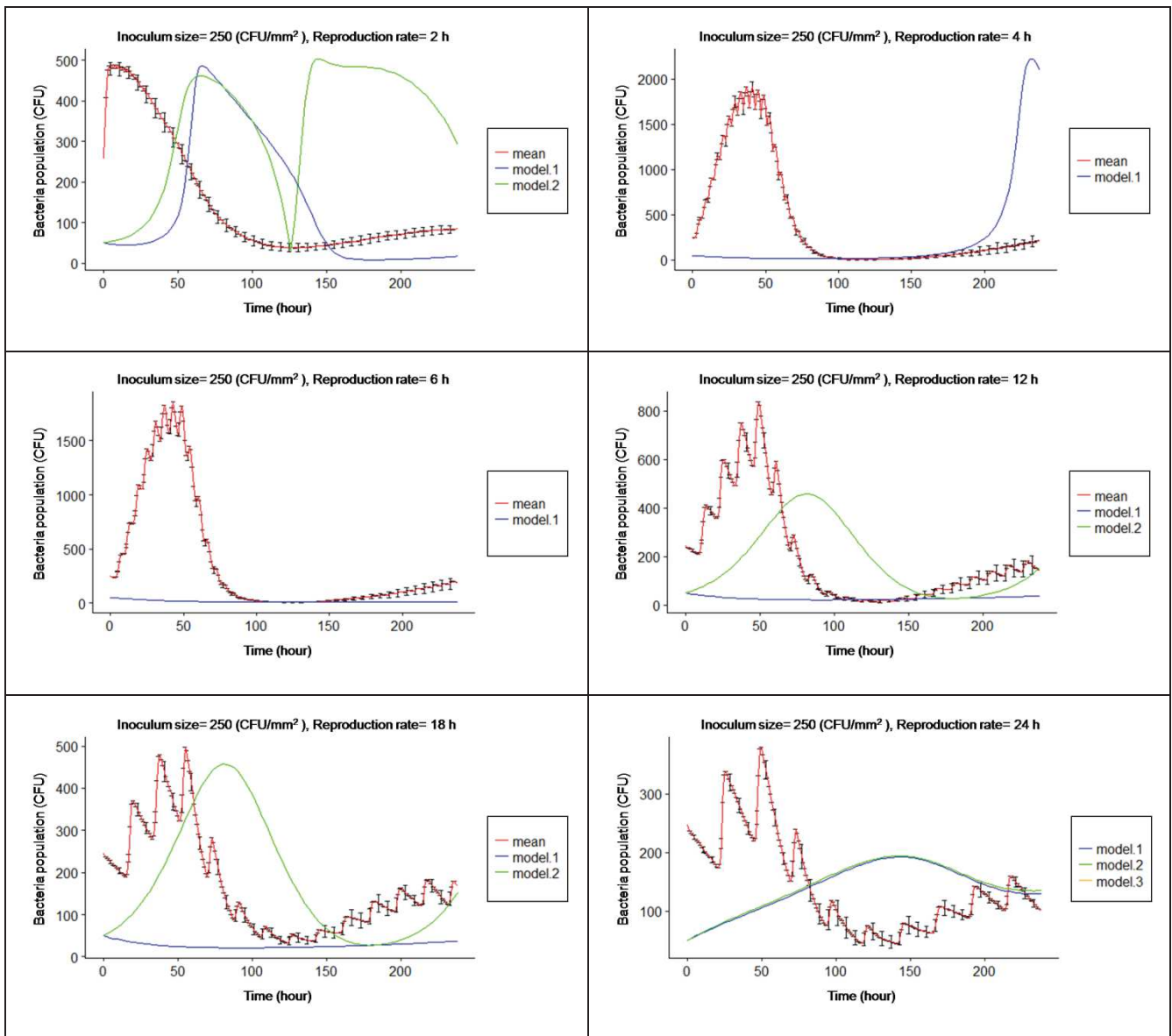


Figure B.3. Comparison between the BJI model simulation outputs and the system dynamics model outputs of bacteria population over time. The outputs were calculated for bacteria inoculum size= 250 (CFU/mm²) and for different values of bacterial reproduction rate= 2, 4, 6, 12, 18, 24 hours, respectively. The red line represents the mean of 20 iterations of simulation output. The other lines represent the three best fit models calculated by Bayesian dynamical system approach for the same data. Blue line represents the first best fit calculated model. Green line represents the second best fit calculated model. Orange line represents the third best fit calculated model.

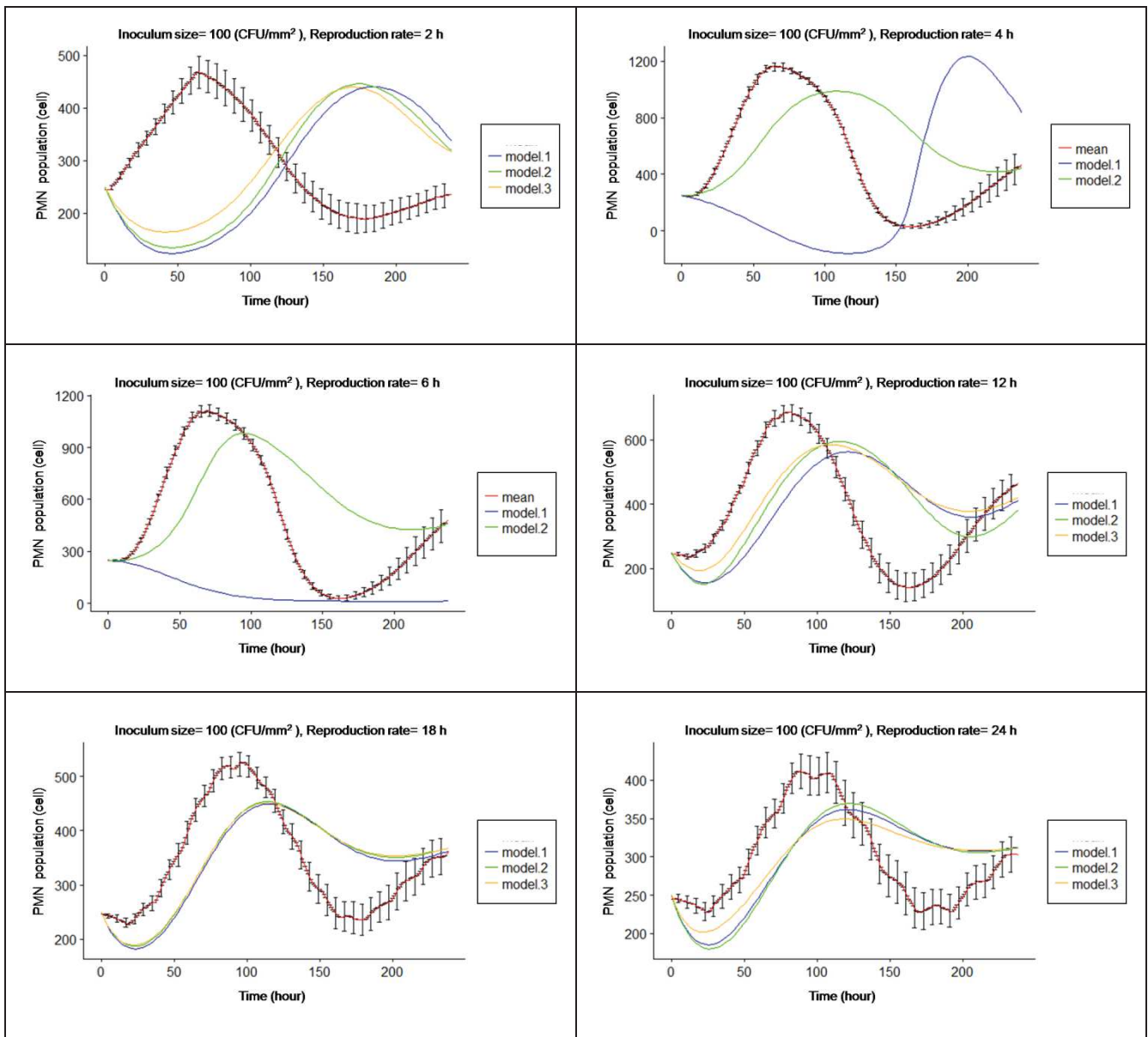


Figure B.4. Comparison between the BJI model simulation outputs and the system dynamics model outputs of neutrophil (PMN) population over time. The outputs were calculated for bacteria inoculum size= 100 (CFU/mm²) and for different values of bacterial reproduction rate= 2, 4, 6, 12, 18, 24 hours, respectively. The red line represents the mean of 20 iterations of simulation output. The other lines represent the three best fit models calculated by Bayesian dynamical system approach for the same data. Blue line represents the first best fit calculated model. Green line represents the second best fit calculated model. Orange line represents the third best fit calculated model.

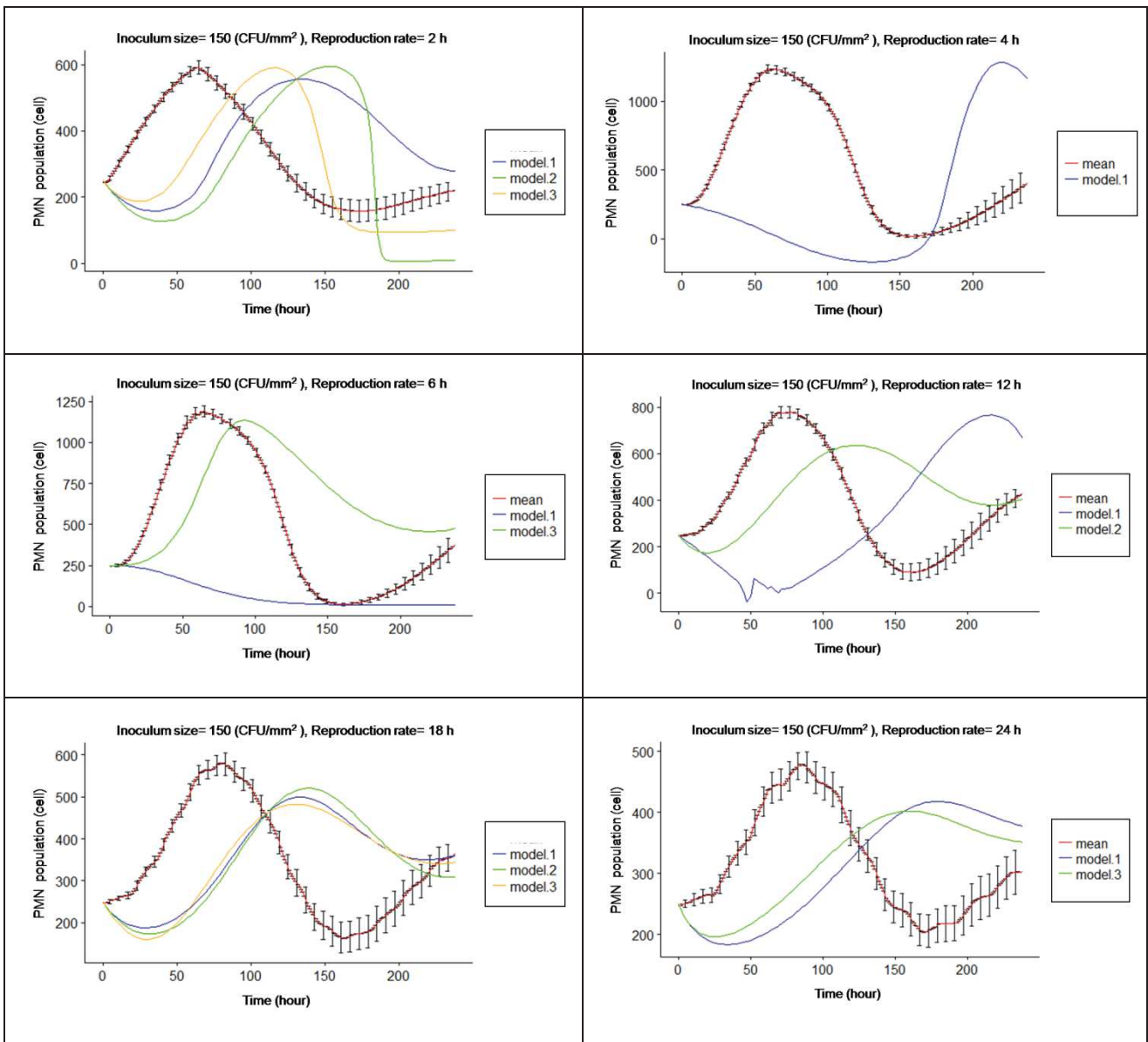


Figure B.5. Comparison between the BJI model simulation outputs and the system dynamics model outputs of neutrophil (PMN) population over time. The outputs were calculated for bacteria inoculum size= 150 (CFU/mm²) and for different values of bacterial reproduction rate= 2, 4, 6, 12, 18, 24 hours, respectively. The red line represents the mean of 20 iterations of simulation output. The other lines represent the three best fit models calculated by Bayesian dynamical system approach for the same data. Blue line represents the first best fit calculated model. Green line represents the second best fit calculated model. Orange line represents the third best fit calculated model.

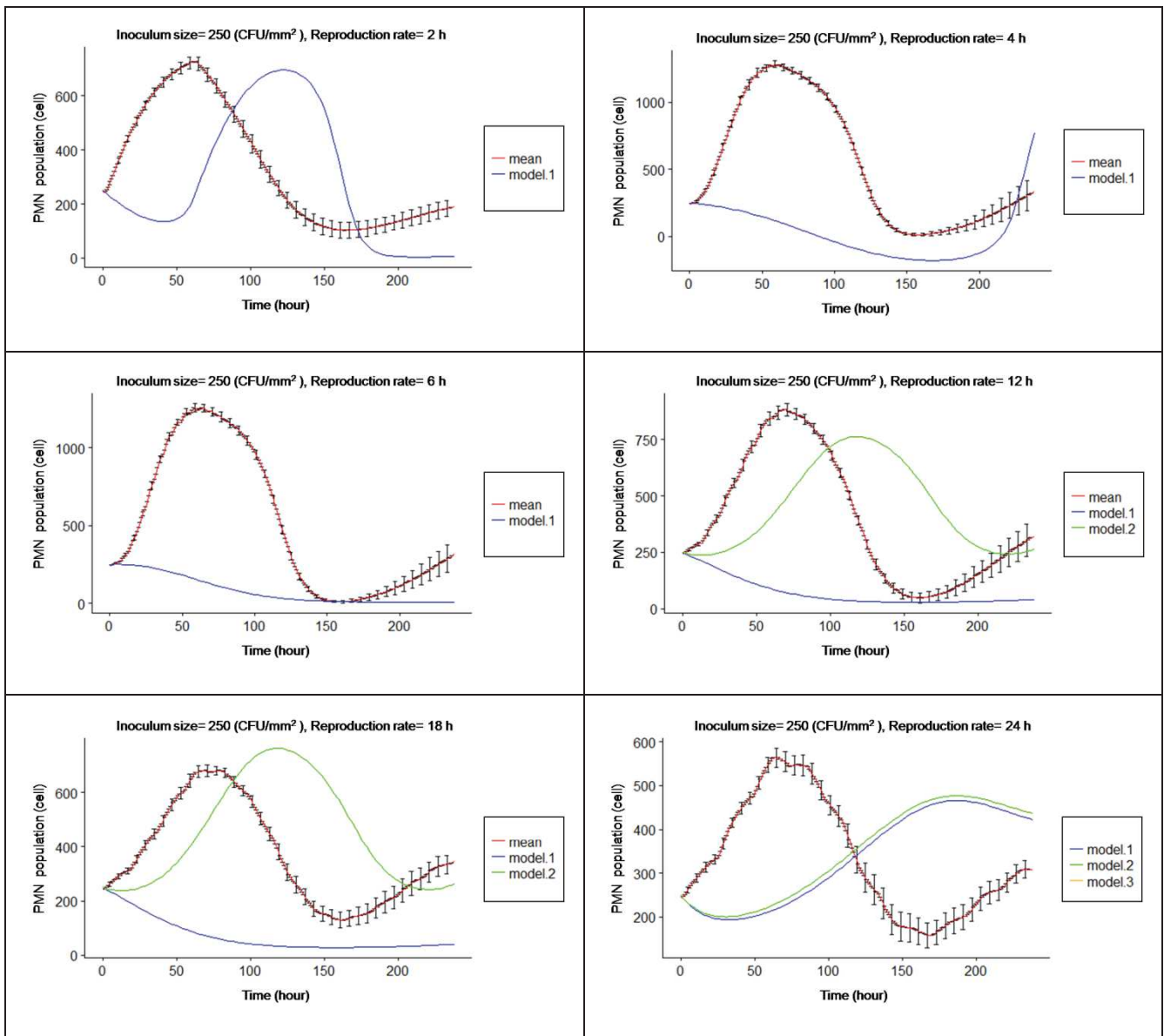


Figure B.6. Comparison between the BJI model simulation outputs and the system dynamics model outputs of neutrophil (PMN) population over time. The outputs were calculated for bacteria inoculum size= 250 (CFU/mm²) and for different values of bacterial reproduction rate= 2, 4, 6, 12, 18, 24 hours, respectively. The red line represents the mean of 20 iterations of simulation output. The other lines represent the three best fit models calculated by Bayesian dynamical system approach for the same data. Blue line represents the first best fit calculated model. Green line represents the second best fit calculated model. Orange line represents the third best fit calculated model.

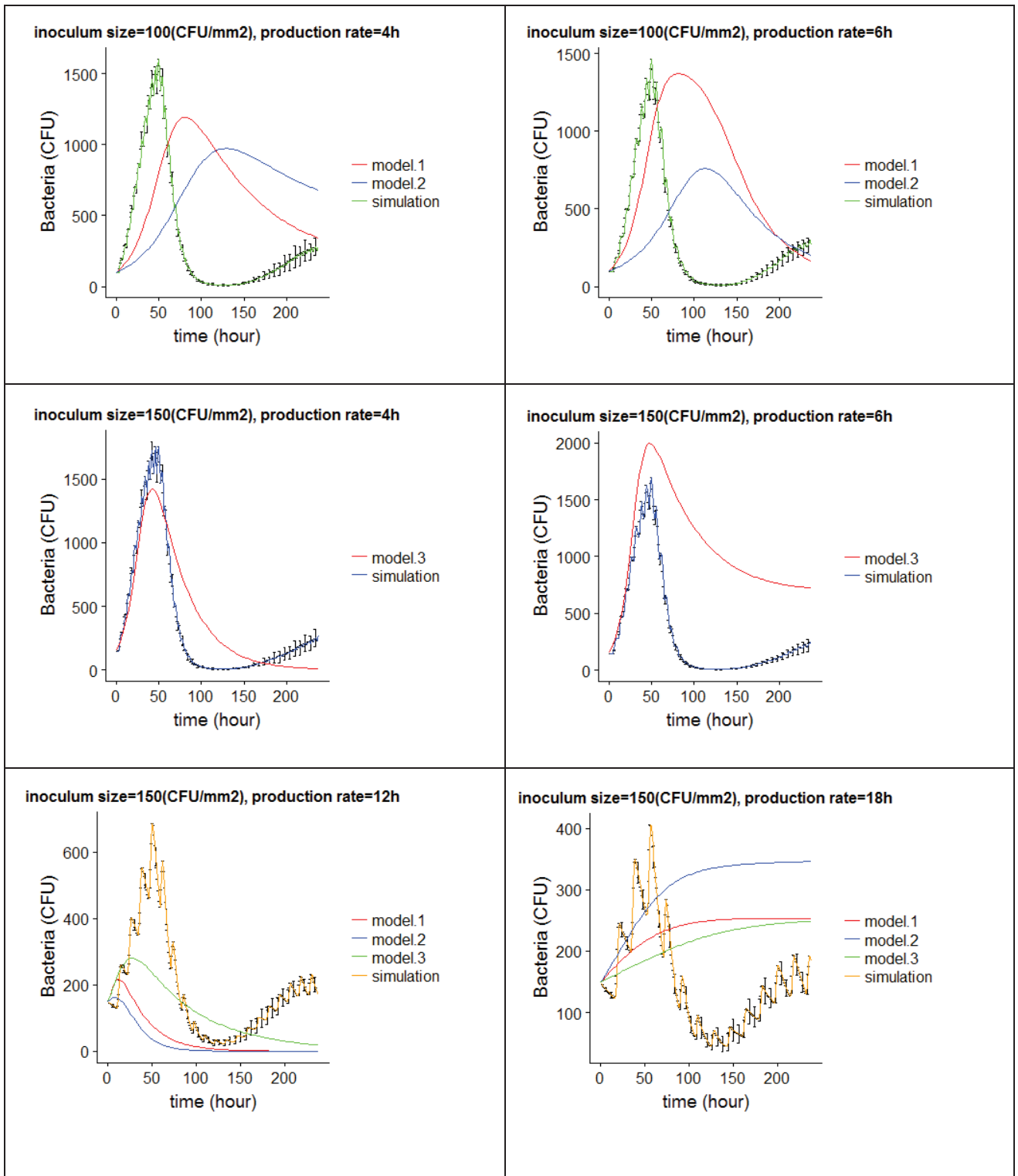


Figure B.7. Comparison between the BJI model simulation outputs and the system dynamics model outputs of bacteria population over time for bacteria and osteocyte dynamic system. The outputs were calculated for bacteria inoculum size= 100 and 150 (CFU/mm²) and for different values of bacterial reproduction rate= 4, 6, 12, 18 hours, respectively.

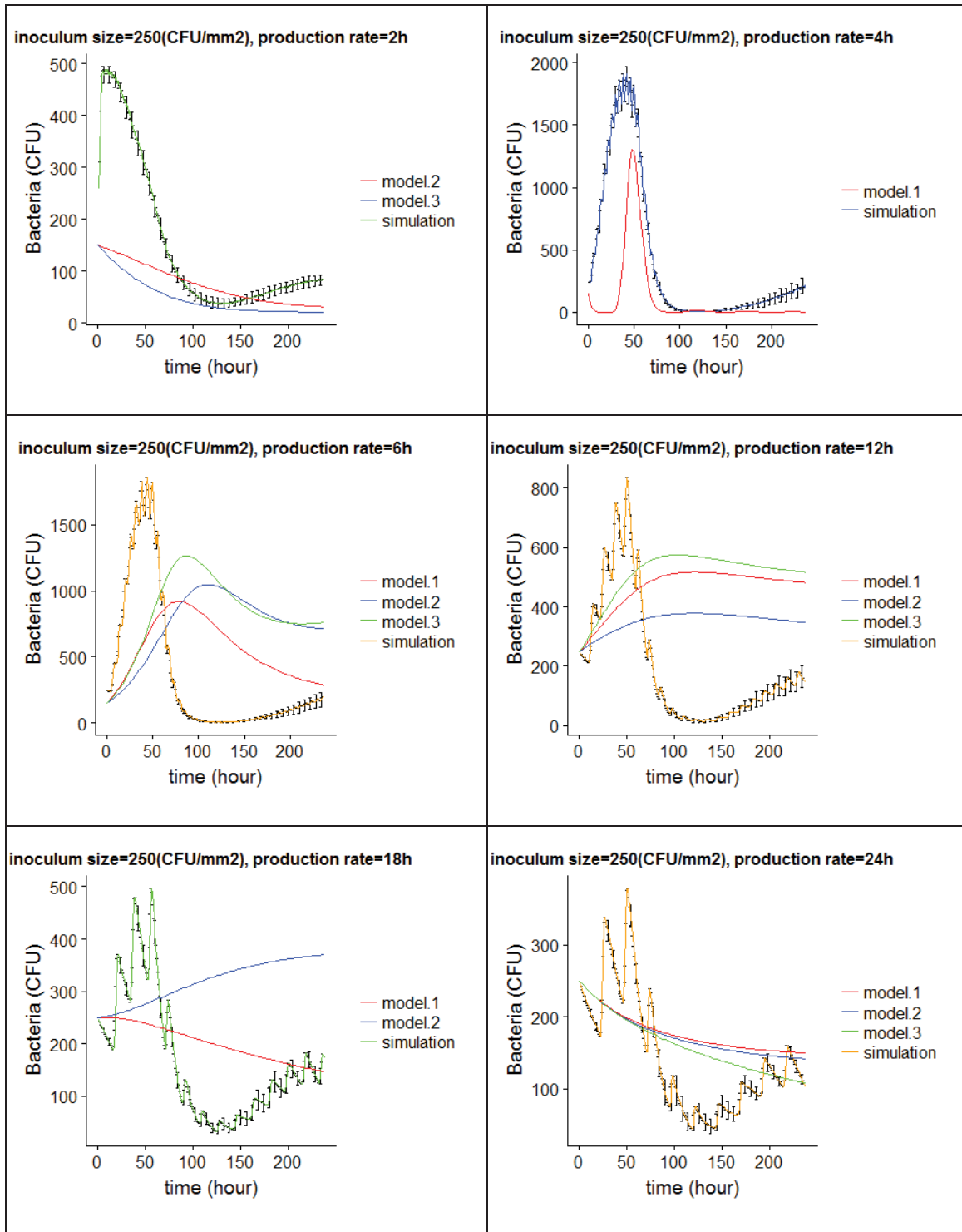


Figure B.8. Comparison between the BJI model simulation outputs and the system dynamics model outputs of bacteria population over time for bacteria and osteocyte dynamic system. The outputs were calculated for bacteria inoculum size= 250 (CFU/mm²) and for different values of bacterial reproduction rate= 2, 4, 6, 12, 18, 24 hours, respectively.

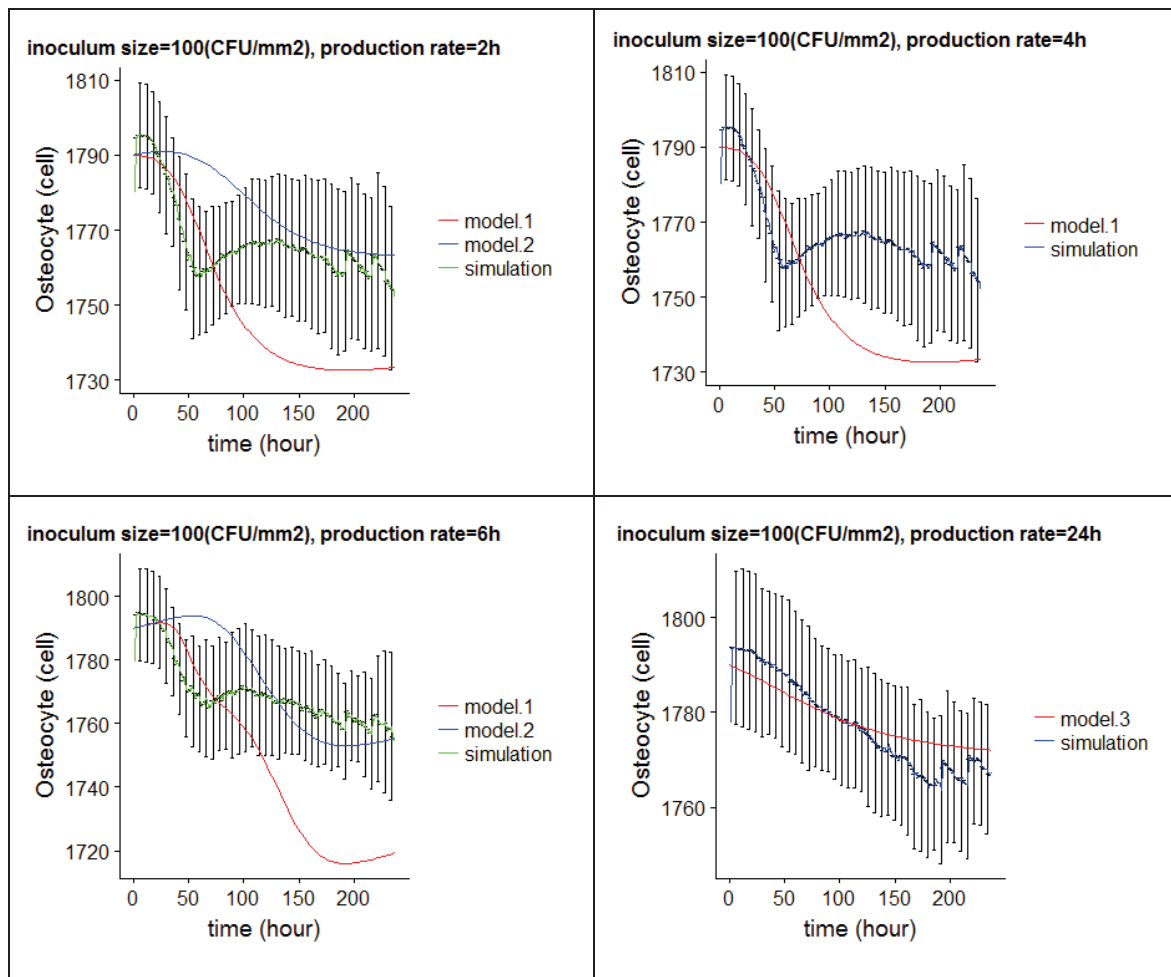


Figure B.9. Comparison between the BJI model simulation outputs and the system dynamics model outputs of osteocyte population over time for bacteria and osteocyte dynamic system. The outputs were calculated for bacteria inoculum size= 100 (CFU/mm²) and for different values of bacterial reproduction rate= 2, 4, 6, 24 hours, respectively.

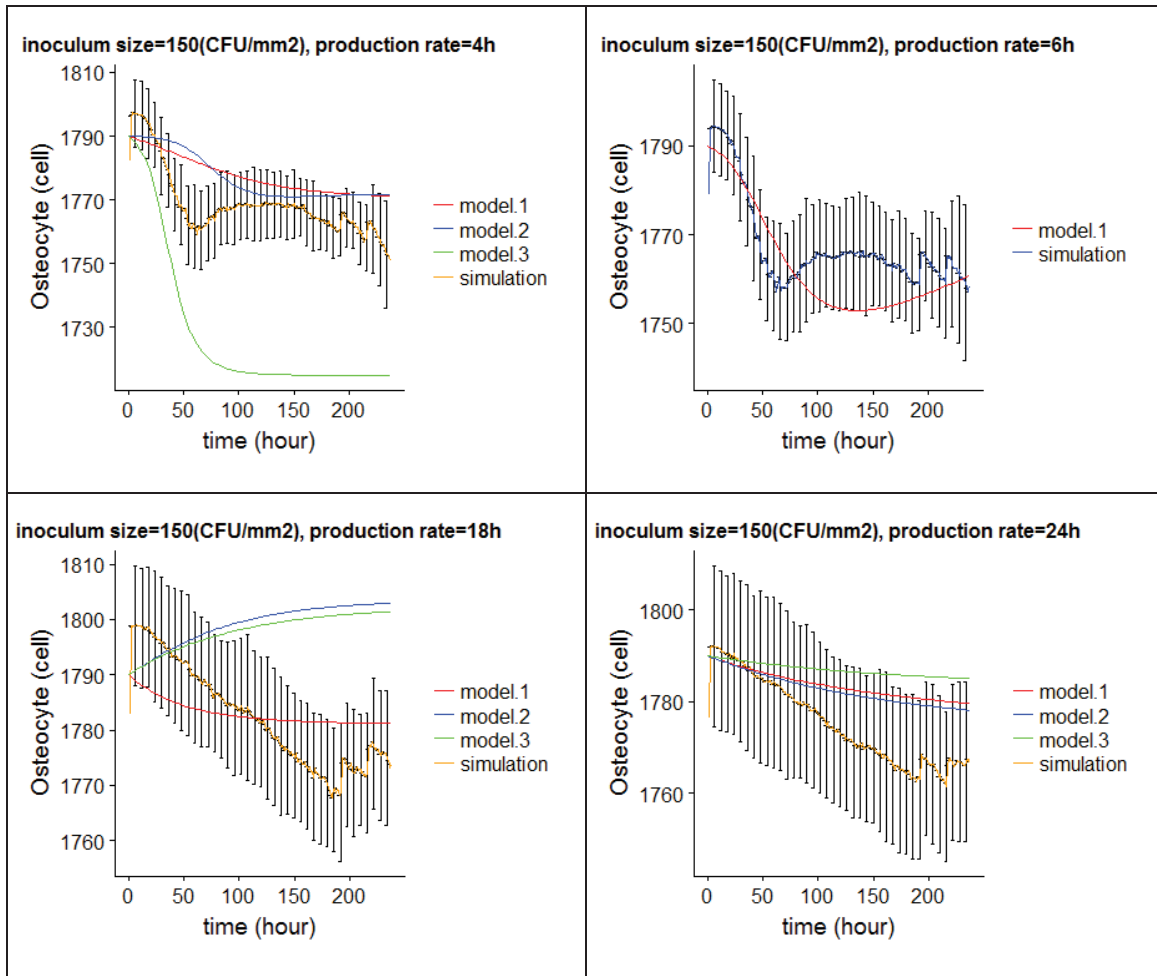


Figure B.10. Comparison between the BJI model simulation outputs and the system dynamics model outputs of osteocyte population over time for bacteria and osteocyte dynamic system. The outputs were calculated for bacteria inoculum size= 150 (CFU/mm²) and for different values of bacterial reproduction rate= 4, 6, 18, 24 hours, respectively.

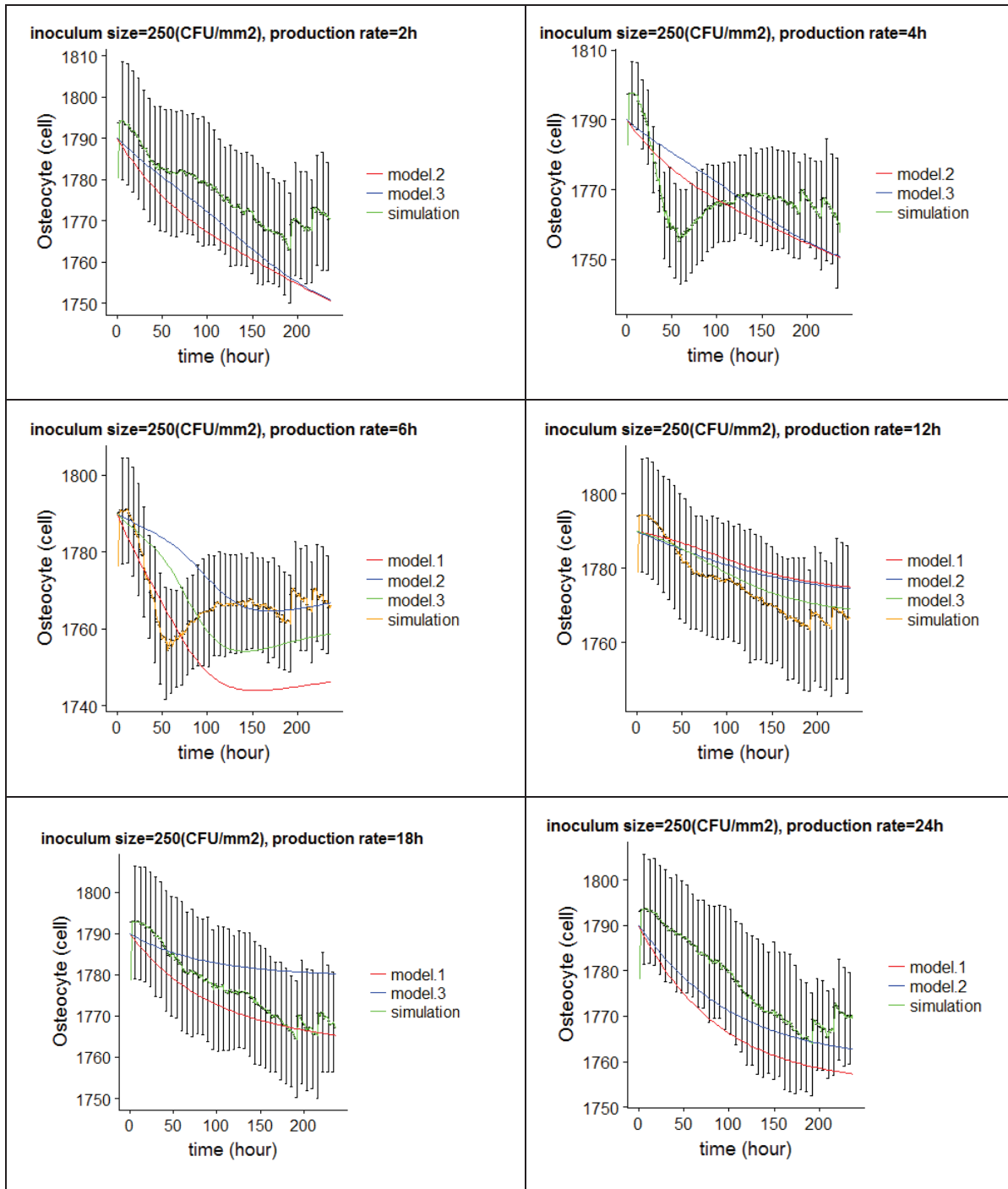


Figure B.11. Comparison between the BJI model simulation outputs and the system dynamics model outputs of osteocyte population over time for bacteria and osteocyte dynamic system. The outputs were calculated for bacteria inoculum size= 250 (CFU/mm²) and for different values of bacterial reproduction rate= 2, 4, 6, 12, 18, 24 hours, respectively.

Titre: Modélisations complexes bi dimensionnelles des infections ostéo-articulaires à base de simulations multi-agents.

Mots clés: Infections ostéo-articulaires, systèmes multi-agents, NetLogo, modélisation par systèmes dynamiques non-linéaires, multi-échelle, remodelage osseux, *Staphylococcus aureus*

Résumé: Le diagnostic et la prise en charge des infections ostéo-articulaires (IOA) sont souvent complexes occasionnant une perte osseuse irréversible. La variabilité intra et inter-patient en terme de présentation clinique rend impossible le recours à une description systématique ou à une analyse statistique pour le diagnostic et l'étude de cette pathologie. Le développement d'IOA résulte d'interactions complexes entre les mécanismes cellulaires et moléculaires du tissu osseux et les bactéries. L'objectif de cette thèse est de modéliser l'IOA afin de simuler le comportement du système suite à des interactions au niveau cellulaire et moléculaire en utilisant l'approche de modélisation à base d'agents. Nous avons utilisé une méthode basée sur l'analyse bibliographique pour extraire les caractéristiques du modèle et les utiliser pour deux aspects. Le premier consiste en l'élaboration de la structure du modèle en identifiant les agents et les interactions, et le deuxième concerne l'estimation quantitative des différents paramètres du modèle. La réponse du système BJI aux différentes tailles d'inoculum bactérien a été simulée par la variation de différents paramètres. L'évolution des agents simulés a ensuite été analysée en utilisant une modélisation par des systèmes dynamiques non linéaires et une méthodologie "Data-driven", grâce auxquelles nous avons décrit le système d'IOA et identifié des relations plausibles entre les agents. Le modèle a réussi à présenter la dynamique des bactéries, des cellules immunitaires innées et des cellules osseuses au cours de la première étape de l'IOA et pour différentes tailles d'inoculum bactérien. La simulation a mis en évidence les conséquences sur le tissu osseux résultant du processus de remodelage osseux au cours de l'IOA. Ces résultats peuvent être considérés comme une base pour une analyse plus approfondie et pour la proposition de différentes hypothèses et scénarios de simulation qui pourraient être étudiés dans ce laboratoire virtuel.

Title: Two-dimensional complex modeling of bone and joint infections using agent-based simulation

Keywords: Bone and joint infections, agent-based modeling, NetLogo, nonlinear system dynamics modeling, multi-scale, bone destruction prediction, bone remodeling process, *Staphylococcus aureus*

Abstract: Bone and joint infections are one of the most challenging bone pathologies that associated with irreversible bone loss and long costly treatment. The high intra and inter patient's variability in terms of clinical presentation makes it impossible to rely on the systematic description or classical statistical analysis for its diagnosis or studying. The development of BJI encompasses a complex interplay between the cellular and molecular mechanisms of the host bone tissue and the infecting bacteria. The objective of this thesis is to provide a novel computational modeling framework that simulates the behavior resulting from the interactions on the cellular and molecular levels to explore the BJI dynamics qualitatively and comprehensively, using an agent-based modeling approach. We relied on a meta-analysis-like method to extract the quantitative and qualitative data from the literature and used it for two aspects. First, elaborating the structure of the model by identifying the agents and the interactions, and second estimating quantitatively the different parameters of the model. The BJI system's response to different microbial inoculum sizes was simulated with respect to the variation of several critical parameters. The simulation output data was then analyzed using a data-driven methodology and system dynamics approach, through which we summarized the BJI complex system and identified plausible relationships between the agents using differential equations. The BJI model succeeded in imitating the dynamics of bacteria, the innate immune cells, and the bone cells during the first stage of BJI and for different inoculum size in a compatible way. The simulation displayed the damage in bone tissue as a result of the variation in bone remodeling process during BJI. These findings can be considered as a foundation for further analysis and for the proposition of different hypotheses and simulation scenarios that could be investigated through this BJI model as a virtual lab.